Control of Vein Network Formation by Auxin Transport in Arabidopsis Leaves

by

Carla De Agostini Verna

A thesis submitted in partial fulfillment of the requirements for the degree of

Doctor of Philosophy

in

Plant Biology

Department of Biological Sciences
University of Alberta

ABSTRACT

Vascular networks transport water, signals and nutrients in both plants and animals; what controls the formation of these networks is thus a central question in biology. In animals, vascular network formation requires direct cell-cell communication and often cell movements, both of which are precluded in plants by a wall that holds cells in place; therefore, plants form vascular networks, such as the vein networks of leaves, by a different mechanism. Furthermore, many animal vascular networks are stereotyped; by contrast, the vein networks of plant leaves are both reproducible and variable. Consider, for example, the vein network of an Arabidopsis leaf: lateral veins branch from a single midvein and connect to distal veins to form loops; minor veins branch from midvein and loops and connect to other veins to form a mesh; and loops and minor veins curve near the leaf margin to lend a scalloped outline to the vein network. Features of the vein network such as these are reproducible from leaf to leaf—so much so that they are used to define species. By contrast, the number of veins differs from leaf to leaf, and whether a vein will connect to another vein on both ends or one end will terminate free of contact with other veins is unpredictable; this is always so for minor veins, but even loops can occasionally fail to connect to other veins at one end. This coexistence of reproducibility and variability argues against a rigid specification of leaf vein networks and instead suggest a self-organizing mechanism that functionally integrates vein network formation with leaf growth.

Varied evidence implicates the plant signal auxin and its polar transport through plant tissues in the control of vein network formation. (i) Expression of the PIN-FORMED1 (PIN1) auxin transporter of Arabidopsis is initiated in broad domains of leaf inner cells that become gradually restricted to files of vascular precursor cells in contact with pre-existing, narrow PIN1 expression domains. Within broad expression domains, PIN1 is localized isotropically—or

nearly so—to the plasma membrane of leaf inner cells. As expression of PIN1 becomes gradually restricted to files of vascular precursor cells, PIN1 localization becomes polarized to the side of the plasma membrane facing the pre-existing, narrow PIN1 expression domains with which the narrowing domains are in contact. (ii) Auxin application to developing leaves induces formation of broad expression domains of isotropically localized PIN1. Such domains become restricted to the sites of auxin-induced vein formation, and PIN1 localization becomes polarized toward the pre-existing vasculature. (iii) Both restriction of PIN1 expression and polarization of PIN1 localization initiate and proceed away from pre-existing, narrow PIN1 expression domains and are delayed by chemical inhibition of auxin transport. (iv) Auxin transport inhibitors induce characteristic vein-pattern defects, similar to—though stronger than—those of *pin1* mutants. Therefore, available evidence suggests that auxin induces the polar formation of veins and that such inductive and orienting property of auxin strictly depends on the function of *PIN1* and of possibly the other seven *PIN* genes in Arabidopsis.

Here I tested these hypotheses. My results suggest that: (i) PIN-mediated auxin transport controls both reproducible and variable features of leaf vein networks. (ii) *PIN1* is the only known gene to be nonredundantly required for both the reproducible features of leaf vein networks and their variable ones. (iii) The expression of PIN1 that is required for vein network patterning depends on a 205-bp region of the *PIN1* promoter that contains conserved putative binding-sites for transcription factors of the MYELOBLASTOMA and DNA-BINDING WITH ONE FINGER families. (iv) Auxin-induced polar-vein-formation occurs in the absence of the function of PIN proteins or of any known intercellular auxin transporter. (v) The auxin-transport-independent vein-patterning activity relies on auxin signaling. (vi) A polarizing signal that depends on the function of the GNOM guanine-nucleotide exchange factor for ADP-

rybosilation-factor GTPases, which regulates vesicle formation in membrane trafficking, acts upstream of both auxin transport and auxin signaling in leaf vein formation. My results define new inputs of auxin in the control of vein network formation.

PREFACE

Parts of my thesis are published.

Chapter 1 was published as Linh, N.M., Verna, C. and Scarpella, E. 2018. “Coordination of cell polarity and the patterning of vein networks”. Current Opinion in Plant Biology 41:116–124. All authors equally shared the responsibility to conceiving, designing and writing the paper.

Chapter 2 was published as Verna, C., Sawchuk, M.G., Linh, N.M. and Scarpella, E. 2015. “Control of vein network topology by auxin transport”. BMC Biology 13:94. I shared equally with my supervisor, Dr. Enrico Scarpella, the responsibility to conceiving and designing the experiments, analyzing the data and writing the paper. I performed 65% of the experiments, while M. Sawchuk and N.M. Linh performed 25% and 10% of the experiments, respectively.

All the authors and publishers have given their permission for the inclusion of these publications in this thesis.

ACKNOWLEGEMENTS

The work I present in this thesis would not have been possible without the help and support of many people.

First and foremost, I thank my supervisor, Dr. Enrico Scarpella. Thank you for the opportunity and mentorship you have given me during my time in your lab. What I learned from you has helped me improve not only professionally but also personally, and I will remember your teachings for the rest of my life.

For kindly providing plasmids and seeds, I thank the Arabidopsis Biological Resource Center (ABRC), Jose Alonso, Eva Benková, Malcom Bennett, Thomas Berleth, Ikram Blilou, Clay Carter, Hyung-Taeg Cho, Pankaj Dhonukshe, Mark Estelle, Jiří Friml, Hidehiro Fukaki, Hiroo Fukuda, Gerd Jürgens, Chris Kuhlemeier, Elliot Meyerowitz, Ranjan Swarup, Ben Scheres and Venkatesan Sundaresan.

I thank the past and current member of the Scarpella Lab for the shared moments of joy and hardship. I thank Megan Sawchuk for all the training she has given me and her help with the analysis of *pin* mutants in Chapter 2 and Chapter 4. For helping with different parts of this thesis, I thank Priyanka Govindaraju, Linh Manh Nguyen, Sree Janani Ravichandran, and Tongbo Zhu. I also thank Jason Gardiner and Ira Sherr for training me in at-the-time unfamiliar molecular biology techniques when I started in the lab. I want to thank Brindhi Amalraj, Tyler Donner, Anmol Krishna, Dhruv Lavania and Osama Odat for providing an uplifting environment in the lab.

I thank the members of my supervisory committee, Dr. Michael Deyholos and Dr. Uwe Hacke, for their guidance and help throughout my Ph.D.

Finally, I thank my family for their support in my journey: my partner Aaron Evans, my parents Elizete and Carlos Verna, my sister Juliana Verna, and my grandmother Jacyra de Agostini. Your emotional support in this period really helped overcome the bad days of homesickness. I can never thank you enough for all the support and words of encouragement.

TABLE OF CONTENT

LIST OF TABLES

LIST OF FIGURES

CHAPTER 1

CHAPTER 2

LIST OF ABBREVIATIONS

ABCB	ATP-BINDING CASSETTE B
AFB2	AUXIN SIGNALLING F-BOX2
AS1	ASYMMETRIC LEAVES 1
ATML1	ARABIDOPSIS THALIANA MERISTEM LAYER1
AXR1	AUXIN RESISTANT1
CDF	CYCLING DOF FACTOR
CFP	CYAN FLUORESCENT PROTEIN
Col-0	Columbia-0
cPIN1	PIN-FORMED1 coding sequence
CVP2	COTYLEDON VASCULAR PATTERN2
DAG	days after germination
DOF	DNA-BINDING WITH ONE FINGER
DR5	DIRECT REPEAT5
EIR1	ETHYLENE INSENSITIVE ROOT1
EMB30	EMBRYO DEFECTIVE30
EP	end point
ER	endoplasmic reticulum
Fig	Figure
GFP	GREEN FLUORESCENT PROTEIN
GN	GNOM
gPIN1	PIN-FORMED1 genomic sequence
IAA	indole-3-acetic acid
KP	break point
LAX	LIKE AUX1
MDR	MULTIDRUG RESISTANCE
MP	MONOPTEROS
MYB	MYELOBLASTOMA
NPA	N-1-naphthylphthalamic acid

nuc	nuclear signal
OBP	OBF BINDING PROTEIN
PEDs	PIN1-expression domains
PGP	P-GLYCOPROTEIN
PIN	PIN-FORMED
PM	plasma membrane
RS2	ROUGH SHEATH2
TIR1	TRANSPORT INHIBITOR RESPONSE1
TOZ	TORMOZEMBRYO DEFECTIVE
TP	touch point
RPS5A	RIBOSOMAL PROTEIN S5A
TWD1	TWISTED DWARF1
WT	Wild type
UCU2	ULTRACURVATA2
XP	exit point
YFP	YELLOW FLUORESCENT PROTEIN
ΔPIN1	*PIN-FORMED1* promoter fragments

Gene and Protein Notation

Uppercase Italics	WT Gene (e.g., *PIN1*)
Uppercase Roman	WT Protein (e.g., PIN1)
Lowercase Italics	Mutant Allele (e.g., *pin1*)
Multiple Mutant of Gene A and B	*a*;*b* (e.g.; *pin1*;*pin6*)

Gene Fusion Notation

Transcriptional Fusion of Gene A to Gene B (Fusion of promoter A to gene B)	A::B
Translational Fusion of Gene A to Gene B (Fusion of gene Ato gene B)	A:B

Gene Coordinates

All gene coordinates are relative to the adenine (position +1) of the start codon.

CHAPTER 1: GENERAL INTRODUCTION

1.1 Cell polarity and its coordination

During development, cell behaviors such as expansion and division are coordinated between cells along preferential or exclusive orientations or directions (Wolpert et al. 2015). In plants, for example, cells in epidermal files of the root form hairs by locally expanding at their basal outer side (Masucci and Schiefelbein 1994; Fischer et al. 2006), and cells in epidermal sheets of shoot organ primordia expand and divide along the proximodistal orientation (Reddy et al. 2004; Kuchen et al. 2012). How are these orientations and directions specified within cells and coordinated between cells?

In animals, where this question has been addressed extensively, the anisotropic localization of cellular components such as proteins provides cells with an internal compass that points in a specific direction (Goodrich and Strutt 2011). These cell anisotropies, or cell polarities, are then coordinated between cells, often by mechanisms that rely on direct interaction between proteins bridging the plasma membranes of neighboring cells. These types of mechanisms are precluded in plants by a wall that separates the cells' plasma membranes. How then is cell polarity coordinated in plants?

1.2 Coordination of cell polarity during auxin-induced vascular-strand formation

That the formation of vascular strands is an expression of coordination of cell polarity was first suggested by experiments in which auxin had been applied to mature plant tissues (Kraus et al. 1936; Jacobs 1952; Sachs 1968). Indeed, application of auxin to various tissues leads to the

formation of continuous files of vascular cells that connect the applied auxin to the pre-existing vascular strands *basally* to the site of auxin application (Fig. 1.1A). This polar response requires the application of polarly transported auxins (Dalessandro and Roberts 1971) and is blocked by inhibitors of polar auxin transport (Gersani 1987), suggesting that it depends on the ability of the responding tissue to transport auxin polarly.

Normally, auxin is produced in large amounts in immature shoot-organs (Thimann and Skoog 1934; Avery 1935) and is transported to the roots through vascular strands (Went 1928; Wangermann 1974) (Fig. 1.1B). This apical-basal polarity of auxin transport is thought to derive from the localization of auxin efflux proteins at the basal end of auxin-transporting cells (Rubery and Sheldrake 1974; Raven 1975) (Fig. 1.1B). Indeed, as a weak acid, auxin is mostly negatively charged at the neutral intracellular pH and can efficiently leave the cell only through specialized plasma-membrane-localized efflux proteins (Fig. 1.1B). This model is certainly a simplification, but calculations based on known parameters suggest that it can account for the observed polar transport (Mitchison 1980b); it can also account for the auxin-induced vascular-differentiation response, provided that auxin movement through a cell positively feed back on the localization of auxin efflux proteins to the site where auxin leaves the cell, as put forward by the "auxin canalization hypothesis" (Sachs 1991a; Sachs 2000).

This hypothesis proposes that in the cells between a site of auxin application and the pre-existing vascular strands, the applied auxin would initially move by diffusion in varied directions, and that in these cells, auxin efflux proteins would be localized isotropically, or nearly so, to the plasma membrane (Fig. 1.1C). By efficiently transporting auxin along their original, apical-basal auxin-transport polarity, the pre-existing vascular strands would act as auxin sinks, thereby directing auxin movement in the neighboring cells and polarizing the localization of auxin efflux proteins in these cells. The induction of polar auxin transport in these cells would be gradually enhanced by positive feedback between auxin transport and efflux protein localization. By draining auxin increasingly more efficiently and polarly, these cells would in turn induce polar auxin transport and polarization of efflux protein localization in the cells above them, and inhibit the same processes in their lateral neighbors. Reiteration of these steps would result in preferential transport of auxin through limited cell files, which would

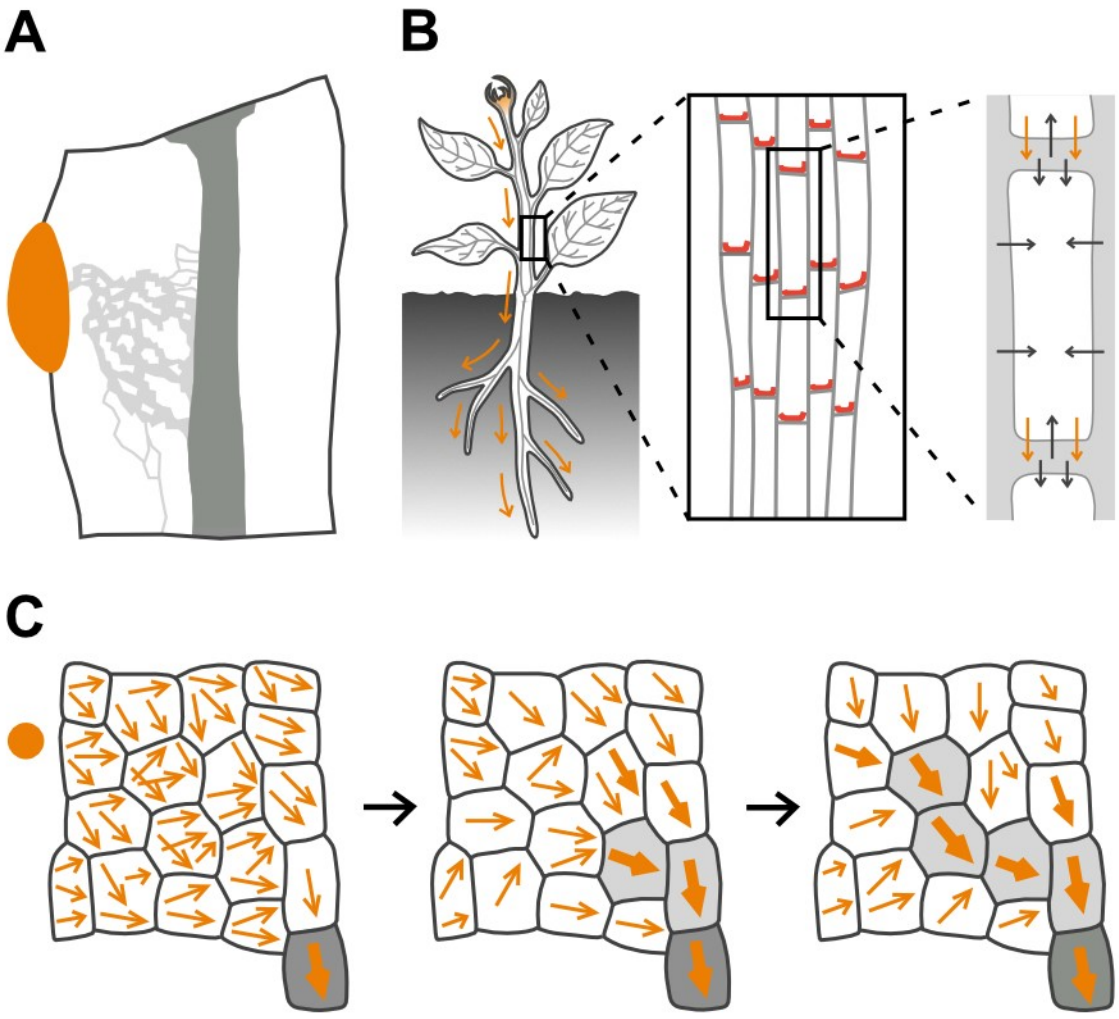

Figure 1.1. Coordination of cell polarity during auxin-induced vascular strand formation. (A) Application of polarly transported auxins (orange) to plant tissues in which auxin is transported from top to bottom induces differentiation of vascular cells in continuous lines to form vascular strands (light gray) that connect the applied auxin to the pre-existing vascular strands (dark gray) basal to the application site. After (Sachs 1968, 1991b). (B) Left: auxin (orange) is produced in large amounts in immature shoot-organs and transported (orange arrows) to the roots by vascular strands. Middle: the shoot-to-root, apical-basal polarity of auxin transport derives from the polar localization of efflux transporters of the PIN-FORMED (PIN) family (red) at the basal plasma-membrane of vascular cells. Right: specialized efflux transporters are required for auxin to leave efficiently the cell (orange arrows) as auxin is mostly negatively charged at intracellular pH; by contrast, auxin is mostly uncharged at extracellular pH

and can thus diffuse efficiently into the cell (dark gray arrows). Auxin can also enter the cell by the activity of transporters of the AUXIN RESISTANT1 (AUX1)/LIKE AUX1 family (Peret et al. 2012) and leave the cell by the activity of transporters of the ATP-BINDING CASSETTE B/P-GLYCOPROTEIN/MULTIDRUG RESISTANCE family (Geisler and Murphy 2006), the nonpolar localization of which is, for simplicity, not shown. (C) Successive stages (connected by arrows) of vascular strand formation in response to application of auxin (orange circle) according to the "auxin canalization hypothesis". Positive feedback between cellular auxin efflux (orange arrows) and localization of auxin efflux proteins to the cellular site of auxin exit gradually polarize auxin transport (increasingly thicker orange-arrows). This occurs first in cells in contact with the pre-existing vascular strands (dark gray), which transport auxin along the original, apical-basal polarity of the tissue and thus orient auxin transport toward themselves. Large polar-auxin-transport capacity in selected cells leads to vascular differentiation (light gray) and drains auxin away from neighboring cells, thus inhibiting their differentiation. Reiteration of the process forms a continuous vascular strand that connects the applied auxin to the pre-existing vascular strands basal to the site of auxin application. Figure inspired by (Sachs 1991a).

eventually differentiate into vascular strands. During this process, chance localization of efflux proteins would be stabilized by positive feedback between auxin transport and efflux protein localization, resulting in random elements in the course of the selected cell files and deviations from the shortest paths for auxin transport.

The localization of the five plasma-membrane-localized members of the PIN- FORMED (PIN) family of auxin efflux proteins of Arabidopsis marks the presumed auxin-efflux side of cells (Petrasek et al. 2006; Wisniewska et al. 2006). Therefore, the polarity of auxin transport can be inferred from the localization of PIN proteins at the plasma membrane. Local application of auxin to mature tissue induces the formation of broad PIN1-expression domains (PEDs hereafter) that connect the applied auxin to the pre-existing vascular strands (Sauer et al. 2006). Initially, PIN1 is localized isotropically, or nearly so, to the plasma membrane of the cells in these broad domains. However, over time, PIN1 localization becomes polarized: toward the pre-existing vascular strands basal to the site of auxin application, in the cells along the domains' midline; and toward the domains' midline, in the cells flanking it. Furthermore, over time, broad PEDs narrow to sites of auxin-induced vascular-strand formation. In these narrow PEDs, PIN1 localization suggests auxin transport away from the applied auxin and toward the pre-existing vascular strands basal to the site of auxin application. Both the narrowing of broad PEDs and the polarization of PIN1 localization initiate and proceed away from the pre-existing vascular strands. Therefore, experimental observations of coordination of cell polarity during auxin-induced vascular-strand formation are consistent with predictions of the auxin canalization hypothesis.

Not all the predictions of the auxin canalization hypothesis seem, however, to be supported by experimental observations (Runions et al. 2014). For example, the prediction of low levels of auxin in developing vascular strands (Mitchison 1980a; Rolland-Lagan and Prusinkiewicz 2005) seems to be inconsistent with experimental observations (Mattsson et al. 2003; Scarpella et al. 2003). However, this apparent inconsistency can be resolved by assuming active import of auxin into vascular cells (Kramer 2004), mobilization of auxin sequestered within vascular cells (Sawchuk et al. 2013; Verna et al. 2015) (Chapter 2), limiting supply of auxin efflux proteins within the cell (Feugier et al. 2005) or auxin transport toward the vascular strand from the cells flanking it (Bayer et al. 2009).

These observations suggest that vascular strand formation in response to auxin application is an expression of coordination of cell polarity the essence of which is captured by the auxin canalization hypothesis. But is that so also for the vascular strands that form during normal development?

1.3 Coordination of cell polarity during vein network patterning

All plant organs and their parts are supplied with interconnected vascular strands. This is nowhere more evident than in leaves, where vascular strands, or veins, form conspicuous networks that largely reflect the shape of the leaf (Ettinghausen 1861; Ash et al. 1999; Dengler and Kang 2001). In the rounded leaves of many eudicots—for example, Arabidopsis—lateral veins branch from a single midvein and contact distal veins to form vein loops; minor veins branch from midvein and loops, and either end freely or contact other veins to form a mesh; and loops and minor veins curve near the leaf margin to lend a scalloped outline to the vein network (Troll 1939; Gifford and Foster 1988; Nelson and Dengler 1997) (Fig. 1.2A). In the elongated leaves of many monocots—for example, grasses like maize—vein loops are compressed laterally and are stretched along the length of the leaf, such that midvein and lateral veins seem to be parallel to one another (Troll 1939; Gifford and Foster 1988; Nelson and Dengler 1997) (Fig. 1.2B).

In both eudicots and monocots, polar localization of PIN1 and related proteins at the plasma membrane of epidermal cells at the shoot apex suggests that auxin transport converges toward sites of leaf primordium formation (Benkova et al. 2003; Reinhardt et al. 2003; Scarpella et al. 2006; Carraro et al. 2006; Lee et al. 2008; Bayer et al. 2009; Johnston et al. 2015) (Fig. 1.2C,D). Epidermal “convergence points” of PIN1 polarity correlated with sites of primordium formation become associated with broad inner PEDs that will narrow to sites of midvein formation. Likewise, sites of leaf lateral growth and positions of broad inner PEDs correlated with lateral vein formation seem to be connected to one another through epidermal convergence points of PIN1 polarity at the leaf margin (Hay et al. 2006; Scarpella et al. 2006; Wenzel et al.

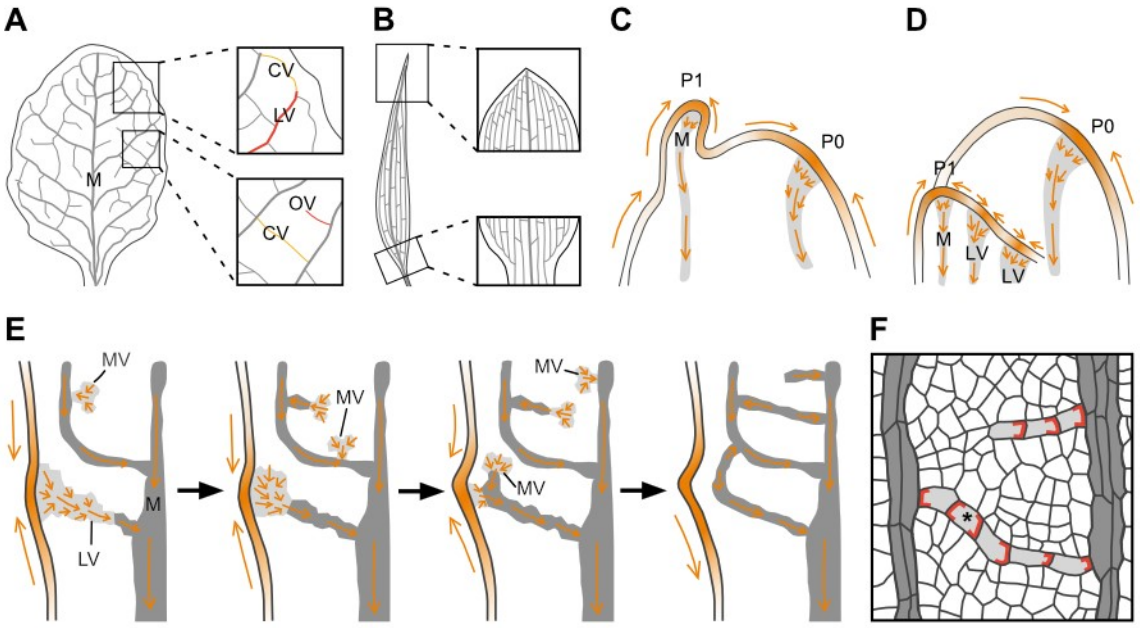

Figure 1.2. Coordination of cell polarity during vein network patterning. (A) In many eudicot leaves, lateral veins (LVs) branch from a single midvein (M); minor veins branch from midvein and lateral veins, and either end freely ("open" veins; OVs; red) or contact other veins ("closed" veins; CVs; yellow); and vein loops form from the fusion of lateral veins (red) and closed minor veins (yellow) (E). (B) In many monocot leaves, vein loops are compressed laterally and are stretched along the length of the leaf, such that midvein and lateral veins seem to be parallel to one another; and midvein and lateral veins are connected laterally by minor veins. (C,D) In both eudicots (C) and monocots (D), polar PIN1 localization in epidermal cells of the shoot apex (orange arrows) suggests auxin transport toward discrete spots (orange) that become associated with sites of leaf primordium formation. Epidermal "convergence points" of PIN1 polarity correlated with sites of primordium formation become associated with broad inner PIN1 expression domains (PEDs hereafter) that will narrow to sites of midvein (M) formation (light gray). Over time, PIN1 localization becomes polarized (orange arrows) in the cells in these broad domains: toward pre-existing PEDs, in the cells along the broad domains' midline; and toward the broad domains' midline, in the cells flanking it. Both the narrowing of broad PEDs and the polarization of PIN1 localization initiate and proceed away from pre-existing PEDs, in which PIN1 localization is polarized. P0 and P1: successive stages of leaf primordium development. (D,E) In both monocots (D) and eudicots (E), polar PIN1 localization in epidermal

cells of the primordium margin (orange arrows) suggests auxin transport toward discrete spots (orange) that become associated with sites of primordium lateral growth. Epidermal convergence points of PIN1 polarity correlated with sites of primordium lateral growth become associated with broad inner PEDs that will narrow to sites of lateral vein (LV) formation (light gray). Over time, PIN1 localization becomes polarized (orange arrows) in the cells in these broad domains: toward pre-existing PEDs (dark gray), in the cells along the broad domains' midline; and toward the broad domains' midline, in the cells flanking it. Both the narrowing of broad PEDs and the polarization of PIN1 localization initiate and proceed away from pre-existing PEDs (dark gray), in which PIN1 localization is polarized (orange arrows). (E) In eudicots, broad inner PEDs correlated with the formation of minor veins (MVs) (light gray) form in contact with pre-existing PEDs (dark gray) within the expanding leaf. Over time, PIN1 localization becomes polarized (orange arrows) in the cells in these broad domains: toward pre-existing PEDs, in the cells along the broad domains' midline; and toward the broad domains' midline, in the cells flanking it. Both the narrowing of broad PEDs and the polarization of PIN1 localization initiate and proceed away from pre-existing PEDs, in which PIN1 localization is polarized (orange arrows). Initially, minor-vein-correlated PEDs contact pre-existing veins at one end only ("open" PEDs), but they can extend to contact other veins at both ends ("closed" PEDs). Open PEDs have a single polarity; closed PEDs have two, opposite polarities, which are coordinated by the formation of a "bipolar" cell: a cell in which PIN1 localization is polarized at both ends (F). Each vein loop form from the fusion of a lateral-vein-correlated PEDs and a minor-vein-correlated closed PEDs. Broad minor-vein-correlated PEDs can gradually disappear instead of narrowing and polarizing. Arrows connect successive stages of leaf development. (F) Polar localization of PIN1 (red) in files of vascular cells (light gray) suggests auxin transport toward pre-existing veins (dark gray; for simplicity, PIN1 expression in pre-existing veins is not shown). In open veins, a single auxin-transport polarity exists; in closed veins, the two opposite polarities are coordinated by a bipolar cell (asterisk): a cell with PIN1 at both ends.

2007) (Fig. 1.2D,E). Inhibition of polar auxin transport or higher auxin levels because of local auxin application reduce spacing of epidermal convergence points of PIN1 polarity and lead to the formation of more closely spaced leaf primordia, and of more and more closely spaced lateral veins, as in *pin1* mutants (Okada et al. 1991; Bennett et al. 1995; Mattsson et al. 1999; Sieburth 1999; Reinhardt et al. 2000; Scarpella et al. 2006; Guenot et al. 2012; Sawchuk et al. 2013; Verna et al. 2015) (Chapter 2).

These observations suggest that a single mechanism controls positioning of leaf primordia at the shoot apex and of midvein and lateral veins in the leaf. This mechanism seems to depend on the positioning of epidermal convergence points of PIN1 polarity, which in turn seems to depend on auxin levels and transport, and is consistent with the hypothesis that broad leaves evolved from branched systems of cylindrical organs with a vein in their center (Beerling and Fleming 2007; Alvarez et al. 2016).

Unlike the broad inner PEDs correlated with the formation of midvein and lateral veins, those correlated with the formation of minor veins in eudicot leaves are not associated with epidermal convergence points of PIN1 polarity; instead, broad inner PEDs correlated with the formation of minor veins form in contact with pre-existing PEDs within the expanding leaf (Scarpella et al. 2006; Wenzel et al. 2007; Marcos and Berleth 2014) (Fig. 1.2E).

Irrespective of whether broad inner PEDs are associated with epidermal convergence points of PIN1 polarity, PIN1 is localized isotropically, or nearly so, to the plasma membrane of the cells in broad inner domains (Carraro et al. 2006; Scarpella et al. 2006; Wenzel et al. 2007; Lee et al. 2008; Marcos and Berleth 2014; Johnston et al. 2015) (Fig. 1.2C–E). Over time, PIN1 localization becomes polarized: toward pre-existing PEDs, in the cells along the broad domains' midline; and toward the broad domains' midline, in the cells flanking it. Furthermore, over time, broad PEDs narrow to sites of vein formation. Both the narrowing of broad PEDs and the polarization of PIN1 localization initiate and proceed away from pre-existing PEDs and are delayed by auxin transport inhibition. Inhibition of polar auxin transport or higher auxin levels, occurring naturally at leaf margin outgrowths or induced experimentally by local direct auxin application, lead to the formation of broader inner PEDs (Aloni et al. 2003; Mattsson et al. 2003; Hay et al. 2006; Scarpella et al. 2006; Wenzel et al. 2007) . Nevertheless, even these broader

PEDs eventually narrow to sites of vein position, and also this narrowing is delayed by auxin transport inhibition.

All these features can be accounted for by the positive feedback between polarization of PIN1 localization and polar auxin transport proposed by the auxin canalization hypothesis (Mitchison 1980a; Mitchison 1981; Sachs 1991a; Sachs 2000; Feugier et al. 2005; Rolland-Lagan and Prusinkiewicz 2005; Fujita and Mochizuki 2006b; Stoma et al. 2008; Bayer et al. 2009; Walker et al. 2013; O'Connor et al. 2014; Cieslak et al. 2015).

Broad inner PEDs associated with the formation of minor veins in eudicot leaves can gradually disappear instead of narrowing and polarizing (Marcos and Berleth 2014) (Fig. 1.2E). This excess of PEDs and reversal of PIN1 expression suggest competition of PEDs for a limiting amount of auxin (Sachs 2003). At any given stage of leaf tissue development, details of PIN1 expression—the number of new PEDs; their shape, size and position; which of these domains will outcompete the others for the limiting amount of auxin—would thus not only depend on positive feedback between polarization of PIN1 localization and polar auxin transport: they would no less depend on chance variation in the local production of auxin; on the number, shape, size and position of pre-existing PEDs; and in their varied efficiency to drain auxin from the tissue. Therefore, the formation of new PEDs would continuously build upon previous ones.

Initially, the broad inner PEDs associated with the formation of minor veins contact pre-existing PEDs at only at one of their two ends (“open” PEDs), but they can extend to contact other PEDs at both their ends (“closed” PEDs) (Scarpella et al. 2006; Wenzel et al. 2007; Marcos and Berleth 2014). The formation of such “closed” PEDs is promoted by auxin transport inhibition (Mattsson et al. 1999; Sieburth 1999; Verna et al. 2015) (Chapter 2), suggesting that contacts are favored, or occur exclusively, between PEDs that have yet to differentiate high polar-auxin-transport capacity or auxin-transport-mediated auxin levels.

Within narrow PEDs, PIN1 localization suggests auxin transport towards pre-existing PEDs (Scarpella et al. 2006; Wenzel et al. 2007; Marcos and Berleth 2014) (Fig. 1.2D–F). In open PEDs, PIN1 localization is polarized to the side of the cells that faces the pre-existing PEDs contacted by the open PED, thus resulting in a single polarity. Also in closed PEDs, PIN1 is polarized to the side of the cells that faces the pre-existing PEDs contacted by the closed PEDs. However, because both ends of the closed PEDs contact pre-existing PEDs, the closed PEDs is

composed of two segments, each with a single polarity, opposite to that of the other. The two opposite polarities are coordinated by the formation of a "bipolar" cell: a cell in which PIN1 localization is polarized at both ends.

In eudicot leaves, individual loops form from the fusion of a lateral-vein-correlated PED, which is associated with an epidermal convergence point of PIN1 polarity, and a minor-vein-correlated closed PED, which is *not* associated with an epidermal convergence point of PIN1 polarity (Scarpella et al. 2006; Wenzel et al. 2007) (Fig. 1.2A,E).

It is currently unknown whether PIN1 expression and localization behave during the formation of minor veins and loops in monocot leaves as they do in eudicot leaves; however, computational modeling suggests that, provided different leaf growth patterns, the same vein-patterning mechanism can account for the different vein networks of monocot and eudicot leaves (Runions et al. 2005; Fujita and Mochizuki 2006a).

In conclusion, available evidence suggests that, as vascular strand formation in response to auxin application, vein network formation in normal leaf development is an expression of coordination of cell polarity, many aspects of which are consistent with computational simulations of the auxin canalization hypothesis (Mitchison 1980a; Mitchison 1981; Sachs 1991a; Sachs 2000; Feugier et al. 2005; Rolland-Lagan and Prusinkiewicz 2005; Feugier and Iwasa 2006; Fujita and Mochizuki 2006b; Stoma et al. 2008; Bayer et al. 2009; Smith and Bayer 2009; Alim and Frey 2010; Wabnik et al. 2010; Walker et al. 2013; Lee et al. 2014; Cieslak et al. 2015; Abley et al. 2016). Nevertheless, in its most basic form, the auxin canalization hypothesis predicts the formation of networks of "open" veins (i.e. veins that contact other veins at only one of their two ends) (Mitchison 1980a; Feugier et al. 2005; Rolland-Lagan and Prusinkiewicz 2005; Fujita and Mochizuki 2006b). However, the formation of "closed" veins (i.e. veins that contact other veins at both their ends) could result from vein meeting at points of maximum auxin levels (Dimitrov and Zucker 2006) or from repeated shifts in the locations of auxin production (Sachs 1975, 1989; Aloni et al. 2003; Rolland-Lagan and Prusinkiewicz 2005; Runions et al. 2005). Both hypotheses are consistent with the observation of bipolar cells, and further predict maximum auxin levels in these cells; however, this prediction remains to be tested experimentally.

1.4 Control of coordinated cell polarity during vein network patterning

Auxin transport inhibition or higher auxin levels delay coordination of cell polarity during vein formation; however, given enough time, eventually cell polarity becomes coordinated even under those conditions (Hay et al. 2006; Scarpella et al. 2006; Wenzel et al. 2007). By contrast, mutation of specific Arabidopsis genes seems to interfere, to varying extents, with coordination of cell polarity during vein formation.

Mutants in *FORKED1*/*VASCULAR-NETWORK3-BINDING PROTEI*N often fail to form bipolar cells (Steynen and Schultz 2003; Naramoto et al. 2009; Hou et al. 2010). This reduced ability to coordinate cell polarity along closed PEDs often leads to their "opening" and thus to vein networks with very few closed veins (Fig. 1.3A,B). Nevertheless, these mutants are still able to coordinate cell polarity along open PEDs, which have a single polarity.

More severe loss-of-function of the same pathway in the *vascular network3*/*scarface* single mutant or in the *cotyledon vascular pattern2* (*cvp2*); *cvp2-like1* double mutant leads to the inability to coordinate cell polarity even along open PEDs (Carland et al. 1999; Deyholos et al. 2000; Koizumi et al. 2000; Carland and Nelson 2004; Koizumi et al. 2005; Scarpella et al. 2006; Sieburth et al. 2006; Carland and Nelson 2009; Naramoto et al. 2009). The inability of these mutants to coordinate cell polarity along PEDs leads to cessation of PIN1 expression in some of the cells in a PED before any of the cells in the domain become coordinately polarized (Scarpella et al. 2006; Naramoto et al. 2009). The cells that cease to express PIN1 differentiate into nonvascular cells, while the remaining "fragments" of PEDs differentiate into isolated stretches of vascular cells (Fig. 1.3C). Nevertheless, these vein "fragments" still form along the paths where continuous veins would form in wild type (Fig. 1.3A,C).

Defects are even more severe in mutants of *EMBRYO DEFECTIVE30*/*GNOM* (*GN* hereafter) (Mayer et al. 1993; Shevell et al. 1994; Busch et al. 1996). In *gn* embryos, individual cells localize PIN1 polarly, but they seem to have entirely lost the ability to coordinate cell polarity between them (Steinmann et al. 1999), leading to shapeless clusters of disconnected and

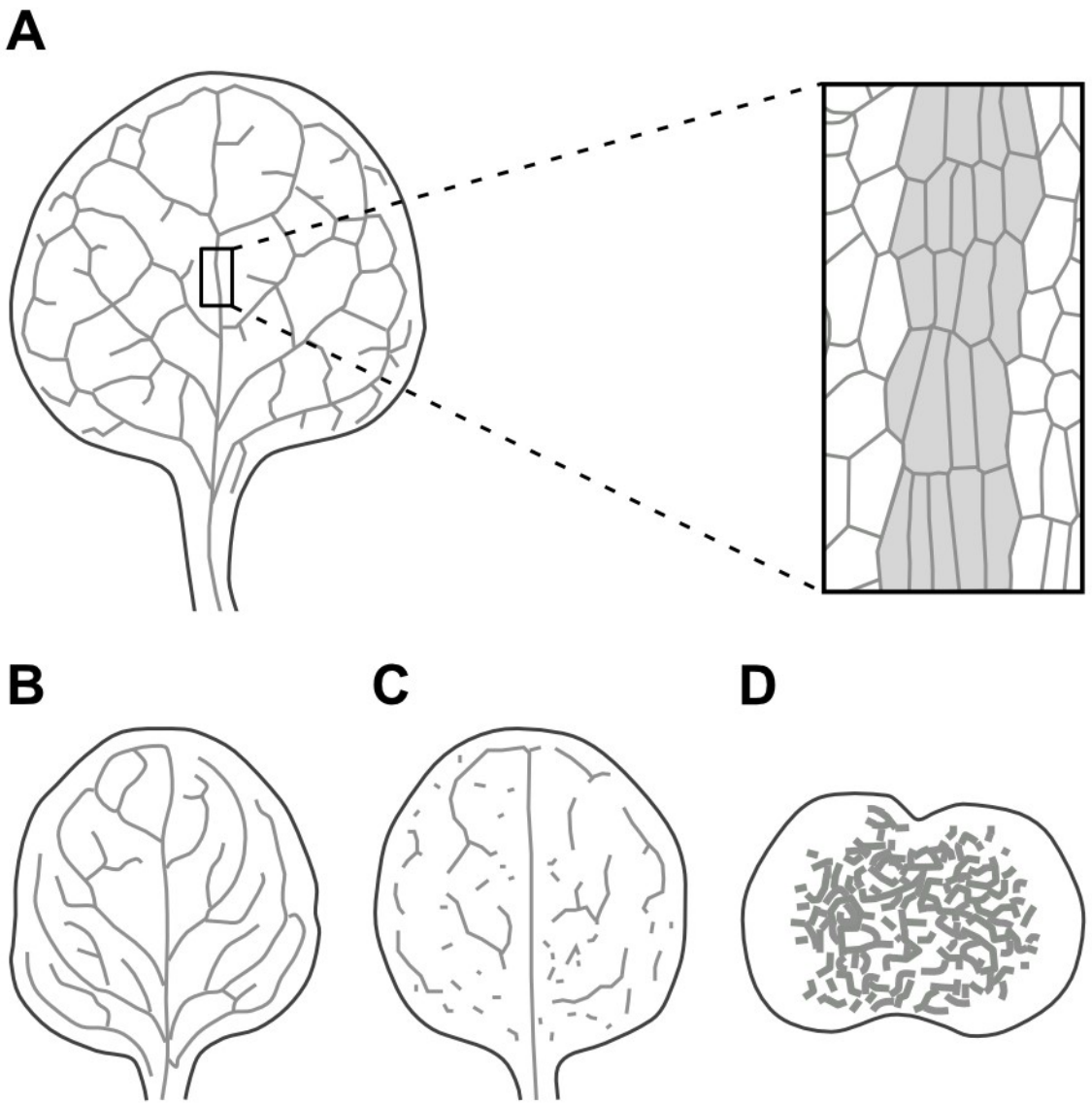

Figure 1.3. Control of coordinated cell polarity during vein network patterning. (A) In wild-type leaves of Arabidopsis, the ability to coordinate cell polarity during vein network patterning leads to networks of continuous veins that are frequently closed and in which the axis of the vascular cells is aligned with the axis of the vein. (B–D) Progressive reduction in the ability to coordinate cell polarity during vein network patterning leads to vein networks with very few closed veins, as in *forked1*/*vascular-network3-binding protein* mutant leaves (B); vein networks in which vein fragments form along paths defined by initially continuous PIN1-expression-domains, as in *vascular network3*/*scarface* mutant leaves (C); or shapeless clusters of disconnected and randomly oriented vascular cells, as in *emb30*/*gnom* mutant cotyledons (D).

randomly oriented vascular cells at the center of the seedling's cotyledons (Mayer et al. 1993; Steinmann et al. 1999; Geldner et al. 2004) (Fig. 1.3D).

Based on their molecular identity and cellular localization, all these proteins have been proposed to localize or retain PIN1 to the plasma membrane, polarize PIN1 localization at the plasma membrane or maintain such polar localization [e.g., (Geldner et al. 2003; Koizumi et al. 2005; Sieburth et al. 2006; Kleine-Vehn et al. 2008; Carland and Nelson 2009; Naramoto et al. 2009; Naramoto et al. 2010; Prabhakaran Mariyamma et al. 2017)]. However, it remains unclear how loss of such proposed function fails to affect the plasma-membrane localization of PIN1 or its polarization, and instead affect the *coordination* of such cell polarity.

1.5 Beyond coordination of PIN1 polar localization

The thought implicit in most of the literature on coordination of cell polarity in plants is that the polar localization of PIN1 and related proteins is not only a marker of cell polarity but is essential to cell polarity and its coordination. And indeed, this seems to be suggested by the most severe phenotype classes of *pin* multiple mutants (Friml et al. 2003). However, evidence is also available that seems to suggest that though PIN1 and related proteins contribute to cell polarity and its coordination, they and their polar localization are not essential to or sufficient for it (Fischer et al. 2006; Bilsborough et al. 2011; Guenot et al. 2012; Kierzkowski et al. 2013). Finally, yet other evidence is consistent with the possibility that PIN1 and related proteins are only a readout of an upstream polarity signal (Heisler et al. 2010). Future research will have to reconcile these seemingly contrasting pieces of evidence if we are to understand how cell polarity is coordinated in plants.

1.6. Scope and outline of the thesis

The evidence discussed above suggests that the formation of leaf vein networks is an expression of coordination of cell polarity that is controlled by auxin transport. The scope of my Ph.D.

thesis was to understand the contribution of auxin transport to vein network formation in Arabidopsis leaves.

Leaf vein networks are characterized by reproducible features such as the presence of lateral veins that branch from a single midvein and connect to distal veins to form loops; of minor veins that branch from midvein and loops and connect to other veins to form a mesh; and of loops and minor veins that curve near the leaf margin to lend a scalloped outline to the vein network. Features such as these are so reproducible that they are used to define species [e.g. (Klucking 1995)]; by contrast, features such as the number of veins and their connectedness are variable.

In Chapter 2 (Verna et al. 2015), we asked whether PIN-mediated auxin transport, which is known to control reproducible features of leaf vein networks (Okada et al. 1991; Mattsson et al. 1999; Bilsborough et al. 2011; Sawchuk et al. 2013), also controlled their variable features. We found that auxin transport mediated by PIN1, PIN5, PIN6 and PIN8 controls the formation of leaf veins and their connection into networks; therefore, our results suggest that PIN-mediated auxin transport controls both reproducible and variable features of leaf vein networks.

PIN1 is the only known gene to be nonredundantly required for both the reproducible features of leaf vein networks and their variable ones. The PIN1 protein is expressed in all the cells of the leaf at early stages of tissue development; over time, however, epidermal expression becomes restricted to the basal-most cells and inner expression becomes restricted to files of vascular precursor cells (Galweiler et al. 1998; Benkova et al. 2003; Reinhardt et al. 2003; Heisler et al. 2005; Petrasek et al. 2006; Scarpella et al. 2006; Wenzel et al. 2007; Bayer et al. 2009; Sawchuk et al. 2013; Marcos and Berleth 2014).

In Chapter 3, we sought to understand the cis-regulation of *PIN1* function in patterning of leaf vein networks. We found that the expression of PIN1 that is required for vein network patterning depends on the 205-bp region of the *PIN1* promoter from -699 to -495, which contains conserved putative binding-sites for transcription factors of the MYELOBLASTOMA and DNA-BINDING WITH ONE FINGER families.

The evidence discussed above also suggests that auxin controls coordination of cell polarity and derived polar-vein-formation and that such inductive and orienting property of auxin

strictly depends on the function of *PIN1* and possibly other *PIN* genes. How auxin precisely controls coordination of cell polarity and derived polar-vein-formation is unclear, but the current hypothesis is that the GN guanine-nucleotide exchange factor for ADP-rybosilation-factor GTPases, which regulates vesicle formation in membrane trafficking, coordinates the cellular localization of PIN1 and possibly other PIN proteins between cells (Steinmann et al. 1999); the resulting cell-to-cell, polar transport of auxin would propagate cell polarity across tissues, and control polar developmental processes such as vein formation (Sachs 1991a).

In Chapter 4, we tested this hypothesis. We found that auxin-induced polar-vein-formation occurs in the absence of PIN proteins or any known intercellular auxin transporter; that the auxin-transport-independent vein-patterning activity relies on auxin signaling; and that a GN-dependent coordinating signal acts upstream of both auxin transport and signaling.

Finally, in Chapter 5, I propose and discuss two hypotheses on the upstream regulators of PIN1 functional expression in leaf vein patterning.

CHAPTER 2: CONTROL OF VEIN NETWORK TOPOLOGY BY AUXIN TRANSPORT

2.1 Introduction

Water, signals and nutrients are transported within and between the organs of most multicellular organisms by tissue networks. What controls the formation of tissue networks is thus a central question in biology. In animals, many of these networks are stereotyped (Lu and Werb 2008); by contrast, the vein networks of plant leaves are both reproducible and variable (Sachs 1989; Berleth et al. 2000). Consider, for example, the vein network of an *Arabidopsis thaliana* leaf (Telfer and Poethig 1994; Nelson and Dengler 1997; Kinsman and Pyke 1998; Candela et al. 1999; Mattsson et al. 1999; Sieburth 1999; Steynen and Schultz 2003): lateral veins branch from a single midvein and connect to distal veins to form loops; minor veins branch from midvein and loops, and connect to other veins to form a mesh; and loops and minor veins curve near the leaf margin to lend a scalloped outline to the vein network. Patterning features of the vein network such as these are reproducible from leaf to leaf—so much so that they are used as a taxonomic characteristic [e.g., (Klucking 1995)]. By contrast, topological features of the vein network are variable (Kinsman and Pyke 1998; Candela et al. 1999; Steynen and Schultz 2003; Kang and Dengler 2004; Scarpella et al. 2004; Sawchuk et al. 2007): the number of veins differs from leaf to leaf, and whether a vein will connect to another vein on both ends or one end will terminate free of contact with other veins is unpredictable; this is always so for minor veins, but even loops can occasionally fail to connect to other veins at one end.

While no evidence is available that associates patterning features of vein networks with the networks' functional traits, abundant evidence exists that associates functional traits of vein networks with the networks' topological features [reviewed in (Roth-Nebelsick et al. 2001; Sack and Scoffoni 2013)]; yet our knowledge of the signals that control vein network topology is limited, and most of such signals also control vein network patterning [e.g., (Koizumi et al. 2000;

Cheng et al. 2006; Sieburth et al. 2006; Petricka et al. 2008; Donner et al. 2009; Garrett et al. 2012; Krogan et al. 2012)]. One of very few exceptions (Casson et al. 2002; Clay and Nelson 2005; Baima et al. 2014) is the control of vein network topology by intracellular transport of the plant signal auxin suggested by genetic evidence: leaves of double mutants in the genes encoding the endoplasmic-reticulum (ER)-localized PIN-FORMED6 (PIN6) and PIN8 auxin transporters of Arabidopsis (Petrasek et al. 2006; Mravec et al. 2009; Bosco et al. 2012; Ding et al. 2012; Bender et al. 2013; Cazzonelli et al. 2013; Sawchuk et al. 2013) have higher vein-density (Sawchuk et al. 2013); the vein density defect of *pin6*;*pin8* leaves is suppressed by mutation of the gene encoding the ER-localized PIN5 auxin transporter (Mravec et al. 2009; Sawchuk et al. 2013; Ganguly et al. 2014); overexpression of *PIN6* or *PIN8* results in lower vein-density, and overexpression of *PIN5* results in the opposite defect (Sawchuk et al. 2013).

In contrast to the control of vein network topology by intracellular auxin transport, no genetic evidence is available in support of a role for the cell-to-cell transport of auxin in control of vein network topology; yet such a role seems to be suggested by imaging and inhibitor studies. Expression of the PIN1 auxin efflux protein (Galweiler et al. 1998; Petrasek et al. 2006) is initiated in broad domains of leaf inner cells that become gradually restricted to files of vascular precursor cells in contact with pre-existing, narrow PIN1 expression domains (Benkova et al. 2003; Reinhardt et al. 2003; Heisler et al. 2005; Scarpella et al. 2006; Wenzel et al. 2007; Bayer et al. 2009; Sawchuk et al. 2013; Marcos and Berleth 2014). Within broad expression domains, PIN1 is localized isotropically—or nearly so—at the plasma membrane (PM) of leaf inner cells. As expression of PIN1 becomes gradually restricted to files of vascular precursor cells, PIN1 localization becomes polarized to the side of the PM facing the pre-existing, narrow PIN1 expression domains with which the narrowing domains are in contact. Initially, PIN1 expression domains are in contact with pre-existing domains at one end only, but they can eventually become connected to other PIN1 expression domains at both ends. Inhibitors of cellular auxin efflux delay the restriction of PIN1 expression domains and the polarization of PIN1 localization (Scarpella et al. 2006; Wenzel et al. 2007), and induce the formation of more veins (Mattsson et al. 1999; Sieburth 1999).

The polar localization of PIN1 to the PM of vascular cells—toward pre-existing veins and ultimately the root tip—is thought to determine the polarity of intercellular auxin transport

(Wisniewska et al. 2006): from the immature shoot-organs, where auxin is produced in large amounts (Thimann and Skoog 1934; Avery 1935), to the roots (Went 1928; Wangermann 1974). By contrast, the directions of ER-PIN-mediated intracellular auxin-transport are unclear. Available evidence suggest that PIN5 transports auxin from the cytoplasm to the ER lumen (Mravec et al. 2009; Sawchuk et al. 2013), and that PIN6 and PIN8 transport it from the ER lumen to the cytoplasm or the nucleus (Bosco et al. 2012; Ding et al. 2012; Bender et al. 2013; Cazzonelli et al. 2013; Sawchuk et al. 2013), the envelope of which is continuous with the ER membrane (Graumann and Evans 2011; Oda and Fukuda 2011); alternatively, PIN5, PIN6 and PIN8 could transport in the same direction but have different affinities for different auxins with different developmental functions [e.g., (Ludwig-Muller 2012)].

Here we asked whether PIN1-mediated intercellular auxin-transport controlled vein network topology and, if so, whether it interacted with the control of vein network topology by ER-PIN-mediated intracellular auxin-transport. To address this question, we introduced descriptors of vein network topology that enable quantification of vein number, connectedness and continuity, and combined these topological descriptors with cellular imaging and molecular genetic analysis to quantify the contribution of *PIN1*, *PIN5*, *PIN6* and *PIN8* to vein network topology. We derived cellular expression and genetic interaction maps of these genes in vein network formation, and suggest that the interaction between PIN1-mediated intercellular auxin-transport and ER-PIN-mediated intracellular auxin-transport controls the formation of veins and their connection into networks.

2.2 Results and discussion

2.2.1 Expression of *PIN1*, *PIN5*, *PIN6* and *PIN8* during leaf development

Veins form sequentially during Arabidopsis leaf development: the formation of the midvein is followed by the formation of the first loops of veins (“first loops”), which in turn is followed by

the formation of second loops and minor veins (Mattsson et al. 1999; Sieburth 1999; Kang and Dengler 2004; Scarpella et al. 2004) (Fig. 2.1A–C).

Two distinct auxin-transport pathways have overlapping functions in control of Arabidopsis vein-network patterning (Sawchuk et al. 2013). One pathway—mediated by the PM-localized PIN1 protein—transports auxin intercellularly (Galweiler et al. 1998; Petrasek et al. 2006); the other pathway—mediated by the ER-localized PIN5, PIN6 and PIN8 proteins—transports auxin intracellularly (Petrasek et al. 2006; Mravec et al. 2009; Bosco et al. 2012; Ding et al. 2012; Bender et al. 2013; Cazzonelli et al. 2013; Sawchuk et al. 2013; Ganguly et al. 2014).

Consistent with their role in control of vein network patterning (Mattsson et al. 1999; Bilsborough et al. 2011; Guenot et al. 2012; Sawchuk et al. 2013), *PIN1* (AT1G73590), *PIN6* (AT1G77110) and *PIN8* (AT5G15100) are expressed in developing veins, though with different dynamics: expression of *PIN1* and *PIN6* is initiated in broad domains of leaf inner cells, domains that over time become restricted to single files of vascular precursor cells (Scarpella et al. 2006; Wenzel et al. 2007; Sawchuk et al. 2013; Marcos and Berleth 2014) (Fig. 2.1D–I); by contrast, *PIN8* expression is restricted from early on to single files of leaf vascular cells (Sawchuk et al. 2013) (Fig. 2.1J–L). It remains unclear, however, whether these different dynamics of *PIN* expression comprise onset of *PIN* expression at different stages of leaf development.

To address this question, we compared expression of *PIN1*, *PIN6* and *PIN8* in first leaves 2, 3 and 4 days after germination (DAG). To visualize *PIN* expression, we used functional translational fusions (*PIN* promoter driving expression of the respective PIN:reporter fusion protein) (Benkova et al. 2003; Gordon et al. 2007; Sawchuk et al. 2013) or transcriptional fusions (*PIN* promoter driving expression of a reporter protein) (Sawchuk et al. 2013) (Table 2.1); whenever we used transcriptional fusions, their expression matched that of the respective, functional translational fusions (Sawchuk et al. 2013) (Fig. 2.2), suggesting that those *PIN* promoters contain all the regulatory elements required for functional expression of the respective genes.

While expression of a PIN1::PIN1:GFP translational fusion (*PIN1* promoter driving expression of PIN1:GFP fusion protein) and of a PIN6::YFPnuc transcriptional fusion (*PIN6* promoter driving expression of a nuclear yellow fluorescent protein) was already visible 2 DAG

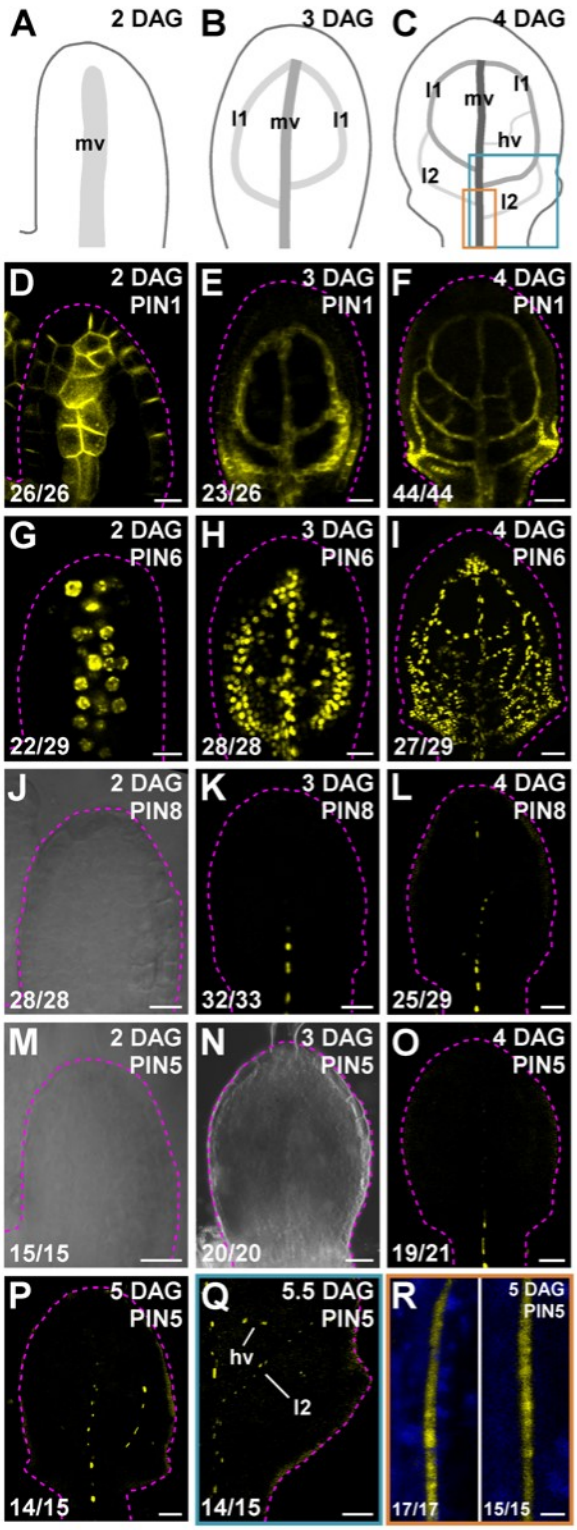

Figure 2.1. Expression of *PIN1*, *PIN5*, *PIN6* and *PIN8* of Arabidopsis during first leaf development. (A–R) Top right: leaf age in days after germination (DAG) and expression-reported gene (D–R). (D–R) Bottom left: reproducibility index. (A–C) Midvein, loops and minor

veins form sequentially during leaf development (Mattsson et al. 1999; Sieburth 1999; Kang and Dengler 2004; Scarpella et al. 2004); increasingly darker gray depicts progression through successive stages of vein development. Boxes in (C) illustrate positions of close-ups in (Q) (cyan) and (R) (orange). (D–R) Confocal laser scanning microscopy with (J,M,N) or without (D–I,K,L,O-R) transmitted light; first leaves. Yellow: expression of PIN1::PIN1:GFP (D-F), PIN6::YFPnuc (G–I), PIN8::YFPnuc (J–L), PIN5::YFPnuc (M–Q), PIN5::PIN5:GFP^{MGS} (R, left) or PIN5::PIN5:GFP^{AG} (R, right). Blue: autofluorescence (R). Dashed magenta line delineates leaf primordium outline. hv, minor veins; l1, first loop; l2, second loop; mv, midvein. Bars: (D,G,J,M,R) 10 μm; (E,H,K,N) 25 μm; (F,I,L,O–Q) 50 μm.

Table 2.1. Origin and nature of lines.

Line	Origin/Nature
PIN1::PIN1:GFP	Benkova et al. 2003
PIN1:PIN1:CFP	Gordon et al. 2007; ABRC; introgressed into Col-0
PIN6::YFPnuc	Sawchuk et al. 2013
PIN6::CFPnuc	Transcriptional fusion of *PIN6* (AT1G77110; -3784 to -1; primers: 'PIN6 prom SalI F' and 'PIN6 prom BamHI R') to ECFP:3xNLS (Clontech Laboratories Inc.)
PIN6::PIN6:GFP^{MGS}	Sawchuk et al. 2013
PIN6::PIN6:GFP^{RLB}	Bender et al. 2013
PIN8::YFPnuc	Sawchuk et al. 2013
PIN8::PIN8:GFP^{MGS}	Sawchuk et al. 2013
PIN8::PIN8:GFP^{ZD}	Ding et al. 2012
PIN5::YFPnuc	Transcriptional fusion of *PIN5* (AT5G16530; -3279 to -3; primers: 'PIN5 SpeI KpnI transc forw' and 'PIN5 AgeI transc rev') to EYFP:3xNLS (Clontech Laboratories Inc.)
PIN5::PIN5:GFP^{MGS}	Translational fusion of *PIN5* (AT5G16530; -4311 to +3606; primers: 'PIN5 extra prom XhoI forw' and 'PIN5 extra prom SalI rev', 'PIN5 prom XhoI forw' and PIN5 4991 BamHI rev', 'PIN5 4992 XbaI forw' and 'PIN5 UTR SacI rev', 'PIN5 extra UTR SmaI forw' and 'PIN5 extra UTR SacI rev') to EGFP (Clontech Laboratories Inc.; insertion at +1712 of *PIN5*; primers: 'EGFP BamHI forw' and 'EGFP XbaI rev'); reverts the cotyledon phenotype of *pin1*;*5*;*6*;*8* to that of *pin1*;*6*;*8*
PIN5:PIN5:GFP^{AG}	Ganguly et al. 2014
DR5rev::YFPnuc	Heisler et al. 2005; Sawchuk et al. 2013
pin1-1	Goto et al. 1987; Galweiler et al. 1998; Sawchuk et al. 2013; WT at the *TTG1* (AT5G24520) locus; contains a G-to-A transition at position +431, resulting in a stop codon after amino acid 143
pin5-4	Mravec et al. 2009
pin6	Sawchuk et al. 2013
pin8-1	Bosco et al. 2012
RPS5A::PIN1	Kind gift of P. Dhonukshe

RPS5A::PIN6	Sawchuk et al. 2013
MP::PIN6	Sawchuk et al. 2013
MP::PIN8	Sawchuk et al. 2013
MP::PIN5	Sawchuk et al. 2013

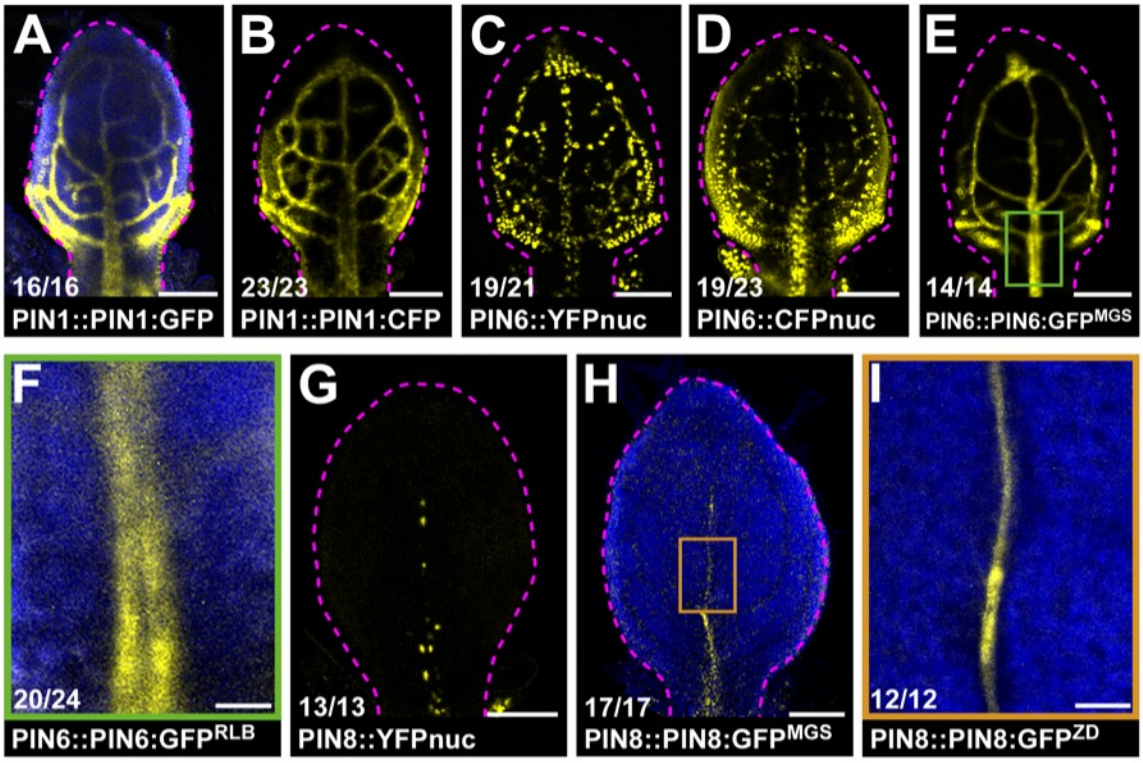

Figure 2.2. Expression of *PIN1*, *PIN6* and *PIN8* in Arabidopsis first leaves. (A–H) Confocal laser scanning microscopy; first leaves 4 days after germination. Bottom left: reproducibility index and reporter identity. Yellow: expression of PIN1::PIN1:GFP (A), PIN1::PIN1:CFP (B), PIN6::YFPnuc (C), PIN6::CFPnuc (D), PIN6::PIN6:GFP^{MGS} (E), PIN6::PIN6:GFP^{RLB} (F), PIN8::YFPnuc (G), PIN8::PIN8:GFP^{MGS} (H), or PIN8::PIN8:GFP^{ZD} (I). Blue: autofluorescence (A,F,H,I). Dashed magenta line delineates leaf primordium outline. Boxes in (E) and (H) illustrate positions of close-ups in (F) and (I), respectively. Bars: (A–E,G,H) 100 μm; (F,I) 20 μm.

(Fig. 2.1D,G), expression of PIN8::YFPnuc was first detected 3 DAG (Fig. 2.1J,K), suggesting that *PIN8* expression is initiated after the onset of expression of both *PIN1* and *PIN6*.

PIN5 (AT5G16530) is expressed in veins of mature leaves (Mravec et al. 2009; She et al. 2010), but its expression during leaf development is unknown. Transcriptional and translational fusions of *PIN5* are expressed in similar domains (Mravec et al. 2009; She et al. 2010; Ganguly et al. 2014), suggesting that the *PIN5* promoter contains all the regulatory elements required for *PIN5* expression. Thus, to visualize *PIN5* expression during leaf development, we imaged PIN5::YFPnuc expression in first leaves 2, 3, 4, 5 and 5.5 DAG.

Expression of PIN5::YFPnuc was first detected in the midvein of 4-DAG leaves (Fig. 2.1M–O); at 5 DAG, PIN5::YFPnuc was additionally expressed in first loops (Fig. 2.1P), and at 5.5 DAG PIN5::YFPnuc was additionally expressed in second loops and minor veins (Fig. 2.1Q). Thus our results suggest that *PIN5* expression is initiated after *PIN8* expression (Fig. 2.1K,N,O) and that, as *PIN8*, *PIN5* is expressed from early on in single files of leaf vascular cells (Fig. 2.1K,L,O–Q).

Expression of *PIN5* in single files of leaf vascular cells—suggested by PIN5::YFPnuc expression—was supported by expression of two functional (Table 2.1) (Ganguly et al. 2014) PIN5::PIN5:GFP translational fusions (Fig. 2.1R).

2.2.2 Expression of *PIN1*, *PIN5*, *PIN6* and *PIN8* in leaf vascular cells

Because *PIN1*, *PIN5*, *PIN6* and *PIN8* are all expressed in developing veins (Fig. 2.1), we asked whether these genes were expressed in the same vascular cells. To address this question, we imaged pairwise combinations of fluorescent reporters of *PIN1*, *PIN5*, *PIN6* and *PIN8* in midvein cells of 4-DAG first leaves—where these genes are expressed (Fig. 2.1F,I,L,O)—and quantified reporter coexpression.

In none of the 20 analyzed leaves coexpressing PIN5::YFPnuc and PIN6::CFPnuc (*PIN6* promoter driving expression of a nuclear cyan fluorescent protein) were cells expressing PIN5::YFPnuc ever on the same plane as cells expressing PIN6::CFPnuc: cells expressing

PIN5::YFPnuc were located ventrally, while cells expressing PIN6::CFPnuc were located dorsally (Fig. 2.3A–C). Likewise, in none of the 20 analyzed leaves coexpressing PIN8::YFPnuc and PIN6::CFPnuc were cells expressing PIN8::YFPnuc ever on the same plane as cells expressing PIN6::CFPnuc: cells expressing PIN8::YFPnuc were located ventrally, while cells expressing PIN6::CFPnuc were located dorsally (Fig. 2.3D–F). And though cells expressing PIN5::YFPnuc or PIN8::PIN8:GFP^{MGS} were both on the same ventral plane (Fig. 2.3G–I), only less than 3% of the cells expressing either reporter expressed both (Fig. 2.3S).

Approximately 95% of PIN5::YFPnuc-expressing cells expressed PIN1::PIN1:GFP, but only ~25% of the PIN1::PIN1:GFP-expressing cells that were on the same ventral plane as cells expressing PIN5::YFPnuc expressed this reporter (Fig. 2.3J–L,S). Likewise, ~90% of PIN8::YFPnuc-expressing cells expressed PIN1::PIN1:GFP, but only ~25% of the PIN1::PIN1:GFP-expressing cells that were on the same ventral plane as cells expressing PIN8::YFPnuc expressed this reporter (Fig. 2.3M–O,S). Finally, consistent with previous observations (Sawchuk et al. 2013), ~95% of PIN6::YFPnuc-expressing cells expressed PIN1::PIN1:GFP, and ~75% of the PIN1::PIN1:GFP-expressing cells that were on the same dorsal plane as cells expressing PIN6::YFPnuc expressed this reporter (Fig. 2.3P–S).

Thus our results suggest that *PIN5*, *PIN6* and *PIN8* are expressed in mutually exclusive domains of leaf vascular cells, and that the *PIN1* cellular-expression domain overlaps with—but extends beyond—the *ER-PIN* cellular-expression domain.

2.2.3 Unique and redundant functions of *PIN1*, *PIN5*, *PIN6* and *PIN8* in control of vein network topology

PIN1, *PIN5*, *PIN6* and *PIN8* control vein network patterning (Mattsson et al. 1999; Bilsborough et al. 2011; Guenot et al. 2012; Sawchuk et al. 2013); we asked what their functions are in control of vein network topology.

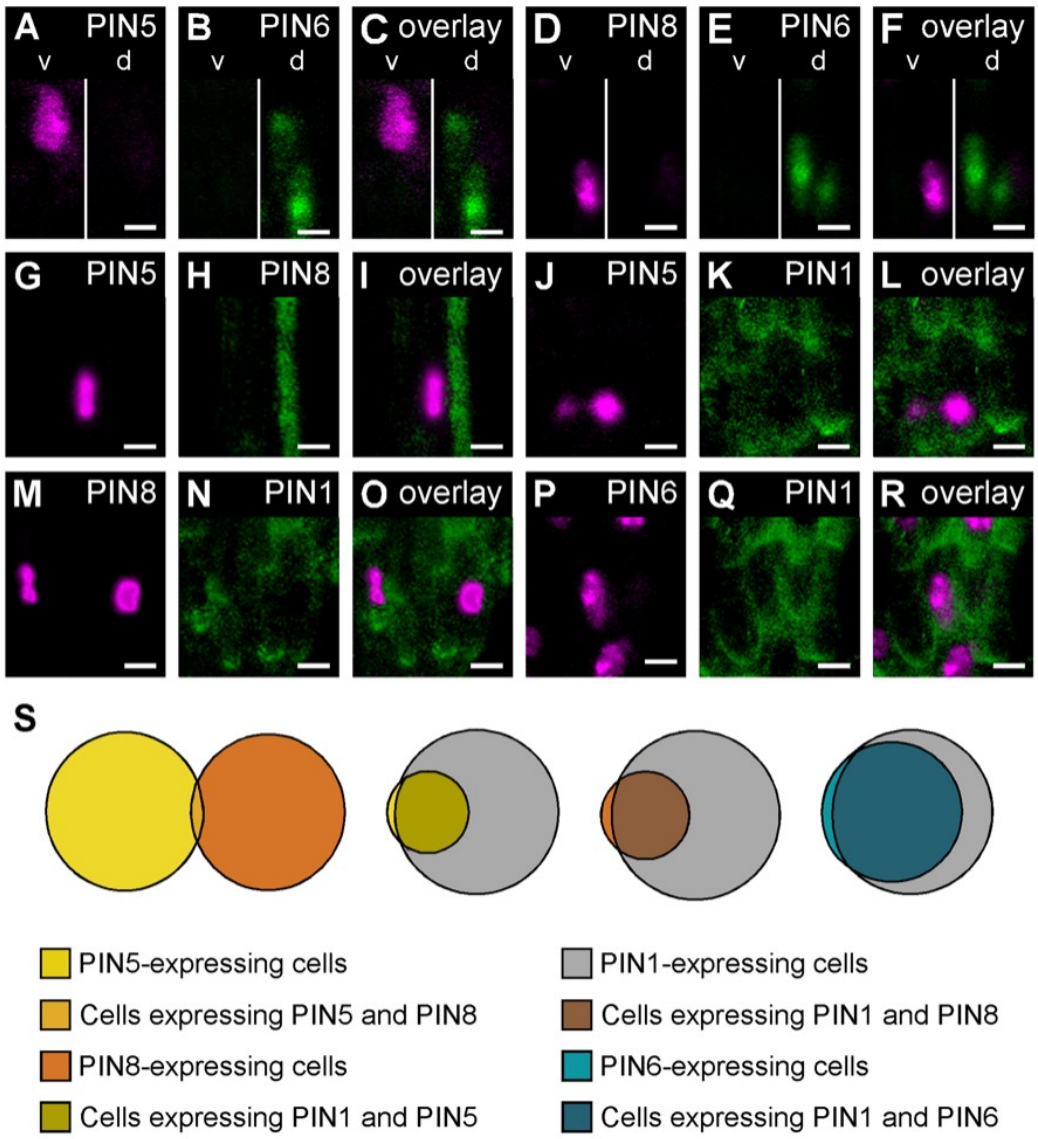

Figure 2.3. Expression of *PIN1*, *PIN5*, *PIN6* and *PIN8* in leaf vascular cells. (A–R) Top right: expression-reported gene. Confocal laser scanning microscopy; first leaves. (A–R) Expression of PIN5::YFPnuc (A,G,J), PIN6::CFPnuc (B,E), PIN8::YFPnuc (D,M), PIN8::PIN8:GFP^{MGS} (H), PIN1::PIN1:GFP (K,N,Q), PIN6::YFPnuc (P), and respective overlays (C,F,I,L,O,R). (S) Proportional Venn diagrams of percentage of cells expressing fluorescent reporters in 25-µm-by-25-µm midvein regions of 4-day-old first leaves (1 region per midvein) in different pairwise combinations of reporters. Sample population sizes: PIN5::YFPnuc;PIN8::PIN8:GFP^{MGS}, 40 leaves (41 PIN5::YFPnuc-expressing cells; 39 PIN8::PIN8:GFP^{MGS}-expressing cells); PIN5::YFPnuc;PIN1::PIN1:GFP, 26 leaves (30

PIN5::YFPnuc-expressing cells; 119 PIN1::PIN1:GFP-expressing cells); PIN8::YFPnuc;PIN1::PIN1:GFP, 25 leaves (34 PIN8::YFPnuc-expressing cells; 122 PIN1::PIN1:GFP-expressing cells); PIN6::YFPnuc;PIN1::PIN1:GFP, 31 leaves (127 PIN6::YFPnuc-expressing cells; 174 PIN1::PIN1:GFP-expressing cells). d, dorsal focal plane; v, ventral focal plane. Bars: (A–R) 5 μm.

To characterize vein network topology, we derived (see Methods and Fig. 2.15 for details) and used three descriptors based on numerical graph invariants: a cardinality index, a continuity index and a connectivity index.

The cardinality index is a proxy for the number of "veins" (i.e. stretches of vascular elements that contact other stretches of vascular elements at least at one of their two ends) in a network (Fig. 2.4A).

The continuity index quantifies how close a vein network is to a network with the same number of veins but in which at least one end of each "vein fragment" (i.e. a stretch of vascular elements that are free of contact with other stretches of vascular elements) contacts a vein. The continuity index ranges from 0—for a network of sole vein fragments—to 1—for a network without vein fragments (Fig. 2.4A).

The connectivity index quantifies how close a vein network is to a network with the same number of veins but in which both ends of each vein or vein fragment contact other veins. The connectivity index ranges from 0—for a network of "open" veins (i.e. veins that contact vein fragments or other veins only at one end)—to 1—for a network of "closed" veins (i.e. veins that contact vein fragments or other veins at both ends) (Fig. 2.4A).

Though the number of veins in a leaf is variable and it is unpredictable whether a developing vein will remain open at maturity (Kinsman and Pyke 1998; Candela et al. 1999; Steynen and Schultz 2003; Kang and Dengler 2004; Scarpella et al. 2004; Sawchuk et al. 2007), the cardinality and connectivity indices of vein networks in different populations of WT leaves grown in identical conditions were reproducible (Figs. 2.4,2.6,2.11 and 2.13). This observation suggests that while the outcome of vein formation events is unpredictable for single veins, it is predictable—within the limits of statistical variation—for networks of veins. Thus—as for non-stereotyped animal-networks [reviewed in (Thompson et al. 2013)]—topology descriptors such as the cardinality and connectivity indices can be compared statistically across genotypes and conditions to identify reproducible patterns and their controls.

The continuity index of vein networks in different populations of WT leaves grown in identical conditions was also reproducible (Fig. 2.5)—a finding consistent with the stringent requirement for continuity of tissue systems with transport function such as vein networks, and

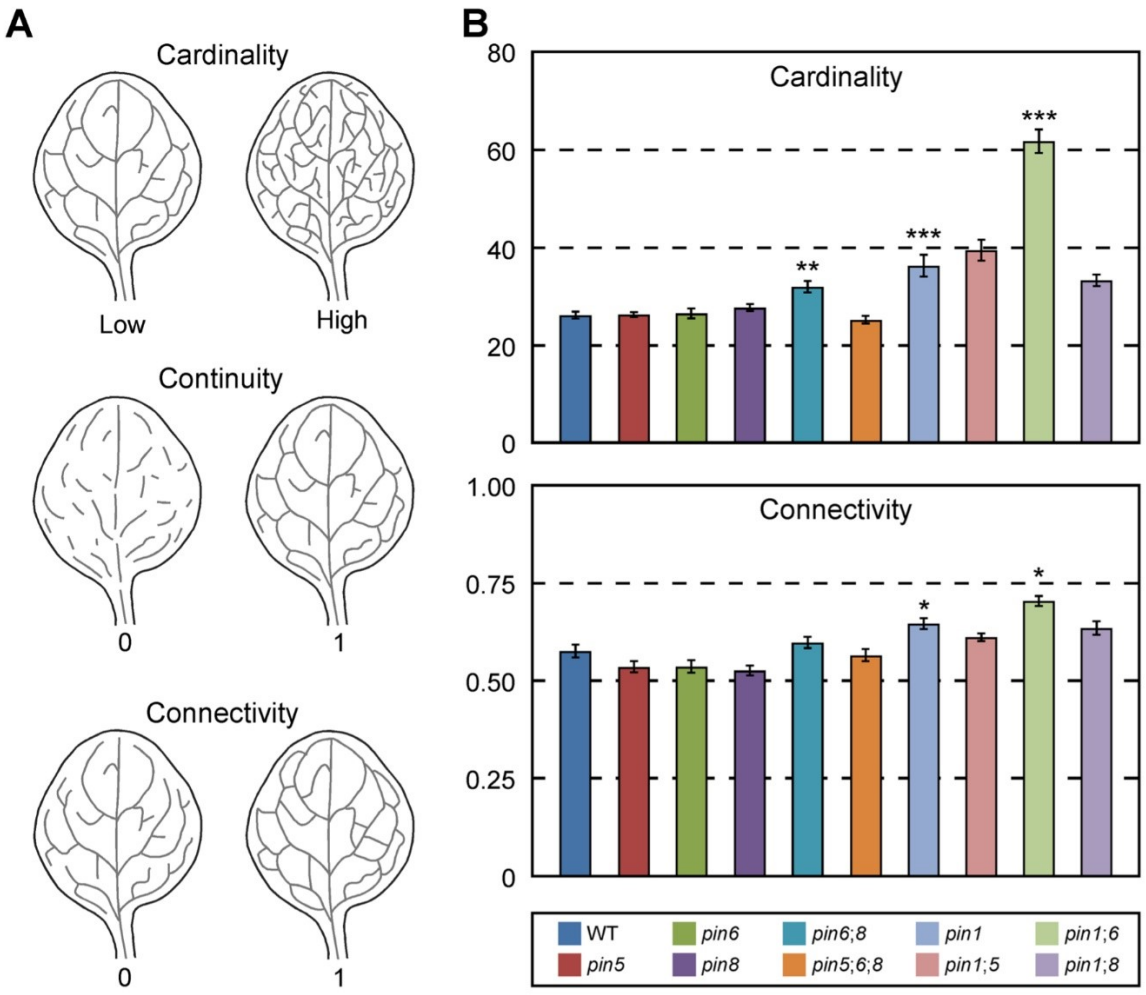

Figure 2.4. Functions of *PIN1*, *PIN5*, *PIN6* and *PIN8* in control of vein network topology. (A) Schematics of vein networks with low or high cardinality index (top row), minimum—i.e. 0—or maximum—i.e. 1—continuity index (middle row), or minimum—i.e. 0—or maximum—i.e. 1—connectivity index (bottom row). (B) First leaves. Indices are expressed as mean ± SE. Difference between *pin6*;*8* and WT cardinality indices, between *pin1* and WT cardinality indices, between *pin1*;*6* and *pin1* cardinality indices, between *pin1* and WT connectivity indices, and between *pin1*;*6* and *pin1* connectivity indices was significant at $P<0.05$ (*), $P<0.01$ (**) or $P<0.001$ (***) by *F*-test and *t*-test with Bonferroni correction. Sample population sizes: WT, 30; *pin5*, 30; *pin6*, 30; *pin8*, 27; *pin6*;*8*, 28; *pin5*;*6*;*8*, 28; *pin1*, 45; *pin1*;*5*, 57; *pin1*;*6*, 47; *pin1*;*8*, 37.

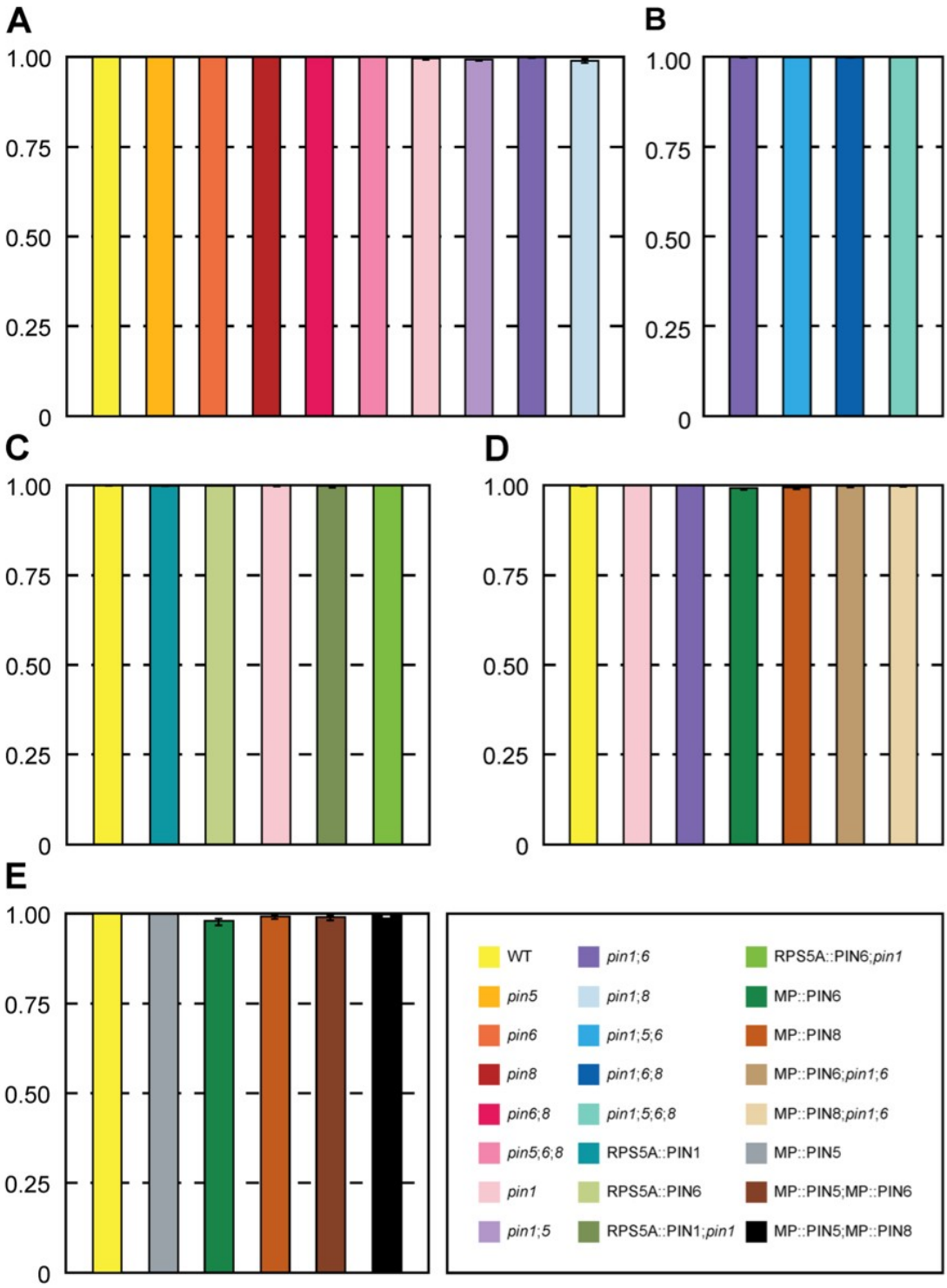

Figure 2.5. Functions of *PIN1*, *PIN5*, *PIN6* and *PIN8* in control of vein continuity. First leaves. Indices are expressed as mean ± SE. Sample population sizes as in Fig. 2.4B (A), Fig. 2.6 (B), Fig. 2.8D (C), Fig. 2.11E (D) or Fig. 2.13 (E).

with the successful use of vein fragmentation as diagnostic criterion for the identification of mutants in genetic screens (Carland et al. 1999; Deyholos et al. 2000; Koizumi et al. 2000).

The continuity index of none of the mutants or transgenics in our study was different from that of WT (Fig. 2.5), suggesting that *PIN1*, *PIN5*, *PIN6* and *PIN8* have no function in control of vein continuity or their functions in this process are redundant.

Consistent with previous observations (Sawchuk et al. 2013), the vein network topology of *pin5*, *pin6* or *pin8* was no different from that of WT (Fig. 2.4B); by contrast, the cardinality and connectivity indices of *pin1* vein networks were higher than those of WT vein networks (Fig. 2.4B), suggesting that *PIN1* inhibits the formation of veins and their connection.

We next asked whether *PIN5*, *PIN6* or *PIN8* acted redundantly with *PIN1* in inhibition of vein formation and connection. The vein network topology of neither *pin1*;*pin5* (*pin1*;*5* hereafter) nor *pin1*;*8* differed from that of *pin1* (Fig. 2.4B); however, the cardinality and connectivity indices of *pin1*;*6* vein networks were higher than those of *pin1* vein networks (Fig. 2.4B), suggesting that *PIN6* acts redundantly with *PIN1* in inhibition of vein formation and connection.

Next, we asked whether *PIN5* or *PIN8* acted redundantly with *PIN6* in *PIN1*-dependent inhibition of vein formation and connection. The vein network topology of *pin1*;*5*;*6* was no different from that of *pin1*;*6* (Fig. 2.6), but the cardinality index of *pin1*;*6*;*8* vein networks was higher than that of *pin1*;*6* vein networks (Fig. 2.6), suggesting that *PIN8* acts redundantly with *PIN6* in *PIN1*-dependent inhibition of vein formation; by contrast, the connectivity index of *pin1*;*6*;*8* vein networks was no different from that of *pin1*;*6* vein networks (Fig. 2.6), suggesting that *PIN8* has no function redundant to that of *PIN6* in *PIN1*-dependent inhibition of vein connection. Because the vein network topology of neither *pin6* nor *pin8* differed from that of WT (Fig. 2.4B), but the cardinality index of *pin6*;*8* vein networks is higher than that of WT (Fig. 2.4B), *PIN6* and *PIN8* also have redundant functions in inhibition of vein formation that are independent of *PIN1*. Thus the enhancement of *pin1*;*6* cardinality defects by *PIN8* could be interpreted as the result of the simultaneous loss of the *PIN1*-dependent pathway and of the parallel, *PIN6*/*PIN8*-dependent, *PIN1*-independent pathway—rather than evidence that *PIN8* acts redundantly with *PIN6* in *PIN1*-dependent inhibition of vein formation. However, we do not

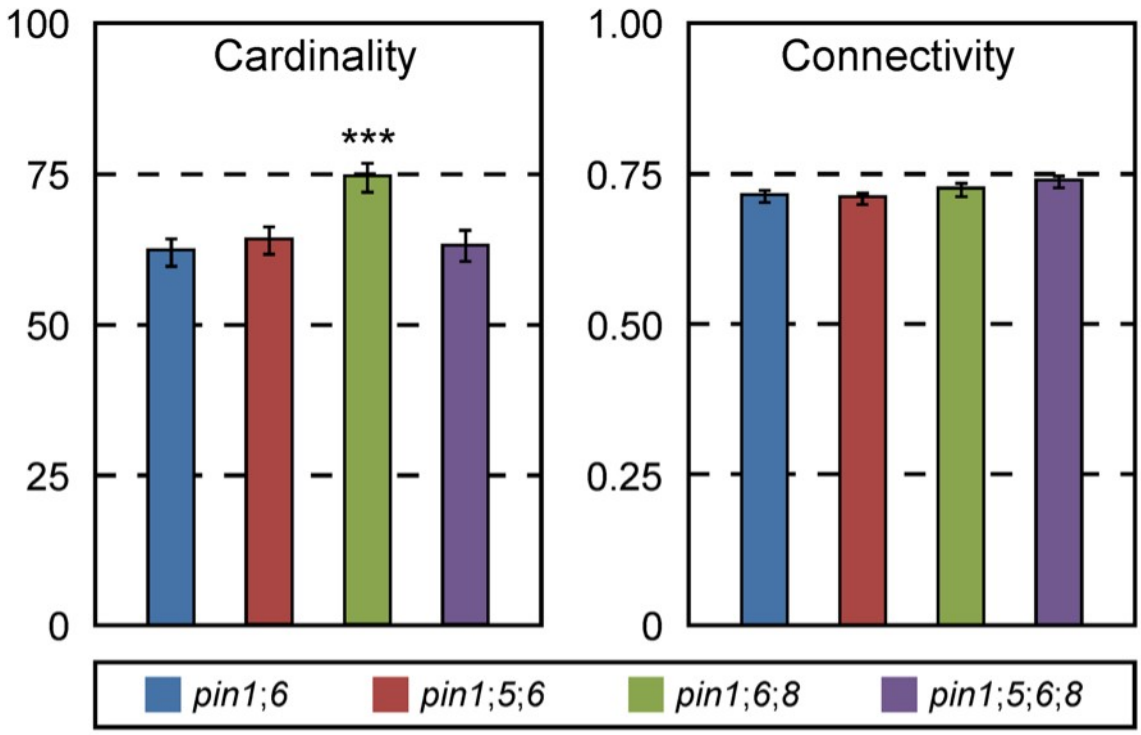

Figure 2.6. Functions of *PIN5* and *PIN8* in *PIN1*/*PIN6*-dependent control of vein network topology. First leaves. Indices are expressed as mean ± SE. Difference between *pin1*;*6*;*8* and *pin1*;*6* cardinality indices was significant at $P<0.001$ (***) by *F*-test and *t*-test with Bonferroni correction. Sample population sizes: *pin1*;*6*, 103; *pin1*;*5*;*6*, 104; *pin1*;*6*;*8*, 98; *pin1*;*5*;*6*;*8*, 109.

favor this interpretation because the cardinality defect of *pin1*;*6*;*8* is much greater than the sum of the cardinality defects of *pin1* and *pin6*;*8*.

We finally asked whether *PIN5* acted redundantly with *PIN6* and *PIN8* in *PIN1*-dependent or *PIN1*-independent inhibition of vein formation. The vein network topology of *pin1*;*5*;*6*;*8* was no different from that of *pin1*;*6* (Fig. 2.6) and that of *pin5*;*6*;*8* was no different from that of WT (Fig. 2.4B), suggesting that *pin5* suppresses the effects of *pin6* and *pin8* on *PIN1*-independent inhibition of vein formation. In agreement with interpretations of similar genetic interactions in other organisms [e.g., (Aguilera and Klein 1989; Hudson et al. 1990; Fan and Klein 1994)], the most parsimonious account for our observations is that *PIN5* promotes vein formation; that *PIN6* and *PIN8* redundantly and completely inhibit *PIN5*-dependent promotion of vein formation; and that these functions of *PIN5*, *PIN6* and *PIN8* are independent of *PIN1*. Further, because expression of *PIN5* and *PIN8* is initiated at post-formative stages of vein development (Sawchuk et al. 2013) (Fig. 2.1), these genes most likely control vein formation indirectly—for example, through feedback on vascular precursor cells located in more-immature parts of the leaf [e.g., Baima et al. 2014; reviewed in (Hsu and Fuchs 2012; Hsu et al. 2014)]. Finally, because *PIN5*, *PIN6* and *PIN8* are expressed in nonoverlapping sets of vascular cells (Fig. 2.3), the genetic interaction between these genes—as that between other genes expressed in mutually exclusive domains [e.g.: (Briscoe et al. 2000; Hirakawa et al. 2008; Sims et al. 2009; Etchells and Turner 2010; Stein et al. 2010) and references therein]—presumably reflects underlying cell-cell interactions.

2.2.4 Redundant functions of *PIN1*, *PIN6* and *PIN8* in control of auxin distribution in developing leaves

PIN1 inhibits vein formation, and *PIN6* acts redundantly with *PIN1* in inhibition of vein formation and with *PIN8* in *PIN1*-independent inhibition of vein formation (Figs. 2.4,2.6). We asked whether such redundancy extended to control of auxin distribution in developing leaves, which is known to control vein formation (Mattsson et al. 1999; Sieburth 1999; Mattsson et al. 2003; Cheng et al. 2006; Scarpella et al. 2006; Wenzel et al. 2007; Sawchuk et al. 2013). To

address this question, we imaged expression of the auxin reporter DR5rev::YFPnuc (Heisler et al. 2005; Brunoud et al. 2012; Sawchuk et al. 2013) in 4-DAG first leaves of WT, *pin6*;*8*, *pin1* and *pin1*;*6*.

As previously reported (Mattsson et al. 2003; Scarpella et al. 2006; Donner et al. 2009; Sawchuk et al. 2013), in WT the DR5 promoter was strongly active in narrow domains that coincide with sites of vein formation (Fig. 2.7A). Consistent with previous observations (Bosco et al. 2012; Ding et al. 2012; Bender et al. 2013; Cazzonelli et al. 2013; Sawchuk et al. 2013), DR5rev::YFPnuc expression was weaker in *pin6*;*8* than in WT, but domains of DR5rev::YFPnuc expression were equally narrow in *pin6*;*8* and WT (Fig. 2.7A,B). Levels of DR5rev::YFPnuc expression were lower, and domains of DR5rev::YFPnuc expression were broader, in *pin1* than in WT or *pin6*;*8* (Fig. 2.7A–D); and DR5rev::YFPnuc expression levels were even lower, and DR5rev::YFPnuc expression domains even broader, in *pin1*;*6* (Fig. 2.7C–F).

Thus our results suggest that the redundancy between *PIN1*, *PIN6* and *PIN8* that underlies control of vein formation extends to control of auxin distribution in developing leaves (see Conclusions).

2.2.5 Homologous and nonhomologous functions of *PIN1* and *PIN6* in vein network formation

PIN6 acts redundantly with *PIN1* in control of vein network patterning (Sawchuk et al. 2013) and topology (Fig. 2.4B); however, the redundancy between *PIN1* and *PIN6* is unequal: the patterning and topology of *pin6* vein networks are no different from those of WT vein networks but those of *pin1* vein networks are, suggesting that *PIN1* can provide all—or nearly all—the functions of *PIN6* in vein network formation and that, by contrast, *PIN6* is unable to provide all the functions of *PIN1* in this process. Such unequal redundancy could reflect nonhomologous functions of *PIN1* and *PIN6* in vein network formation—a possibility consistent with the different localization of PIN1 and PIN6: PIN1 is predominantly localized to the PM (Galweiler et al. 1998), while PIN6 is predominantly localized to the ER (Sawchuk et al. 2013). On the

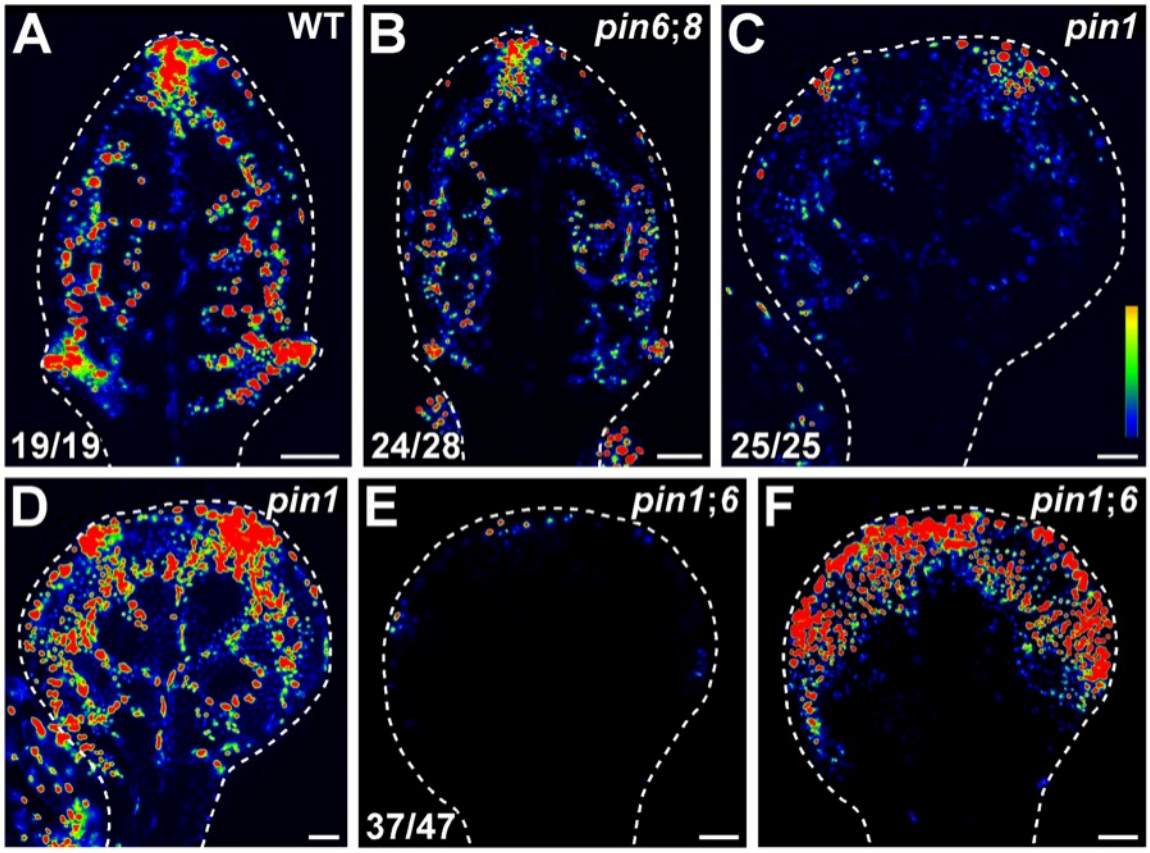

Figure 2.7. Expression of DR5rev::YFPnuc in *pin* developing leaves. (A–D) Confocal laser scanning microscopy; first leaves 4 days after germination. Look-up table (ramp in C) visualizes expression levels. Top right: genotype. Bottom left: reproducibility index. Dashed white line delineates leaf primordium outline. Images in A, B, C and E were taken at identical settings and show increasingly weaker DR5rev::YFPnuc expression in *pin6*;*8*, *pin1* and *pin1*;*6*. Images in A, D and F were taken by matching signal intensity to detector's input range (~4% saturated pixels), and show increasingly broader DR5rev::YFPnuc expression domains in *pin1* and *pin1*;*6*. Bars: (A–F) 50 μm.

other hand—at least in other organisms—redundant, homologous functions can be provided by proteins that are localized to different cellular compartments [e.g.:(Jin et al. 2008; Kouranti et al. 2010) and references therein]. Further, at least some of the functions of *PIN1* in vein network formation depend on *PIN1* expression in leaf epidermal cells (Bilsborough et al. 2011; Kierzkowski et al. 2013)—leaf epidermal cells that fail, by contrast, to express *PIN6* (Sawchuk et al. 2013) (Fig. 2.1). Thus the unequal redundancy of *PIN1* and *PIN6* in vein network formation could alternatively be accounted for by their different expression domains.

To test these possibilities, we used the promoter of the *RIBOSOMAL PROTEIN S5A* (*RPS5A*) gene (AT3G11940)—highly active in developing organs, including their epidermal cells (Weijers et al. 2001)—to express *PIN1* (RPS5A::PIN1) or *PIN6* (RPS5A::PIN6) in the *pin1* background, and compared phenotype features of RPS5A::PIN1;*pin1* and RPS5A::PIN6;*pin1* with those of *pin1* and WT.

We first asked whether *PIN6* could provide functions in control of vein network patterning homologous to those of *PIN1*. The patterning of ~15% of the vein networks of RPS5A::PIN1 and RPS5A::PIN6, and—as previously reported (Sawchuk et al. 2013)—of nearly 50% of *pin1* vein networks was abnormal (Fig. 2.8A–D). RPS5A::PIN1 shifted the spectrum of vein network patterning of *pin1* toward the vein network patterning of WT but RPS5A::PIN6 failed to do so (Fig 2.8A–D), suggesting that *PIN6* is unable to provide functions in control of vein network patterning homologous to those of *PIN1*.

We next asked whether *PIN6* could provide functions in control of vein network topology homologous to those of *PIN1*. The cardinality and connectivity indices of RPS5A::PIN1 vein networks were lower than those of WT vein networks (Fig. 2.8E), supporting that *PIN1* inhibits vein formation and connection. The cardinality index of RPS5A::PIN6 vein networks was higher than that of WT vein networks (Fig. 2.8E), suggesting that ectopic expression of *PIN6* in the epidermis promotes vein formation. As reported above (Fig. 2.4B), the cardinality and connectivity indices of *pin1* vein networks were higher than those of WT vein networks (Fig. 2.8E). RPS5A::PIN1 shifted the cardinality index of *pin1* vein networks toward that of WT vein networks but RPS5A::PIN6 failed to do so (Fig. 2.8E), suggesting that *PIN6* is unable to provide functions in vein formation homologous to those of *PIN1*. By contrast, both RPS5A::PIN1 and RPS5A::PIN6 shifted the connectivity index of *pin1* vein networks toward that of WT vein

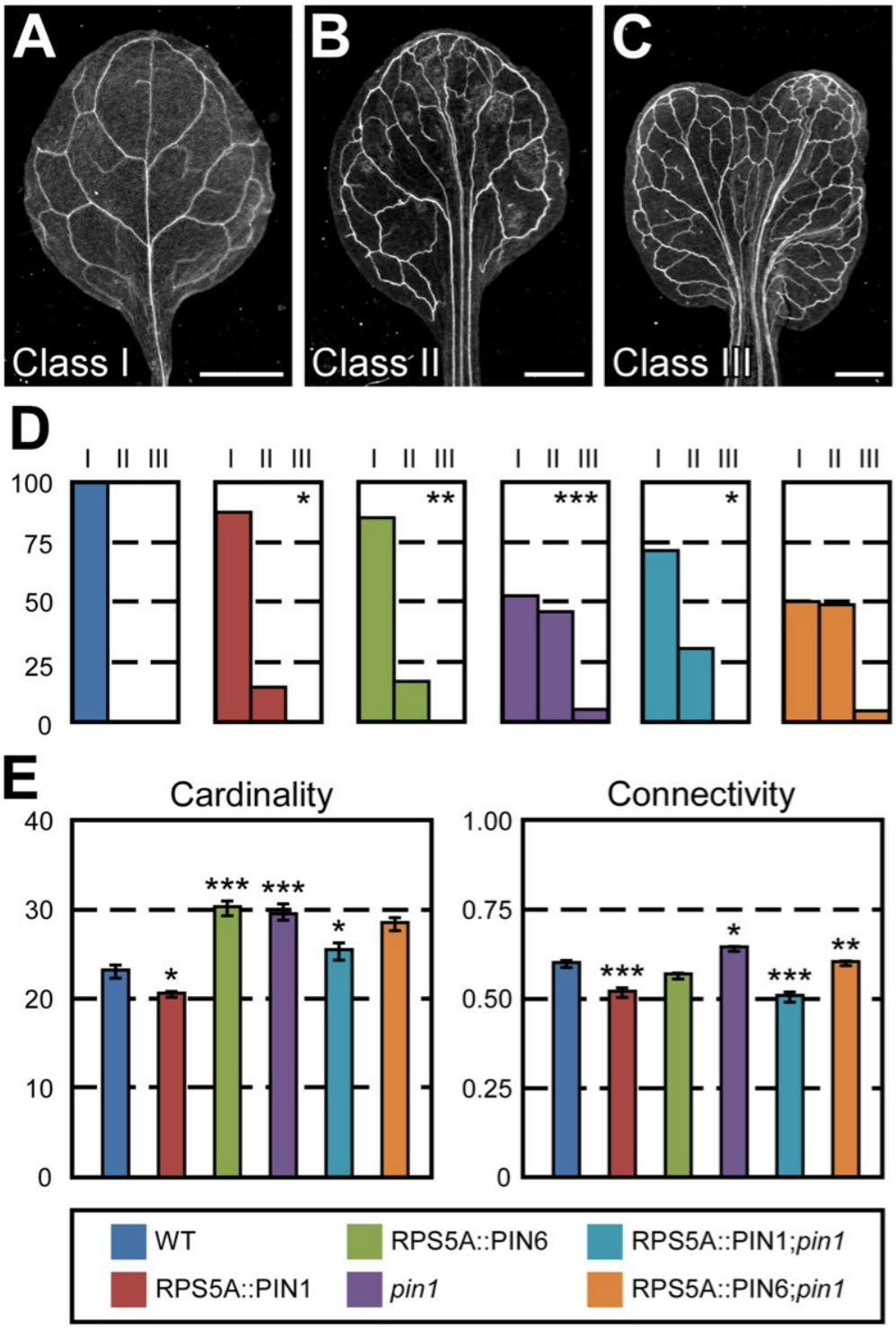

Figure 2.8. Functions of *PIN1* and *PIN6* in vein network formation. (A–C) Dark-field illumination of mature first leaves illustrating phenotype classes: unbranched, narrow midvein and scalloped vein-network outline (A); bifurcated midvein and scalloped vein-network outline

(B); fused leaves with scalloped vein-network outline (C). (D) Percentages of leaves in phenotype classes. Difference between RPS5A::PIN1 and WT, between RPS5A::PIN6 and WT, between *pin1* and WT, and between RPS5A::PIN1;*pin1* was significant at $P<0.05$ (*), $P<0.01$ (**) or $P<0.001$ (***) by Kruskal-Wallis and Mann-Whitney test with Bonferroni correction. Sample population sizes: WT, 65; RPS5A::PIN1, 55; RPS5A::PIN6, 58; *pin1*, 116; RPS5A::PIN1;*pin1*, 71; RPS5A::PIN6;*pin1*, 140. (E) First leaves. Indices are expressed as mean ± SE. Difference between RPS5A::PIN1 and WT cardinality indices, between RPS5A::PIN6 and WT cardinality indices, between *pin1* and WT cardinality indices, between RPS5A::PIN1;*pin1* and *pin1* cardinality indices, between RPS5A::PIN1 and WT connectivity indices, between *pin1* and WT connectivity indices, between RPS5A::PIN1;*pin1* and *pin1* connectivity indices, and between RPS5A::PIN6;*pin1* and *pin1* connectivity indices was significant at $P<0.05$ (*), $P<0.01$ (**) or $P<0.001$ (***) by *F*-test and *t*-test with Bonferroni correction. Sample population sizes as in (D). Bars: (A–C) 1 mm.

networks (Fig. 2.8E), suggesting that *PIN6* can provide functions in vein connection homologous to those of *PIN1*. Interpretations of similar genetic interactions in other organisms [e.g., (Hodgkin 1986; Maruyama et al. 1989; Han et al. 1990)] suggest that the suppression of vein connectedness defects of *pin1* by RPS5A::PIN6 can be accounted for by at least two mechanisms. One possibility is that *PIN6* acts downstream of *PIN1* in the same pathway that controls vein connection; we do not favor this hypothesis, however, because it fails to predict the observed (Figs. 2.4,2.6) enhancement of vein connectedness defects of *pin1* by *pin6*. Alternatively, vein connection may be unfavored at high auxin levels (Sachs 1968), which would be the result of at least two separate pathways: PIN1-mediated auxin transport toward sites of vein formation (Scarpella et al. 2006; Wenzel et al. 2007; Bayer et al. 2009; Marcos and Berleth 2014) (Fig. 2.7) and PIN6-mediated increase in auxin levels within developing vascular cells (Bender et al. 2013; Cazzonelli et al. 2013; Sawchuk et al. 2013) (Fig. 2.7) (see Conclusions).

In addition to vein network formation, *PIN6* acts redundantly with *PIN1* in cotyledon patterning, and as in vein network formation, the redundancy between *PIN1* and *PIN6* in cotyledon patterning is unequal (Sawchuk et al. 2013). We thus asked whether *PIN6* could provide functions in cotyledon patterning homologous to those of *PIN1*; our results (Fig. 2.9) suggest that it cannot.

Finally, RPS5A::PIN1 reverted the pin-shaped, sterile inflorescences of *pin1* to WT-looking, fertile inflorescences but RPS5A::PIN6 failed to do so (Fig. 2.10), suggesting that *PIN6* is unable to provide functions in inflorescence development homologous to those of *PIN1*.

In summary, *PIN6* was unable to provide functions homologous to those of *PIN1* in control of vein network patterning, vein formation, cotyledon patterning and inflorescence development. Thus the unequal redundancy between *PIN1* and *PIN6* in these processes is unlikely the result of their different expression and might instead be accounted for by their nonhomologous functions—a conclusion consistent with the opposite effects of *PIN1* and *PIN6* on intercellular auxin transport (Cazzonelli et al. 2013). By contrast, *PIN6* was able to provide functions in vein connection homologous to those of *PIN1*, suggesting that *PIN6* expression normally limits *PIN6*'s ability to compensate for the effects of loss of *PIN1* function in vein connection.

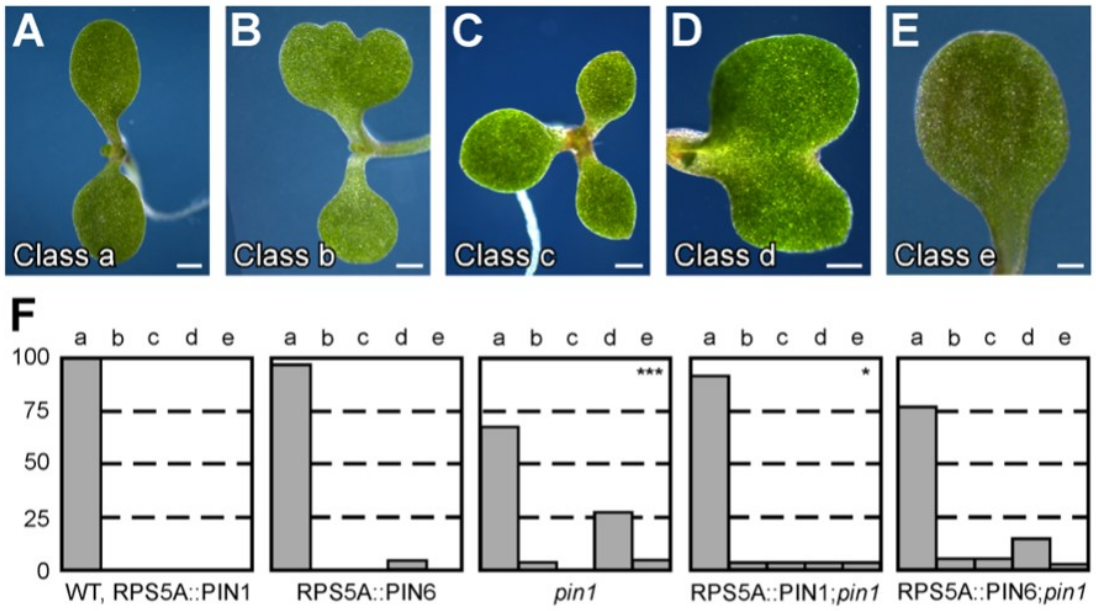

Figure 2.9. Functions of *PIN1* and *PIN6* in cotyledon patterning. (A–E) Dark-field illumination of 4-day old seedlings illustrating phenotype classes: two separate cotyledons (A); fused cotyledons and separate single cotyledon (B); three separate cotyledons (C); fused cotyledons (D); single cotyledon (E). (F) Percentages of seedlings in phenotype classes. Difference between *pin1* and WT, and between RPS5A::PIN1;*pin1* and *pin1* was significant at $P<0.05$ (*) or $P<0.001$ (***) by Kruskal-Wallis and Mann-Whitney test with Bonferroni correction. Sample population sizes: WT, 78; RPS5A::PIN1, 68; RPS5A::PIN6, 32; *pin1*, 88; RPS5A::PIN1;*pin1*, 47; RPS5A::PIN1;*pin1*, 73. Bars: (A–C) 1 mm; (D,E) 0.5 mm.

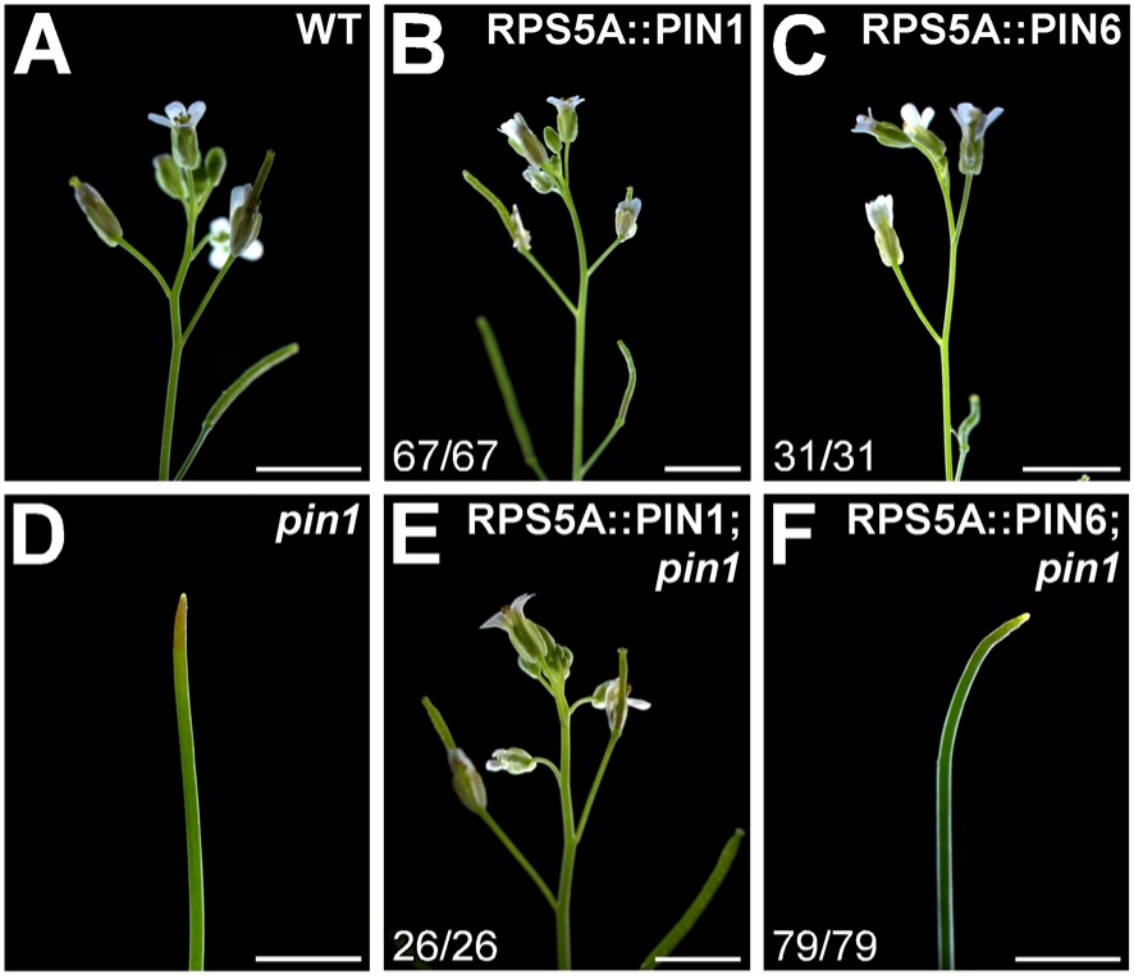

Figure 2.10. Functions of *PIN1* and *PIN6* in inflorescence development. (A–F) Four-week-old plants. Top right: genotype. Bottom left: reproducibility index. WT plants normally form fertile flowers (A), while *pin1* plants never do (Goto et al. 1987; Okada et al. 1991) (D). Bars: 5 mm.

2.2.6 Homologous functions of *PIN6* and *PIN8* in *PIN1*-dependent vein-network formation

PIN8 acts redundantly with *PIN6* in *PIN1*-dependent control of vein network patterning (Sawchuk et al. 2013) and vein formation (Fig. 2.6); however, the redundancy between *PIN6* and *PIN8* in *PIN1*-dependent control of vein network formation is unequal: the patterning and cardinality index of *pin1*;*8* vein networks are no different from those of *pin1* vein networks, but those of *pin1*;*6* vein networks are; thus *PIN6* can provide all the functions of *PIN8* in *PIN1*-dependent control of vein network patterning and vein formation, but *PIN8* is unable to provide all the functions of *PIN6* in these processes. Further, *PIN8* seems to have no function in *PIN1*/*PIN6*-dependent vein connection. The unequal functions of *PIN6* and *PIN8* in vein network formation could be accounted for by the different expression of *PIN6* and *PIN8* during vein development (Sawchuk et al. 2013) (Figs. 2.1,2.3), but it could also reflect nonhomologous functions of *PIN6* and *PIN8* in this process.

To test these possibilities, we expressed *PIN6* or *PIN8* by the promoter of the *MONOPTEROS* (*MP*) gene (AT1G19850) (MP::PIN6 or MP::PIN8)—highly active in developing veins (Sawchuk et al. 2013)—in the *pin1*;*6* background, and compared defects of MP::PIN6;*pin1*;*6* and MP::PIN8;*pin1*;*6* with those of *pin1*;*6* and *pin1*.

We first asked whether *PIN8* could provide functions in *PIN1*-dependent control of vein network patterning homologous to those of *PIN6*. As previously reported (Sawchuk et al. 2013), the vein network patterning of MP::PIN6 and MP::PIN8 was no different from that of WT (Fig. 2.11A–E). By contrast, the patterning of nearly 60% of *pin1* vein networks was abnormal, and *pin6* shifted the spectrum of vein network patterning of *pin1* toward more severe phenotype classes (Sawchuk et al. 2013) (Fig. 2.11A–E). The spectrum of vein network patterning of MP::PIN6;*pin1*;*6* was no different from that of *pin1* and that of MP::PIN8;*pin1*;*6* was no different from that of MP::PIN6;*pin1*;*6* (Fig. 2.11A–E), suggesting that *PIN8* can provide functions in *PIN1*-dependent control of vein network patterning homologous to those of *PIN6*.

We next asked whether *PIN8* could provide functions in *PIN1*-dependent control of vein network topology homologous to those of *PIN6*. Consistent with previous observations

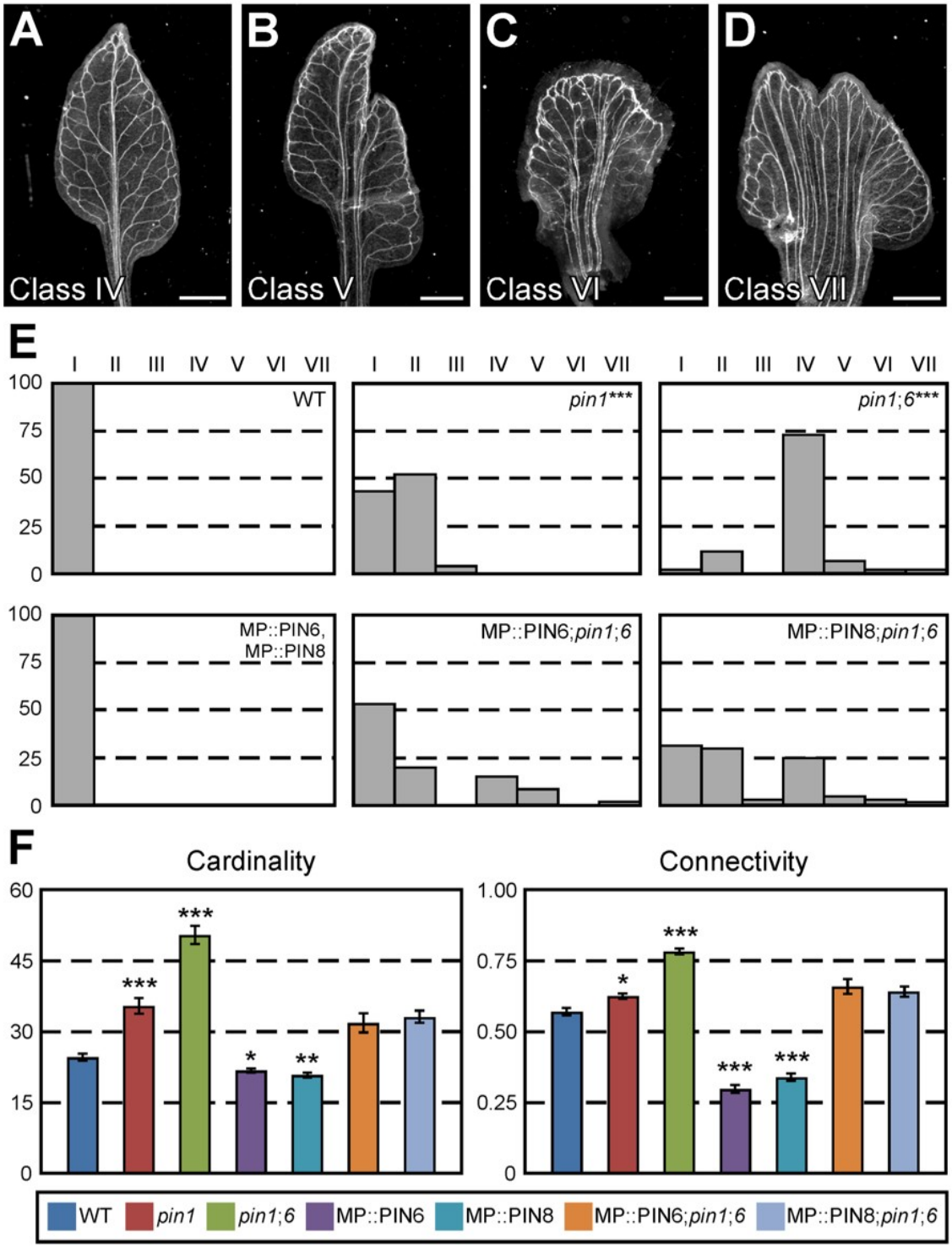

Figure 2.11. Functions of *PIN6* and *PIN8* in *PIN1*-dependent vein network formation. (A–D) Dark-field illumination of mature first leaves illustrating phenotype classes: conspicuous marginal vein (A); fused leaves with conspicuous marginal vein (B); wide midvein (C); fused

leaves with wide midvein (D). Phenotype classes I–III as in Fig. 2.5. (E) Percentages of leaves in phenotype classes. Difference between *pin1* and WT, and between *pin1*;*6* and *pin1* was significant at $P<0.001$ (***) by Kruskal-Wallis and Mann-Whitney test with Bonferroni correction. Sample population sizes: WT, 53; *pin1*, 46; *pin1*;*6*, 42; MP::PIN6, 54; MP::PIN8, 49; MP::PIN6;*pin1*;*6*, 45; MP::PIN8;*pin1*;*6*, 60. (F) First leaves. Indices are expressed as mean ± SE. Difference between *pin1* and WT cardinality indices, between *pin1*;*6* and *pin1* cardinality indices, between MP::PIN6 and WT cardinality indices, between MP::PIN8 and WT cardinality indices, between *pin1* and WT connectivity indices, between *pin1*;*6* and *pin1* connectivity indices, between MP::PIN6 and WT connectivity indices, and between MP::PIN8 and WT connectivity indices was significant at $P<0.001$ (***) by *F*-test and *t*-test with Bonferroni correction. Sample population sizes as in (E). Bars: (A,B,D) 1 mm; (C) 0.25 mm.

(Sawchuk et al. 2013), MP::PIN6 and MP::PIN8 induced similar defects—as it frequently results from overexpression of genes with homologous functions [e.g., (Balcells et al. 1988; Hadwiger et al. 1989; Parkhurst et al. 1990)]: the cardinality and connectivity indices of both MP::PIN6 and MP::PIN8 vein networks were lower than those of WT vein networks (Fig. 2.11F), supporting that *PIN6* inhibits vein formation and connection, and suggesting that *PIN8* can inhibit vein connection in addition to vein formation. As reported above (Fig. 2.4B), the cardinality and connectivity indices of *pin1* vein networks were higher than those of WT vein networks and those of *pin1*;*6* vein networks were higher than those of *pin1* vein networks (Fig. 2.11F). The vein network topology of MP::PIN6;*pin1*;*6* was no different from that of *pin1* and that of MP::PIN8;*pin1*;*6* was no different from that of MP::PIN6;*pin1*;*6* (Fig. 2.11F), suggesting that *PIN8* can provide functions in *PIN1*-dependent control of vein network topology homologous to those of *PIN6*.

In addition to *PIN1*-dependent vein-network formation, *PIN8* acts redundantly with *PIN6* in *PIN1*-dependent cotyledon patterning, and as in *PIN1*-dependent vein network formation, the redundancy between *PIN6* and *PIN8* in *PIN1*-dependent cotyledon patterning is unequal (Sawchuk et al. 2013). We thus asked whether *PIN8* could provide functions in *PIN1*-dependent cotyledon patterning homologous to those of *PIN6*; our results (Fig. 2.12) suggest that it can.

In summary, *PIN8* was able to provide functions homologous to *PIN6* in *PIN1*-dependent vein network formation and cotyledon patterning. Thus the unequal redundancy between *PIN6* and *PIN8* is unlikely the result of nonhomologous functions and might instead be accounted for by their different expression. Just as the *ER-PIN* genes *PIN6* and *PIN8* redundantly control *PIN1*-dependent vein network formation, the redundancy between the *PM-PIN* genes *PIN1*, *PIN2*, *PIN3*, *PIN4* and *PIN7* underlies—to varying extents—many other developmental processes [e.g., (Benkova et al. 2003; Friml et al. 2003; Blilou et al. 2005; Vieten et al. 2005; Fischer et al. 2006; Guenot et al. 2012)]. In the development of embryos and roots, *PM-PIN* genes compensate for loss of one another's function by their ectopic expression in the domain of the gene whose function has been lost (Blilou et al. 2005; Vieten et al. 2005). For example, in *pin7* embryos PIN4 becomes expressed at earlier stages of development and in the domain in which PIN7 is normally expressed, thereby compensating for loss of *PIN7* function (Vieten et al. 2005). By contrast, in the *pin1*;*6* background *PIN8* expression remains restricted to post-

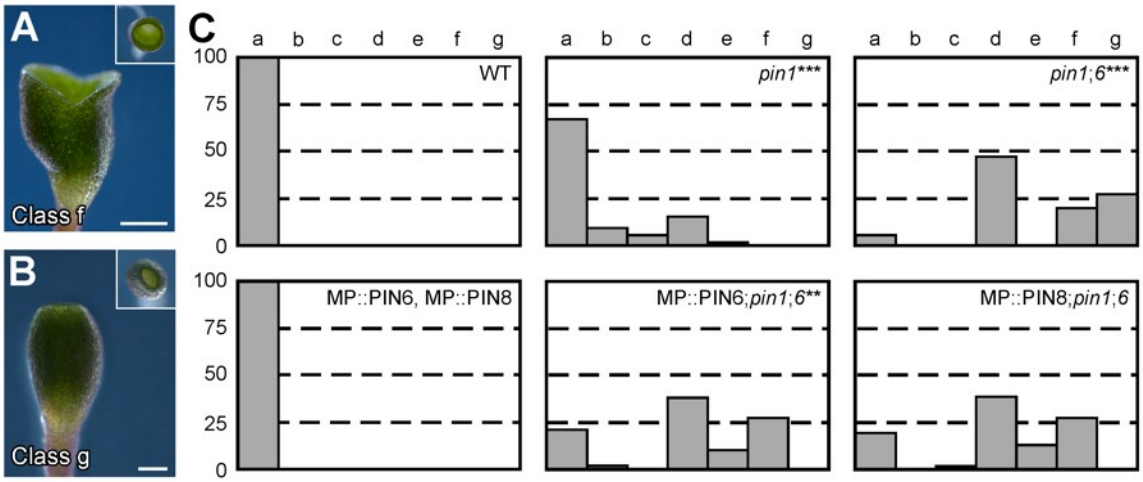

Figure 2.12. Functions of *PIN6* and *PIN8* in *PIN1*-dependent cotyledon patterning. (A,B) Dark-field illumination of 4-day old seedlings illustrating phenotype classes: partially fused cup-shaped cotyledons, side view; inset: top view (A); completely fused cup-shaped cotyledon, side view; inset: top view (B). Phenotype classes a–e as in Fig. 2.9. (C) Percentages of seedlings in phenotype classes. Difference between *pin1* and WT, between *pin1*;*6* and *pin1*, and between MP::PIN6;*pin1*;*6* and *pin1*;*6* was significant at $P<0.01$ (**) or $P<0.001$ (***) by Kruskal-Wallis and Mann-Whitney test with Bonferroni correction. Sample population sizes: WT, 53; *pin1*, 52; *pin1*;*6*, 55; MP::PIN6, 54; MP::PIN8, 49; MP::PIN6;*pin1*;*6*, 47; MP::PIN8;*pin1*;*6*, 62. Bars: (A) 0.5 mm; (B) 0.25 mm.

formative stages of vein development (Sawchuk et al. 2013), supporting that *PIN8* controls vein network formation by feeding back on vascular precursor cells located in more-immature parts of the leaf.

2.2.7 Functions of *PIN5* in *PIN6*/*PIN8*-dependent control of vein network topology

PIN6 has functions in control of vein network topology beyond control of *PIN5* function (Fig. 2.6). We asked whether *PIN5* could provide functions in control of vein network topology that are independent of control by *PIN6* or *PIN8*.

To address this question, we used plants expressing *PIN5* by the *MP* promoter (MP::PIN5) because the vein density of MP::PIN5 leaves is higher than that of WT leaves (Sawchuk et al. 2013). We reasoned that if *PIN5* could provide functions that are independent of control by *PIN6* or *PIN8*, at least some of the effects of MP::PIN5 on vein network topology should persist in the MP::PIN6 or MP::PIN8 backgrounds. By contrast, if all *PIN5*'s functions depended on control by *PIN6* or *PIN8*, the effects of MP::PIN6 or MP::PIN8 on vein network topology should mask those of MP::PIN5.

Consistent with previous observations (Sawchuk et al. 2013), the cardinality index of MP::PIN5 vein networks was higher than that of WT vein networks (Fig. 2.13), supporting that *PIN5* promotes vein formation. As reported above (Fig. 2.11), the cardinality and connectivity indices of MP::PIN6 and MP::PIN8 vein networks were lower than those of WT vein networks (Fig. 2.13). Because the vein network topology of MP::PIN5;MP::PIN6 was no different from that of MP::PIN6 and that of MP::PIN5;MP::PIN8 was no different from that of MP::PIN8 (Fig. 2.13), we conclude that no function of *PIN5* escapes control by *PIN6* or *PIN8*.

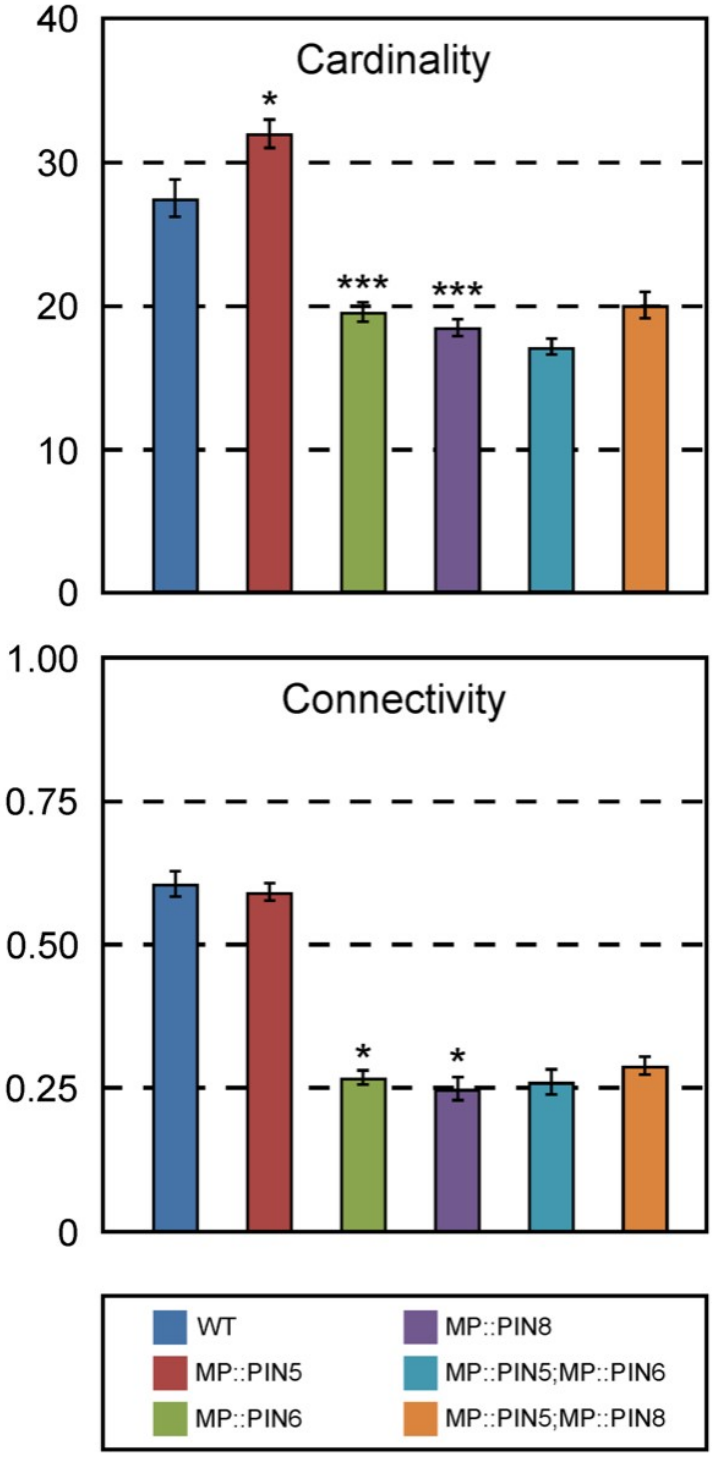

Figure 2.13. Functions of *PIN5* in *PIN6*/*PIN8*-dependent control of vein network topology. First leaves. Indices are expressed as mean ± SE. Difference between MP::PIN5 and WT cardinality indices, between MP::PIN6 and WT cardinality indices, between MP::PIN8 and WT cardinality indices, between MP::PIN6 and WT connectivity indices, and between MP::PIN8 and

WT connectivity indices was significant at $P<0.05$ (*) or $P<0.001$ (***) by *F*-test and *t*-test with Bonferroni correction. Sample population sizes: WT, 27; MP::PIN5, 48; MP::PIN6, 32; MP::PIN8, 32; MP::PIN5;MP::PIN6, 31; MP::PIN5;MP::PIN8, 40.

2.2.8 Conclusions

Vein network formation is redundantly, but nonhomologously, controlled by PIN1-mediated intercellular auxin transport and PIN6/PIN8-mediated intracellular auxin transport (Fig. 2.14A,B). How to account for such functional overlap?

The "auxin canalization hypothesis" proposes that a positive feedback between auxin movement through a cell and localization of auxin efflux proteins to the site where auxin leaves the cell leads to the selection of cell files from within a field of cells; such cell files would become exposed to inductive levels of auxin, would differentiate into efficient auxin-transport canals—the veins—and would drain auxin from the surrounding areas (Sachs 1991a; Sachs 2000). Auxin drainage by developing veins would lower auxin levels in the surrounding areas below those levels which inhibit growth (Ljung et al. 2001; Keller et al. 2004), growth would resume, and new fields of cells would be generated in which the whole process could be repeated (Sachs 1989).

The predictions of the auxin canalization hypothesis have been rigorously tested and are supported by computer simulation of mathematical models (Mitchison 1980a; Mitchison 1981; Rolland-Lagan and Prusinkiewicz 2005); nevertheless, inconsistencies seem to exist between experimental evidence and hypothesis' predictions. For example, the hypothesis appears unable to predict the experimentally observed high levels of auxin in veins (Mattsson et al. 2003; Brunoud et al. 2012); however, such levels could be, at least in part, the result of PIN1-mediated auxin transport toward sites of vein formation (Bayer et al. 2009) (Figs. 2.7,2.14D), and of PIN6/PIN8-mediated increase in auxin levels within developing vascular cells (Bosco et al. 2012; Ding et al. 2012; Bender et al. 2013; Cazzonelli et al. 2013; Sawchuk et al. 2013) (Fig. 2.7,2.14D). We suggest that because of the lower auxin levels in *pin6*;*8* (Bosco et al. 2012; Ding et al. 2012; Bender et al. 2013; Cazzonelli et al. 2013; Sawchuk et al. 2013) (Fig. 2.7), auxin would be drained more efficiently in leaves of this background, leaf growth would resume sooner, and veins would form faster—a prediction supported by the faster formation of vein-associated domains of *PIN1* expression in *pin6*;*8* (Sawchuk et al. 2013)—thus leading to the formation of networks of more veins (Fig. 2.14C). Because of the reduced intercellular auxin-

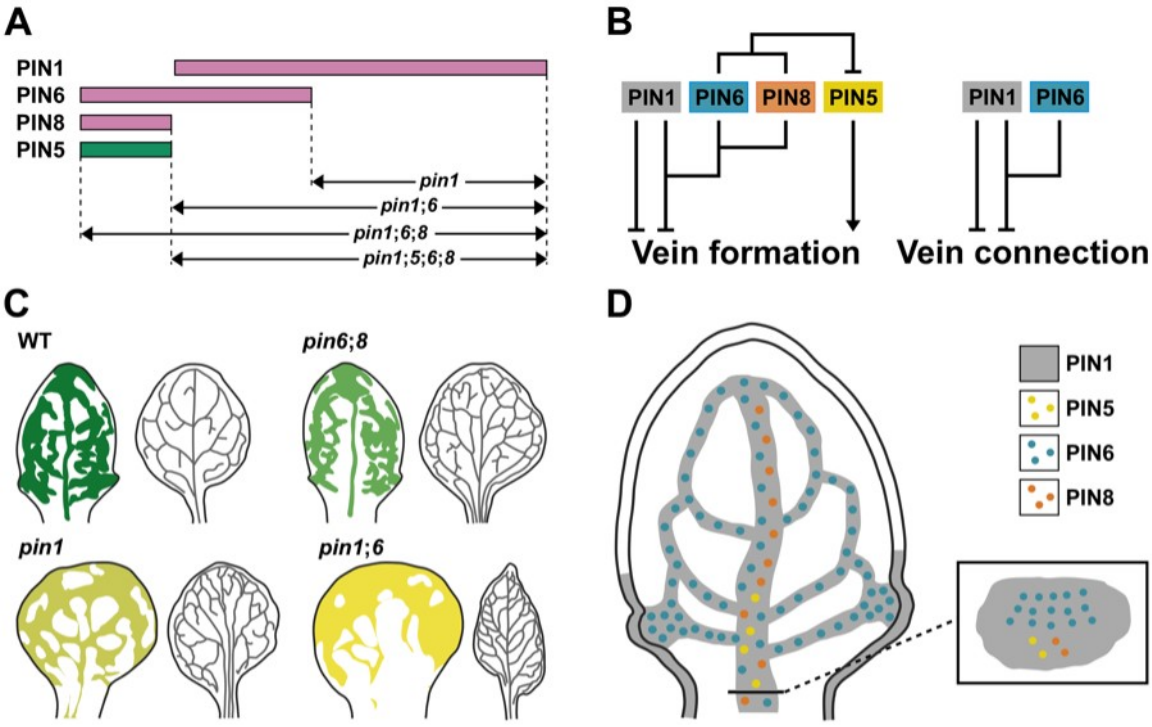

Figure 2.14. Summary and interpretations. (A) Unique and redundant functions of *PIN1*, *PIN5*, *PIN6* and *PIN8* in vein network formation (magenta, inhibiting functions; green, promoting functions), and derived mutant phenotypes. It is possible that *PIN8*'s functions extend to overlap with *PIN6*'s in *PIN1*-dependent inhibition of vein network formation. (B) Genetic interaction map of *PIN1*, *PIN5*, *PIN6* and *PIN8* in vein network topology. Arrows indicate positive effects; blunt-ended lines indicate negative effects. (C) DR5-promoter-activity-derived auxin levels and distribution in developing leaves (left; lower levels are in lighter tints; for simplicity, differences within leaves are ignored), and vein networks in mature leaves (right). (D) Cellular expression map of *PIN1*, *PIN5*, *PIN6* and *PIN8* in vein development. See text for details.

transport in *pin1* (Okada et al. 1991), auxin would accumulate for longer periods in leaves of this background before inducing efficient drainage canals, thereby exposing more cells to inductive levels of auxin—a prediction consistent with the broader domains of DR5rev::YFPnuc expression in *pin1* (Fig. 2.7)—and thus leading to the formation of networks of more veins (Fig 2.14C). Because of the additionally lower levels of auxin in *pin1*;*6*—suggested by the mimicry of *pin1*;*6* defects by reduction of auxin levels in *pin1* (Sawchuk et al. 2013) and by the lower levels of DR5rev::YFPnuc expression in *pin1*;*6* than in *pin1* (Fig. 2.7)—auxin would accumulate for even longer periods before inducing efficient drainage canals, thereby exposing even more cells to inductive levels of auxin—a prediction consistent with the broader domains of DR5rev::YFPnuc expression in *pin1*;*6* than in *pin1* (Fig. 2.7)—and thus leading to the formation of networks of even more veins (Fig. 2.14C).

Closed veins form during leaf development from open-vein precursors that become connected with other vein precursors at both ends (Kang and Dengler 2004; Scarpella et al. 2004; Scarpella et al. 2006; Sawchuk et al. 2007; Wenzel et al. 2007; Marcos and Berleth 2014). Accounting for the formation of closed veins has long been a challenge for the auxin canalization hypothesis [reviewed in (Smith and Bayer 2009; Jönsson and Krupinski 2010; Scarpella and Helariutta 2010; Prusinkiewicz and Runions 2012; Sawchuk and Scarpella 2013)]. Loss of function of *PIN1* and *PIN6* leads to network of veins that are more frequently closed, and overexpression of *PIN1*, *PIN6* or *PIN8* leads to the opposite defect; thus—consistently with the observation that vein connections form at early stages of tissue development (Kang and Dengler 2004; Scarpella et al. 2004; Scarpella et al. 2006; Sawchuk et al. 2007; Wenzel et al. 2007; Marcos and Berleth 2014)—our results suggest that connection may be favored—or occur exclusively—between vein precursors that have yet to differentiate high auxin-transport capacity or high auxin-transport-mediated auxin levels.

2.3 Materials and methods

2.3.1 Plants

Origin and nature of lines, genotyping strategies and oligonucleotide sequences are Table 2.1, Table 2.2 and Table 2.3, respectively. Seeds were sterilized and germinated, plants were grown and transformed, and representative lines were selected as described in Sawchuk et al. 2008.

2.3.2 Imaging

Developing leaves were mounted and imaged as in Sawchuk et al. 2013. Marker-line-specific imaging parameters are in Table 2.4 and Table 2.5. Mature leaves were fixed in 3:1 ethanol:acetic acid, rehydrated in 70% ethanol and water, cleared briefly (few seconds to few minutes) in 0.4 M sodium hydroxide, washed in water and mounted in 1:3:8 water:glycerol:chloral hydrate (Sigma-Aldrich Co. LLC). Mounted leaves were imaged as in (Odat et al. 2014). Image brightness and contrast were adjusted by linear stretching of the histogram with ImageJ (National Institutes of Health). Images were cropped with Photoshop (Adobe Systems Inc.) and assembled into figures with Canvas (ACD Systems International Inc.).

2.3.3 Analysis of vein network topology

We define a “touch point” (TP) as the point where a vein end contacts another vein or a vein fragment, an “end point” (EP) as the point where an open vein terminates free of contact with another vein or a vein fragment, and a “break point” (KP) as each of the two points where a vein fragment terminates free of contact with veins or other vein fragments (Fig. 2.15). Because it is impractical to determine the TP between a vein that exits a leaf and the vein system of the plant axis, or the KP in proximity of the vein system of the plant axis of a vein fragment that exits a leaf, we define an “exit point” (XP) as the point where a vein or a vein fragment exits the leaf lamina and enters the leaf petiole (Fig. 2.15), and equate an XP to a TP. The number of TPs, EPs,

Table 2.2. Genotyping strategies.

Line	Strategy
pin1-1	In RPS5A::PIN1 background: '0.28 PIN1p SalI' and 'pin1-1 R', and *Tat*I. In all other backgrounds: 'pin1-1 F' and 'pin1-1 R', and *Tat*I; or 'Pin1-1 WT KpnI Fwd' and 'Pin1-1 WT KpnI Rev', and *Kpn*I
pin5-4	*PIN5*: 'SALK_042994 LP' and 'SALK_042994 RP'; *pin5*: 'SALK_042994 RP' and 'LBb1.3'
pin6	*PIN6* (in MP::PIN6 background): 'PIN6 prom seq forw' and 'PIN6 spm R'; *PIN6* (in all other backgrounds): 'PIN6 spm F' and 'PIN6 spm R'; *pin6*: 'PIN6 spm F' and 'Spm32'
pin8-1	*PIN8*: 'SALK_107965 LP' and 'SALK_107965 RP'; *pin8*: 'SALK_107965 RP' and 'LBb1.3'
RPS5A::PIN6	'PIN6 ox SmaI forw' and 'PIN6 ox Ecl136II rev'
MP::PIN6	'PIN6 ox SmaI forw' and 'PIN6 ox Ecl136II rev'
MP::PIN8	'SALK_107965 RP' and 'WiscDsLox489-492C10 RP'
MP::PIN5	'PIN5 ox SmaI forw' and 'PIN5 ox BamHI rev 2'

Table 2.3. Oligonucleotide sequences.

Name	Sequence (5' to 3')
PIN5 SpeI KpnI transc forw	ATAACTAGTGGTACCGAGAGAGAGAGAGAGAGAC
PIN5 AgeI transc rev	CTCACCGGTTTTTATCAGAAAAATAGAAATGTTGCAG
PIN5 extra prom XhoI forw	ATACTCGAGAGCAGGCGAATCAGGAAGATCAAC
PIN5 extra prom SalI rev	ATTGTCGACTCTCTCTCTCTCTCTCTCTCTCTC
PIN5 prom XhoI forw	ATTCTCGAGACGGAGAAAGGAGAAGAAC
PIN5 4991 BamHI rev	ATAGGATCCTCCATATTCCTTAGCAAAAATGAAC
PIN5 4992 XbaI forw	ATGTCTAGATTACATGCAGATGTTCTAAG
PIN5 UTR SacI rev	ATAGAGCTCATTCGGTTGAGGAGAAAG
PIN5 extra UTR SmaI forw	ATTCCCGGGCAATATGAAGATAAAAGGG
PIN5 extra UTR SacI rev	ATAGAGCTCAGCCACGAACAGAAACCATCAAG
EGFP BamHI forw	TATGGATCCGTGAGCAAGGGCGAGGAG
EGFP XbaI rev	TATTCTAGACTTGTACAGCTCGTCCATGC
PIN6 prom SalI F	GCGGTCGACTGATGATTGTTTAAGATAAG
PIN6 prom BamHI R	TCTGGATCCTCTTTGCCTCTTCTTCTTC
0.28 PIN1p SalI	GCGGTCGACTACACGTAAACTACTTTTG
pin1-1 R	TTCCGACCACCACCAGAAGCC
pin1-1 F	ATGATTACGGCGGCGGACTTCTA
Pin1-1 WT KpnI Fwd	TTCTCTCTCTCGACACTCCCC
Pin1-1 WT KpnI Rev	CAAAGAGAAAGAGCATGAGTGGGTAC
SALK_042994 LP	TGTGGTTGTGGGAGAGAAGTC
SALK_042994 RP	AAATTTGGACTTACGCTGTGC

LBb1.3	ATTTTGCCGATTTCGGAAC
PIN6 prom seq forw	GGTAATCTCGTCAACAAGTCTC
PIN6 spm R	GGAGTTCAAAGAGGAATAGTAGCAGAG
PIN6 spm F	CATAACGAAGCTAACTAAGGGGTAATCTC
Spm32	TACGAATAAGAGCGTCCATTTTAGAGTG
SALK_107965 LP	TGAAAGACATTTTGATGGCATC
SALK_107965 RP	CCAAATCAAGCTTTGCAAGAC
PIN6 ox SmaI forw	ATACCCGGGATGATAACGGGAAACGAATTCTAC
PIN6 ox Ecl136II rev	ATTGAGCTCTCATAGGCCCAAGAGGACG
WiscDsLox489-492C10 RP	TTGGAAAGGAAAAGAACACCC
PIN5 ox SmaI forw	ATACCCGGGATGATAAATTGTGGAGA
PIN5 ox BamHI rev 2	ATTGGATCCTCAATGAATAAACTCCAGAGC

Table 2.4. Imaging parameters: single-marker lines.

Line	Laser	Wavelength (nm)	Main dichroic beam splitter	First secondary dichroic beam splitter	Second secondary dichroic beam splitter	Emission filter (detector)
PIN1::PIN1:CFP	Ar	458	HFT 458/543	NFT 595	NFT 545	BP 475–525
PIN6::YFPnuc	Ar	514	HFT 405/514/594	NFT 595	NFT 515	BP 520–555 IR (PMT3)
PIN6::CFPnuc	Ar	458	HFT 458/543	NFT 595	NFT 545	BP 475–525
PIN8::YFPnuc	Ar	514	HFT 405/514/594	NFT 595	NFT 515	BP 520–555 IR (PMT3)
PIN1::PIN1:GFP	Ar	488	HFT 405/488/594	NFT 545	NFT 490	BP 505–530 (PMT3)
PIN5::YFPnuc	Ar	514	HFT 405/514/594	NFT 595	NFT 515	BP 520–555 IR (PMT3)
DR5rev::YFPnuc	Ar	514	HFT 405/514/594	NFT 595	NFT 515	BP 520–555 IR (PMT3)

Table 2.5. Imaging parameters: double-marker lines.

Double-marker lines	Single-marker lines	Laser	Wavelength (nm)	Main dichroic beam splitter	First secondary dichroic beam splitter	Second secondary dichroic beam splitter	Emission filter (detector)
PIN1::PIN1:GFP; autofluorescence	PIN1::PIN1:GFP	Ar	488	HFT 405/488/594			507–593 (META)
	Autofluorescence	Ar	488	HFT 405/488/594			507–593 (META)
PIN6::PIN6:GFP^{MGS}; autofluorescence	PIN6::PIN6:GFP^{MGS}	Ar	488	HFT 405/488/594			507–593 (META)
	Autofluorescence	Ar	488	HFT 405/488/594			507–593 (META)
PIN6::PIN6:GFP^{RLB}; autofluorescence	PIN6::PIN6:GFP^{RLB}	Ar	488	HFT 405/488/594	Mirror	NFT 545	BP 505–530 (PMT2)
	Autofluorescence	Ar	488	HFT 405/488/594	Mirror	NFT 545	BP 600–650 (PMT3)
PIN8::PIN8:GFP^{MGS}; autofluorescence	PIN5::PIN5:GFP	Ar	488	HFT 405/488/594			507–593 (META)
	Autofluorescence	Ar	488	HFT 405/488/594			507–593 (META)

PIN8::PIN8:GFP^{ZD}; autofluorescence	PIN8::PIN8:GFP^{ZD}	Ar	488	HFT 405/488/594	Mirror	NFT 545	BP 505–530 (PMT2)
	Autofluorescence	Ar	488	HFT 405/488/594	Mirror	NFT 545	BP 600–650 (PMT3)
PIN5::PIN5:GFP; autofluorescence	PIN5::PIN5:GFP	Ar	488	HFT 405/488/594			507–593 (META)
	Autofluorescence	Ar	488	HFT 405/488/594			507–593 (META)
PIN1::PIN1:GFP; PIN5::YFPnuc	PIN1::PIN1:GFP	Ar	488	HFT 405/488/594			507–593 (META)
	PIN5::YFPnuc	Ar	488	HFT 405/488/594			507–593 (META)
PIN1::PIN1:GFP; PIN6::YFPnuc	PIN1::PIN1:GFP	Ar	488	HFT 405/488/594			507–593 (META)
	PIN6::YFPnuc	Ar	488	HFT 405/488/594			507–593 (META)
PIN1::PIN1:GFP; PIN8::YFPnuc	PIN1::PIN1:GFP	Ar	488	HFT 405/488/594			507–593 (META)
	PIN8::YFPnuc	Ar	488	HFT 405/488/594			507–593 (META)

PIN6::CFPnuc; PIN5::YFPnuc	PIN6::CFPnuc	Ar	458	HFT 458/514	NFT 595	NFT 545	BP 475–525 (PMT2)
	PIN5::YFPnuc	Ar	514	HFT 458/514	NFT 595	NFT 515	BP 520–355 IR (PMT3)
PIN8::PIN8:GFP; PIN5::YFPnuc	PIN8::PIN8:GFP	Ar	488	HFT 405/488/594			507–593 (META)
	PIN5::YFPnuc	Ar	488	HFT 405/488/594			507–593 (META)
PIN6::CFPnuc; PIN8::YFPnuc	PIN6::CFPnuc	Ar	458	HFT 458/514	NFT 595	NFT 545	BP 475–525 (PMT2)
	PIN8::YFPnuc	Ar	514	HFT 458/514	NFT 595	NFT 515	BP 520–355 (PMT3)

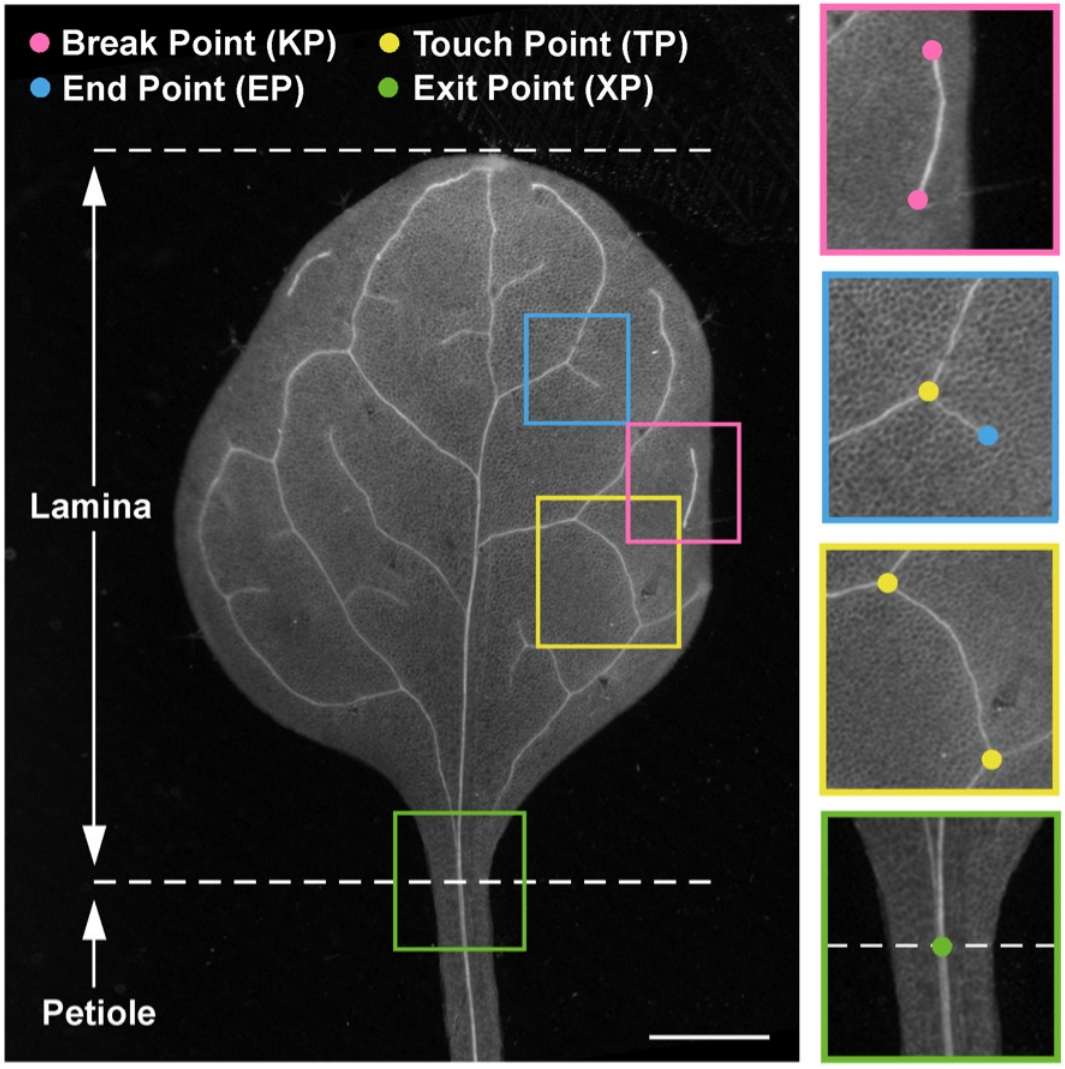

Figure 2.15. Analysis of vein network topology. Dark-field illumination of cleared mature first leaf (MP::PIN6) illustrating vein network elements. A "vein fragment" (magenta box) is incident to two "break points" (KPs; magenta dots)—the points where a vein fragment terminates free of contact with veins or other vein fragments. An "open vein" (blue box) is incident to a "touch point" (TP; yellow dot)—a point of contact between a vein and vein fragments or other veins—and an "end point" (EP; blue dot)—the point where an open vein terminates free of contact with another vein or a vein fragment. A "closed vein" (yellow box) is incident to two TPs. A vein or a vein fragment exits the leaf lamina and enters the leaf petiole (green box) by an "exit point" (XP; green dot). See text for details. Bar: 1 mm.

KPs and XPs in dark-field images of cleared mature leaves was calculated with the Cell Counter plugin of ImageJ (National Institutes of Health).

A vein network can be understood as an undirected graph in which TPs, EPs, KPs and XPs are vertices, and veins and vein fragments are edges. Because each vein is incident to two TPs, a TP and an XP, a TP and an EP, or an XP and an EP, the cardinality index—a measure of the size (i.e. the number of edges) of a graph—is a proxy for the number of veins and is calculated as: $[(TP+XP-EP)/2]+EP$, or: $(TP+XP+EP)/2$.

The continuity index quantifies how close a vein network is to a network with the same number of veins but in which at least one end of each vein fragment contacts a vein, and is thus calculated as the ratio of the cardinality index of the first network to the cardinality index of the second network: $[(TP+XP+EP)/2]/[(TP+XP+EP+KP)/2]$, or: $(TP+XP+EP)/(TP+XP+EP+KP)$.

The connectivity index quantifies how close a vein network is to a network with the same number of veins but in which both ends of each vein or vein fragment contact other veins, and is thus calculated as the ratio of the number of closed veins in the first network to the number of closed veins in the second network (i.e. the cardinality index of the second network): $[(TP+XP-EP)/2]/[(TP+XP+EP+KP)/2]$, or: $(TP+XP-EP)/(TP+XP+EP+KP)$.

CHAPTER 3: TRANSCRIPTIONAL CONTROL OF *PIN1*-DEPENDENT VEIN NETWORK PATTERNING

3.1 Introduction

The problem of long-distance transport is solved in most multicellular organisms by tissue networks; how these networks form is thus a key question in biology. In some tissue networks, such as the vessel networks of mammals and the airway systems of insects, the formation of network elements is driven by cell movements [e.g., (Samakovlis et al. 1996; Gerhardt et al. 2003)]; in others, such as the vein networks of insect wings and plant leaves, it is not (Bryant 1970; García-Bellido and Merriam 1971).

Unlike the vein networks of insect wings, which are invariant [compare, for example, (Bier 2000) and (De Celis 2003)], the vein networks of plant leaves are both reproducible and variable (Sachs 1989; Berleth et al. 2000). Consider, for example, the vein network of an Arabidopsis leaf (Telfer and Poethig 1994; Nelson and Dengler 1997; Kinsman and Pyke 1998; Candela et al. 1999; Mattsson et al. 1999; Sieburth 1999; Steynen and Schultz 2003): lateral veins branch from an I-shaped midvein and connect to distal veins to form loops; minor veins branch from midvein and loops and connect to other veins to form a mesh; and loops and minor veins curve near the leaf margin to lend a scalloped outline to the vein network. Features of the vein network such as these are reproducible from leaf to leaf, so much so that they are used as a taxonomic characteristic [e.g., (Klucking 1995)]. By contrast, features such as the number of veins; their shape, length and position; and whether they contact other veins at both their ends or only one of them, and if so which one, differ from leaf to leaf (Kinsman and Pyke 1998; Candela et al. 1999; Steynen and Schultz 2003; Kang and Dengler 2004; Scarpella et al. 2004; Sawchuk et al. 2007; Rolland-Lagan et al. 2009; Price et al. 2011; Dhondt et al. 2012; Verna et al. 2015) (Chapter 2).

The *PIN-FORMED1* (*PIN1*) gene of Arabidopsis is the only known gene to be nonredundantly required for both the reproducible features of leaf vein networks and their variable ones. Leaves of *pin1* mutants occasionally fail to separate ("fused leaves"), and their midvein often branches near the leaf tip into a Y-shaped vein (Okada et al. 1991; Mattsson et al. 1999; Bilsborough et al. 2011; Sawchuk et al. 2013). Furthermore, the vein networks of *pin1* leaves have more veins, which are more frequently connected to other veins on both ends (Verna et al. 2015) (Chapter 2). The plasma-membrane-localized PIN1 protein catalyzes cellular efflux of the plant signal auxin and is expressed in all the cells of the leaf at early stages of tissue development; over time, however, epidermal expression becomes restricted to the basal-most cells and inner expression becomes restricted to files of vascular precursor cells (Galweiler et al. 1998; Benkova et al. 2003; Reinhardt et al. 2003; Heisler et al. 2005; Petrasek et al. 2006; Scarpella et al. 2006; Wenzel et al. 2007; Bayer et al. 2009; Sawchuk et al. 2013; Marcos and Berleth 2014).

Here we sought to understand the cis-regulation of *PIN1* function in the patterning of leaf vein networks. We found that the expression of PIN1 that is required for vein network patterning depends on the 205-bp region of the *PIN1* promoter from -699 to -495, which contains conserved putative binding-sites for transcription factors of the MYELOBLASTOMA and DNA-BINDING WITH ONE FINGER families.

3.2 Results and Discussion

3.2.1 Functional activity of the Arabidopsis *PIN-FORMED1* promoter in vein network patterning

In Arabidopsis leaf development, the formation of the midvein is followed by the formation of the first loops of veins ("first loops"), which in turn is followed by the formation of the second and third loops, and of minor veins in the area delimited by midvein and first loops (Mattsson et

al. 1999; Sieburth 1999; Kang and Dengler 2004; Scarpella et al. 2004; Sawchuk et al. 2007) (Fig. 3.1A–D). Loops and minor veins form first in the apical part of the leaf and then progressively closer to the base of it, and minor veins form after loops in the same area of the leaf (Fig. 3.1B–D).

Consistent with previous reports (Benkova et al. 2003; Reinhardt et al. 2003; Heisler et al. 2005; Scarpella et al. 2006; Sawchuk et al. 2007; Wenzel et al. 2007; Bayer et al. 2009; Sawchuk et al. 2013; Marcos and Berleth 2014), a fusion of the *PIN-FORMED1* (*PIN1*) open reading frame to YFP driven by the 4,171-bp *PIN1* upstream sequence ("promoter") and 1,173-bp *PIN1* downstream sequence (PIN1::gPIN1:YFP) (Xu et al. 2006) was expressed in all the cells of the leaf at early stages of tissue development; over time, however, epidermal expression became restricted to the basal-most cells and inner expression became restricted to files of vascular precursor cells (Fig. 3.1E–H).

We first asked whether PIN1::gPIN1:YFP expression were recapitulated by the activity of the 4,171-bp *PIN1* promoter. To address this question, we imaged expression of a nuclear YFP driven by the 4,171-bp *PIN1* promoter (PIN1::nYFP) in first leaves 2, 2.5, 3 and 4 days after germination (DAG).

Just as PIN1::gPIN1:YFP expression (Fig. 3.1E–H), PIN1::nYFP was expressed in all the inner cells of the leaf at early stages of tissue development, and over time this expression became restricted to files of vascular precursor cells (Fig. 3.1I–M). Unlike PIN1::gPIN1:YFP and PIN1::gPIN1:CFP [a fusion of the *PIN1* open reading frame to CFP driven by the 3,506-bp *PIN1* promoter and 2,181-bp *PIN1* downstream sequence (Gordon et al. 2007)] (Fig. 3.1E–H,M), however, PIN1::nYFP was only expressed in very few epidermal cells at the tip of 2-DAG leaves and at the margin of 2.5-DAG leaves (Fig. 3.1I–M), and this expression was very infrequent (Fig. 3.1I,J); PIN1::nYFP expression in epidermal cells at the leaf margin was more frequent at 3 and 4 DAG but was still limited to very few cells (Fig. 3.1K–M). Because a fusion of the *PIN1* coding sequence to GFP driven by the 4,168-bp *PIN1* promoter (PIN1::cPIN1:GFP) was hardly expressed in epidermal cells, we conclude that the already limited activity of the 4,168-bp *PIN1* promoter in the leaf epidermis is suppressed post-transcriptionally by the *PIN1* coding sequence and that the epidermal expression characteristic of PIN1 is encoded in the gene's introns or downstream sequence.

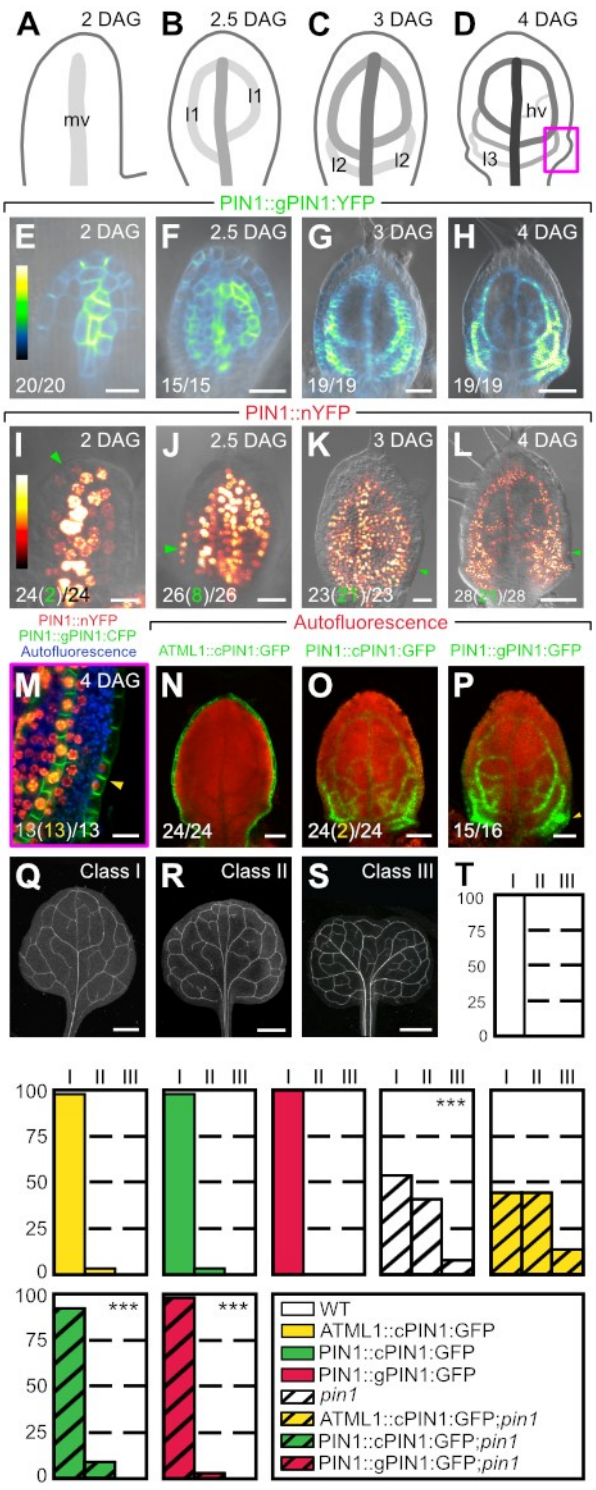

Figure 3.1. PIN1 expression in Arabidopsis first-leaf development. (A–P). Top right: leaf age in days after germination (DAG); bottom left: reproducibility index (in white for inner-tissue expression; in green or yellow for epidermal expression). (A–D) Midvein, loops and minor veins

form sequentially in leaf development (Mattsson et al. 1999; Sieburth 1999; Kang and Dengler 2004; Scarpella et al. 2004; Sawchuk et al. 2007); increasingly darker greys depict progressively later stages of vein development. Box in (D) illustrates position of closeup in (M). (E–P) Confocal laser scanning microscopy with (E–L) or without (M–P) transmitted light; first leaves. Lookup tables in (E–H)—ramp in (E)—and in (I–L)—ramp in (I)—visualize expression levels. Green arrowheads in (I–L) and yellow arrowheads in (M,P) point to epidermal expression. (Q–S) Dark-field illumination of mature first leaves illustrating phenotype classes: I-shaped midvein and scalloped vein-network outline (Q); Y-shaped midvein and scalloped vein-network outline (R); fused leaves with scalloped vein-network outline (S). (T) Percentages of leaves in phenotype classes. Difference between *pin1* and WT, between PIN1::cPIN1:GFP;*pin1* and *pin1* and between PIN1::gPIN1:GFP;*pin1* and *pin1* was significant at $P < 0.001$ (***) by Kruskal-Wallis and Mann-Whitney test with Bonferroni correction. Sample population sizes: WT, 40; *pin1*, 60; ATML1::cPIN1:GFP, 49; PIN1::cPIN1:GFP, 48; PIN1::gPIN1:GFP, 55; ATML1::cPIN1:GFP;*pin1*, 55; PIN1::cPIN1:GFP;*pin1*, 51; PIN1::gPIN1:GFP;*pin1*, 60. hv, minor vein; l1, first loop; l2, second loop; l3, third loop; mv, midvein. Bars: (E,I,M) 10 μm; (J,K) 15 μm; (C,G) 20 μm; (H,L,N–P) 50 μm; (Q) 1 mm; (R–S) 2 mm.

We next asked what the function in vein network patterning was of PIN1 expression in leaf epidermis and inner tissue. To address this question, we expressed in WT and *pin1* mutant backgrounds: (1) cPIN1:GFP driven by the epidermis-specific *ARABIDOPSIS THALIANA MERISTEM LAYER1* promoter (Sessions et al. 1999) (ATML1::cPIN1:GFP) (Fig. 3.1N); (2) PIN1::cPIN1:GFP, which is expressed in the leaf inner tissue (Fig. 3.1O); (3) PIN1::gPIN1:GFP [a fusion of the *PIN1* open reading frame to GFP driven by the 4,171-bp *PIN1* promoter and 1,173-bp *PIN1* downstream sequence; (Xu et al. 2006)], which as PIN1::gPIN1:YFP and PIN1::gPIN1:CFP (Fig. 3.1E–H,M) is expressed in both leaf epidermis and inner tissue (Fig. 3.1P). We then compared vein network patterns of mature first leaves of WT, *pin1*, ATML1::cPIN1:GFP, PIN1::cPIN1:GFP, PIN1::gPIN1:GFP, ATML1::cPIN1:GFP;*pin1*, PIN1::cPIN1:GFP;*pin1* and PIN1::gPIN1:GFP;*pin1*.

Consistent with previous reports (Sawchuk et al. 2013; Verna et al. 2015) (Chapter 2), the vein network patterns of nearly 50% of *pin1* leaves were abnormal (Fig. 3.1Q–T). The vein network patterns of ATML1::cPIN1:GFP, PIN1::cPIN1:GFP and PIN1::gPIN1:GFP were no different from the vein network pattern of WT (Fig. 3.1Q–T). Both PIN1::gPIN1:GFP and PIN1::cPIN1:GFP shifted the phenotype spectrum of the vein network patterns of *pin1* toward the vein network pattern of WT, but ATML1::cPIN1:GFP failed to do so (Fig. 3.1Q–T).

These observations suggest that PIN1 expression in epidermal cells is insufficient for *PIN1*-dependent vein-network patterning. By contrast, *PIN1* function in vein network patterning depends mainly, or only, on the expression of PIN1 in leaf inner tissue, which is controlled by the activity of the *PIN1* promoter.

3.2.2 Cis-regulation of *PIN1* function in vein network patterning

We next asked what cis-regulatory elements were required for *PIN1* function in vein network patterning. To address this question, we deleted increasingly longer regions from the 5'-end of the 4,168-bp *PIN1* promoter avoiding the disruption of putative transcription-factor binding-sites identified by bioinformatics tools (see Materials & Methods) (Fig. 3.2A); used the resulting 15

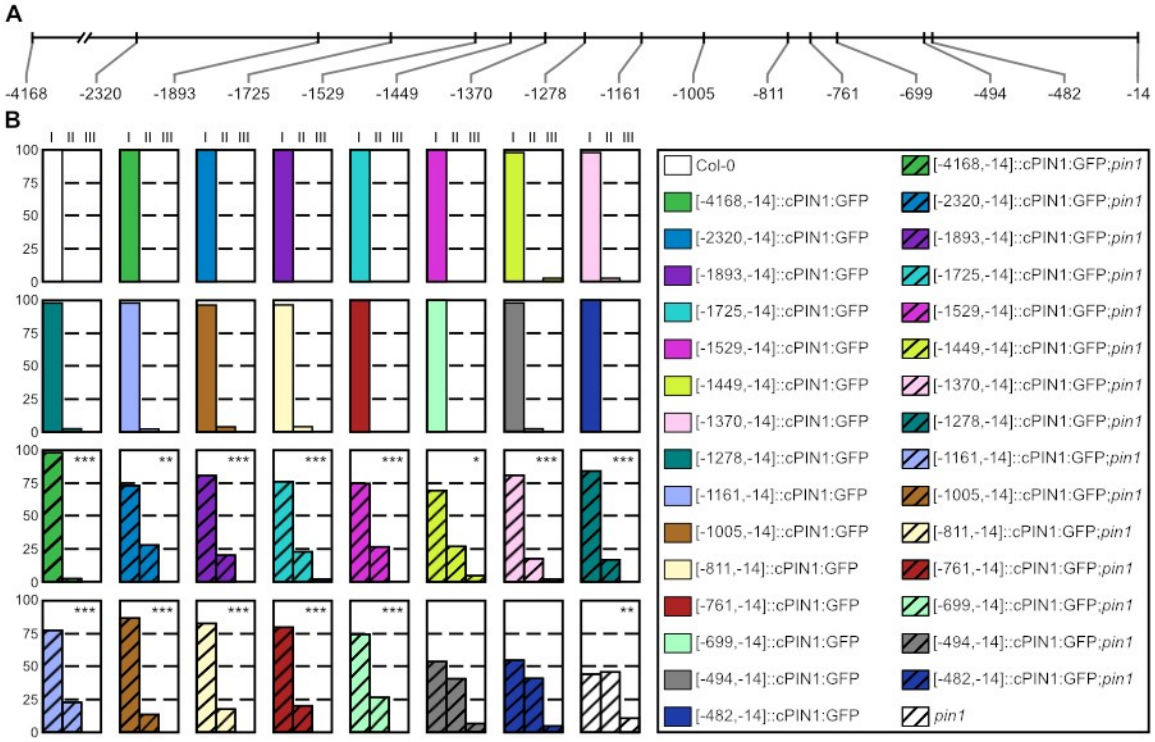

Figure 3.2. Function of *PIN1* promoter fragments in *PIN1*-dependent vein-network formation. (A) *PIN1* promoter. Coordinates relative to start-codon's first nucleotide. (B) Percentages of leaves in phenotype classes (defined in Fig. 3.1). Difference between *pin1* and WT, between [-2,320,-14]::cPIN1:GFP;*pin1* and *pin1*, between [-1,893,-14]::cPIN1:GFP;*pin1* and *pin1*,between [-1,725,-14]::cPIN1:GFP;*pin1* and *pin1*, between [-1,529,-14]::cPIN1:GFP;*pin1* and *pin1*,between [-1,449,-14]::cPIN1:GFP;*pin1* and *pin1*, between [-1,370,-14]::cPIN1:GFP;*pin1* and *pin1*,between [-1,278,-14]::cPIN1:GFP;*pin1* and *pin1*, between [-1,161,-14]::cPIN1:GFP;*pin1* and *pin1*,between [-1,005,-14]::cPIN1:GFP;*pin1* and *pin1*, between [-811,-14]::cPIN1:GFP;*pin1* and *pin1*,between [-761,-14]::cPIN1:GFP;*pin1* and *pin1* and between [-699,-14]::cPIN1:GFP;*pin1* and *pin1* was significant at $P < 0.05$ (*), $P < 0.01$ (**) or $P < 0.001$ (***) by Kruskal-Wallis and Mann-Whitney test. Sample population sizes: WT, 41; *pin1*, 57; PIN1::cPIN1:GFP, 47; [-2,320,-14]::cPIN1:GFP, 47; [-1,893,-14]::cPIN1:GFP, 54; [-1,725,-14]::cPIN1:GFP, 51; [-1,529,-14]::cPIN1:GFP, 51; [-1,449,-14]::cPIN1:GFP, 53; [-1,370,-14]::cPIN1:GFP, 50; [-1,278,-14]::cPIN1:GFP, 52; [-1,161,-14]::cPIN1:GFP, 51; [-1,005,-14]::cPIN1:GFP, 53; [-811,-14]::cPIN1:GFP, 27; [-761,-14]::cPIN1:GFP, 51; [-699,-14]::cPIN1:GFP, 49; [-494,-14]::cPIN1:GFP, 47; [-482,-14]::cPIN1:GFP, 52; PIN1::cPIN1:GFP;pin1, 54; [-2,320,-14]::cPIN1:GFP;*pin1*, 51; [-1,893,-14]::cPIN1:GFP;*pin1*,

56; [-1,725,-14]::cPIN1:GFP;*pin1*, 58; [-1,529,-14]::cPIN1:GFP;*pin1*, 58; [-1,449,-14]::cPIN1:GFP;*pin1*, 45; [-1,370,-14]::cPIN1:GFP;*pin1*, 58; [-1,278,-14]::cPIN1:GFP;*pin1*, 62; [-1,161,-14]::cPIN1:GFP;*pin1*, 58; [-1,005,-14]::cPIN1:GFP;*pin1*, 52; [-811,-14]::cPIN1:GFP;*pin1*, 29; [-761,-14]::cPIN1:GFP;*pin1*, 40; [-699,-14]::cPIN1:GFP;*pin1*, 58; [-494,-14]::cPIN1:GFP;*pin1*, 67; [-482,-14]::cPIN1:GFP;*pin1*, 44.

PIN1 promoter fragments (Fig. 3.2A)—collectively referred to as *ΔPIN1* hereafter—to drive cPIN1:GFP expression in WT and *pin1* mutant backgrounds; and compared vein network patterns of mature first leaves of WT, *pin1*, PIN1::cPIN1:GFP, ΔPIN1::cPIN1:GFP, PIN1::cPIN1:GFP;*pin1* and ΔPIN1::cPIN1:GFP;*pin1*.

Consistent with previous reports (Sawchuk et al. 2013; Verna et al. 2015) (Chapter 2) and as shown above (Fig. 3.1Q–T), the vein network patterns of nearly 50% of *pin1* leaves were abnormal (Fig. 3.2B). As also shown above (Fig. 3.1Q–T), the vein network patterns of PIN1::cPIN1:GFP were no different from the vein network pattern of WT (Fig. 3.2B). The vein network patterns of ΔPIN1::cPIN1:GFP were also no different from the vein network pattern of WT (Fig. 3.2B). As shown above (Fig. 3.1Q–T), PIN1::cPIN1:GFP shifted the phenotype spectrum of the vein network patterns of *pin1* toward the vein network pattern of WT (Fig. 3.2B). Also [-2,320,-14]::cPIN1:GFP, [-1,893,-14]::cPIN1:GFP, [-1,725,-14]::cPIN1:GFP, [-1,529,-14]::cPIN1:GFP, [-1,449,-14]::cPIN1:GFP, [-1,370,-14]::cPIN1:GFP, [-1,278,-14]::cPIN1:GFP, [-1,161,-14]::cPIN1:GFP, [-1,005,-14]::cPIN1:GFP, [-811,-14]::cPIN1:GFP, [-761,-14]::cPIN1:GFP and [-699,-14]::cPIN1:GFP shifted the phenotype spectrum of the vein network patterns of *pin1* toward the vein network pattern of WT (Fig. 3.2B). By contrast, [-494,-14]::cPIN1:GFP and [-482,-14]::cPIN1:GFP failed to do so (Fig. 3.2B).

The [-699,-14] fragment was thus the shortest *PIN1* promoter fragment that drove cPIN1:GFP expression so as to shift the phenotype spectrum of the vein network patterns of *pin1* toward the vein network pattern of WT, and the [-494,-14] fragment was the longest promoter fragment that failed to do so. We therefore conclude that the 205-bp region of the *PIN1* promoter between -699 and -495 is required for *PIN1* function in vein network patterning.

3.2.3 Cis-regulation of PIN1 functional expression in vein network patterning

We then asked what the domains of activity were of the 15 *PIN1* promoter fragments (Fig. 3.2A). To address this question, we imaged ΔPIN1::cPIN1:GFP expression in 4-DAG first leaves.

Consistent with the activity of the *PIN1* promoter reported by PIN1::nYFP expression (Fig. 3.1I–M), and as shown above (Fig. 3.1O), the 4,168-bp *PIN1* promoter drove cPIN1:GFP expression in all the veins and in nearly all the inner cells in the area delimited by the midvein and by second and third loops (Fig. 3.3A). The [-2,320,-14], [-1,893,-14], [-1,725,-14], [-1,529,-14] and [-1,449,-14] fragments drove cPIN1:GFP expression in all the veins (Fig. 3.3B–F). The [-1,370,-14], [-1,278,-14] and [-1,161,-14] fragments drove cPIN1:GFP expression in the midvein, first loops and very few epidermal cells at the leaf margin (Fig. 3.3G–I). The [-1,005,-14], [-811,-14], [-761,-14] and [-699,-14] fragments drove cPIN1:GFP expression in the most apical part of the midvein and first loops, and in very few epidermal cells at the leaf margin (Fig. 3.3K–M). Finally, the [-494,-14] and [-482,-14] fragments drove cPIN1:GFP expression only in very few epidermal cells at the leaf margin (Fig. 3.3N,O).

Because the [-699,-14] fragment was the shortest *PIN1* promoter fragment that drove cPIN1:GFP expression in midvein and first loops and the [-494,-14] was the longest one that failed to do so, we conclude that the 205-bp region of the *PIN1* promoter between -699 and -495 is required for expression in midvein and first loops. Because this same region of the *PIN1* promoter is also required for *PIN1* function in vein network patterning (Fig. 3.2B), we further conclude that PIN1 expression in midvein and first loops is required for *PIN1* function in vein network patterning.

3.2.4 Cis-regulatory elements controlling PIN1 functional expression in vein network patterning

To identify conserved transcription-factor binding sites in the 205-bp region of the *PIN1* promoter that is required for PIN1 functional expression in vein network patterning, we compared the sequence of this promoter region of *Arabidopsis thaliana* with that of the corresponding promoter region in species of the Brassicaceae family of Lineage I (Franzke et al. 2011) and for which whole-genome sequence is available.

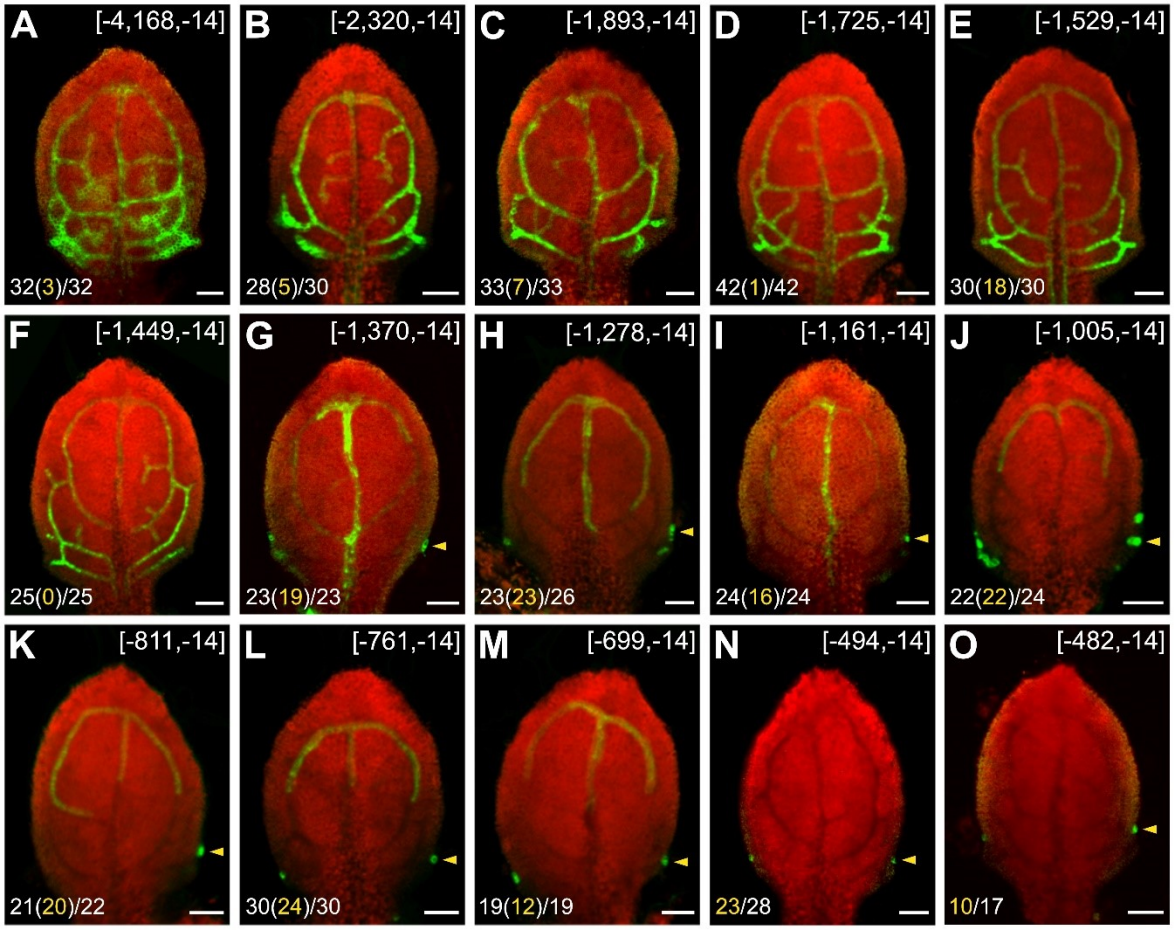

Figure 3.3. Activity of *PIN1* promoter fragments in developing leaves. (A–O). Confocal laser scanning microscopy; first leaves 4 days after germination. Green, cPIN1:GFP expression; red, autofluorescence. Yellow arrowheads point to epidermal expression. Top right: promoter fragment coordinates; bottom left: reproducibility index (in white for inner-tissue expression; in yellow for epidermal expression). Bars: (A–O) 50 μm.

The 205-bp region of the *PIN1* promoter that is required for PIN1 functional expression in vein network patterning contains two conserved putative binding-sites for transcription factors of the MYELOBLASTOMA (MYB) family (Prouse and Campbell 2012) and three conserved putative binding-sites for transcription factors of the DNA-BINDING WITH ONE ZINC FINGER (DOF) family (Yanagisawa 2002) (Fig 3.4). Therefore, it is possible that MYB or DOF transcription factors control PIN1 functional expression in vein network patterning.

However, it is also possible that PIN1 functional expression in vein network patterning depends on unknown transcription-factor binding sites that overlap the 3'-end of the 205-bp region of the *PIN1* promoter or are in the conserved parts of that promoter region where no known transcription-factor binding sites were identified.

It is also possible that the cis-regulatory elements controlling PIN1 functional expression in vein network patterning are highly degenerate and thus that their sequence is not conserved, or that the sequence of such elements is conserved but that of the surrounding promoter context is not, as in some gene regulatory networks of both plants and animals (Wilson and Odom 2009; Dowell 2010; Moyroud et al. 2011).

Finally, consistent with some findings in animals [reviewed in (Carroll et al. 2005; Wray 2007)], it is also possible that PIN1 expression is not conserved in Brassicaceae and that the cis-regulatory elements controlling PIN1 functional expression in vein network patterning of *Arabidopsis thaliana* are thus in the non-conserved parts of the 205-bp promoter region.

Though it will be interesting to identify the transcription factors that bind the 205-bp region of the *PIN1* promoter that is required for PIN1 functional expression in vein network patterning, our results already define cis-regulation of *PIN1* function in this process.

3.3 Materials and methods

Figure 3.4. Conserved cis-regulatory elements in *PIN1* promoter in Brassicaceae species. Sequence alignment of the 205-bp region of the *PIN1* promoter of *Arabidopsis thaliana* between -699 and -495 (chromosome 1, position 27,659,063–27,659,287) that is required for *PIN1* function in vein network patterning with corresponding regions in *Arabidopsis hallerii* (scaffold 146, position 30,168–30,215; and scaffold 21,076, position 5,681–5,807), *Arabidopsis lyrata* (scaffold 2, position 3,670,880–3,670,921; and scaffold 2, position 15,881,035–15,881,162), *Boechera stricta* (scaffold 697, position 125,664–125,703; and scaffold 10,273, position 35,418–35,541), *Capsella grandiflora* (scaffold 8,914, position 410–434; and scaffold 17,308, position 11,728–11,822) and *Capsella rubella* (scaffold 5, position 384,331–384,361; scaffold 1, position 6,467,999–6,468,037; and scaffold 2, position 11,229,465–11,229,560). Grey highlight, sequence identity. Conserved, putative transcription-factor binding sites are below sequence alignment.

3.3.1 Plants

Origin and nature of lines and oligonucleotide sequences are in Tables 3.1 and 3.2. Seeds were sterilized and sown as in Sawchuk et al. 2008. Stratified seeds were germinated and seedlings were grown at 22°C under continuous fluorescent light (~80 μmol $m^{-2}s^{-1}$). Plants were grown at 25°C under fluorescent light (~100 μmol $m^{-2}s^{-1}$) in a 16-h-light/8-h-dark cycle. *pin1-051* was genotyped with the "pin1 GK LP" and "pin1 GK RP" primers (WT allele) and with the "pin1 GK RP" and "o8409" primers (mutant allele). Plants were transformed and representative lines were selected as described in Sawchuk et al. 2008.

3.3.2 Imaging

Developing leaves were mounted and imaged as in Sawchuk et al. 2013. Light paths are in Tables 3.3. and Table 3.4 Images in stacks were aligned with the Scale Invariant Feature Transform algorithm (Lowe 2004) and maximum-intensity projection was applied to aligned image stacks in the Fiji distribution (Schindelin et al. 2012) of ImageJ (Schneider et al. 2012; Schindelin et al. 2015; Rueden et al. 2017). Mature leaves were fixed in 6 : 1 ethanol : acetic acid, rehydrated in 70% ethanol and water, mounted in 8 : 2 : 1 chloral hydrate : glycerol : water and imaged as in Odat et al. 2014. Image brightness and contrast were adjusted by linear stretching of the histogram in Fiji. Images were rotated and cropped in Affinity Photo (Serif Europe Ltd. Nottingham, UK) and assembled into figures in Affinity Designer.

3.3.3 Bioinformatics

Sequences were retrieved with Phytozome 12 (Goodstein et al. 2012) (http://www.phytozome.net/). Putative transcription-factor binding sites were identified with

Table 3.1. Origin and nature of lines.

Line	Origin/Nature
PIN1::gPIN1:YFP	Xu et al. 2006
PIN1::nYFP	Transcriptional fusion of *PIN1* (AT1G73590; -4,171 to -1; primers: 'PIN1 transc 4171 forw' and 'PIN1 transc rev') to HTA6:EYFP (Zhang et al. 2005)
PIN1::gPIN1:CFP	Gordon et al. 2007
PIN1::cPIN1:GFP	Transcriptional fusion of *PIN1* (-4,168 to -14; primers 'XhoI full length PIN1p F' and 'BamHI PIN1p rev') to translational fusion of *PIN1* cDNA (GenBank accession no. AY093960; ABRC clone no. U12338; primers 'BamHI PIN1 cDNA F' and 'KpnI PIN1 cDNA R') to EGFP (Clontech insertion after +651 of *PIN1*; primers 'XhoI GFP no ATG Fwd' and 'XhoI GFP no* Rev')
ATML1::cPIN1:GFP	Transcriptional fusion of *ATML1* (AT4G21750; -5,016 to -1,597, primers 'XhoI ATML1 p F' and 'BamHI ATML1p R') to translational fusion of *PIN1* cDNA (GenBank accession no. AY093960; ABRC clone no. U12338; primers 'BamHI PIN1 cDNA F' and 'KpnI PIN1 cDNA R') to EGFP (Clontech; insertion after +651 of *PIN1*; primers 'XhoI GFP no ATG Fwd' and 'XhoI GFP no* Rev')
PIN1::gPIN1:GFP	Xu et al. 2006
pin1-051	NASC; GK-051A10-012139 (Kleinboelting et al. 2012); contains a T-DNA insertion after +2234 of *PIN1*
[-2,320,-14]::cPIN1:GFP	Transcriptional fusion of *PIN1* (-2,120 to -14, primers 'XhoI 2300 PIN1p F' and 'BamHI PIN1p rev') to translational fusion of *PIN1* cDNA (GenBank accession no.: AY093960; ABRC clone no.:

	U12338; primers 'BamHI PIN1 cDNA F' and 'KpnI PIN1 cDNA R') to a sequence encoding EGFP (Clontech; insertion after +651 of *PIN1*; primers 'XhoI GFP no ATG Fwd' and 'XhoI GFP no* Rev')
[-1,893,-14]::cPIN1:GFP	Transcriptional fusion of *PIN1* (-1,893 to -14, primers 'SalI 1900 PIN1p F' and 'BamHI PIN1p rev') to translational fusion of *PIN1* cDNA (GenBank accession no.: AY093960; ABRC clone no.: U12338; primers 'BamHI PIN1 cDNA F' and 'KpnI PIN1 cDNA R') to a sequence encoding EGFP (Clontech; insertion after +651 of *PIN1*; primers 'XhoI GFP no ATG Fwd' and 'XhoI GFP no* Rev')
[-1,725,-14]::cPIN1:GFP	Transcriptional fusion of *PIN1* (-1,725 to -14, primers 'SalI 1700 PIN1p F' and 'BamHI PIN1p rev') to translational fusion of *PIN1* cDNA (GenBank accession no.: AY093960; ABRC clone no.: U12338; primers 'BamHI PIN1 cDNA F' and 'KpnI PIN1 cDNA R') to a sequence encoding EGFP (Clontech; insertion after +651 of *PIN1*; primers 'XhoI GFP no ATG Fwd' and 'XhoI GFP no* Rev')
[-1,529,-14]: cPIN1:GFP	Transcriptional fusion of *PIN1* (-1,529 to -14, primers 'PIN1 prom 1.5 SalI Fwd' and 'BamHI PIN1p rev') to translational fusion of *PIN1* cDNA (GenBank accession no.: AY093960; ABRC clone no.: U12338; primers 'BamHI PIN1 cDNA F' and 'KpnI PIN1 cDNA R') to a sequence encoding EGFP (Clontech; insertion after +651 of *PIN1*; primers 'XhoI GFP no ATG Fwd' and 'XhoI GFP no* Rev')
[-1,449,-14]::cPIN1:GFP	Transcriptional fusion of *PIN1* (-1,449 to -14, primers 'SalI 1450 PIN1p F' and 'BamHI PIN1p rev') to translational fusion of *PIN1* cDNA (GenBank accession no.: AY093960; ABRC clone no.: U12338; primers 'BamHI PIN1 cDNA F' and 'KpnI PIN1 cDNA R') to a sequence encoding EGFP (Clontech; insertion after +651 of *PIN1*; primers 'XhoI GFP no ATG Fwd' and 'XhoI GFP no* Rev')

[-1,370,-14]::cPIN1:GFP	Transcriptional fusion of *PIN1* (-1,370 to -14, primers 'SalI 1350 PIN1p F' and 'BamHI PIN1p rev') to translational fusion of *PIN1* cDNA (GenBank accession no.: AY093960; ABRC clone no.: U12338; primers 'BamHI PIN1 cDNA F' and 'KpnI PIN1 cDNA R') to a sequence encoding EGFP (Clontech; insertion after +651 of *PIN1*; primers 'XhoI GFP no ATG Fwd' and 'XhoI GFP no* Rev')
[-1,278,-14]::cPIN1:GFP	Transcriptional fusion of *PIN1* (-1,278 to -14, primers 'SalI 1270 PIN1p F' and 'BamHI PIN1p rev') to translational fusion of *PIN1* cDNA (GenBank accession no.: AY093960; ABRC clone no.: U12338; primers 'BamHI PIN1 cDNA F' and 'KpnI PIN1 cDNA R') to a sequence encoding EGFP (Clontech; insertion after +651 of *PIN1*; primers 'XhoI GFP no ATG Fwd' and 'XhoI GFP no* Rev')
[-1,161,-14]::cPIN1:GFP	Transcriptional fusion of *PIN1* (-1,161 to -14, primers 'SalI 1160 PIN1p F' and 'BamHI PIN1p rev') to translational fusion of *PIN1* cDNA (GenBank accession no.: AY093960; ABRC clone no.: U12338; primers 'BamHI PIN1 cDNA F' and 'KpnI PIN1 cDNA R') to a sequence encoding EGFP (Clontech; insertion after +651 of *PIN1*; primers 'XhoI GFP no ATG Fwd' and 'XhoI GFP no* Rev')
[-1,005,-14]::cPIN1:GFP	Transcriptional fusion of *PIN1* (-1,005 to -14, primers 'SalI 1kb PIN1p F' and 'BamHI PIN1p rev') to translational fusion of *PIN1* cDNA (GenBank accession no.: AY093960; ABRC clone no.: U12338; primers 'BamHI PIN1 cDNA F' and 'KpnI PIN1 cDNA R') to a sequence encoding EGFP (Clontech; insertion after +651 of *PIN1*; primers 'XhoI GFP no ATG Fwd' and 'XhoI GFP no* Rev')
[-811,-14]::cPIN1:GFP	Transcriptional fusion of *PIN1* (-811 to -14, primers 'SalI 800 PIN1p F' and 'BamHI PIN1p rev') to translational fusion of *PIN1* cDNA (GenBank accession no.: AY093960; ABRC clone no.: U12338; primers 'BamHI PIN1 cDNA F' and 'KpnI PIN1 cDNA

	R') to a sequence encoding EGFP (Clontech; insertion after +651 of *PIN1*; primers 'XhoI GFP no ATG Fwd' and 'XhoI GFP no* Rev')
[-761,-14]::cPIN1:GFP	Transcriptional fusion of *PIN1* (-761 to -14, primers 'PIN1 prom 0.75 Sal1 Fwd' and 'BamHI PIN1p rev') to translational fusion of *PIN1* cDNA (GenBank accession no.: AY093960; ABRC clone no.: U12338; primers 'BamHI PIN1 cDNA F' and 'KpnI PIN1 cDNA R') to a sequence encoding EGFP (Clontech; insertion after +651 of *PIN1*; primers 'XhoI GFP no ATG Fwd' and 'XhoI GFP no* Rev')
[-699,-14]::cPIN1:GFP	Transcriptional fusion of *PIN1* (-699 to -14, primers 'SalI 700 PIN1p F' and 'BamHI PIN1p rev') to translational fusion of *PIN1* cDNA (GenBank accession no.: AY093960; ABRC clone no.: U12338; primers 'BamHI PIN1 cDNA F' and 'KpnI PIN1 cDNA R') to a sequence encoding EGFP (Clontech; insertion after +651 of *PIN1*; primers 'XhoI GFP no ATG Fwd' and 'XhoI GFP no* Rev')
[-494,-14]::cPIN1:GFP	Transcriptional fusion of *PIN1* (-494 to -14, primers 'PIN1p no DOFs SalI FWD' and 'BamHI PIN1p rev') to translational fusion of *PIN1* cDNA (GenBank accession no.: AY093960; ABRC clone no.: U12338; primers 'BamHI PIN1 cDNA F' and 'KpnI PIN1 cDNA R') to a sequence encoding EGFP (Clontech; insertion after +651 of *PIN1*; primers 'XhoI GFP no ATG Fwd' and 'XhoI GFP no* Rev')
[-482,-14]::cPIN1:GFP	Transcriptional fusion of *PIN1* (-482 to -14, primers '0.47 PIN1p SalI' and 'BamHI PIN1p rev') to translational fusion of *PIN1* cDNA (GenBank accession no.: AY093960; ABRC clone no.: U12338; primers 'BamHI PIN1 cDNA F' and 'KpnI PIN1 cDNA R') to a sequence encoding EGFP (Clontech; insertion after +651 of *PIN1*; primers 'XhoI GFP no ATG Fwd' and 'XhoI GFP no* Rev')

Table 3.2. Oligonucleotide sequences.

Name	Sequence (5' to 3')
PIN1 transc 4171 forw	GGGGACAAGTTTGTACAAAAAAGCAGGCTATGATCCGATTGGATTCG
PIN1 transc rev	GGGGACCACTTTGTACAAGAAAGCTGGGTCTTTTGTTCGCCGGAGAAG
XhoI full length PIN1p F	TGTCTCGAGATCCGATTGGATTCGGTCTG
BamHI PIN1p rev	AAGGGATCCGAGAAGAGAGAGGGAAGAGAG
BamHI PIN1 cDNA F new	TTAGGATCCATGATTACGGCGGCGGACTTC
KpnI PIN1 cDNA R	CTCGGTACCTCATAGACCCAAGAGAATGTAG
XhoI GFP no ATG Fwd	TTACTCGAGAGTGAGCAAGGGCGAGGAGCTGTT
XhoI GFP no* Rev	TATCTCGAGTACTTGTACAGCTCGTCCATGCCGAG
XhoI ATML1 p F	GCCCTCGAGTTTACATTGATTCTGAACTG
BamHI ATML1p R	GATGGATCCTAACCGGTGGATTCAGGGAG
pin GK LP	ACTCTTTGGCAAACACAAACG
pin1 GK RP	CTCTCAGATGCAGGTCTAGGC
o8409	ATATTGACCATCATACTCATTGC
XhoI 2300 PIN1p F	CCGCTCGAGTAAATTATTCCATTGGCGTTG
SalI 1900 PIN1p F	ACCGTCGACCATAACCATAAGTCAAGCCG
SalI 1700 PIN1p F	CCTGTCGACTGGAATGTGAAAAAATCCTGC
PIN1 prom 1.5 SalI Fwd	GGCGTCGACTTCGGATTGCATAACCTA
SalI 1450 PIN1p F	CGGGTCGACGTACTATATATTATTATTATGC
SalI 1350 PIN1p F	GGTGTCGACGAACTGTGTTTGTATGGGATG
SalI 1270 PIN1p F	CCTGTCGACCATCAACCCATTGCTTTTTG
SalI 1160 PIN1p F	GGCGTCGACCTACGTATTTATGTTCAATAAAAC
SalI 1kb PIN1p F	ACCGTCGACCGCAACTACAACTGTAAATG
SalI 800 PIN1p F	GCCGTCGACAGACTTCTATCTTTAAAACC
PIN1 prom 0.75 Sal1 Fwd	GCCGTCGACTCGAGCCTTATATCATCA
SalI 700 PIN1p F	GCCGTCGACTCAATACCAAAAATCCCATC
PIN1p no DOFs SalI FWD	AATGTCGACCACAAGGCCGCCTCTTTCAC
0.47 PIN1p SalI	TAAGTCGAC TCTTTCACTATCCCCAAAGC

Table 3.3. Light paths: single-marker lines.

Line	Laser	Wavelength (nm)	Main dichroic beam splitter	First secondary dichroic beam splitter	Second secondary dichroic beam splitter	Emission filter (detector)
PIN1::gPIN1:YFP	Ar	514	HFT 405/514/594	NFT 595	NFT 515	BP 520–555 IR (PMT3)
PIN1::YFPnuc	Ar	514	HFT 405/514/594	NFT 595	NFT 515	BP 520–555 IR (PMT3)

Table 3.4. Light paths: multiple-marker lines.

Multiple-marker lines	Single-marker lines	Laser	Wavelength (nm)	Main dichroic beam splitter	First secondary dichroic beam splitter	Second secondary dichroic beam splitter	Emission filter (detector)
PIN1::gPIN1:CFP; PIN1::nYFP; autofluorescence	PIN1::gPIN1:CFP	Ar	458	HFT 458/514	NFT 595	NFT 545	BP 475–525 (PMT2)
	PIN1::nYFP	Ar	514	HFT 458/514	NFT 595	NFT 515	BP 520–355 IR (PMT3)
	Autofluorescence	Ar	458	HFT 458/543			BP 475–525
PIN1::cPIN1:GFP; autofluorescence	PIN1::cPIN1:GFP	Ar	488	HFT 405/488/594			507–593 (META)
	Autofluorescence	Ar	488	HFT 405/488/594			507–593 (META)
ATML1::cPIN1:GFP; autofluorescence	ATML1::cPIN1:GFP	Ar	488	HFT 405/488/594			507–593 (META)
	Autofluorescence	Ar	488	HFT 405/488/594			507–593 (META)
PIN1::gPIN1:GFP; autofluorescence	PIN1::gPIN1:GFP	Ar	488	HFT 405/488/594			507–593 (META)
	Autofluorescence	Ar	488	HFT 405/488/594			507–593 (META)
ΔPIN1::cPIN1:GFP; autofluorescence	ΔPIN1::cPIN1:GFP	Ar	488	HFT 405/488/594			507–593 (META)
	Autofluorescence	Ar	488	HFT 405/488/594			507–593 (META)

AthaMap (Steffens et al. 2004) (http://www.athamap.de/), PLACE (Higo et al. 1999) (http://www.dna.affrc.go.jp/PLACE/), Plant CARE (Lescot et al. 2002) (http://bioinformatics.psb.ugent.be/webtools/plantcare/html/) and rVISTA 2.0 (Loots and Ovcharenko 2004) (http://rvista.dcode.org) using the TRANSFAC professional V10.2 library for plants and 0.75-similarity matrix.

CHAPTER 4: A TISSUE-CELL-POLARIZING SIGNAL UPSTREAM OF AUXIN TRANSPORT AND SIGNALING CONTROLS VEIN PATTERNING

4.1 Introduction

How cell polarity is coordinated between cells within tissues is a central question in biology. In animals, this tissue cell polarization requires direct cell-cell communication and often cell movements (Goodrich and Strutt 2011), both of which are precluded in plants by a wall that holds cells in place; therefore, plants coordinate tissue cell polarity by a different mechanism.

The formation of veins is a spectacular expression of tissue cell polarization in plants (Sachs 1991a; Sachs 2000; Boutte et al. 2007; Nakamura et al. 2012). This is already reflected in the relation between the parts of the mature vein, and between the mature vein and the parts of the plant: vascular elements are elongated along the axis of the vein and connected to one another at their ends (Esau 1942); and because veins primarily connect shoot organs with roots (Dengler 2006), veins and their elements are unequal at their ends—one end connects to shoot tissues, the other to root tissues—and are therefore polar (Sachs 1975). Not all the mature veins in closed networks such as those of Arabidopsis leaves have unambiguous shoot-to-root polarity, but the vein networks themselves are polar (Sachs 1975).

But that vein formation is an expression of tissue cell polarization is most evident in developing leaves. Consider, for example, the formation of the midvein at the centre of the cylindrical leaf primordium. Initially, the plasma-membrane (PM)-localized PIN-FORMED1 (PIN1) protein of Arabidopsis (Galweiler et al. 1998), which catalyzes cellular efflux of the plant signal auxin (Petrasek et al. 2006), is uniformly expressed in all the inner cells of the leaf primordium (Benkova et al. 2003; Reinhardt et al. 2003; Heisler et al. 2005; Scarpella et al. 2006; Wenzel et al. 2007; Bayer et al. 2009); over time, however, PIN1 expression becomes

gradually restricted to the file of cells that will form the midvein. PIN1 localization at the PM of the inner cells is initially isotropic, or nearly so, but as PIN1 expression becomes restricted to the site of midvein formation, PIN1 localization becomes polarized: in the cells surrounding the developing midvein, PIN1 localization gradually changes from isotropic to medial, i.e. toward the developing midvein, to mediobasal; in the cells of the developing midvein, PIN1 becomes uniformly localized toward the base of the leaf primordium, where the midvein will connect to the pre-existing vasculature. Both the restriction of PIN1 expression and the polarization of PIN1 localization initiate and proceed away from pre-existing vasculature, and are therefore polar.

The correlation between tissue cell polarization, as expressed by the polarization of PIN1 localization; polar auxin transport, as expressed by the auxin-transport-polarity-defining localization of PIN1 (Wisniewska et al. 2006); and polar vein formation does not seem to be coincidental. Auxin application to developing leaves induces the formation of broad expression domains of isotropically localized PIN1; such domains become restricted to the sites of auxin-induced vein formation, and PIN1 localization becomes polarized toward the pre-existing vasculature (Scarpella et al. 2006). Both the restriction of PIN1 expression and the polarization of PIN1 localization are delayed by chemical inhibition of auxin transport (Scarpella et al. 2006; Wenzel et al. 2007), which induces vein pattern defects similar to, though stronger than, those of *pin1* mutants (Mattsson et al. 1999; Sieburth 1999; Sawchuk et al. 2013).

Therefore, available evidence suggests that auxin induces tissue cell polarization and derived polar-vein-formation, and it seems that such inductive and orienting property of auxin strictly depends on the function of *PIN1* and possibly other *PIN* genes. How auxin precisely induces tissue cell polarization and derived polar-vein-formation is unclear, but the current hypothesis is that the GNOM (GN) guanine-nucleotide exchange factor for ADP-rybosilation-factor GTPases, which regulates vesicle formation in membrane trafficking, coordinates the cellular localization of PIN1 and possibly other PIN proteins between cells (Steinmann et al. 1999); the resulting cell-to-cell, polar transport of auxin would propagate cell polarity across tissues, and control polar developmental processes such as vein formation (Sachs 1991a).

Here we experimentally tested this hypothesis. We found that auxin-induced polar-vein-formation occurs in the absence of PIN proteins or any known intercellular auxin transporter;

that the auxin-transport-independent vein-patterning activity relies on auxin signaling; and that a GN-dependent tissue-cell-polarizing signal acts upstream of both auxin transport and signaling.

4.2 Results

4.2.1 Contribution of the *GNOM* gene to Arabidopsis vein patterning

We asked whether defects in coordination of PIN1 polarity and possible derived defects in polar auxin transport during embryogenesis of *gnom* (*gn*) mutants (Steinmann et al. 1999) were associated with vein pattern defects in mature leaves.

WT Arabidopsis grown under normal conditions forms separate leaves whose vein networks are defined by at least four reproducible features (Telfer and Poethig 1994; Nelson and Dengler 1997; Kinsman and Pyke 1998; Candela et al. 1999; Mattsson et al. 1999; Sieburth 1999; Steynen and Schultz 2003; Sawchuk et al. 2013) (Fig. 4.1A,B): (1) a narrow I-shaped midvein that runs the length of the leaf; (2) lateral veins that branch from the midvein and join distal veins to form closed loops; (3) minor veins that branch from midvein and loops and either end freely or join other veins; (4) minor veins and loops that curve near the leaf margin, lending a scalloped outline to the vein network.

In the leaves of both gn^{fwr} (Okumura et al. 2013) and $gn^{B/E}$ (Geldner et al. 2004), veins were often replaced by "vein fragments", i.e. stretches of vascular elements that failed to contact other stretches of vascular elements at least at one end (Fig. 4. 1C,D,L). In addition, the vein network of $gn^{B/E}$ leaves was denser and its outline was thicker near the leaf tip (Fig. 4.1D,L).

The vein network was denser also in all the leaves of gn^{R5} (Geldner et al. 2004), in nearly 70% of those of gn^{van7} (Koizumi et al. 2000) and in ~40% of those of $gn^{van7+fwr}$;*gn-13*—in which we combined the *van7* and *fwr* mutations (Table 4.1) (Fig. 4.1E,L). However, in those

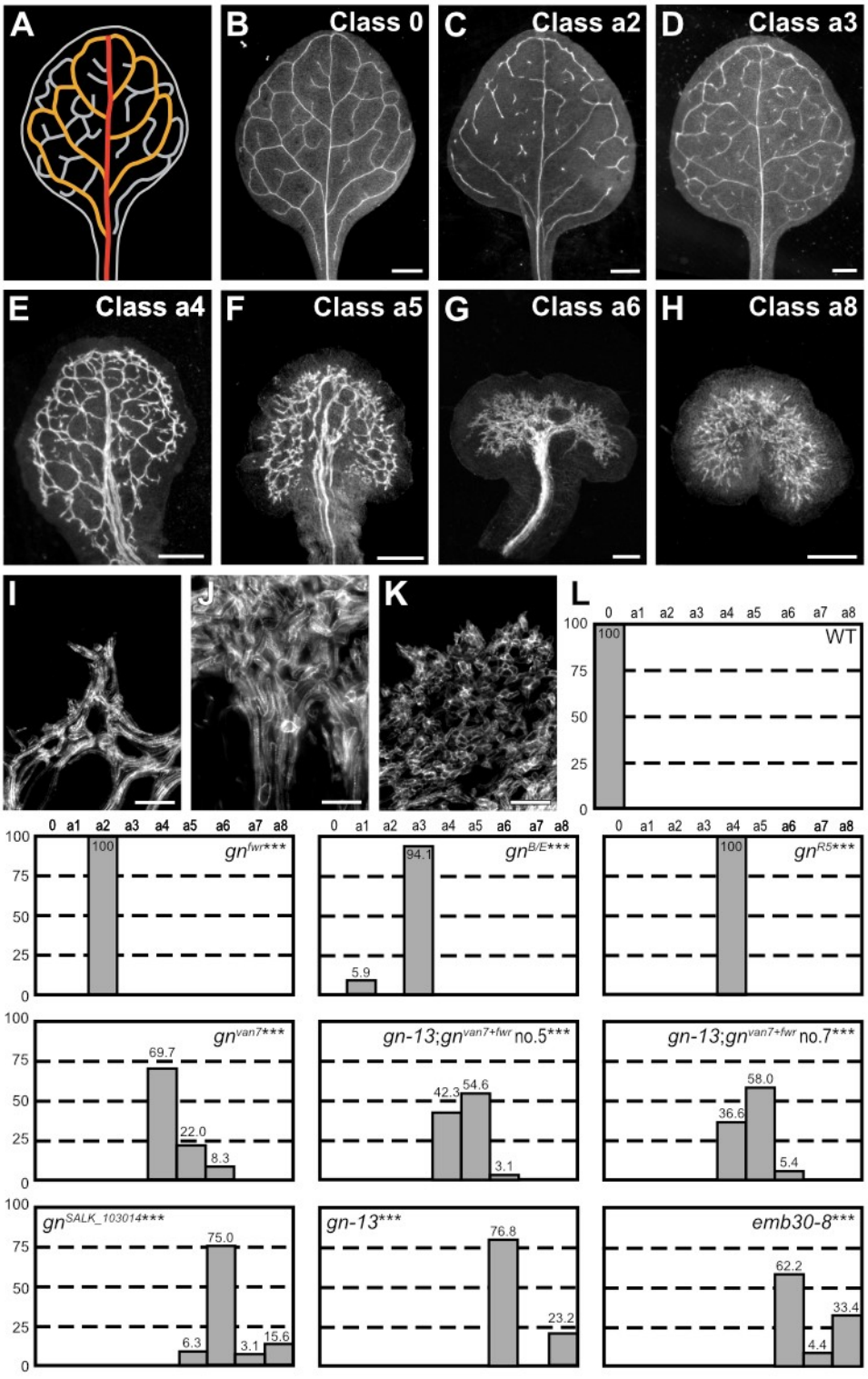

Figure 4.1. Contribution of the *GNOM* gene to Arabidopsis vein patterning. (A,B) Vein pattern of WT mature first leaf. In (A): red, midvein; orange, loops; gray, minor veins. (B–K) Dark-field illumination of mature first leaves illustrating phenotype classes (top right in B–H):

class 0, narrow I-shaped midvein and scalloped vein-network outline (B); class a1, dense vein network and apically thickened vein-network outline (not shown); class a2, narrow I-shaped midvein and fragmented vein network (C); class a3, dense, fragmented vein network and apically thickened vein-network outline (D); class a4, wide midvein, dense network of thick veins and jagged vein-network outline (E); class a5, dense network of thick veins that fail to join the midvein in the bottom half of the leaf and pronouncedly jagged vein-network outline (F); class a6, wide midvein and shapeless vascular cluster (G); class a7, fused leaves with wide midevin and shapeless vascular cluster (not shown); class a8, shapeless vascular cluster (H). (I–K) Details of vascular clusters illustrating vascular elements uniformly oriented perpendicular to the leaf margin (I) (class a4), vascular elements oriented randomly at the apical side of the cluster and parallel to the leaf axis at the proximal side of the cluster (J) (classes a6 and a7) and random orientation of vascular elements (K) (class a8). (L) Percentages of leaves in phenotype classes. Difference between gn^{fwr} and WT, between $gn^{B/E}$ and WT, between gn^{R5} and WT, between gn^{van7} and WT, between *gn-13*;$gn^{van7+fwr}$ and WT, between gn^{SALK}*103014* and WT, between *gn-13* and WT and between *emb30-8* and WT was significant at $P<0.001$ (***) by Kruskal-Wallis and Mann-Whitney test with Bonferroni correction. Sample population sizes: WT, 58; gn^{fwr}, 43; $gn^{B/E}$, 80; gn^{R5}, 93; gn^{van7}, 109; *gn-13*;$gn^{van7+fwr}$no.5, 97, *gn-13*; $gn^{van7+fwr}$no.7, 93; gn^{SALK_103014}, 32; *gn-13*, 56; *emb30-8*, 45. Bars: (B) 1 mmm; (C,E) 0.75 mm; (D,F) 0.5 mm; (G,H) 0.25 mm;(I–K) 50 µm.

Table 4.1. Origin and nature of lines.

Line	Origin/Nature
fwr (*gn*^{fwr})	Okumura et al. 2013
gn$^{B/E}$	Geldner et al. 2004
gn^{R5}	Geldner et al. 2004
van7/*emb30-7* (*gn*^{van7})	Koizumi et al. 2000
gn$^{van7+fwr}$	*gn*^{van7} (-2127 to +5388; primers: 'GN Fwd NotI' and 'GN Rev NotI') containing the *fwr* mutation (primers: 'fwr-mutagenesis F' and 'fwr-mutagenesis R')
gn$^{SALK\_103014}$	ABRC; Okumura et al. 2013
emb30-8	ABRC; Moriwaki et al. 2013)
gn-13	ABRC; SALK_045424 (Alonso et al. 2003); contains a T-DNA insertion after +2835 of *GN* (AT1G13980)
PIN1::PIN1:GFP	Benkova et al. 2003
PIN2::PIN2:GFP	Xu and Scheres 2005
PIN3::PIN3:GFP	Zadnikova et al. 2010
PIN4::PIN4:GFP	Translational fusion of *PIN4* (AT2G01420; -4598 to +3095; primers: 'PIN4 prom PstI forw' and 'PIN4 1032 SalI rev', 'PIN4 1033 SalI forw' and 'PIN4 UTR EcoRI rev') to EGFP (Clontech; insertion after +1032 of *PIN4*; primers: 'EGFP SalI Forw' and 'EGFP SalI Rev')
PIN7::PIN7:GFP	Translational fusion of *PIN7* (AT1G23080; -1537 to +2830; primers: 'PIN7 prom SalI forw' and 'PIN7 UTR KpnI rev') to

	EGFP (Clontech; insertion after +921 of *PIN7*; primers: 'EGFP SacI forw' and 'EGFP SacI rev')
pin1-1	ABRC; WT at the TTG1 (AT5G24520) locus (Galweiler et al. 1998; Goto et al. 1987; Sawchuk et al. 2013)
pin1-134	Derived from *Atpin1::En134* (Galweiler et al. 1998); contains a 4-bp (AATT) insertion between +134 and +135 of *PIN1* (AT1G73590), resulting in a stop codon after amino acid 62.
pin3-3	Friml et al. 2002b
pin4-2	Friml et al. 2002a
$pin7^{En}$	Blilou et al. 2005
eir1-1 (*pin2*)	ABRC; Roman et al. 1995; Luschnig et al. 1998
toz-1	Griffith et al. 2007
mp^{G12}	Hardtke and Berleth 1998
pin6	ABRC; Sawchuk et al. 2013
pin8-1	ABRC; Bosco et al. 2012
ABCB1::ABCB1:GFP	Dhonukshe et al. 2008; Mravec et al. 2008
ABCB19::ABCB19:GFP	Mravec et al. 2008; Dhonukshe et al. 2008
pgp1-100 (*abcb1*)	ABRC; Lin and Wang 2005
mdr1-101 (*abcb19*)	ABRC; Lin and Wang 2005
ucu2-4 (*twd1*)	ABRC; Perez-Perez et al. 2004
AUX1::AUX1:YFP	Band et al. 2014
LAX1::LAX1:YFP	Peret et al. 2012

LAX2::LAX2:YFP	Peret et al. 2012
LAX3::LAX3:YFP	Fabregas et al. 2015
aux1-21;*lax1*;*2-1*;*3*	Bainbridge et al. 2008
aux1-355	ABRC; SALK_020355 (Alonso et al. 2003); contains a T-DNA insertion after +631 of *AUX1* (AT2G38120)
lax1-064	ABRC; SALK_071064 (Alonso et al. 2003); contains a T-DNA insertion after +814 of *LAX1* (AT5G01240)
axr1-3	ABRC; Lincoln et al. 1990
axr1-12	ABRC; Lincoln et al. 1990
tir1-1;*afb2-3*	Savaldi-Goldstein et al. 2008
DR5rev::nYFP	Heisler et al. 2005; Sawchuk et al. 2013

leaves *all* the veins were thicker, lateral veins failed to join the midvein and ran parallel to it to form a "wide midvein", and the vein network outline was jagged because of narrow clusters of vascular elements that were oriented perpendicular to the leaf margin and that were laterally connected by veins (Fig. 4.1E,I,L). These features were enhanced in ~20% of the leaves of gn^{van7}, in ~55% of those of $gn^{van7+fwr}$;*gn-13* and in ~5% of those of gn^{SALK_103014} (Okumura et al. 2013): the vein network was denser, veins failed to join the midvein in the bottom half of the leaf, and the vein network outline was pronouncedly jagged (Fig. 4.1F,L).

In the few remaining leaves of gn^{van7} and $gn^{van7+fwr}$;*gn-13* and in most of those of gn^{SALK_103014}, of *emb30-8* (Moriwaki et al. 2013) and of the new allele *gn-13* (Table 4.1), a central, shapeless vascular cluster was connected with the basal part of the leaf by a wide midvein; vascular elements were oriented randomly at the distal side of the cluster and progressively more parallel to the leaf axis toward the proximal side of the cluster (Fig. 4.1G,J–L).

Finally, in the remaining leaves of gn^{SALK_103014}, *gn-13* and *emb30-8*, vascular differentiation was limited to a central, shapeless cluster of randomly oriented vascular elements (Fig. 4.1H,K,L).

4.2.2 Contribution of plasma-membrane-localized PIN proteins to vein patterning

Were the vein pattern defects of *gn* the sole result of loss of *PIN1*-dependent polar auxin-transport induced by defects in coordination of PIN1 polarity, the vein pattern defects of *gn* would be phenocopied by mutation in all the *PIN* genes with function in *PIN1*-dependent vein patterning; we asked whether that were so.

In Arabidopsis, the PIN family of auxin transporters is composed of eight members (Paponov et al. 2005; Krecek et al. 2009; Viaene et al. 2012): PIN5, PIN6 and PIN8, which are primarily localized to the endoplasmic reticulum (ER) (Mravec et al. 2009; Bosco et al. 2012; Ding et al. 2012; Sawchuk et al. 2013); and PIN1, PIN2, PIN3, PIN4 and PIN7, which are

primarily localized to the plasma membrane (PM), and catalyze cellular auxin efflux (Chen et al. 1998; Galweiler et al. 1998; Luschnig et al. 1998; Muller et al. 1998; Friml et al. 2002a; Friml et al. 2002b; Friml et al. 2003; Petrasek et al. 2006). Sequence analysis divides the PM-localized subfamily of PIN (PM-PIN) proteins into three groups: the PIN1 group, the PIN2 group and the PIN3 group, which also contains PIN4 and PIN7 (Krecek et al. 2009; Viaene et al. 2012).

Mutants of the *PM-PIN* gene *PIN1* are the only *pin* single mutants with vein pattern defects, and the vein pattern defects of double mutants between *pin1* and mutants of the *PM-PIN* genes *PIN2*, *PIN3*, *PIN4* or *PIN7* are no different from those of *pin1* single mutants (Sawchuk et al. 2013), suggesting that either *PIN2*, *PIN3*, *PIN4* and *PIN7* have no function in *PIN1*-dependent vein patterning or their function in this process is redundant. To discriminate between these possibilities, we first assessed the collective contribution to *PIN1*-dependent vein patterning of the *PM-PIN* genes of the *PIN3* group (*PIN3*, *PIN4* and *PIN7*), whose translational fusions to GFP (Zadnikova et al. 2010) (Table 4.1) are all expressed—as are translational fusions of PIN1 to GFP (Benkova et al. 2003; Heisler et al. 2005; Scarpella et al. 2006; Sawchuk et al. 2007; Wenzel et al. 2007; Bayer et al. 2009; Marcos and Berleth 2014)—in both epidermal and inner cells of the developing leaf (Fig. 4.2A,C–E).

Consistent with previous reports (Sawchuk et al. 2013; Verna et al. 2015) (Chapter 2), the vein patterns of most of the *pin1* leaves were abnormal (Fig. 4.2F,G,L).

pin3pin4pin7 (*pin3*;*4*;*7* hereafter) embryos were viable and developed into seedlings (Table 4.2) whose vein patterns were no different from those of WT (Fig. 4.2L). *pin1*;*3*;*4*;*7* embryos were viable (Table 4.3) and developed into seedlings (Table 4.4) whose vein pattern defects were more severe than those of *pin1*: no *pin1*;*3*;*4*;*7* leaf had a WT vein pattern; *pin1*;*3*;*4*;*7* veins were thicker; and ~15% of *pin1*;*3*;*4*;*7* leaves were fused (Fig. 4.2H–L). Cotyledon pattern defects of *pin1*;*3*;*4*;*7* were no different from those of *pin1* (Fig. 4.3A–H), but *pin1*;*3*;*4*;*7* seedlings were smaller than *pin1* seedlings (Fig. 4.4A,B).

Next, we asked whether mutation of *PIN2*—whose translational fusion to GFP (Xu and Scheres 2005) is only expressed in epidermal cells in the developing leaf (Fig. 4.2B)—changed the spectrum of vein pattern defects of *pin1*;*3*;*4*;*7*. *pin2*;*3*;*4*;*7* embryos were viable and developed into seedlings (Table 4.2) whose vein patterns were no different from those of WT (Fig. 4.2L). *pin1*;*2*;*3*;*4*;7 embryos were viable (Table 4.3) and developed into seedlings (Table 4.4) whose

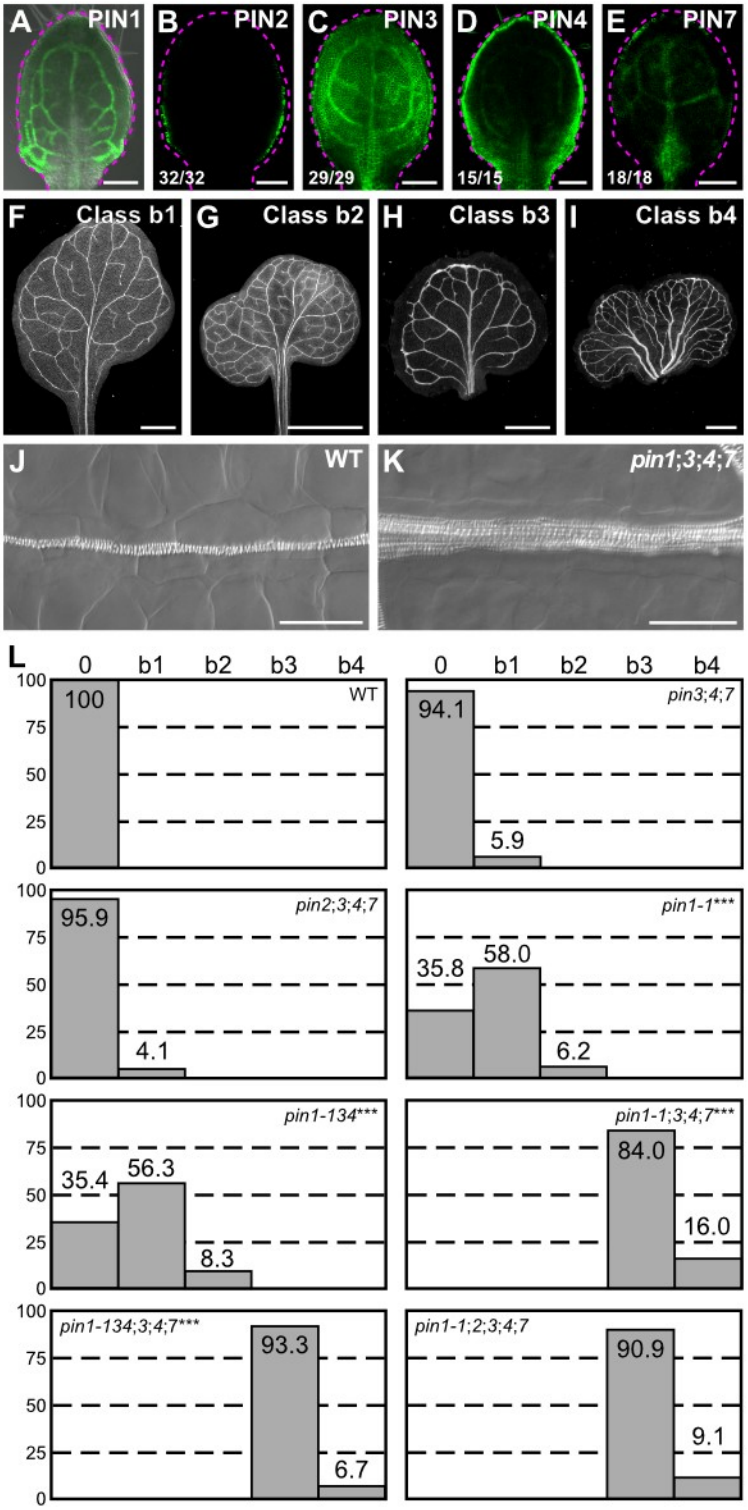

Figure 4.2. Contribution of plasma-membrane-localized PIN proteins to vein patterning. (A–K) Top right: expression-reported gene, phenotype class or genotype. (B–E) Bottom left: reproducibility index. (A–E) Confocal laser scanning microscopy with (A) or without (B–E)

transmitted light; 4-day-old first leaves. Dashed magenta line delineates leaf outline. (A) PIN1::PIN1:GFP expression. (B) PIN2::PIN2:GFP expression. (C) PIN3::PIN3:GFP expression. (D) PIN4::PIN4:GFP expression. (E) PIN7::PIN7:GFP expression. (F–I) Dark-field illumination images of mature first leaves illustrating phenotype classes: class b1, Y-shaped midvein and scalloped vein-network outline (F); class b2, fused leaves with scalloped vein-network outline (G); class b3, thick veins and scalloped vein-network outline (H); class b4, fused leaves with thick veins and scalloped vein-network outline (I). (J,K) Differential interference images of details of WT (J) or *pin1-1*;*3*;*4*;*7* (K) illustrating normal (classes 0, b1 and b2) or thick (classes b3 and b4) veins, respectively. (L) Percentages of leaves in phenotype classes. Difference between *pin1-1* and WT, between *pin1-134* and WT, between *pin1-1*;*3*;*4*;*7* and *pin1-1*, and between *pin1-134*;*3*;*4*;*7* and *pin1-134* was significant at $P<0.001$ (***) by Kruskal-Wallis and Mann-Whitney test with Bonferroni correction. Sample population sizes: WT, 58; *pin2*;*3*;*4*;*7*, 49; *pin3*;*4*;*7*, 102; *pin1-1*, 81; *pin1-134*, 48; *pin1-1*;*3*;*4*;*7*, 75; *pin1-134*;*3*;*4*;*7*, 45; *pin1-1*;*pin2*;*3*;*4*;*7*, 99. Bars: (A–E) 0.1 mm; (F–H) 1 mm; (I) 5 mm; (J,K) 50 μm.

Table 4.2. Embryo viability of WT, *pin3*;*4*;*7* and *pin2*;*3*;*4*;*7*.

Genotype of self-fertilized parent	Proportion of viable embryos in siliques of self-fertilized parent (no. of non-aborted seeds / total no. of seeds)	Percentage of viable seeds in siliques of self-fertilized parent
WT (Col-0)	293/293	100
pin3/*pin3*;*pin4*/*pin4*;*pin7*/*pin7*	275/276	99.6
pin2/*pin2*;*pin3*/*pin3*;*pin4*/*pin4*;*pin7*/*pin7*	271/271	100

Difference between *pin3*;*4*;*7* and WT and between *pin2*;*3*;*4*;*7* and WT was not significant by Kruskal-Wallis and Mann-Whitney test with Bonferroni correction.

Table 4.3. Embryo viability of *toz*, *mp*, *pin1*, *pin1*;*3*;*4*;*7*, *pin1*;*2*;*3*;*4*;*7* and *pin1*;*3*;*4*;*6*;*7*;*8*.

Genotype of self-fertilized parent	Proportion of viable embryos in siliques of self-fertilized parent (no. of non-aborted seeds / total no. of seeds)	Percentage of viable seeds in siliques of self-fertilized parent
TOZ/*toz-1*	202/278	72.7
MP/*mp*^{G12}	264/265***	99.6
PIN1/*pin1-1*	254/260***	97.7
PIN1/*pin1-134*	257/258***	99.6
PIN1/*pin1-1*;*pin3*/*pin3*;*pin4*/*pin4*;*pin7*/*pin7*	269/272***	98.9
PIN1/*pin1-134*;*pin3*/*pin3*;*pin4*/*pin4*;*pin7*/*pin7*	280/281***	99.6
PIN1/*pin1-1*;*pin2*/*pin2*;*pin3*/*pin3*;*pin4*/*pin4*;*pin7*/*pin7*	276/278***	99.3
PIN1/*pin1-1*;*pin3*/*pin3*;*pin4*/*pin4*;*pin6*/*pin6*;*pin7*/*pin7*;*pin8*/*pin8*	266/268***	99.2

Difference between negative control for completely penetrant embryo lethality (*mp*^{G12}) and positive control for completely penetrant embryo lethality (*toz-1*), between *pin1-1* and *toz-1*, between *pin1-134* and *toz-1*, between *pin1-1*;*3*;*4*;*7* and *toz-1*, between *pin1-134*;*3*;*4*;*7* and *toz-1*, between *pin1-1*;*2*;*3*;*4*;*7* and *toz-1* and between *pin1-1*;*3*;*4*;*6*;*7*;*8* and *toz-1* was significant at $P<0.001$ (***) by Kruskal-Wallis and Mann-Whitney test with Bonferroni correction. Difference between *pin1-1* and *mp*^{G12}, between *pin1-134* and *mp*^{G12}, between *pin1-1*;*3*;*4*;*7* and *mp*^{G12}, between *pin1-134*;*3*;*4*;*7* and *mp*^{G12}, between *pin1-1*;*2*;*3*;*4*;*7* and *mp*^{G12} and between *pin1-1*;*3*;*4*;*6*;*7*;*8* and *mp*^{G12} was not significant by Kruskal-Wallis and Mann-Whitney test with Bonferroni correction.

Table 4.4. Embryo viability of *pin1*, *pin1*;*3*;*4*;*7*, *pin1*;*2*;*3*;*4*;*7* and *pin1*;*3*;*4*;*6*;*7*;*8*.

Genotype of self-fertilized parent	Proportion of embryo-viable mutants in progeny of self-fertilized parent (no. of mutant seedlings / total no. of seedlings)	Percentage of embryo-viable mutants in progeny of self-fertilized parent
PIN1/*pin1-1*	66/239	27.6
PIN1/*pin1-134*	53/227	23.3
PIN1/*pin1-1*;*pin3*/*pin3*;*pin4*/*pin4*;*pin7*/*pin7*	52/196	26.5
PIN1/*pin1-1-134*;*pin3*/*pin3*;*pin4*/*pin4*;*pin7*/*pin7*	56/228	24.6
PIN1/*pin1-1*;*pin2*/*pin2*;*pin3*/*pin3*;*pin4*/*pin4*;*pin7*/*pin7*	61/263	23.2
PIN1/*pin1-1*;*pin3*/*pin3*;*pin4*/*pin4*;*pin6*/*pin6*;*pin7*/*pin7*;*pin8*/*pin8*	65/260	25.0

Difference between observed and theoretical frequency distributions of embryo-viable mutants in the progeny of self-fertilized heterozygous parents was not significant by Pearson's chi-squared (χ^2) goodness-of-fit test (α=0.05, dF=1).

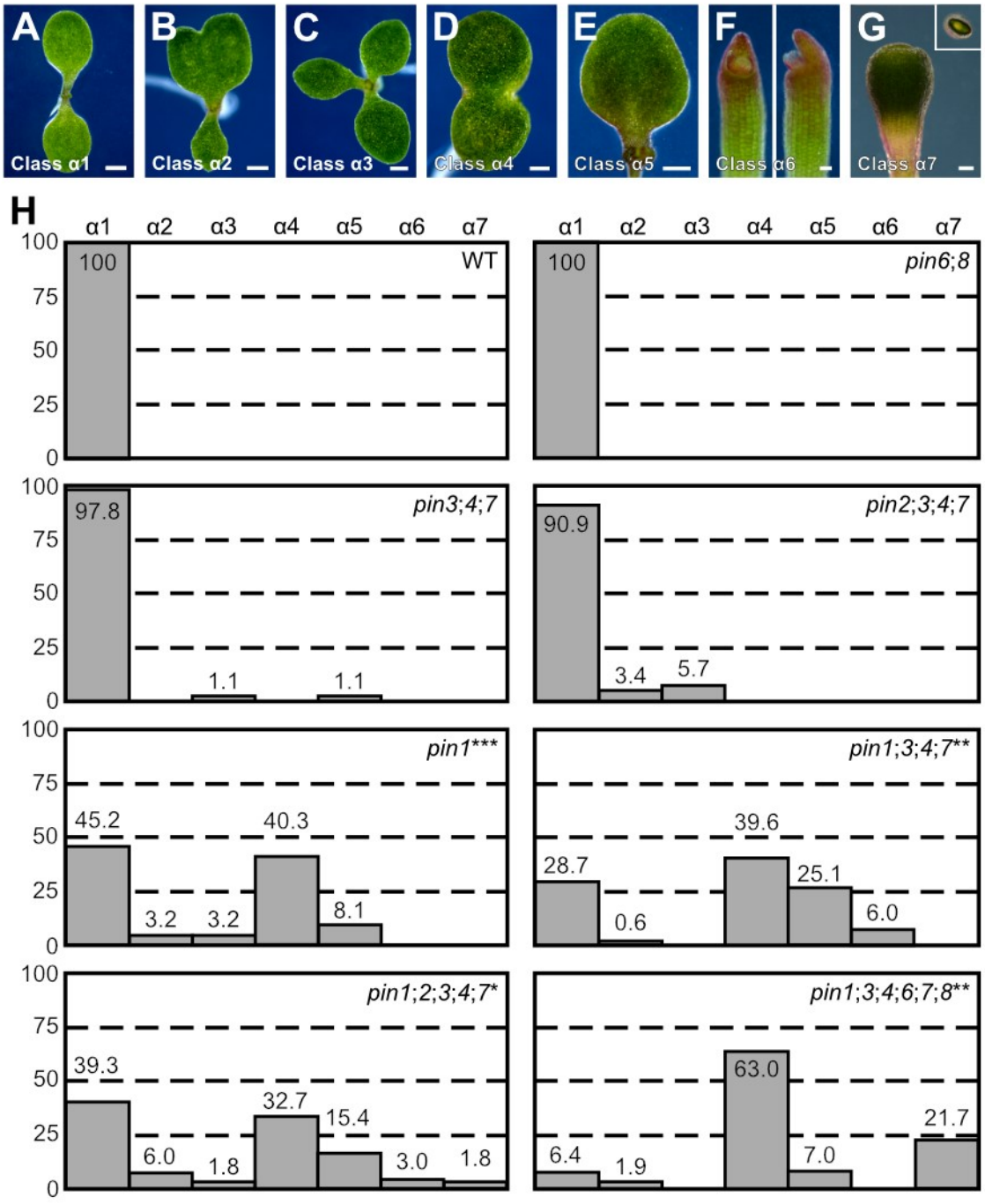

Figure 4.3. Cotyledon patterns of *pin* mutants. (A–G) Dark-field illumination of 3-day-old seedlings illustrating phenotype classes (bottom left): class α1, two separate cotyledons (A); class α2, fused cotyledons and separate single cotyledon (B); class α3, three separate cotyledons (C); class α4, fused cotyledons (D); class α5, single cotyledon (E); class α6, small, hood-like cotyledon (F: left, front view; right, side view); class α7, cup-shaped cotyledon, side view (inset:

top view) (G). (H) Percentages of seedlings in phenotype classes. Difference between *pin1-1* and WT was significant at $P<0.001$ (***), between *pin1-1*;*3*;*4*;*7* and *pin1-1* and between *pin1-1*;*3*;*4*;*6*;*7*;*8* and *pin1-1* was significant at $P<0.01$ (**) and between *pin1-1*;*2*;*3*;*4*;*7* and *pin1-1* was significant at $P<0.05$ (*) by Kruskal-Wallis and Mann-Whitney test with Bonferroni correction. Sample population sizes: WT, 58; *pin3*;*4*;*7*, 55; *pin2*;*3*;*4*;*7*, 55; *pin6*;*8*, 50; *pin1-1*;*3*;*4*;*7*, 76; *pin1-1*;*2*;*3*;*4*;*7*, 80; *pin1-1*;*3*;*4*;*6*;*7*;*8*, 65. Bars: (A–E) 0.5 mm; (F) 0.25 mm; (G) 0.2 mm.

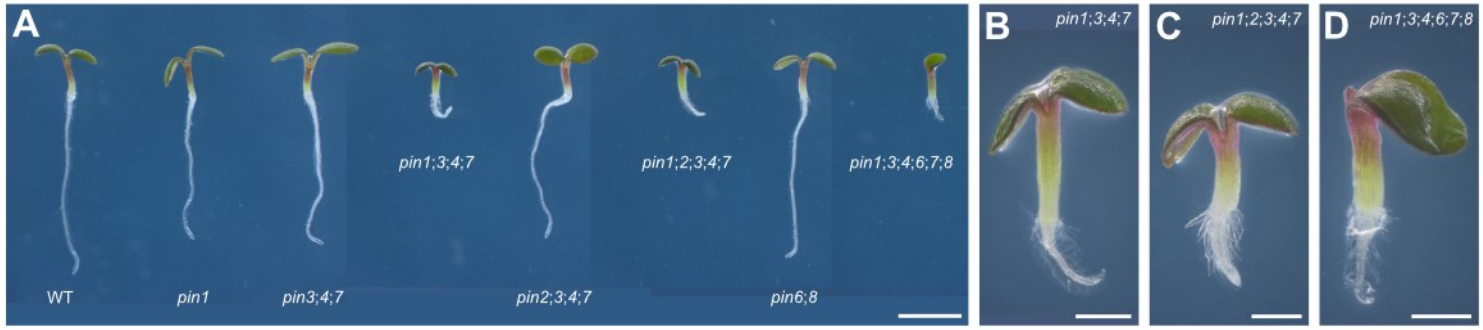

Figure 4.4. *pin* mutant seedlings. (A–D) Dark-field illumination composite of 3-day-old seedlings; genotypes below respective seedlings (A) or top right (B–D). (A) Overview. Because the seedling lineup was wider than the stereomicroscope's field of view, overlapping images of parts of the lineup were acquired and combined to reconstruct the original lineup. (B–D) Details. Bars: (A) 2 mm; (B–D) 0.5 mm.

vein pattern defects were no different from those of *pin1*;*3*;*4*;*7* (Fig. 4.2L). Cotyledon pattern defects of *pin1*;*2*;*3*;*4*;7 were no different from those of *pin1*;*3*;*4*;*7* (Fig. 4.3A–H), and size of *pin1*;*2*;*3*;*4*;7 seedlings was similar to that of *pin1*;*3*;*4*;*7* seedlings (Fig. 4.4A–C).

In conclusion, the *PIN3* group of *PM-PIN* genes (*PIN3*, *PIN4* and *PIN7*) provides no nonredundant function in vein patterning, but it contributes to *PIN1*-dependent vein patterning; *PIN1* and the *PIN3* group of *PM-PIN* genes redundantly restrict vascular differentiation to narrow zones; and *PIN2* seems to have no function in any these processes. Most important, loss of *PM-PIN* function fails to phenocopy the vein pattern defects of *gn* (Figs. 4.1,4.2).

4.2.3 Contribution of *PIN* genes to vein patterning

Expression and genetic analyses suggest that the PM-PIN proteins PIN1, PIN3, PIN4 and PIN7 redundantly define a single intercellular auxin-transport pathway with vein patterning functions whose loss fails to phenocopy the vein pattern defects of *gn* (Figs. 4.1,4.2). The ER-localized PIN (ER-PIN) proteins PIN6 and PIN8 define a distinct, intracellular auxin-transport pathway with vein patterning functions that overlap with those of *PIN1* (Sawchuk et al. 2013; Verna et al. 2015) (Chapter 2). We asked what the collective contribution of these two auxin-transport pathways were to vein patterning and whether mutation in all the *PIN* genes with vein patterning function phenocopied the vein pattern defects of *gn*.

As previously reported (Sawchuk et al. 2013), the vein pattern of *pin6*;*8* was no different from that of WT (Fig. 4.5C). *pin1*;*3*;*4*;*6*;*7*;*8* embryos were viable (Table 4.3) and developed into seedlings (Table 4.4) whose vein patterns differed from those of *pin1*;*3*;*4*;*7* in three respects: (1) the vein network comprised more lateral veins; (2) lateral veins failed to join the midvein but ran parallel to it to form a wide midvein; (3) lateral veins ended in a marginal vein that closely paralleled the leaf margin, lending a smooth outline to the vein network (Figs. 4.2,4.5A–C). Mutation of *PIN6* and *PIN8* in the *pin1*;*3*;*4*;*7* background shifted the distribution of *pin1*;*3*;*4*;*7* cotyledon pattern phenotypes toward stronger classes (Fig. 4.3A–H), but the size of *pin1*;*3*;*4*;*6*;*7*;*8* seedlings was similar to that of *pin1*;*3*;*4*;*7* seedlings (Fig. 4.4A,B,D).

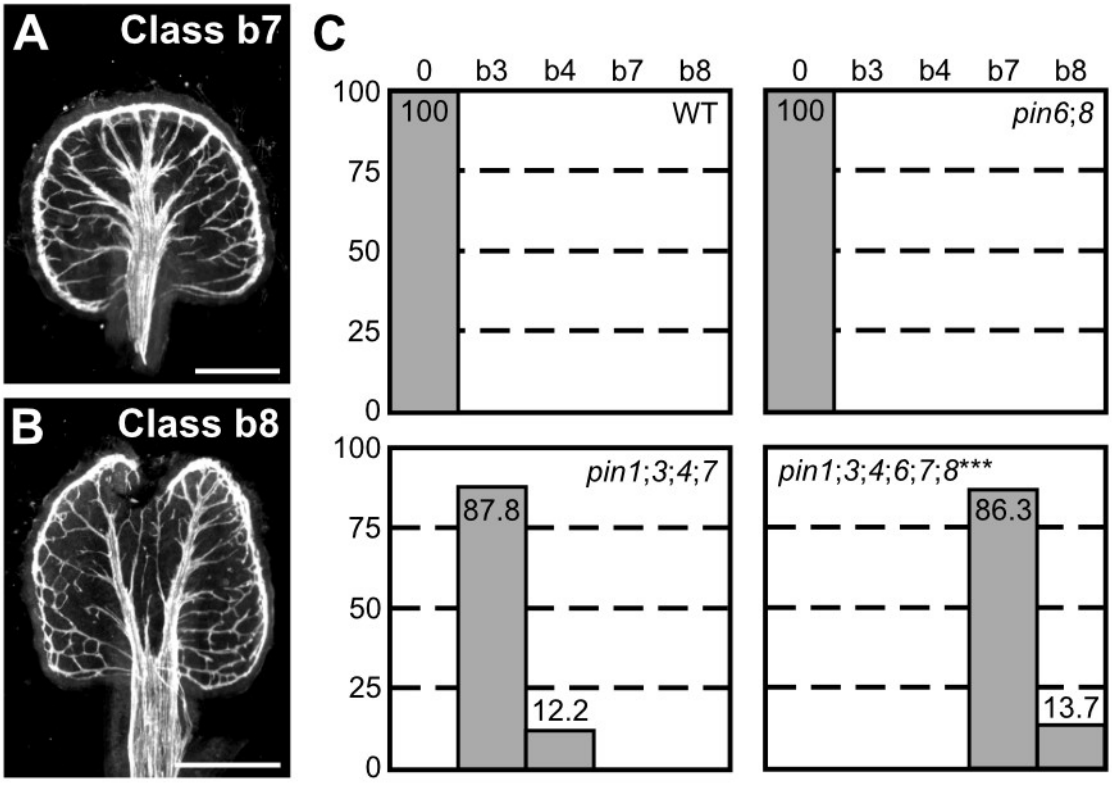

Figure 4.5. Contribution of *PIN* genes to vein patterning. (A,B) Dark-field illumination of mature first leaves illustrating phenotype classes (top right): class b7, wide midvein, more lateral-veins and conspicuous marginal vein (A); class b8, fused leaves with wide midvein, more lateral-veins and conspicuous marginal vein (B). (C) Percentages of leaves in phenotype classes (Classes 0, b3 and b4 defined in Figs. 4.1,4.2). Difference between *pin1-1*;*3*;*4*;*6*;*7*;*8* and *pin1-1*;*3*;*4*;*7* was significant at $P<0.001$ (***) by Kruskal-Wallis and Mann-Whitney test with Bonferroni correction. Sample population sizes: WT, 51; *pin6*;*8*, 47; *pin1-1*;*3*;*4*;*7*, 49; *pin1-1*;*3*;*4*;*6*;*7*;*8*, 73. Bars: (A,B) 0.5 mm.

Because *pin6*;*8* synthetically enhanced vein pattern defects of *pin1*;*3*;*4*;*7*, we conclude that the intercellular auxin-transport pathway mediated by the PM-PIN proteins and the intracellular auxin-transport pathway mediated by the ER-PIN proteins provide overlapping functions in vein patterning. Nevertheless, loss of *PIN*-dependent vein patterning function fails to phenocopy the vein pattern defects of *gn* (Figs. 4.1,4.5).

4.2.4 Genetic versus chemical interference of auxin transport

Loss of *PIN*-dependent vein patterning function fails to phenocopy the vein pattern defects of *gn* (Figs. 4.1,4.5), suggesting that these latter are not the sole result of loss of *PIN*-dependent polar auxin-transport induced by defects in coordination of PIN polarity. However, it is possible that the vein pattern defects of *gn* result from additional or exclusive defects in *PIN*-independent polar auxin-transport pathways; we asked whether that were so.

Cellular auxin efflux is inhibited by a class of structurally related compounds referred to as phytotropins, exemplified by N-1-naphthylphthalamic acid (NPA) (Katekar and Geissler 1980; Sussman and Goldsmith 1981). Because PM-PIN proteins catalyze cellular auxin efflux (Chen et al. 1998; Petrasek et al. 2006), we first asked whether defects resulting from simultaneous mutation of all the *PM-PIN* genes with vein patterning function were phenocopied by growth of WT in the presence of NPA. To address this question, we compared defects of *pin1*;*3*;*4*;*7* to those induced in WT by growth in the presence of 100 µM NPA, which is the highest concentration of NPA without toxic, auxin-efflux-unrelated effects (Petrasek et al. 2003; Dhonukshe et al. 2008). Because leaves develop more slowly at this concentration of NPA (Mattsson et al. 1999; Sieburth 1999), to ensure maximal vascular differentiation we allowed them to grow for four weeks before analysis.

Consistent with previous reports (Mattsson et al. 1999; Sieburth 1999), high concentration of NPA only rarely induced leaf fusion in WT (see Fig. 4.7I for one such rare occurrence) but reproducibly induced characteristic vein-pattern defects: (1) the vein network comprised more lateral veins; (2) lateral veins failed to join the midvein but ran parallel to it to

form a wide midvein; (3) lateral veins ended in a marginal vein that closely paralleled the leaf margin, lending a smooth outline to the vein network; (4) veins were thicker (Fig. 4.6A,D,E,H).

By contrast, 20% of *pin1*;*3*;*4*;*7* leaves were fused, and though *pin1*;*3*;*4*;*7* veins were thick, *pin1*;*3*;*4*;*7* vein patterns lacked all the other characteristic defects induced in WT by NPA (Fig. 4.6B,H). However, such defects were induced in *pin1*;*3*;*4*;*7* by 100 µM NPA (Fig. 4.6F,H), suggesting that this background has residual NPA-sensitive vein-patterning activity. The vein pattern defects induced in WT or *pin1*;*3*;*4*;*7* by NPA were no different from those of *pin1*;*3*;*4*;*6*;*7*;*8* (Fig. 4.6C,D–F,H). Because no additional defects were induced in *pin1*;*3*;*4*;*6*;*7*;*8* by 100 µM NPA (Fig. 4.6G,H), the residual NPA-sensitive vein-patterning activity of *pin1*;*3*;*4*;*7* is likely provided by *PIN6* and *PIN8*.

In conclusion, our results suggest that growth in the presence of 100 µM NPA phenocopies defects of loss of *PIN*-dependent vein patterning function; that in the absence of this function any residual NPA-sensitive vein-patterning activity—if existing—becomes inconsequential; and that loss of neither *PIN*-dependent vein-patterning function nor NPA-sensitive vein-patterning activity phenocopies the vein pattern defects of *gn* (Figs. 4.1,4.6).

4.2.5 Contribution of *ABCB* genes to vein patterning

Loss of *PIN*-dependent vein-patterning function or NPA-sensitive vein-patterning activity fails to phenocopy the vein pattern defects of *gn* (Figs. 4.1,4.6), suggesting that these latter are not the sole result of loss of *PIN*-dependent or NPA-sensitive polar auxin-transport induced by defects in coordination of PIN polarity. However, it is possible that the vein pattern defects of *gn* result from additional or exclusive defects in another polar auxin-transport pathway; we asked whether that were so.

Cellular auxin efflux is catalyzed not only by PM-PIN proteins but by the PM-localized ATP-BINDING CASSETTE B1 (ABCB1) and ABCB19 proteins (Geisler et al. 2003; Geisler et al. 2005; Bouchard et al. 2006; Petrasek et al. 2006; Blakeslee et al. 2007; Wu et al. 2007), whose fusions to GFP (Dhonukshe et al. 2008; Mravec et al. 2008) are expressed at early stages

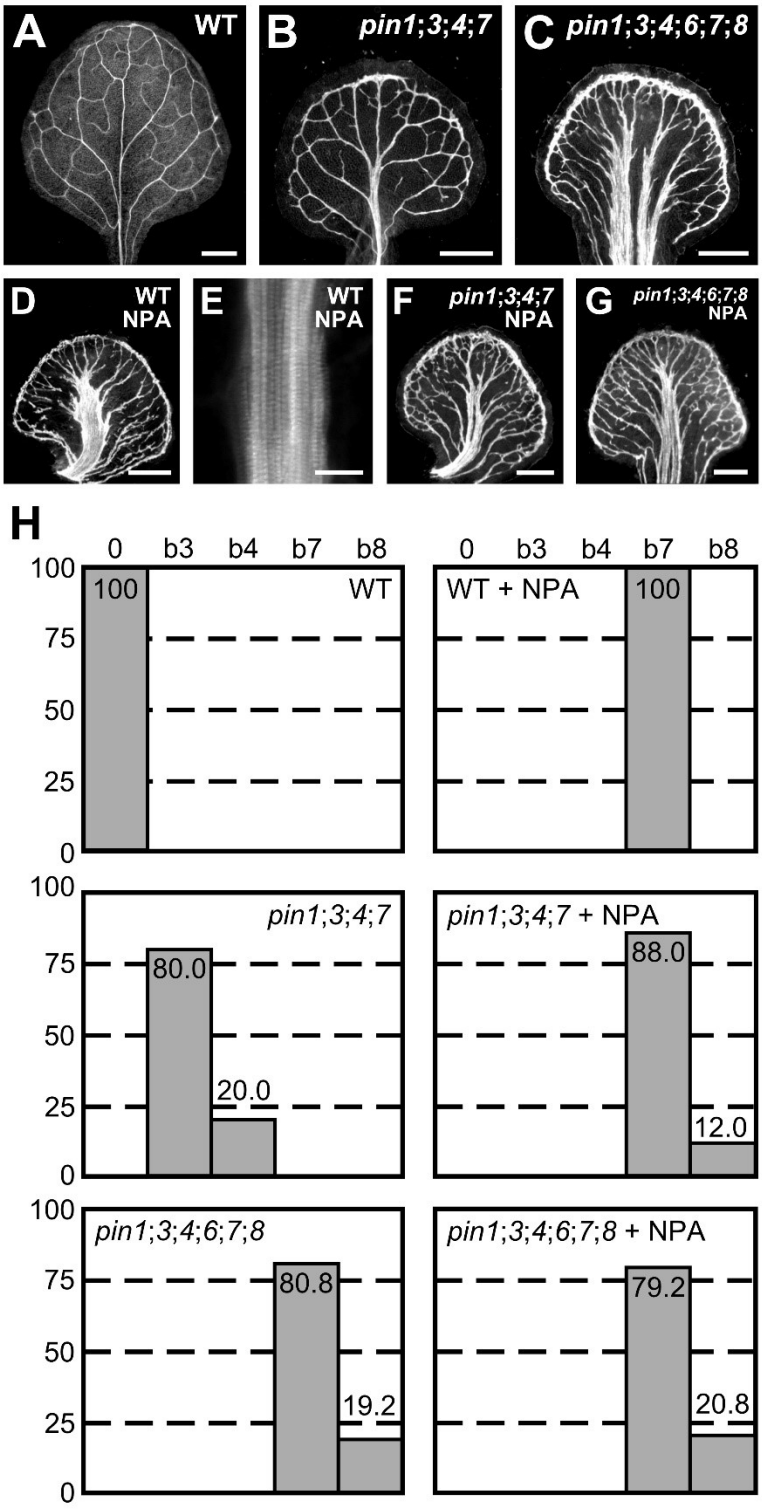

Figure 4.6. Genetic versus chemical interference of auxin transport. (A–G) Top right: genotype and treatment. (A–G) Dark-field illumination (A–D,F,G) or confocal laser scanning microscopy (E) of mature first leaves. (A) WT. (B) *pin1-1*;*3*;*4*;*7*. (C) *pin1-1*;*3*;*4*;*6*;*7*;*8*. (D)

NPA-grown WT. (E) Detail illustrating thick veins in NPA-grown WT (compare with Fig. 4.2J). (F) NPA-grown *pin1-1*;*3*;*4*;*7*. (G) NPA-grown *pin1-1*;*3*;*4*;*6*;*7*;*8*. (G) Percentages of leaves in phenotype classes (defined in Figs. 4.1,4.2,4.5). Sample population sizes: WT, 38; *pin1-1*;*3*;*4*;*7*, 30; *pin1-1*;*3*;*4*;*6*;*7*;*8*, 73; NPA-grown WT, 41; NPA-grown *pin1-1*;*3*;*4*;*7*, 58; NPA-grown *pin1-1*;*3*;*4*;*6*;*7*;*8*, 48. Bars: (A–D,F,G) 0.5 mm, (E) 25 μm.

of leaf development (Fig. 4.7A,B). We asked whether ABCB1/19-mediated auxin efflux was required for vein patterning.

Embryos of *abcb1* and *abcb19* were viable, but ~15% of *abcb1*;*19* embryos died during embryogenesis (Tables 4.5); nevertheless, the vein patterns of *abcb1*, *abcb19* and *abcb1*;*19* were no different from the vein pattern of WT (Fig. 4.7E,F,I), suggesting that ABCB1/19-mediated auxin efflux is dispensable for vein patterning.

Developmental functions of ABCB1/19-mediated auxin transport overlap with those of PIN-mediated auxin transport (Blakeslee et al. 2007 ; Mravec et al. 2008). We therefore asked whether vein pattern defects resulting from simultaneous loss of function of *PIN1*, *PIN3* and *PIN6* or induced in WT by 100 μM NPA, which phenocopies loss of *PIN*-dependent vein-patterning activity (Fig. 4.6), were enhanced by simultaneous mutation of *ABCB1* and *ABCB19*.

pin1;*3*;*6* embryos were viable (Table 4.6) and developed into seedlings (Table 4.7). The proportion of embryos derived from the self-fertilization of *PIN1*/*pin1*;*pin3*/*pin3*;*pin6*/*pin6*;*abcb1*/*abcb1*;*abc19*/*abcb19* that died during embryogenesis was no different from the proportion of embryos derived from the self-fertilization of *abcb1*/*abcb1*;*abc19*/*abcb19* that died during embryogenesis (Table 4.7), suggesting no nonreduntant functions of *PIN1*, *PIN3* and *PIN6* in *ABCB1*/*19*-dependent embryo viability.

Consistent with previous reports (Blakeslee et al. 2007 ; Mravec et al. 2008), mutation of *ABCB1* and *ABCB19* in the *pin1*;*3*;*6* background shifted the distribution of *pin1*;*3*;*6* cotyledon pattern phenotypes toward stronger classes (Fig. 4.8). However, the spectrum of vein pattern phenotypes of *pin1*;*3*;*6*;*abcb1*;*19* was no different from that of *pin1*;*3*;*6* and the vein pattern defects induced in *abcb1*;*19* by NPA were no different from those induced in WT by NPA (Fig. 4.7C,D,G–I), suggesting no vein-patterning function of *ABCB1* and *ABCB19* in the absence of function of *PIN1*, *PIN3* and *PIN6* or of *PIN*-dependent vein-patterning activity.

ABCB1 and ABCB19 are members of a large family (Geisler and Murphy 2006); therefore, vein patterning functions of ABCB1/19-mediated auxin efflux might be masked by redundant functions provided by other ABCB transporters. The TWISTED DWARF1/ULTRACURVATA2 (TWD1/UCU2; TWD1 hereafter) protein (Kamphausen et al. 2002; Perez-Perez et al. 2004) is a positive regulator of ABCB-mediated auxin transport

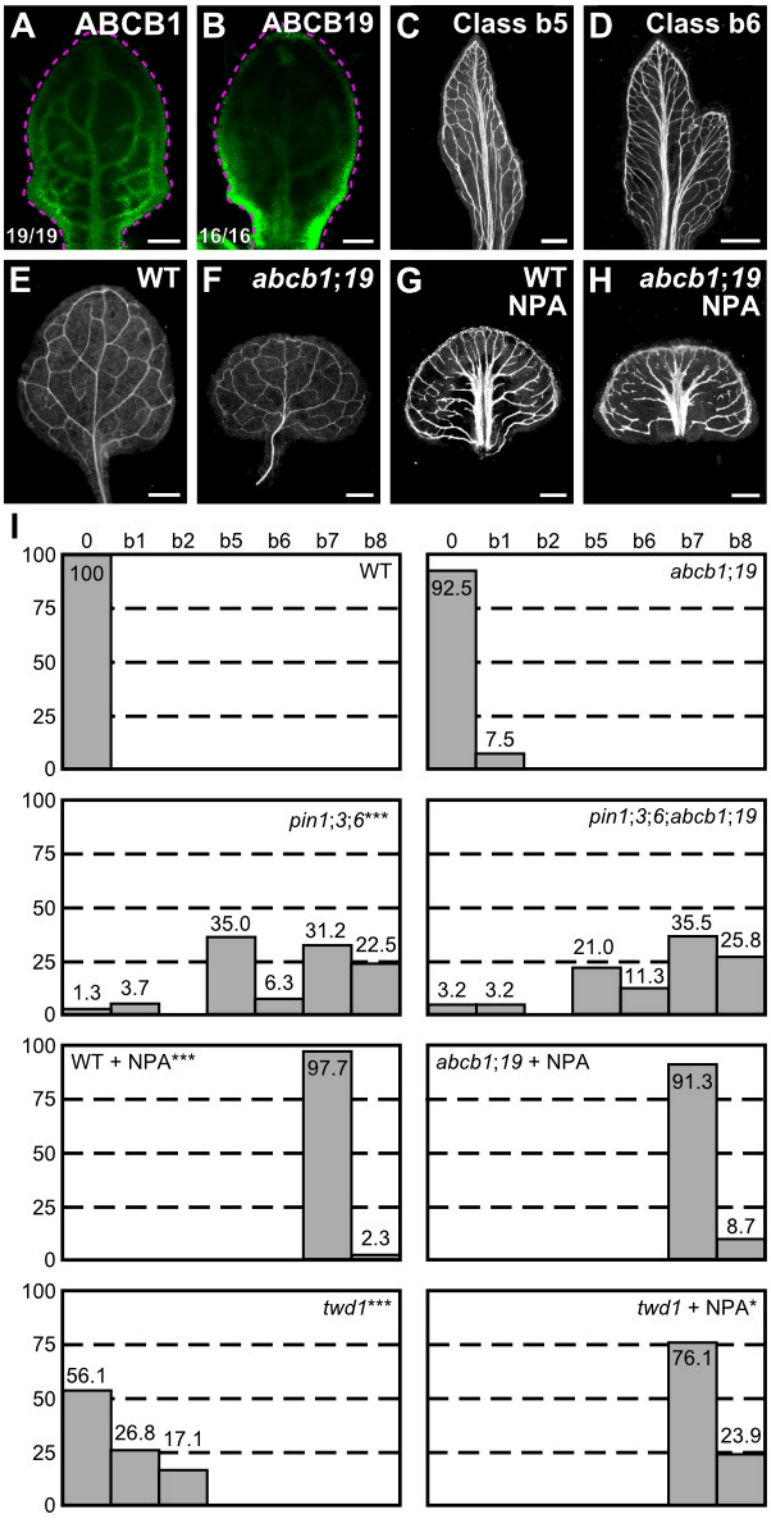

Figure 4.7. Contribution of *ABCB* genes to vein patterning. (A,B,E–H) Top right: expression-reported gene, genotype and treatment. (A–B) Bottom left: reproducibility index. (A–B) Confocal laser scanning microscopy; 5-day-old first leaves. Dashed magenta line delineates leaf

outline. (A) ABCB1::ABCB1:GFP expression. (B) ABCB19::ABCB19:GFP expression. (C–H) Dark-field illumination of mature first leaves. (C,D) Phenotype classes: class b5, thick veins and conspicuous marginal vein (C); class b6, fused leaves with thick veins and conspicuous marginal vein (D). (I) Percentages of leaves in phenotype classes (Classes 0, b1, b2, b7 and b8 defined in Figs.4.1,4.2,4.5). Difference between *pin1-1*;*3*;*6* and WT, between *twd1* and WT and between NPA-grown WT and WT was significant at $P<0.001$ (***) and between NPA-grown *twd1* and NPA-grown WT was significant at $P<0.05$ (*) by Kruskal-Wallis and Mann-Whitney test with Bonferroni correction. Sample population sizes: WT, 41; *abcb1*;*19*, 40; *pin1-1*;*3*;*6*, 80; *pin1-1*;*3*;*6*;*abcb1*;*19*, 62; NPA-grown WT, 43; NPA-grown *abcb1*;*19*, 46; *twd1*, 41; NPA-grown *twd1*, 46. Bars: (A–B) 0.1 mm; (C–H) 0.5 mm.

Table 4.5. Embryo viability of WT, *abcb1*, *abcb19*, *abcb1*;*19* and *twd1*.

Genotype of self-fertilized parent	Proportion of viable embryos in siliques of self-fertilized parent (no. of non-aborted seeds / total no. of seeds)	Percentage of viable seeds in siliques of self-fertilized parent
WT (Col-0)	294/294	100
abcb1/*abcb1*	269/272	98.9
abcb19/*abcb19*	271/276	98.2
abcb1/*abcb1*;*abcb19*/*abcb19*	276/332***	83.1
twd1/*twd1*	245/265***	92.4

Difference between *abcb1*;*19* and WT and between *twd1* and WT was significant at $P<0.001$ (***) and between *abcb1* and WT and between *abcb19* and WT was not significant by Kruskal-Wallis and Mann-Whitney test with Bonferroni correction.

Table 4.6. Embryo viability of *toz*, *mp*, *pin1*;*3*;*6* and *pin1*;*3*;*6*;*abcb1*;*19*.

Genotype of self-fertilized parent	Proportion of viable embryos in siliques of self-fertilized parent (no. of non-aborted seeds / total no. of seeds)	Percentage of viable seeds in siliques of self-fertilized parent
TOZ/*toz-1*	202/277	72.9
MP/*mp*^{G12}	255/256***	99.6
PIN1/*pin1-1*;*pin3*/*pin3*;*pin6*/*pin6*	263/266***	98.9
PIN1/*pin1-1*;*pin3*/*pin3*;*pin6*/*pin6*;*abcb1*/*abcb1*;*abcb19*/*abcb19*	240/284$^{*/***}$	84.5

Difference between negative control for completely penetrant embryo lethality (*mp*^{G12}) and positive control for completely penetrant embryo lethality (*toz-1*) and between *pin1-1*;*3*;*6* and *toz-1* was significant at $P<0.001$ (***) and between *pin1-1*;*3*;*6*;*abcb1*;*19* and *toz-1* was significant at $P<0.05$ (*) by Kruskal-Wallis and Mann-Whitney test with Bonferroni correction. Difference between *pin1-1*;*3*;*6*;*abcb1*;*19* and *mp*^{G12} was significant at $P<0.001$ (***) and between *pin1-1*;*3*;*6* and *mp*^{G12} was not significant by Kruskal-Wallis and Mann-Whitney test with Bonferroni correction.

Table 4.7. Embryo viability of *pin1*;*3*;*6* and *pin1*;*3*;*6*;*abcb1*;*19*.

Genotype of self-fertilized parent	Proportion of embryo-viable mutants in progeny of self-fertilized parent (no. of mutant seedlings / total no. of seedlings)	Percentage of embryo-viable mutants in progeny of self-fertilized parent
PIN1/*pin1-1*;*pin3*/*pin3*;*pin6*/*pin6*	80/361	22.2
PIN1/*pin1-1*;*pin3*/*pin3*;*pin6*/*pin6*;*abcb1*/*abcb1*;*abcb19*/*abcb19*	74/335	22.1

Difference between observed and theoretical frequency distributions of embryo-viable mutants in the progeny of self-fertilized heterozygous parents was not significant by Pearson's chi-squared ($\chi 2$) goodness-of-fit test ($\alpha=0.05$, dF=1).

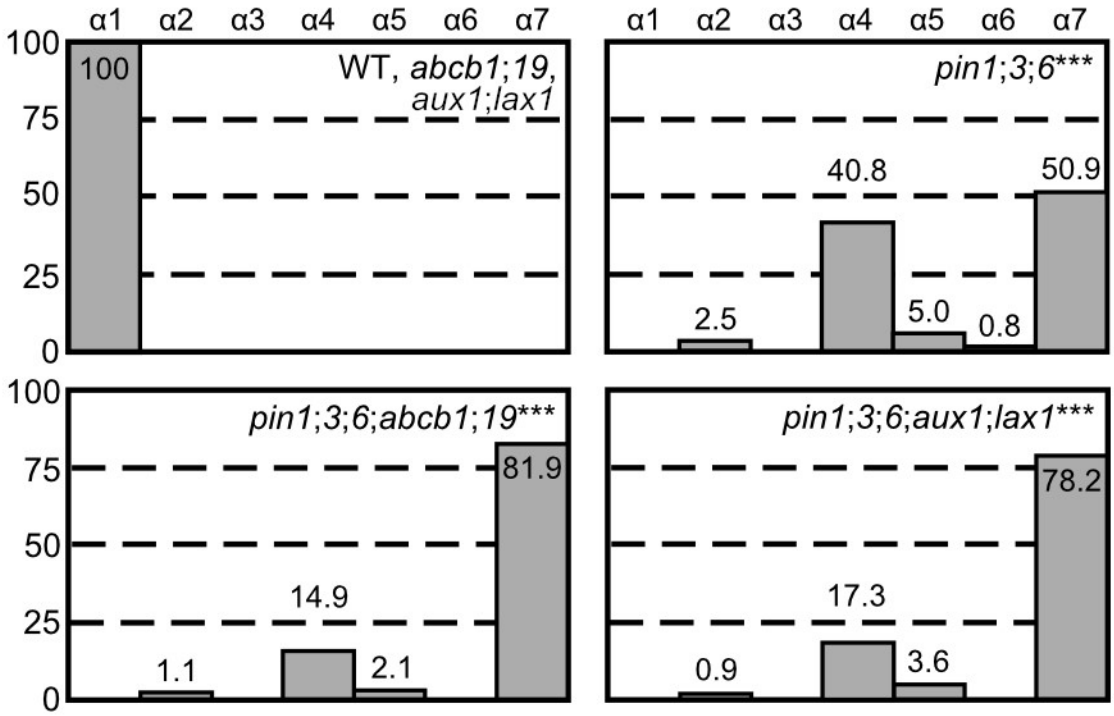

Figure 4.8. Cotyledon patterns of *pin*, *abcb* and *aux1*/*lax* mutants. Percentages of seedlings in phenotype classes (defined in Fig. 4.3). Difference between *pin1-1*;*3*;*6* and WT, between *pin1-1*;*3*;*6*;*abcb1*;*19* and *pin1-1*;*3*;*6* and between *pin1-1*;*3*;*6*;*aux1-355*;*lax1-064* and *pin1-1*;*3*;*6* was significant at $P<0.001$ (***) by Kruskal-Wallis and Mann-Whitney test with Bonferroni correction. Sample population sizes: WT, 56; *abcb1*;*19*, 75; *aux1-355*;*lax1-064*, 87; *pin1-1*;*3*;*6*, 120; *pin1-1*;*3*;*6*;*abcb1*;*19*, 94; *pin1-1*;*3*;*6*;*aux1-355*;*lax1-064*, 110.

(Geisler et al. 2003; Bouchard et al. 2006; Bailly et al. 2008; Wu et al. 2010; Wang et al. 2013). Consistent with this observation, defects of *twd1* are more severe than, though similar to, those of *abcb1*;*19* (Geisler et al. 2003; Bouchard et al. 2006; Bailly et al. 2008; Wu et al. 2010; Wang et al. 2013). We therefore reasoned that analysis of *twd1* vein patterns might uncover vein patterning functions of ABCB-mediated auxin transport that could not be inferred from the analysis of *abcb1*;*19*.

Approximately 25% of *twd1* leaves had Y-shaped midveins and ~15% of *twd1* leaves were fused (Fig. 4.7I), suggesting possible vein-patterning functions of *TWD1*-dependent *ABCB*-mediated auxin transport. However, vein pattern defects induced in *twd1* by 100 μM NPA were no different from those induced in WT or *abcb1*;*19* by NPA (Fig. 4.7I), suggesting that vein patterning functions of *TWD1*-dependent ABCB-mediated auxin transport—if existing—become inconsequential in the absence of *PIN*-dependent vein-patterning activity. By contrast, NPA enhanced leaf separation defects of *twd1* (Fig. 4.7I), suggesting overlapping functions of *TWD1*-dependent ABCB-mediated auxin transport and NPA-sensitive auxin transport in leaf separation.

In conclusion, the residual vein patterning activity in *pin* mutants or their NPA-induced phenocopy is not provided by *ABCB1*, *ABCB19* or *TWD1*-dependent ABCB-mediated auxin transport and loss of PIN- and ABCB-mediated auxin transport fails to phenocopy vein pattern defects of *gn* (Figs. 4.1,4.7).

4.2.6 Contribution of *AUX1*/*LAX* genes to vein patterning

Loss of PIN- and ABCB-mediated auxin transport fails to phenocopy vein pattern defects of *gn* (Figs. 4.1,4.7), suggesting that these latter are not the sole result of loss of *PIN*-dependent, NPA-sensitive or *ABCB*-dependent polar auxin-transport. However, it is possible that the vein pattern defects of *gn* result from additional or exclusive defects in yet another auxin-transport pathway; we asked whether that were so.

Auxin is predicted to enter the cell by diffusion and through an auxin influx carrier (Rubery and Sheldrake 1974; Raven 1975). In Arabidopsis, auxin influx activity is encoded by

the *AUX1*, *LAX1*, *LAX2* and *LAX3* (*AUX1*/*LAX*) genes (Parry et al. 2001; Yang et al. 2006; Swarup et al. 2008; Peret et al. 2012), whose translational fusions to YFP (Peret et al. 2012) are all expressed at early stages of vein development (Fig. 4.9A–D). We thus asked whether AUX1/LAX-mediated auxin influx was required for vein patterning. *aux1*;*lax1*;*2*;*3* embryos were viable (Table 4.8). Because the vein patterns of *aux1*;*lax1*;*2*;*3* were no different from those of WT (Fig. 4.8E,G,I), we conclude that *AUX1*/*LAX* function is dispensable for vein patterning.

We next asked whether contribution of *AUX1*/*LAX* genes to vein patterning only became apparent in conditions of extremely reduced PIN-mediated auxin transport. To address this question, we tested whether vein pattern defects resulting from simultaneous loss of function of *PIN1*, *PIN3* and *PIN6* or induced in WT by 100 μM NPA, which phenocopies mutation of all the *PIN* genes with vein patterning function (Fig. 4.6), were enhanced by simultaneous mutation of *AUX1* and *LAX1* or of all *AUX1*/*LAX* genes, respectively.

pin1;*3*;*6*;*aux1*;*lax1* embryos were viable (Table 4.9) and developed into seedlings (Table 4.10). The spectrum of vein pattern phenotypes of *pin1*;*3*;*6*;*aux1*;*lax1* was no different from that of *pin1*;*3*;*6*, and the vein pattern defects induced in *aux1*;*lax1*;*2*;*3* by NPA were no different from those induced in WT by NPA (Fig. 4.9F,H,I), suggesting no vein-patterning function of *AUX1*/*LAX* genes in conditions of extremely reduced auxin transport. On the other hand, mutation of *AUX1* and *LAX1* in the *pin1*;*3*;*6* background shifted the distribution of *pin1*;*3*;*6* cotyledon pattern phenotypes toward stronger classes (Fig. 4.8), and NPA induced leaf fusion in *aux1*;*lax1*;*2*;*3* but not in WT (Fig. 4.9I), suggesting that AUX1/LAX-mediated auxin influx and NPA-sensitive auxin transport have overlapping functions in cotyledon and leaf separation and that—consistent with previous observations (Reinhardt et al. 2003; Bainbridge et al. 2008; Kierzkowski et al. 2013)—AUX1/LAX-mediated auxin influx contributes to maintaining cotyledon and leaves separate in conditions of reduced auxin transport. Nevertheless, loss of PIN- and AUX1/LAX-mediated auxin transport fails to phenocopy the vein pattern defects of *gn* (Figs. 4.1,4.9).

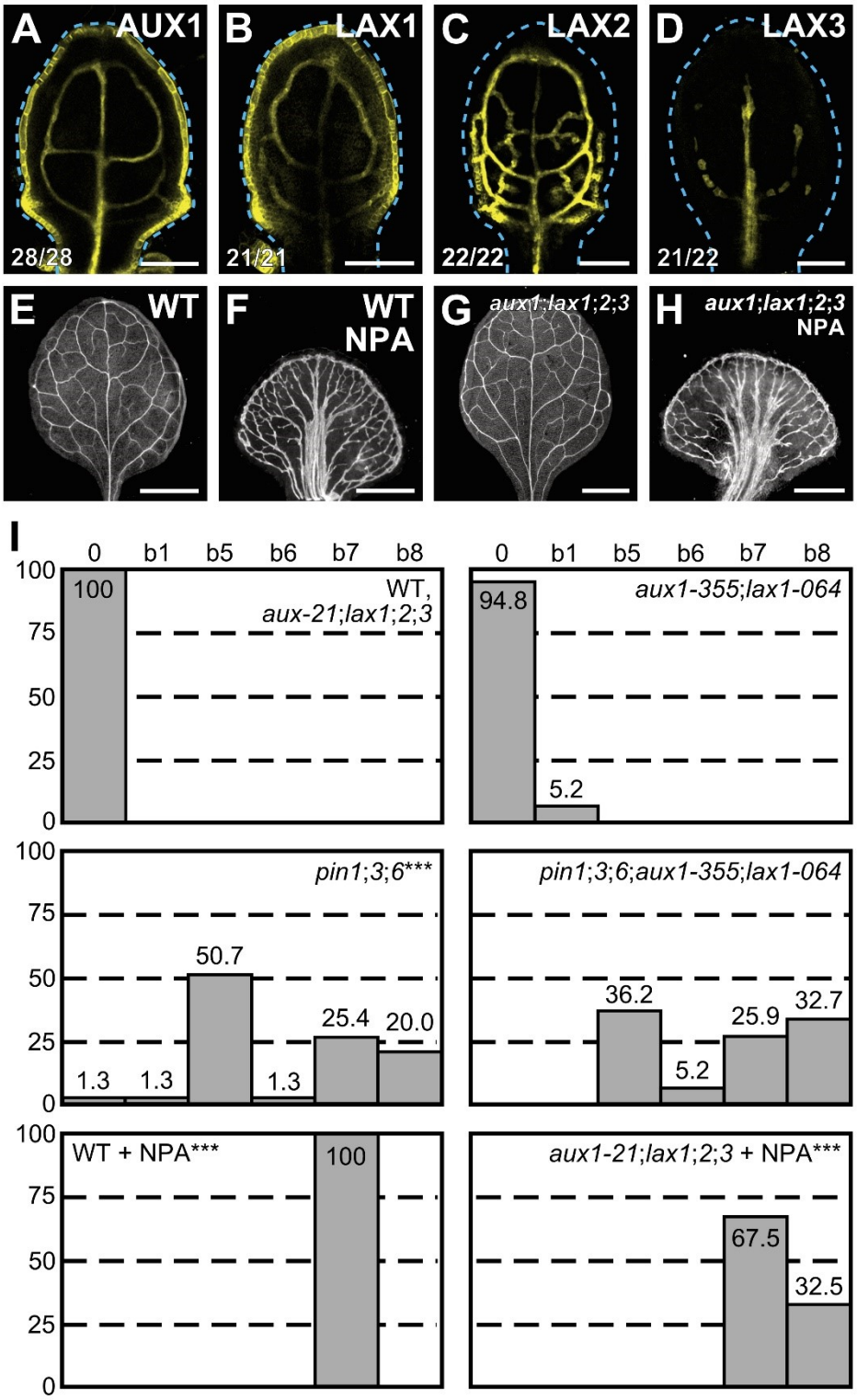

Figure 4.9. Contribution of *AUX1*/*LAX* genes to vein patterning. (A–H) Top right: expression-reported gene, genotype and treatment. (A–D) Bottom left: reproducibility index. (A–D) Confocal laser scanning microscopy; 4-day-old first leaves. Dashed cyan line delineates leaf

outline. (A) AUX1::AUX1:YFP expression. (B) LAX1::LAX1:YFP expression. (C) LAX2::LAX2:YFP expression. (D) LAX3::LAX3:YFP expression. (E–H) Dark-field illumination of mature first leaves. (I) Percentages of leaves in phenotype classes (defined in Figs. 4.1,4.2,4.5,4.7). Difference between *pin1-1*;*3*;*6* and WT, between NPA-grown WT and WT and between NPA-grown *aux1-21*;*lax1*;*2*;*3* and NPA-grown WT was significant at $P<0.001$ (***) by Kruskal-Wallis and Mann-Whitney test with Bonferroni correction. Sample population sizes: WT, 53; *aux1-21*;*lax1*;*2*;*3*, 60; *aux1-355*;*lax1-064*, 77; *pin1-1*;*3*;*6*, 75; *pin1-1*;*3*;*6*;*aux1-355*;*lax1-064*, 58; NPA-grown WT, 46; NPA-grown *aux1-21*;*lax1*;*2*;*3*, 40. Bars: (A–D) 0.1 mm; (E–H) 1 mm.

Table 4.8. Embryo viability of WT, *aux1*, *lax1*, *aux1*;*lax1* and *aux1*;*lax1*;*2*;*3*.

Genotype of self-fertilized parent	Proportion of viable embryos in siliques of self-fertilized parent (no. of non-aborted seeds / total no. of seeds)	Percentage of viable seeds in siliques of self-fertilized parent
WT (Col-0)	272/274	99.3
aux1/*aux1-355*	266/267	99.6
lax1/*lax1-064*	265/267	99.2
aux1/*aux1-355*;*lax1*/*lax1-064*	278/281	98.9
aux1/*aux1-21*;*lax1*/*lax1*;*lax2*/*lax2-1*;*lax3*/*lax3*	261/262	99.6

Difference between *aux1-355* and WT, between *lax1-064* and WT, between *aux1-355*;*lax1-064* and WT and between *aux1-21*;*lax1*;*2-1*;*3* and WT was not significant by Kruskal-Wallis and Mann-Whitney test with Bonferroni correction.

Table 4.9. Embryo viability of *toz*, *mp*, *pin1*;*3*;*6* and *pin1*;*3*;*6*;*aux1*;*lax1*.

Genotype of self-fertilized parent	Proportion of viable embryos in siliques of self-fertilized parent (no. of non-aborted seeds / total no. of seeds)	Percentage of viable seeds in siliques of self-fertilized parent
TOZ/*toz-1*	185/244***	75.8
MP/*mp*^{G12}	220/220	100
PIN1/*pin1-1*;*pin3*/*pin3*;*pin6*/*pin6*	259/261***	99.2
PIN1/*pin1-1*;*pin3*/*pin3*;*pin6*/*pin6*;*aux1*/*aux1-355*;*lax1*/*lax1-064*	280/282***	99.3

Difference between negative control for completely penetrant embryo lethality (*mp*^{G12}) and positive control for completely penetrant embryo lethality (*toz-1*), between *pin1-1*;*3*;*6* and *toz-1* and between *toz-1* and *pin1-1*;*3*;*6*;*aux1-355*;*lax1-064* was significant at $P<0.001$ (***) and between *pin1-1*;*3*;*6* and *mp*^{G12} and between *pin1-1*;*3*;*6*;*aux1-355*;*lax1-064* and *mp*^{G12} was not significant by Kruskal-Wallis and Mann-Whitney test with Bonferroni correction.

Table 4.10. Embryo viability of *pin1*;*3*;*6* and *pin1*;*3*;*6*;*aux1*;*lax1*.

Genotype of self-fertilized parent	Proportion of embryo-viable mutants in progeny of self-fertilized parent (no. of mutant seedlings / total no. of seedlings)	Percentage of embryo-viable mutants in progeny of self-fertilized parent
PIN1/*pin1-1*;*pin3*/*pin3*;*pin6*/*pin6*	87/390	22.3
PIN1/*pin1-1*;*pin3*/*pin3*;*pin6*/*pin6*;*aux1*/*aux1-355*;*lax1*/*lax1-064*	109/489	22.3

Difference between observed and theoretical frequency distributions of embryo-viable mutants in the progeny of self-fertilized heterozygous parents was not significant by Pearson's chi-squared ($\chi 2$) goodness-of-fit test ($\alpha=0.05$, $dF=1$).

4.2.7 Genetic interaction between *GN* and *PIN* genes

The vein pattern defects of *gn* are not the sole result of loss of *PIN*-dependent auxin transport (Figs. 4.1,4.5,4.6); however, they could be the result of abnormal polarity of PIN-mediated auxin transport induced by defects in coordination of PIN polarity. Were that so, the vein pattern defects of *gn* would depend on *PIN* genes and therefore the vein pattern defects of *gn*;*pin* mutants would resemble those of *pin* mutants; we tested whether that were so.

We first asked what the phenotype were of the quintuple mutant between the strong allele *gn-13* (Fig. 4.1) and mutation in *PIN1*, *PIN3*, *PIN4* and *PIN7*—i.e. the *PM-PIN* genes with vein patterning function (Fig. 4.2).

Consistent with previous observations (Mayer et al. 1993; Shevell et al. 1994), in *gn* seedlings hypocotyl and root were replaced by a basal peg and the cotyledons were most frequently fused (Figs. 4.10A,C;4.11A,B).

As shown above (Figs. 4.3A,H;4.4A,B), *pin1*;*3*;*4*;*7* seedlings had hypocotyl, short root and a single cotyledon or two, either separate or fused, cotyledons (Figs. 4.10A,B;4.11B).

A novel phenotype segregated in approximately one-sixteenth of the progeny of plants homozygous for *pin3*, *pin4* and *pin7* and heterozygous for *pin1* and *gn* (256/3624)—no different from the one-sixteenth frequency expected for the *gn*;*pin1*;*3*;*4*;*7* homozygous mutants by Pearson's chi-squared (χ^2) goodness-of-fit test (α=0.05, dF=1). We genotyped 10 of the seedlings with the novel mutant phenotype and found they were *gn*;*pin1*;*3*;*4*;*7* homozygous mutants. *gn*;*pin1*;*3*;*4*;*7* seedlings had hypocotyl, no root and the cotyledons were fused (Figs. 4.10A,D;4.11B).

WT cotyledons had an unbranched midvein and three or four loops (Figs. 4.12A,B,K). All the veins of *pin1*;*3*;*4*;*7* cotyledons were thick, and all *pin1*;*3*;*4*;*7* cotyledons had three or four loops (Figs. 4.12C,D,K). In *pin1*;*3*;*4*;*7* cotyledons, the distal end of the first loops joined the midvein more proximally than in WT and minor veins branched from midvein and loops

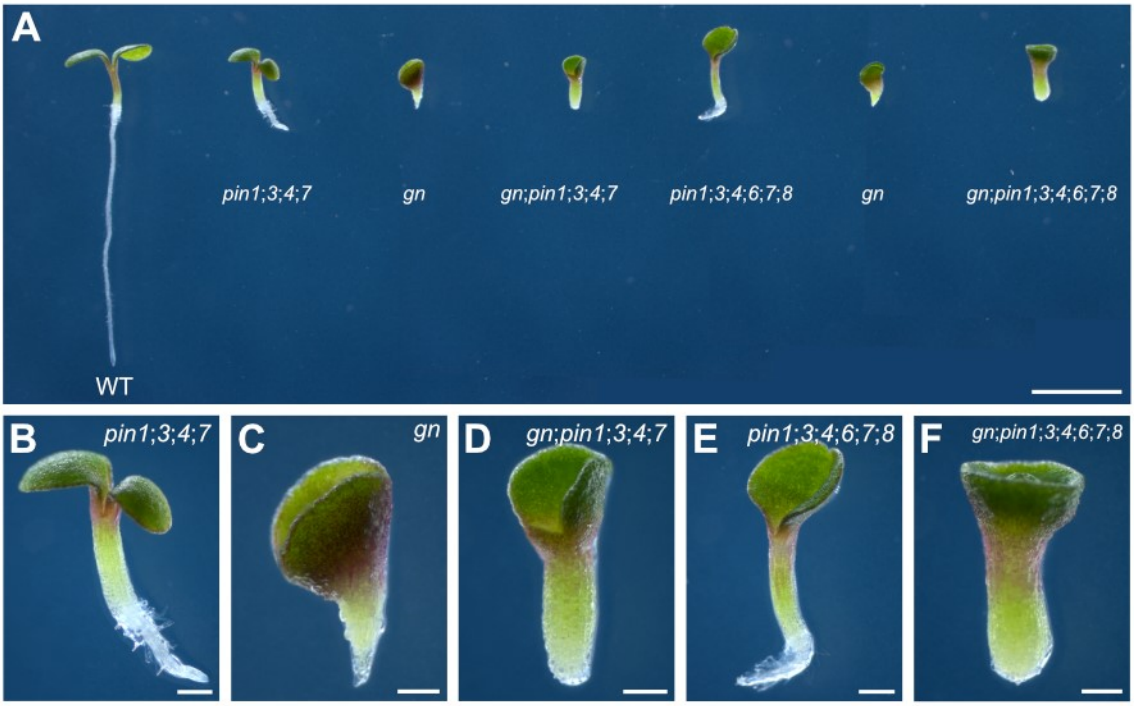

Figure 4.10. *pin* and *gn* mutant seedlings. (A–F) Dark-field illumination composite of 3-day-old seedlings. (A) Overview. (B–F) Details. Genotypes below respective seedlings (A) or top right (B–F). Bars: (A) 2 mm; (B–F) 0.25 mm.

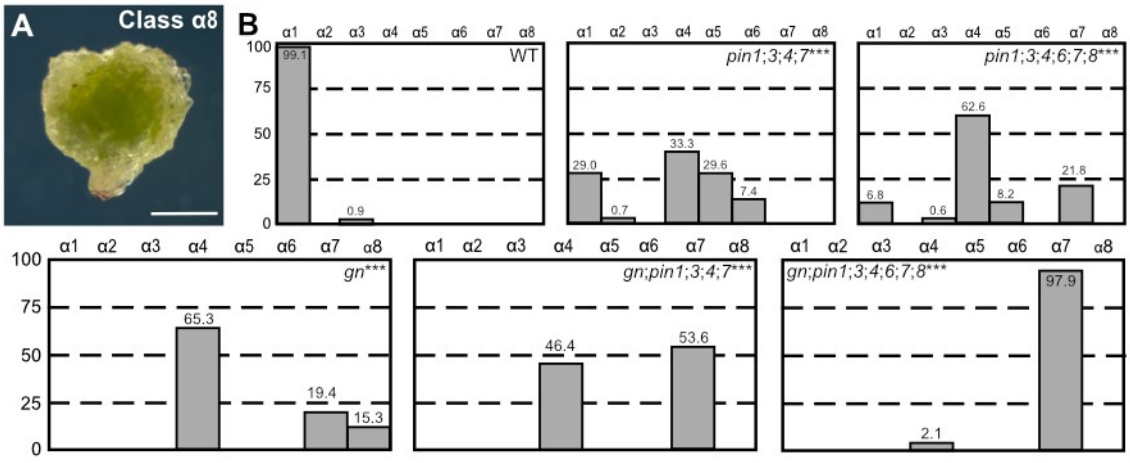

Figure 4.11. Cotyledon patterns of *pin* and *gn* mutants. (A) Dark-field illumination of a 5-day-old seedling illustrating phenotype class α8 (no cotyledons). (B) Percentages of seedlings in phenotype classes (classes α1–α7 defined in Fig. 4.3). Difference between *pin1-1*;*3*;*4*;*7* and WT, between *pin1-1*;*3*;*4*;*6*;*7*;*8* and WT, between *gn-13* and WT, between *gn-13*;*pin1-1*;*3*;*4*;*7* and *pin1-1*;*3*;*4*;*7* and between *gn-13*;*pin1-1*;*3*;*4*;*6*;*7*;*8* and *pin1-1*;*3*;*4*;*6*;*7*;*8* was significant at $P<0.001$ (***) by Kruskal-Wallis and Mann-Whitney test with Bonferroni correction. Sample population sizes: WT, 111; *pin1-1*;*3*;*4*;*7*, 135; *pin1-1*;*3*;*4*;*6*;*7*;*8*, 147; *gn-13*, 72; *gn-13*;*pin1-1*;*3*;*4*;*7*, 84; *gn-13*;*pin1-1*;*3*;*4*;*6*;*7*;*8*, 93. Bar: (A) 0.5 mm.

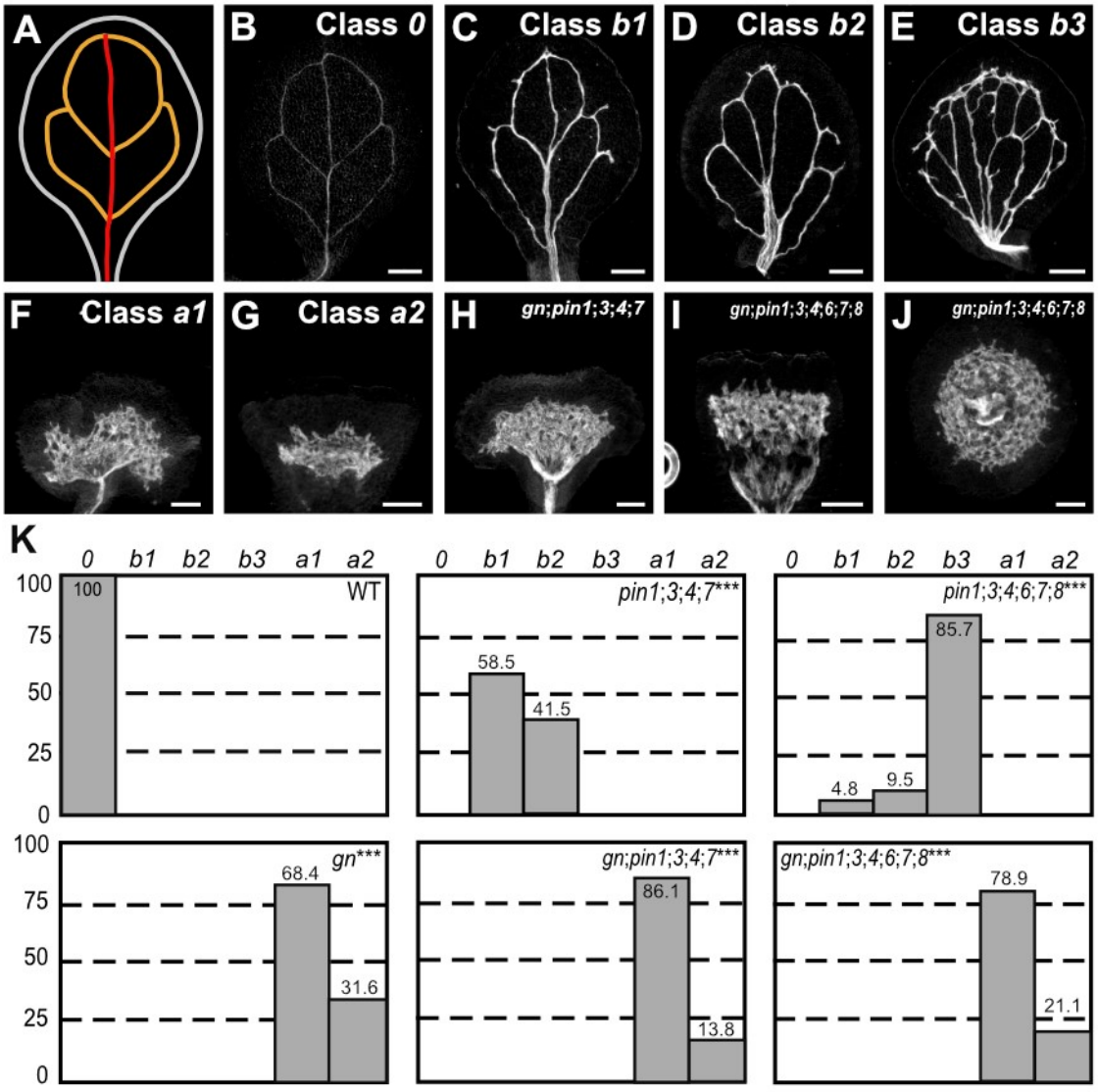

Figure 4.12. Cotyledon vein patterns of *pin* and *gn* mutants. (A,B) Vein pattern of WT mature cotyledon. In (A): red, midvein; orange, vein loops. (B–J) Dark-field illumination of mature cotyledons. Top right: phenotype class or genotype. (B–G) Phenotype classes: class *0*, I-shaped midvein and three or four loops (B); class *b1*, I-shaped midvein, thick veins and minor veins (I); class *b2*, Y-shaped midvein, thick veins and minor veins (J); class *b3*, thick veins, loops joining midvein at base of cotyledon and apically thickened vein-network outline (K); class *a1*, shapeless vascular cluster with short stretches of vascular elements connecting cluster to base of cotyledon (L); class *a2*, shapeless vascular cluster (M). (H–J) Dark-field illumination of mature cotyledons of *gn-13*;*pin1-1*;*3*;*4*;*7* (class *a1*) (N) or *gn-13*;*pin1-1*;*3*;*4*;*6*;*7*;*8* (class *a1*) (I, side view; J, top view). (Q) Percentages of cotyledons in phenotype classes. Difference between

pin1-1;*3*;*4*;*7* and WT, between *pin1-1*;*3*;*4*;*6*;*7*;*8* and WT, between *gn-13* and WT, between *gn-13*;*pin1-1*;*3*;*4*;*7* and *pin1-1*;*3*;*4*;*7* and between *gn-13*;*pin1-1*;*3*;*4*;*6*;*7*;*8* and *pin1-1*;*3*;*4*;*6*;*7*;*8* was significant at $P<0.001$ (***) by Kruskal-Wallis and Mann-Whitney test with Bonferroni correction. Sample population sizes: WT, 52; *pin1-1*;*3*;*4*;*7*, 65; *pin1-1*;*3*;*4*;*6*;*7*;*8*, 63; *gn-13*, 57; *gn-13*;*pin1-1*;*3*;*4*;*7*, 65; *gn-13*;*pin1-1*;*3*;*4*;*6*;*7*;*8*, 57. Bars: (B–J) 0.25 mm.

(Fig. 4.12C,D,K). Approximately 60% of *pin1*;*3*;*4*;*7* cotyledons had an I-shaped midvein, while the remaining ~40% of them had a Y-shaped midvein (Fig. 4.12C,D,K).

Consistent with previous observations (Mayer et al. 1993; Shevell et al. 1994), in ~70% of *gn* cotyledons short stretches of vascular elements connected the proximal side of a central, shapeless cluster of randomly oriented vascular elements with the basal part of the cotyledon, while vascular differentiation was limited to a central, shapeless vascular cluster in the remaining ~30% of *gn* cotyledons (Fig. 4.12F,G,K). The vein pattern defects of *gn*;*pin1*;*3*;*4*;*7* cotyledons were no different from those of *gn* cotyledons (Fig. 4.12H,K), suggesting that the vein pattern phenotype of *gn* cotyledons is epistatic to that of *pin1*;*3*;*4*;*7* cotyledons. Likewise, the vein pattern defects of *gn*;*pin1*;*3*;*4*;*7* leaves were no different from those of *gn* leaves (Fig. 4.13A,B,E), suggesting that the vein pattern phenotype of *gn* leaves is epistatic to that of *pin1*;*3*;*4*;*7* leaves.

We next asked what the phenotype were of the septuple mutant between the strong allele *gn-13* (Fig. 4.1) and mutation in all the *PIN* genes with vein patterning function (Fig. 4.5).

As shown above (Figs. 4.3A,H;4.4A,D), *pin1*;*3*;*4*;*6*;*7*;*8* seedlings had hypocotyl, short root and a single cotyledon or two fused cotyledons (Figs. 4.10A,E;4.11B).

A phenotype similar to that of *gn*;*pin1*;*3*;*4*;*7* segregated in approximately one-sixteenth of the progeny of plants homozygous for *pin3*, *pin4*, *pin6*, *pin7* and *pin8* and heterozygous for *pin1* and *gn* (222/3231)—no different from the one-sixteenth frequency expected for the *gn*;*pin1*;*3*;*4*;*6*;*7*;*8* homozygous mutants by Pearson's χ^2 goodness-of-fit test (α=0.05, dF=1). We genotyped 10 of the seedlings with the novel mutant phenotype and found they were *gn*;*pin1*;*3*;*4*;*6*;*7*;*8* homozygous mutants. As *gn*;*pin1*;*3*;*4*;*7* seedlings, *gn*;*pin1*;*3*;*4*;*6*;*7*;*8* seedlings had hypocotyl and no root, but unlike *gn*;*pin1*;*3*;*4*;*7* seedlings ~90% of *gn*;*pin1*;*3*;*4*;*6*;*7*;*8* seedlings had completely fused cup-shaped cotyledons (Figs. 4.10A,F;4.11B).

The vein pattern defects of *pin1*;*3*;*4*;*6*;*7*;*8* cotyledons were similar to those of *pin1*;*3*;*4*;*7* cotyledons, but in ~85% of *pin1*;*3*;*4*;*6*;*7*;*8* cotyledons the loops joined the midvein at the base of the cotyledon and the top half of the vein network outline was thick (Fig. 4.12C–E,K). The vein pattern defects of *gn*;*pin1*;*3*;*4*;*6*;*7*;*8* cotyledons were no different from those of *gn* cotyledons (Fig. 4.12I–K), suggesting that the vein pattern phenotype of *gn* cotyledons is epistatic to that of

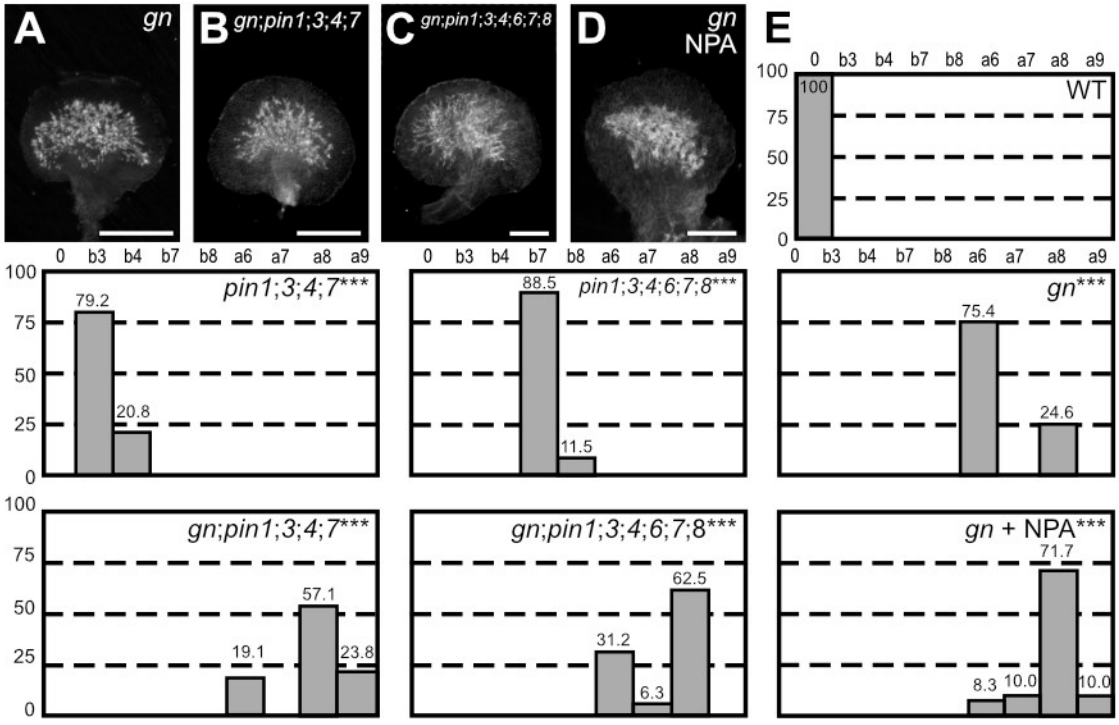

Figure 4.13. Genetic interaction between *GN* and *PIN* genes. (A–D) Dark-field illumination of mature first leaves. Top right: genotype and treatment. (E) Percentages of leaves in phenotype classes (defined in Fig. 4.1,4.2,4.5). Difference between *pin1-1*;*3*;*4*;*7* and WT, between *pin1-1*;*3*;*4*;*6*;*7*;*8* and WT, between *gn* and WT, between *gn-13*;*pin1-1*;*3*;*4*;*7* and *pin1-1*;*3*;*4*;*7*, between *gn-13*;*pin1-1*;*3*;*4*;*6*;*7*;*8* and *pin1-1*;*3*;*4*;*6*;*7*;*8* and between NPA-grown *gn-13* and *pin1-1*;*3*;*4*;*6*;*7*;*8* was significant at $P<0.001$ (***) by Kruskal-Wallis and Mann-Whitney test with Bonferroni correction. Sample population sizes: WT, 63; *pin1-1*;*3*;*4*;*7*, 53; *pin1-1*;*3*;*4*;*6*;*7*;*8*, 52; *gn-13*, 69; *gn-13*;*pin1-1*;*3*;*4*;*7*, 21; *gn-13*;*pin1-1*;*3*;*4*;*6*;*7*;*8*, 15; NPA-grown *gn-13*, 60. Bars: (A–D) 0.5 mm.

pin1;*3*;*4*;*6*;*7*;*8* cotyledons. Likewise, the vein pattern defects of *gn*;*pin1*;*3*;*4*;*6*;*7*;*8* leaves were no different from those of *gn* leaves (Fig. 4.13C,E), suggesting that the vein pattern phenotype of *gn* leaves is epistatic to that of *pin1*;*3*;*4*;*6*;*7*;*8* leaves. Finally, 100 μM NPA, which phenocopies loss of *PIN*-dependent vein-patterning activity (Fig. 4.6), failed to induce additional vein pattern defects in *gn* leaves (Fig. 4.13D,E).

In conclusion, our results suggest that the vein pattern defects of *gn* are *not* the result of either the sole loss of *PIN*-dependent auxin transport or the sole abnormal polarity of PIN-mediated auxin transport induced by defects in coordination of PIN polarity.

4.2.8 Response of *pin* leaves to auxin application

The uniform vein-pattern phenotype of *pin1*;*3*;*4*;*6*;*7*;*8* was phenocopied by growth of WT in the presence of high concentration of NPA (Fig. 4.6). Moreover, the vein-pattern phenotype of *pin1*;*3*;*4*;*6*;*7*;*8* was unchanged by NPA treatment, and the NPA-induced vein-pattern phenocopy of *pin1*;*3*;*4*;*6*;*7*;*8* was unchanged by mutation in any known intercellular auxin-transporter (Fig. 4.7,4.9). These observations suggest that the function of known intercellular auxin-transporters in vein patterning is dispensable in the absence of the auxin transport activity of PIN1, PIN3, PIN4, PIN6, PIN7 and PIN8. Because auxin transport is thought to be essential for auxin-induced vascular-strand formation [reviewed in (Sachs 1981; Berleth and Mattsson 2000; Aloni 2010; Sawchuk and Scarpella 2013)], we asked whether auxin induced vein formation in *pin1*;*3*;*4*;*6*;*7*;*8,* and consequently whether veins were formed by an auxin-dependent mechanism in *pin1*;*3*;*4*;*6*;*7*;*8*. To address this question, we applied lanolin paste containing 1% of the natural auxin indole-3-acetic acid (IAA) to one side of developing leaves of WT and *pin1*;*3*;*4*;*6*;*7*;*8* and recorded tissue response in mature leaves.

Consistent with previous reports (Scarpella et al. 2006; Sawchuk et al. 2007), IAA induced formation of extra veins in ~70% of WT leaves (27/38) (Fig. 4.14A,B), while ~30% of WT leaves (9/38) failed to respond to IAA application.

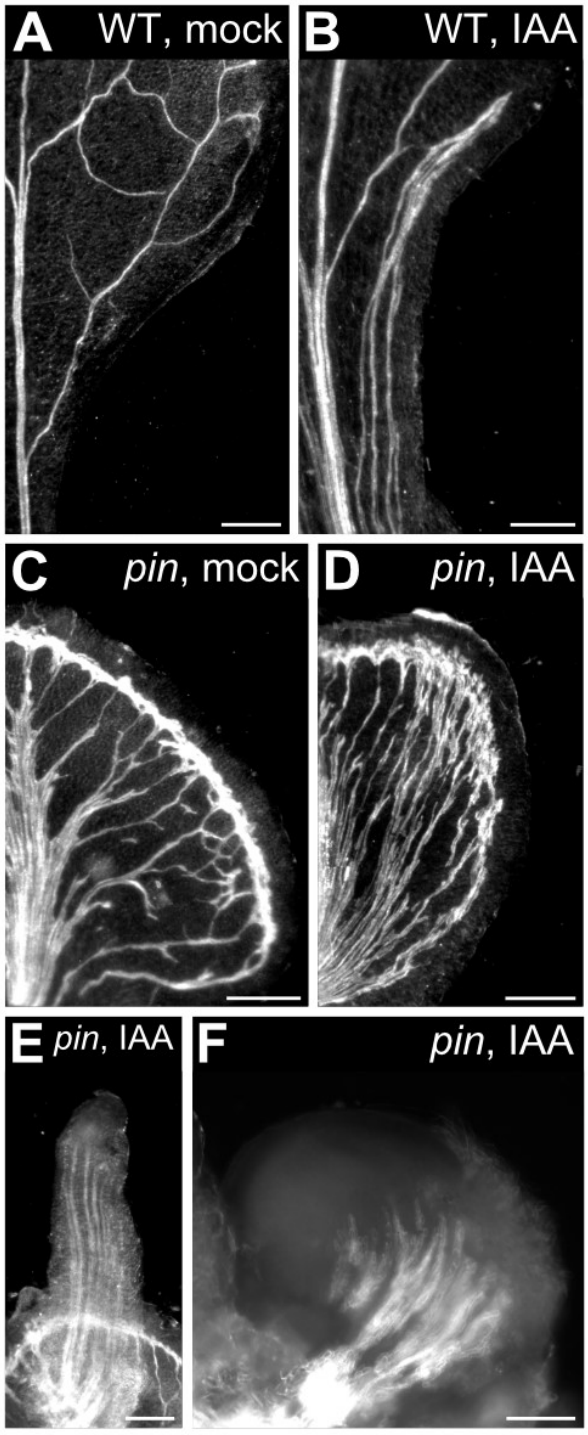

Figure 4.14. Response of *pin* leaves to auxin application. (A–F) Top right: genotype and treatment. Dark-field illumination of mature first leaves of WT (A,B) or *pin1-1*;*3*;*4*;*6*;*7*;*8* (C–F) at side of application of lanolin paste (A,C) or lanolin paste containing 1% IAA (B,D–F). Bars: (A) 0.5 mm; (B–E) 0.25 mm; (F) 0.1 mm.

The effects of IAA on *pin1*;*3*;*4*;*6*;*7*;*8* leaves were variable. In 40% of the leaves (28/70), IAA induced formation of extra veins (Fig. 4.14C,D). In ~60% of the leaves in which IAA induced formation of extra veins (17/28), IAA also induced tissue outgrowth of varied shape (Fig. 4.14E,F). In 30% of *pin1*;*3*;*4*;*6*;*7*;*8* leaves (21/70), IAA induced tissue outgrowth but failed to induce formation of extra veins in the leaf; however, in nearly 80% of the *pin1*;*3*;*4*;*6*;*7*;*8* leaves in which IAA induced tissue outgrowth [30/(17+21)=30/38], IAA also induced formation of vascular strands in the outgrowth (Fig. 4.14E,F). Finally, as in WT, 30% of *pin1*;*3*;*4*;*6*;*7*;*8* leaves (21/70) failed to respond to IAA application in any noticeable way.

We conclude that *pin1*;*3*;*4*;*6*;*7*;*8* leaves respond to vein-formation-inducing auxin signals and consequently that veins are formed by an auxin-dependent mechanism in the absence of PIN-mediated auxin transport.

4.2.9 Contribution of auxin signaling to vein patterning

Leaves of *pin1*;*3*;*4*;*6*;*7*;*8* respond to vein-formation-inducing auxin signals (Fig. 4.14), suggesting that the residual vein-patterning activity in those leaves may be provided by an auxin-dependent mechanism. We therefore asked what the contribution of auxin signaling to vein patterning were in the absence of *PIN*-dependent vein patterning activity.

To address this question, we used mutants in *AUXIN-RESISTANT1* (*AXR1*), which lack a required post-translational modification of the auxin receptor complex [reviewed in (Calderon-Villalobos et al. 2010)], and double mutants in *TRANSPORT INHIBITOR RESPONSE1* (*TIR1*) and *AUXIN SIGNALING F-BOX2* (*AFB2*), which lack the two auxin receptors that most contribute to auxin signaling (Dharmasiri et al. 2005).

As in leaves of weak *gn* alleles (Fig. 4.1), in ~40–50% of the leaves of both *axr1* and *tir1*;*afb2* veins were replaced by vein fragments (Fig. 4.15B,F). In addition, loops were open in most of the leaves of *axr1* and *tir1*;*afb2* (Fig. 4.15A,B,F).

We next asked whether *axr1* or *tir1*;*afb2* enhanced the vein pattern defects induced by 100 μM NPA, which phenocopies loss of *PIN*-dependent vein-patterning activity (Fig. 4.6).

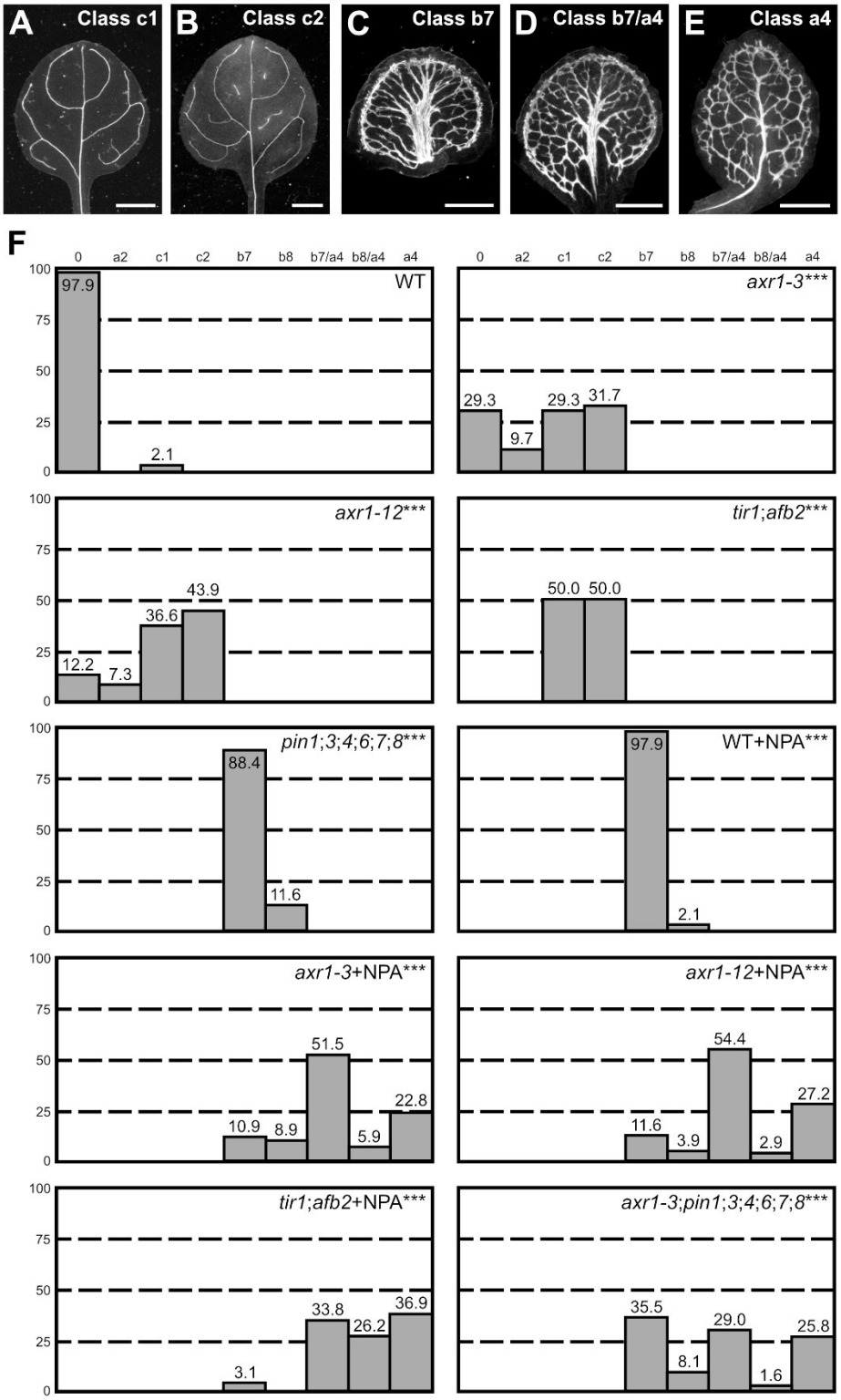

Figure 4.15. Contribution of auxin signaling to vein patterning. (A–E) Dark-field illumination of mature first leaves illustrating phenotype classes (top right): class c1, open vein-network outline (A); class c2, open vein-network outline and fragmented vein network (B); class

b7 (defined in Fig. 4.5) (C); class b7/a4, wide midvein, more lateral-veins, dense network of thick veins and conspicuous marginal vein (D); class b8/a4, fused leaves with wide midvein, more lateral-veins, dense network of thick veins and conspicuous marginal vein (not shown); class a4 (defined in Fig. 4.1) (E). (F) Percentages of leaves in phenotype classes (Classes 0, a2 and b8 defined in Figs. 4.1,4.5). Difference between *axr1-3* and WT, between *axr1-12* and WT, between *tir1*;*afb2* and WT, between *pin1-1*;*3*;*4*;*6*;*7*;*8* and WT, between NPA-grown WT and WT, between NPA-grown *axr1-3* and NPA-grown WT, between NPA-grown *axr1-12* and NPA-grown WT, between NPA-grown *tir1*;*afb2* and NPA-grown WT and between *axr1-3*;*pin1-1*;*3*;*4*;*6*;*7*;*8* and *pin1-1*;*3*;*4*;*6*;*7*;*8* was significant at $P<0.001$ (***) by Kruskal-Wallis and Mann-Whitney test with Bonferroni correction. Sample population sizes: WT, 47; *axr1-3*, 41; *axr1-12*, 41; *tir1*;*afb2*, 42; *pin1-1*;*3*;*4*;*6*;*7*;*8*, 63; NPA-grown WT, 146; NPA-grown *axr1-3*, 101; NPA-grown *axr1-12*, 103; NPA-grown *tir1*;*afb2*, 65; *axr1-3*;*pin1-1*;*3*;*4*;*6*;*7*;*8*, 62. Bars: (A,B) 1 mm; (C–E) 0.75 mm.

Approximately 20% of the leaves of NPA-grown *axr1* and ~3% of those of NPA-grown *tir1*;*afb2* resembled those of NPA-grown WT or of *pin1*;*3*;*4*;*6*;*7*;*8* (Fig. 4.15C,F). However, ~25% of the leaves of NPA-grown *axr1* and nearly 40% of those of NPA-grown *tir1*;*afb2* resembled those of intermediate *gn* alleles: veins were thicker, the vein network was denser and its outline was jagged because of narrow clusters of vascular elements that were oriented perpendicular to the leaf margin and that were laterally connected by veins (Figs. 4.1;4.15E,F). Finally, nearly 60% of the leaves of NPA-grown *axr1* and *tir1*;*afb2* had features intermediate between those of NPA-grown WT or of *pin1*;*3*;*4*;*6*;*7*;*8* and those of intermediate *gn* alleles (Fig. 4.15D,F).

We next asked whether the spectrum of vein pattern defects of NPA-grown *axr1* and *tir1*;*afb2* were recapitulated by the *axr1*;*pin1*;*3*;*4*;*6*;*7*;*8* septuple mutant.

axr1;*pin1*;*3*;*4*;*6*;*7*;*8* embryos were viable (Table 4.11) and developed into seedlings (Table 4.12) that resembled *pin1*;*3*;*4*;*6*;*7*;*8* seedlings (Figs. 4.16A,B;4.17); however, the spectrum of vein pattern defects of *axr1*;*pin1*;*3*;*4*;*6*;*7*;*8* was no different from that of NPA-grown *axr1* (Fig. 4.15D–F).

These observations suggest that the residual vein-patterning activity in *pin1*;*3*;*4*;*6*;*7*;*8* is provided, at least in part, by AXR1- and TIR1/AFB2-mediated auxin signaling. Because reduction of AXR1- and TIR1/AFB2-mediated auxin signaling synthetically enhanced vein pattern defects resulting from loss of *PIN*-dependent vein-patterning activity, we conclude that PIN-mediated auxin transport and AXR1- and TIR1/AFB2-mediated auxin signaling provide overlapping functions in vein patterning. Finally, the similarity between the vein pattern defects of NPA-grown *axr1* and *tir1*;*afb2* and of *axr1*;*pin1*;*3*;*4*;*6*;*7*;*8*, on the one hand, and those of intermediate *gn* alleles, on the other, suggest that the vein pattern defects of *gn* are caused by simultaneous defects in auxin transport and signaling.

4.2.10 Auxin response in *gn*

Were the vein pattern defects of *gn* the result not only of abnormal polarity or loss of PIN-mediated auxin transport but of defects in auxin signaling, the vein pattern defects of *gn* might be

Table 4.11. Embryo viability of *toz*, *mp*, *pin1*;*3*;*4*;*6*;*7*;*8*, *pin1*;*3*;*4*;*6*;*7*;*8*;*axr1*, *gn* and *gn*;*axr1*.

Genotype of self-fertilized parent	Proportion of viable embryos in siliques of self-fertilized parent (no. of non-aborted seeds / total no. of seeds)	Percentage of viable seeds in siliques of self-fertilized parent
TOZ/*toz-1*	190/239	79.5
MP/*mp*^{G12}	261/262***	99.6
PIN1/pin1-1;*pin3/pin3*;*pin4/pin4*;*pin6/pin6*;*pin7/pin7*;*pin8/pin8*	243/244***	99.6
axr1/*axr1-3*;*PIN1/pin1-1* ;*pin3/pin3*;*pin4/pin4*;*pin6/pin6*;*pin7/pin7*;*pin8/pin8*	240/248***	96.8
GN/*gn-13*	248/252***	98.4
GN/*gn-13*;*axr1*/*axr1-3*	264/270***	97.8
GN/*gn-13*;*axr1*/*axr1-12*	178/183***	97.3

Difference between negative control for completely penetrant embryo lethality (*mp*^{G12}) and positive control for completely penetrant embryo lethality (*toz-1*), between *pin1-1*;*3*;*4*;*6*;*7*;*8* and *toz-1*, between *pin1-1*;*3*;*4*;*6*;*7*;*8*;*axr1-3* and *toz-1*, between *gn-13* and *toz-1*, between *gn-13*;*axr*1-3 and *toz-1* and between *gn-13*;*axr1-12* and *toz-1* was significant at $P<0.001$ (***), between *pin1-1*;*3*;*4*;*6*;*7*;*8* and *mp*^{G12}, between *pin1-1*;*3*;*4*;*6*;*7*;*8*;*axr1-3* and *mp*^{G12}, between *gn-13* and *mp*^{G12}, between *gn-13*;*axr1-3* and *mp*^{G12} and between *gn-13*;*axr1-12* and *mp*^{G12} was not significant by Kruskal-Wallis and Mann-Whitney test with Bonferroni correction.

Table 4.12. Embryo viability of *pin1*;*3*;*4*;*6*;*7*;*8*;*axr1*, *gn*, *gn*;*axr1*.

Genotype of self-fertilized parent	Proportion of embryo-viable mutants in progeny of self-fertilized parent (no. of mutant seedlings / total no. of seedlings)	Percentage of embryo-viable mutants in progeny of self-fertilized parent
axr1/*axr1-3*;*PIN1*/*pin1-1* ;*pin3*/*pin3*;*pin4*/*pin4*;*pin6*/*pin6*;*pin7*/*pin7*;*pin8*/*pin8*	66/277	23.8
GN/*gn-13*	101/411	24.6
GN/*gn1-13*; *axr1*/*axr1-3*	74/321	23.0
GN/*gn1-13*; *axr1*/*axr1-12*	70/276	25.4

Difference between observed and theoretical frequency distributions of embryo-viable mutants in the progeny of self-fertilized heterozygous parents was not significant by Pearson's chi-squared (χ^2) goodness-of-fit test (α=0.05, dF=1).

Figure 4.16. *pin* and *axr1* mutant seedlings. (A–C) Dark-field illumination composite of 3-day-old seedlings; genotypes below respective seedlings (A) or top right (B,C). (A) Overview. Because the seedling lineup was wider than the stereomicroscope's field of view, overlapping images of parts of the lineup were acquired and combined to reconstruct the original lineup. (B,C) Details. Bars: (A) 2 mm; (B,C) 0.5 mm.

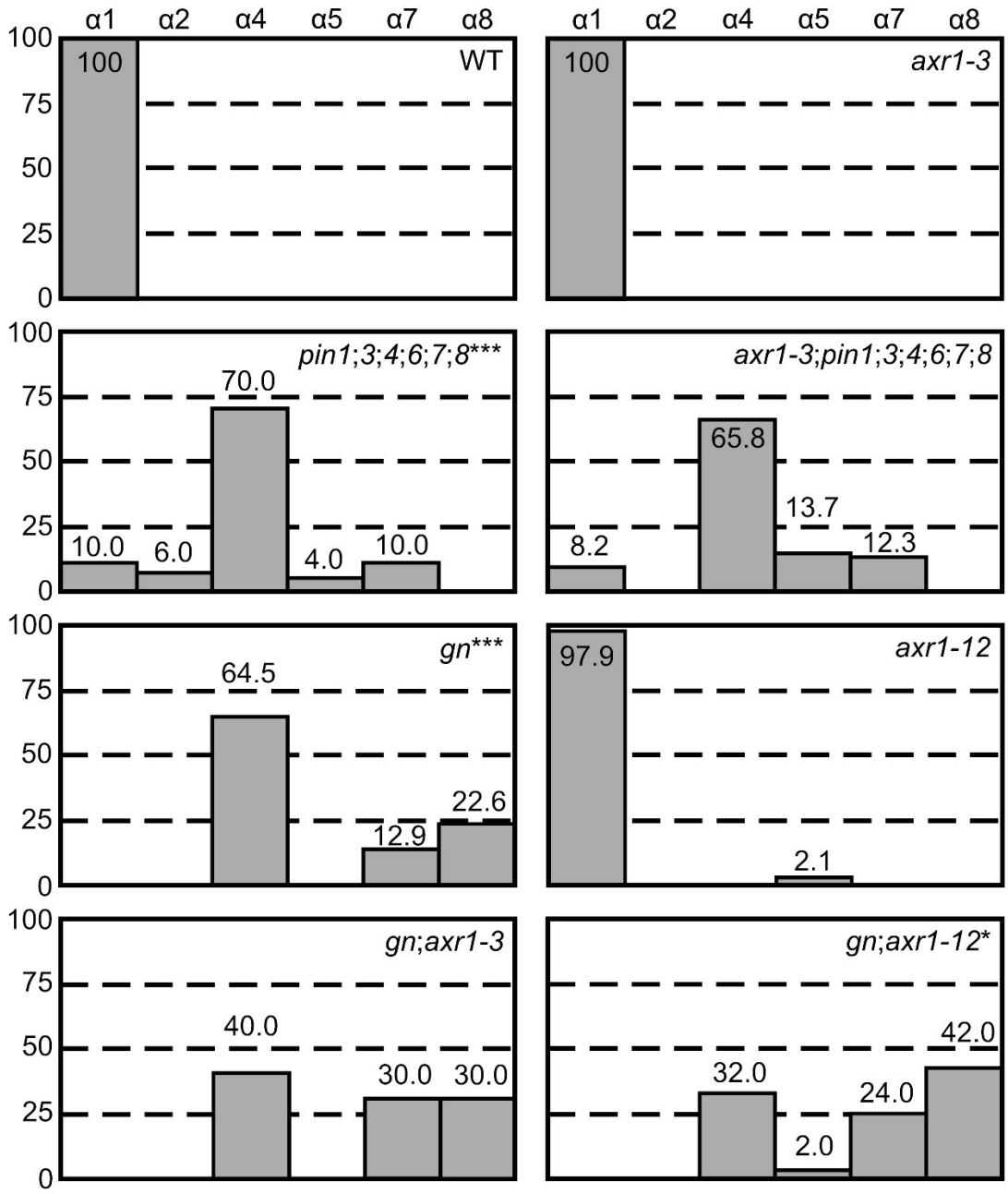

Figure 4.17. Cotyledon patterns of *pin* and *axr1* mutants. Percentages of seedlings in phenotype classes (defined in Fig. 4.3). Difference between *pin1-1*;*3*;*4*;*6*;*7*;*8* and WT and between *gn-13* and WT was significant at $P<0.001$ (***) and between *gn-13*;*axr1-12* was significant at $P<0.05$ (*) by Kruskal-Wallis and Mann-Whitney test with Bonferroni correction. Sample population sizes: WT, 59; *axr1-3*, 49; *pin1-1*;*3*;*4*;*6*;*7*;*8*, 50; *axr1-3*;*pin1-1*;*3*;*4*;*6*;*7*;*8*, 146; *gn-13*, 62; *axr1-12*, 47; *gn-13*;*axr1-3*, 70; *gn-13*;*axr1-12*, 50.

associated with reduced auxin response and the reduced auxin response of *gn* should be recapitulated by that of NPA-grown *axr1*; we asked whether that were so.

To address this question, we imaged and compared expression of the auxin response reporter DR5rev::nYFP (Heisler et al. 2005; Sawchuk et al. 2013) in first leaves of WT, *pin1*;*3*;*4*;*6*;*7*;*8*, NPA-grown WT, *axr1*, *gn* and NPA-grown *axr1* 4 days after germination.

As previously shown (Sawchuk et al. 2013; Verna et al. 2015) (Chapter 2), strong DR5rev::nYFP expression was mainly associated with developing veins in WT (Fig. 4.18A). In *pin1*;*3*;*4*;*6*;*7*;*8* and NPA-grown WT, DR5rev::nYFP expression was weaker and mainly confined to areas near the margin of the leaf (Fig. 4.18B–E). DR5rev::nYFP expression was weaker also in *axr1* but was still associated with developing veins (Fig. 4.18F,G). Finally, in both *gn* and NPA-grown *axr1*, DR5rev::nYFP expression was much weaker and diffused across large areas of the leaf (Fig. 4.18H–K), suggesting that the vein pattern defects of *gn* are associated with reduced auxin response and that the reduced auxin response of *gn* is recapitulated by NPA-grown *axr1*.

Did PIN-mediated auxin transport and AXR1- and TIR1/AFB2-mediated auxin signaling provide overlapping functions in vein patterning and were the vein pattern defects of *gn* caused by simultaneous defects in auxin transport and signaling, the vein pattern defects of *gn*;*axr1* mutants would resemble those of *gn* mutants; we tested whether that were so.

gn;*axr1* seedlings resembled *gn* seedlings (Figs. 4.17;4.19A–C) and the vein pattern defects of *gn*;*axr1* were no different from those of *gn* (Fig. 4.20A–C), suggesting that the phenotype of *gn* is epistatic to that of *axr1*.

We conclude that that the vein pattern defects of *gn* are caused by simultaneous defects in auxin transport and signaling.

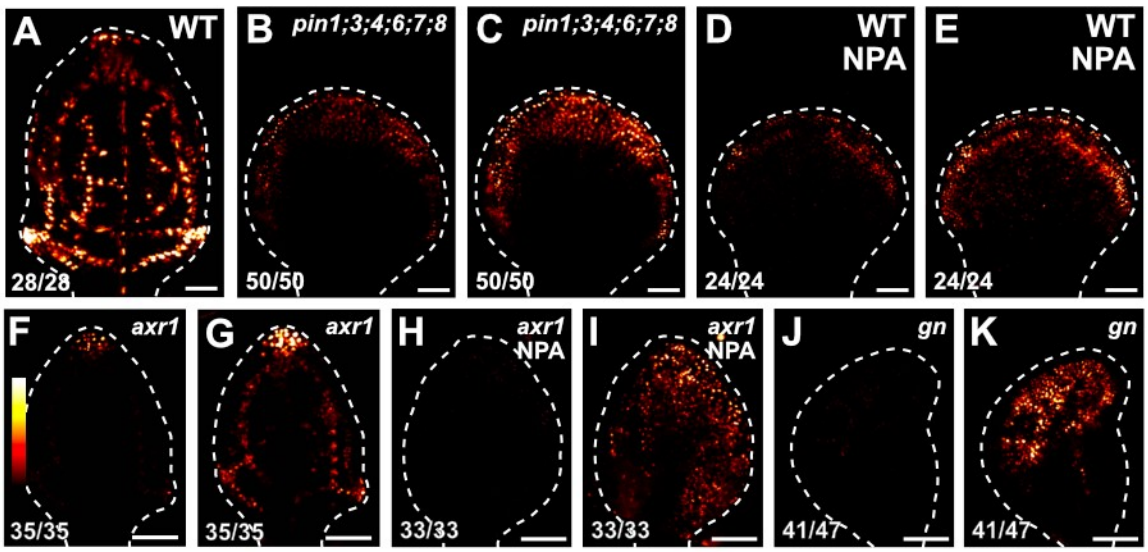

Figure 4.18. Expression of DR5rev::nYFP in developing leaves. (A–K). Confocal laser scanning microscopy; first leaves 4 days after germination. Look-up table (ramp in F) visualizes expression levels. Top right: genotype and treatment. Bottom left: reproducibility index. Dashed white line delineates leaf outline. Images in A,B,D,F,H,J were taken at identical settings. Images in A,C,E,G,I,K were taken by matching signal intensity to detector's input range (~5% saturated pixels). Bars: (A–K) 50 µm

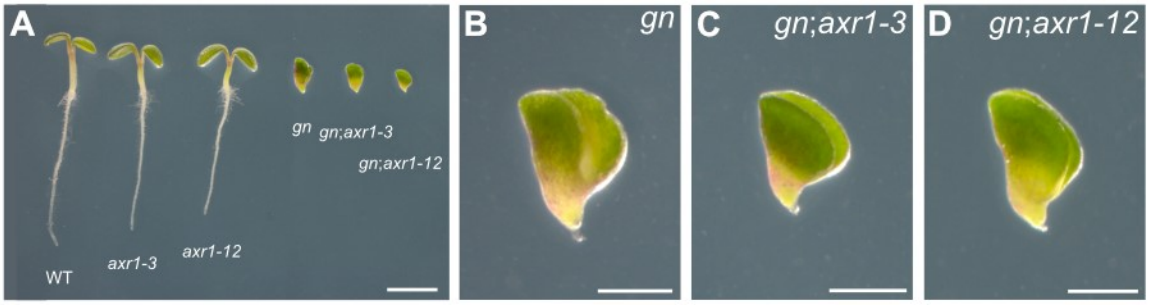

Figure 4.19. *gn* and *axr1* mutant seedlings. (A–D) Dark-field illumination composite of 3-day-old seedlings; genotypes below respective seedlings (A) or top right (B–D). (A) Overview. Because the seedling lineup was wider than the stereomicroscope's field of view, overlapping images of parts of the lineup were acquired and combined to reconstruct the original lineup. (B–D) Details. Bars: (A) 2 mm; (B–C) 0.5 mm.

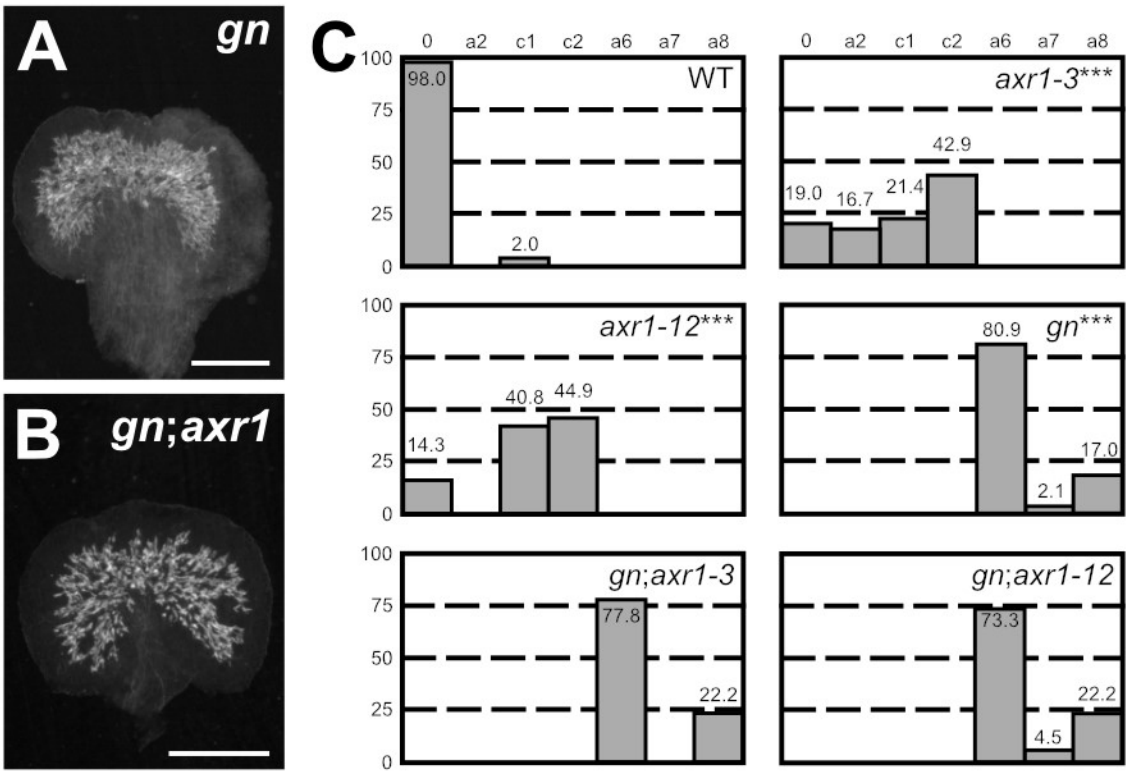

Figure 4.20. Genetic interaction between *GN* and *AXR1*. (A,B) Dark-field illumination mature first leaves. Top right: genotype. (C) Percentages of leaves in phenotype classes (defined in Figs. 4.1,4.2,4.5). Difference between *axr1-3* and WT, between *axr1-12* and WT and between *gn-13* and WT was significant at $P<0.001$ (***) by Kruskal-Wallis and Mann-Whitney test with Bonferroni correction. Sample population sizes: WT, 49; *axr1-3*, 42; *axr1-12*, 49; *gn-13*, 47; *gn-13*;*axr1-3*, 45; *gn-13*;*axr1-12*, 45. Bars: (A,B) 0.75 mm.

4.3 Discussion

4.3.1 Control of vein patterning by carrier-mediated auxin transport

Overwhelming experimental evidence places polar auxin transport at the core of the mechanism that defines sites of vein formation [reviewed in (Sachs 1991a; Berleth and Mattsson 2000; Sawchuk and Scarpella 2013)]. The polarity of auxin transport is determined by the asymmetric localization of auxin effluxers of the PIN family at the plasma membrane (PM) of auxin-transporting cells (Wisniewska et al. 2006). Therefore, one would predict that loss of the function of all the PM-localized PIN (PM-PIN) proteins should lead to loss of reproducible vein-pattern features, or perhaps even, in the most extreme case, to the inability to form veins. Neither prediction is, however, supported by evidence: mutants in all the *PM-PIN* genes with vein patterning function—*PIN1*, *PIN3*, *PIN4* and *PIN7*—or in all the *PM-PIN* genes—*PIN1–PIN4* and *PIN7*—form veins, and these veins are arranged in reproducible, though abnormal, patterns. The most parsimonious account for the discrepancy between the observed and expected mutant defects is that vein patterning is controlled by additional, PM-PIN-independent auxin-transport pathways.

The existence of PM-PIN-independent auxin-transport pathways with vein patterning function can also be inferred from the discrepancy between the vein pattern defects resulting from simultaneous mutation in all the *PM-PIN* genes with vein patterning function, or in all the *PM-PIN* genes, and the vein pattern defects induced by NPA, which is thought to be a specific inhibitor of carrier-mediated cellular auxin-efflux (Rubery 1990; Dhonukshe et al. 2008). The vein pattern defects of WT grown in the presence of NPA are more severe than those of *pin1*;*3*;*4*;*7* or *pin1*;*2*;*3*;*4*;*7*, suggesting the existence of NPA-sensitive auxin-transport pathways with vein patterning function in addition to the PM-PIN-dependent pathway, a suggestion that is supported by the observation that growth in the presence of NPA enhances the vein pattern defects of *pin1*;*3*;*4*;*7* to match those induced in WT by NPA.

Such PM-PIN-independent NPA-sensitive auxin-transport pathway with vein patterning function depends on the activity of the endoplasmic-reticulum (ER)-localized PIN6 and PIN8, as inferred from the identity of the vein pattern defects resulting from simultaneous mutation of *PIN1*, *PIN3*, *PIN4* and *PIN6-PIN8* and those induced in WT by NPA, and from the inability of NPA to induce further defects in *pin1*;*3*;*4*;*6*;*7*;*8*. Moreover, that NPA- grown WT phenocopies *pin1*;*3*;*4*;*6*;*7*;*8*, that no further defects can be induced in *pin1*;*3*;*4*;*6*;*7*;*8* by NPA, and that *pin1*;*3*;*4*;*6*;*7*;*8* and growth on NPA lead to the formation of veins arranged in reproducible patterns suggest no residual NPA-sensitive vein-patterning activity beyond that provided by PIN1, PIN3, PIN4, PIN6, PIN7 and PIN8, and therefore also the existence of NPA-insensitive vein-patterning pathways. It is of course possible that PIN6 and PIN8 are partially localized to the PM, and PM-localization of PIN6 and of the ER-PIN PIN5 has been reported (Ganguly et al. 2014; Bennett et al. 2016; Simon et al. 2016; Ditengou et al. 2018). Most important, however, that would not preclude the existence of NPA-insensitive vein patterning pathways.

These NPA-insensitive vein-patterning pathways are unlikely to be mediated by known intercellular auxin transporters—the AUX1/LAX auxin influxers (Yang et al. 2006; Swarup et al. 2008; Peret et al. 2012) and the ABCB auxin effluxers (Geisler et al. 2005; Bouchard et al. 2006; Petrasek et al. 2006)—as their mutation fails to enhance the vein pattern defects of *pin1*;*3*;*6* and of the NPA-induced phenocopy of *pin1*;*3*;*4*;*6*;*7*;*8*. Though it remains undetermined whether the NPA-insensitive vein-patterning pathways depend on the function of known intracellular auxin transporters [e.g., (Barbez et al. 2012)], such pathways contribute to the polar propagation of the inductive auxin signal: indeed, as in WT, application of auxin to *pin1*;*3*;*4*;*6*;*7*;*8* leaves induces the formation of veins that connect the applied auxin to the pre-exiting vasculature basal to the site of auxin application.

4.3.2 Control of vein patterning by auxin signaling

The residual NPA-insensitive auxin-dependent vein-patterning activity of *pin1*;*3*;*4*;*6*;*7*;*8* depends, at least in part, on the signal transduction mediated by the TIR1/AFB auxin receptors

and their post-translational regulator AXR1. Loss of AXR1 or of TIR1 and AFB2, the two auxin receptors that most contribute to auxin signaling (Dharmasiri et al. 2005), induces entirely new vein-pattern defects in *pin1*;*3*;*4*;*6*;*7*;*8* or in its NPA-induced phenocopy, defects never observed in *pin1*;*3*;*4*;*6*;*7*;*8* or NPA-grown WT: in the more-severely affected leaves of *axr1*;*pin1*;*3*;*4*;*6*;*7*;*8* and NPA-grown *tir1*;*afb2*, the end-to-end alignment of vascular elements oriented with their axis along the axis of the vein is often replaced by the clustered differentiation of abnormally oriented vascular cells. Not only are these defects never observed in *pin1*;*3*;*4*;*6*;*7*;*8* or NPA-grown WT, but they are more severe than the predicted sum of the defects of *pin1*;*3*;*4*;*6*;*7*;*8* and NPA-grown WT. These observations are particularly interesting because genetic analysis of auxin signaling components had so far implicated auxin signaling only in the differentiation of normally patterned veins (Przemeck et al. 1996; Hardtke and Berleth 1998; Hardtke et al. 2004; Alonso-Peral et al. 2006; Candela et al. 2007; Pérez-Pérez et al. 2010). Instead, the mutual synthetic enhancement between the vein pattern defects of reduced auxin signaling and those of reduced auxin transport suggests nonhomologous redundancy of auxin signaling and transport in vein patterning. Such redundancy is unequal, however: whereas auxin transport is required for vein patterning even in the presence of normal auxin signaling, the vein patterning activity of auxin signaling is only exposed in conditions of compromised auxin transport.

How auxin signaling, inherently non-directional, could propagate polar information is unclear. One possibility is that auxin diffuses through plasmodesmata (PD) intercellular channels—a possibility that had previously been suggested (Mitchison 1981) and that has recently encountered some experimental support (Han et al. 2014)—and that the size of the PD aperture or the proportion of PD in the transverse walls of incipient vascular cells are positively regulated by auxin signaling. Rapid, efficient PIN-mediated transport of auxin across the PM would normally limit or dominate the slow, inefficient diffusion of auxin through PD. But in the absence of PM-PIN-mediated transport, auxin would predominantly or exclusively move through PD, thereby exposing the relevance of such movement for vein patterning. Though PD aperture is greater at sites that seem to overlap with sites of maximum auxin signaling and vein formation (Mattsson et al. 2003; Kim et al. 2005), and though mathematical models of diffusion-mediated auxin transport successfully recapitulate aspects of vein formation (Mitchison 1981; Rolland-Lagan and Prusinkiewicz 2005), the possibility that auxin movement through PD controls vein patterning remains to be experimentally tested.

4.3.3 A tissue-cell-polarizing signal upstream of auxin transport and signaling

The vein pattern defects of leaves in which both transport and transduction of the auxin signal are compromised are never observed in leaves in which either process is; yet those defects are not unprecedented: they are observed—though in more extreme form—in leaves of *gn* mutants, suggesting that GN might control both transport and transduction of the auxin signal.

Though it is unclear how the ARF GEF activity of GN might control auxin signaling, the suggestion is supported by the epistasis of the vein pattern defects of *gn* to those of *axr1* and is consistent with genetic analysis placing *GN* upstream of auxin signal transduction in the formation of the apical-basal polarity of the embryo (Mayer et al. 1993), a process that depends on polar auxin signaling from the embryo vascular strand (Weijers et al. 2006).

Seemingly less surprising is the conclusion that GN controls PM-PIN-mediated auxin transport: indeed, the ARF GEF activity of GN is required for the coordinated polarization of PIN1 localization during embryogenesis (Steinmann et al. 1999). However, if failure to coordinate the polarization of the localization of PIN1—and possibly other PM-PIN proteins—were the cause of the vein pattern defects of *gn*, one would predict these defects to be dependent on *PM-PIN* function and therefore masked by those of *pin1*;*3*;*4*;*7* in the *gn*;*pin1*;*3*;*4*;*7* mutant. The epistasis of the vein pattern defects of *gn* to those of *pin1*;*3*;*4*;*7* instead suggests that: (i) the vein pattern defects of *gn* are independent of *PM-PIN* function and therefore *not* the sole result of loss or abnormal polarity of PIN-mediated auxin transport; (ii) *GN* acts upstream of *PM-PIN* genes in vein patterning; (iii) the tissue-cell-polarizing function of GN entails more than the regulation of PM-PIN-mediated auxin transport and of the coordinated polarization of PM-PIN localization. Our conclusions are consistent with more-severe epidermal-cell-polarity defects in *gn* than in *pm-pin* mutants, defects which are associated with normal localization of PM-PIN proteins (Fischer et al. 2006).

Polarization of PIN1 localization and orientation of microtubule arrays during patterned formation of shoot lateral organs seem to be controlled by an upstream mechanical signal from the cell wall (Heisler et al. 2010). Because cell wall composition and properties are abnormal in

gn (Shevell et al. 2000), it will be interesting to test whether *GN* contributes to the production of such mechanical signal with functions beyond the polarization of PIN1 localization and whether the functions of this mechanical signal overlap with those of the *GN*-dependent signal upstream of auxin transport in vein patterning.

Independently of a possible function of *GN* in mechanical signaling, one of the functions of GN beyond the regulation of PM-PIN-mediated auxin transport is the control of auxin transport mediated by the endoplasmic-reticulum (ER)-localized PIN6 and PIN8, a conclusion suggested by the epistasis of the vein pattern defects of *gn* to those of *pin1*;*3*;*4*;*6*;*7*;*8*. Though it is unclear how GN could control ER-PIN-mediated auxin transport, it is possible that such control is indirect and mediated by GN function in ER-Golgi trafficking (Richter et al. 2007).

As severe as they may be, the defects resulting from mutations in *GN* and *PIN* genes neither interfere with completion of embryogenesis nor obliterate embryo patterning or vein formation, suggesting that additional tissue-cell-polarizing signals exist beyond those provided by these genes. It will be focus of future research the identification of such signals.

4.4 Materials and methods

4.4.1 Plants

Origin and nature of lines, genotyping strategies and oligonucleotide sequences are in Tables 4.1, 4.13 and 4.14. Seeds were sterilized and sown as in Sawchuk et al. 2008. Stratified seeds were germinated and seedlings were grown at 22°C under continuous fluorescent light (~80 µmol $m^{-2}s^{-1}$). Plants were grown at 25°C under fluorescent light (~110 µmol m^{-2} s^{-1}) in a 16-h-light/8-h-dark cycle. Plants were transformed and representative lines were selected as described in Sawchuk et al. 2008.

Table 4.13. Genotyping strategies.

Line	Strategy
fwr (*gn*^{fwr})	'FWR for' and 'FWR REV2'; *Eco*RI
van7/*emb30-7* (*gn*^{van7})	'van7 Hpa1 FP' and 'van7 Hpa1 RP'; *Hpa*I
gn-13	*GN*: 'SALK_045424 gn LP' and 'SALK_045424 gn RP'; *gn*: 'SALK_045424 gn RP' and 'LBb1.3'
pin1-1	'pin1-1 F' and 'pin1-1 R'; *Tat*I
pin1-134	'pin1-1 F' and 'pin1-134 R mse-I'; *Mse*I
pin3-3	'pin3-3 F' and 'pin3-3 R'; *Sty*I
pin4-2	*PIN4*: 'PIN4 forw geno II' and 'PIN4en rev Ikram'; *pin4*: 'PIN4en rev Ikram' and 'en primer'
pin7^{En}	*PIN7*: 'PIN7en forw Ikram' and 'PIN7en rev'; *pin7*: 'PIN7en rev Ikram II' and 'en primer'
eir1-1 (*pin2*)	'eir1-1 F' and 'eir1-1 R'; *Bse*LI
pin6	*PIN6*: 'PIN6 spm F' and 'PIN6 spm R'; *pin6*: 'PIN6 spm F' and 'Spm32'
pin8-1	*PIN8*: 'SALK_107965 LP' and 'SALK_107965 RP'; *pin8*: 'SALK_107965 RP' and 'LBb1.3'
pgp1-100 (*abcb1*)	*ABCB1*: 'SALK_083649 pgp1-100 LP' and 'SALK_083649 pgp1-100 RP'; *abcb1*: 'SALK_083649 pgp1-100 RP' and 'LBb1.3'
mdr1-101 (*abcb19*)	*ABCB19*: 'SALK_033455 atmdr1-101 LP' and 'SALK_033455 atmdr1-101 RP'; *abcb19*: 'SALK_033455 atmdr1-101 RP' and 'LBb1.3'
ucu2-4 (*twd1*)	*UCU2*: 'SALK_012836 twd1 LP' and 'SALK_012836 twd1 RP'; *ucu2*: 'SALK_012836 twd1 RP' and 'LBb1.3'
aux1-21	'aux1-21 Fwd' and 'aux1-21 Rev'; *ApaL*I
lax1	*LAX1*: 'lax1 Fwd' and 'lax1 WT Rev'; *lax1*: 'lax1 fwd' and 'lax123 mutant Rev'
lax2-1	*LAX2*: 'lax2 Fwd' and 'lax2 WT Rev'; *lax2*: 'lax2 fwd' and 'lax123 mutant Rev'

lax3	*LAX3*: 'lax3 Fwd' and 'lax3 WT Rev'; *lax3*: 'lax3 fwd' and 'dSpm5'
aux1-355	*AUX1*: 'SALK_020355 LP (aux1)' and 'SALK_020355 RP (aux1)'; *aux1*: 'SALK_020355 RP (aux1)' and 'LBb1.3'
lax1-064	*LAX1*: 'SALK_071064 lax1 LP' and 'SALK_071064 lax1 RP'; *lax1*: 'SALK_071064 lax1 RP' and 'LBb1.3'
axr1-3	'AXR1-Acc1' and 'AXR1-15'; *Sal*I
axr1-12	'axr1-12 forw' and 'axr1-12 rev'; *Dra*I
tir1-1	'tir1-1F2' and 'tir1-1R2', *Bsa*I
afb2-3	*AFB2*: 'AFB2+F' and 'AFB2-TR'; *afb2*: 'pROK-LB' and 'AFB2-TR'

Table 4.14. Oligonucleotide sequences.

Name	Sequence (5' to 3')
FWR for	AAGAGCCAAGATCACAGCCTACTG
FWR REV2	GAGAGCACGCGCAAGCTGCAACAAG
van7 Hpa1 FP	ATCCGTGCCCTTGATCTAATGGGAG
van7 Hpa1 RP	CACTTTTCTTAGTCCTTGAACAAGCGTTAA
GN Fwd NotI	TCTGCGGCCGCTCTAGAGGTGTGTATGATAATG
GN Rev NotI	TTTGCGGCCGCTCTAGAAATCGAAATCCGTCTC
fwr-mutagenesis F	GCTTGCGCGTGCTCTCATTTGGGC
fwr-mutagenesis R	TGCAACAAAAATTCAGCTTGTAGAAACTTGCTTTCG
SALK_045424 gn LP	TGATCCAAATCACTGGGTTTC
SALK_045424 gn RP	AGCTGAAGATAGGGAATTCGC
LBb1.3	ATTTTGCCGATTTCGGAAC
PIN4 prom PstI forw	TCTCTGCAGTTTGTGTATCTTAATTATTTGAGTATG
PIN4 1032 SalI rev	TATGTCGACGTCATGGCTCGCTTTGCTATC
PIN4 1033 SalI forw	TATGTCGACGCTAAGGAGCTTCACATG
PIN4 UTR EcoRI rev	TACGAATTCCAGTATAAACCACTTAACTAGAAAC
EGFP SalI Forw	TATGTCGACGTGAGCAAGGGCGAGGAG
EGFP SalI Rev	TATGTCGACCTTGTACAGCTCGTCCATGC
PIN7 prom SalI forw	TAAGTCGACAAAAATAATATTTTTATTTAAGATAATTATG
PIN7 UTR KpnI rev	TATGGTACCCTTTCTCAAATAATCTC
EGFP SacI forw	TAAGAGCTCAGGTGAGCAAGGGCGAGGAG
EGFP SacI rev	TATGAGCTCCCTTGTACAGCTCGTCCATGC
pin1-1 F	ATGATTACGGCGGCGGACTTCTA
pin1-1 R	TTCCGACCACCACCAGAAGCC
pin1-134 R mse-I	CTCAGCTTCAGTTTCCAAAGGTTG
pin3-3 F	GGAGCTCAAACGGGTCACCCG
pin3-3 R	GCTGGATGAGCTACAGCTATATTC
PIN4 forw geno II	GTCCGACTCCACGGCCTTC
PIN4en rev Ikram	ATCTTCTTCTTCACCTTCCACTCT

en primer	GAGCGTCGGTCCCCACACTTCTATAC
PIN7en forw Ikram	CCTAACGGTTTCCACACTCA
PIN7en rev	TAGCTCTTTAGGGTTTAGCTC
PIN7en rev Ikram II	GGTTTAGCTCTGCTGTGGAGTT
eir1-1 F	TTGTTGATCATTTTACCTGGGACA
eir1-1 R	GGTTGCAATGCCATAAATAGAC
PIN6 spm F	CATAACGAAGCTAACTAAGGGGTAATCTC
PIN6 spm R	GGAGTTCAAAGAGGAATAGTAGCAGAG
Spm32	TACGAATAAGAGCGTCCATTTTAGAGTG
SALK_107965 LP	TGAAAGACATTTTGATGGCATC
SALK_107965 RP	CCAAATCAAGCTTTGCAAGAC
SALK_083649 pgp1-100 LP	GAAGACTGCGACAAGGACAAG
SALK_083649 pgp1-100 RP	GCAAGAGCGATGTTGAAGAAC
SALK_033455 atmdr1-101 LP	GCAATTGCAATTCTCTGCTTC
SALK_033455 atmdr1-101 RP	CTCAGGCAATTGCTCAAGTTC
SALK_012836 twd1 LP	GTGAAGCTGAGGTCTTGGATG
SALK_012836 twd1 RP	TATGGCCTGAAACAGCAAACC
aux1-21 Fwd	CTGGAAAGCACTAGGACTCGC
aux1-21 Rev	AAGCGGCGAAGAAACGATACAG
lax1 Fwd	ATATGGTTGCAGGTGGCACA
lax1 WT Rev	GTAACCGGCAAAAGCTGCA
lax123 mutant Rev	AAGCACGACGGCTGTAGAATAG
lax2 Fwd	ATGGAGAACGGTGAGAAAGCAGC
lax2 WT Rev	CGCAGAAGGCAGCGTTAGCG
lax3 Fwd	TACTTCACCGGAGCCACCA
lax3 WT Rev	TGATTGGTCCGAAAAAGG

dSpm5	CGGGATCCGACACTCTTTAATTAACTGACACTC
SALK_020355 LP (aux1)	GGCTCCCGTAAAATAAAGCAC
SALK_020355 RP (aux1)	AATTATCGTTGGTTTCAGGTGG
SALK_071064 lax1 LP	CAATAGTAGTCTCCGGGGAGG
SALK_071064 lax1 RP	ACAACACAAGCTTGGTTGGAC
AXR1-Acc1	AAACCAACTTAACGTTTGCATGTCG
AXR1-15	TCTCATATGTACTTTTCCTCGTCCTCTTCAC
axr1-12 forw	CCGAGCAGCATCCCAAAAC
axr1-12 rev	GTTGGCAGCAAATCTGTCCG
SALK_045424 gn LP	TGATCCAAATCACTGGGTTTC
SALK_045424 gn RP	AGCTGAAGATAGGGAATTCGC
tir1-1F2	AGCGACGGTGATTAGGAGG
tir1-1R2	CAGGAACAACGCAGCAAAA
AFB2+F	TTCTCCTTCGATCATTGTCAAC
AFB2-TR	TAGCGGCAATAGAGGCAAGA
pROK-LB	GGAACCACCATCAAACAGGA

4.4.2 Chemicals

N-1-naphthylphthalamic acid (Chem Service Inc.) was dissolved in dimethyl sulfoxide; dissolved NPA was added to growth medium just before sowing. Indole-3-acetic acid (Sigma-Aldrich Co. LLC.) was dissolved in melted (55°C) lanolin (Sigma-Aldrich Co. LLC.); the IAA-lanolin paste was applied to first leaves 4 days after germination and was reapplied weekly.

4.4.3 Imaging

Developing leaves were mounted and imaged as in Sawchuk et al. 2013. Light paths are in Table 4.15. Mature leaves were fixed in 3 : 1 or 6 : 1 ethanol : acetic acid, rehydrated in 70% ethanol and water, cleared briefly (few seconds to few minutes) in 0.4 M sodium hydroxide, washed in water and mounted in 1 : 2 : 8 or 1 : 3 : 8 water : glycerol : chloral hydrate (Sigma-Aldrich Co. LLC.) and imaged as in Odat et al. 2014. Image brightness and contrast were adjusted by linear stretching of the histogram in in the Fiji distribution (Schindelin et al. 2012) of ImageJ (Schneider et al. 2012; Schindelin et al. 2015; Rueden et al. 2017). Images were rotated and cropped in Affinity Photo (Serif Europe Ltd. Nottingham, UK) and assembled into figures in Affinity Designer.

Table 4.15. Fluorescent-protein-specific light paths.

Fluorescent protein	Laser	Wavelength	Main dichroic beam splitter	First secondary dichroic beam splitter	Second secondary dichroic beam splitter	Emission filter (detector)
GFP	Ar	488	HFT 405/488/594	NFT 545	NFT 490	BP 505–530 (PMT3)
YFP	Ar	514	HFT 405/514/594	NFT 595	NFT 515	BP 520–555 IR (PMT3)

CHAPTER 5: GENERAL DISCUSSION

5.1 Conclusion summary

The scope of my Ph.D. thesis was to understand the contribution of the transport of the plant signal auxin to vein network formation in Arabidopsis leaves.

Leaf vein networks are characterized by reproducible features such as the presence of lateral veins that branch from a single midvein and connect to distal veins to form loops; of minor veins that branch from midvein and loops and connect to other veins to form a mesh; and of loops and minor veins that curve near the leaf margin to lend a scalloped outline to the vein network. Features such as these are so reproducible that they are used to define species [e.g., (Klucking 1995)]; by contrast, features such as the number of veins and their connectedness are variable. We found that auxin transport mediated by PIN-FORMED (PIN) proteins controls both reproducible and variable features of leaf vein networks (Verna et al. 2015) (Chapter 2).

PIN1 is the only known gene to be nonredundantly required for both the reproducible features of leaf vein networks and their variable ones. The PIN1 protein is expressed in all the cells of the leaf at early stages of tissue development; over time, however, epidermal expression becomes restricted to the basal-most cells and inner expression becomes restricted to files of vascular precursor cells (Galweiler et al. 1998; Benkova et al. 2003; Reinhardt et al. 2003; Heisler et al. 2005; Petrasek et al. 2006; Scarpella et al. 2006; Wenzel et al. 2007; Bayer et al. 2009; Sawchuk et al. 2013; Marcos and Berleth 2014). We found that the expression of PIN1 that is required for vein network patterning depends on the 205-bp region of the *PIN1* promoter from -699 to -495, which contains conserved putative binding-sites for transcription factors of the MYELOBLASTOMA and DNA-BINDING WITH ONE FINGER families (Chapter 3).

The current hypothesis of auxin control of vein formation is that the GN guanine-nucleotide exchange factor for ADP-rybosilation-factor GTPases, which regulates vesicle

formation in membrane trafficking, coordinates the cellular localization of PIN1 and possibly other PIN proteins between cells (Steinmann et al. 1999); the resulting cell-to-cell, polar transport of auxin would propagate cell polarity across tissues and control vein formation (Sachs 1991a). Instead, we found that auxin-induced vein formation occurs in the absence of PIN proteins or any known intercellular auxin transporter; that the auxin-transport-independent vein-patterning activity relies on auxin signaling; and that a GN-dependent coordinating signal acts upstream of both auxin transport and signaling (Chapter 4).

In the Discussion section of the respective chapters, I provided an account of how I reached these conclusions from the experimental data, how these conclusions could be integrated with one another and with those in studies of others to advance our understanding of vascular development, and what the implications of such conclusions are for aspects of plant development beyond the formation of leaf vascular tissue (e.g. Fig 5.1). Here I instead wish to propose and discuss two hypotheses on the upstream regulators of PIN1 functional expression in leaf vein patterning. These hypotheses should be understood as an attempt to develop a conceptual framework to guide future experimentation and not as an exhaustive mechanistic account.

5.2 Hypothesis 1: a MYELOBLASTOMA transcription factor is the upstream regulator of PIN1 functional expression in leaf vein patterning

The results in Chapter 3 suggest that the region of the *PIN1* promoter between -699 and -495 is required for PIN1 functional expression in leaf vein patterning. This promoter region contains two conserved, putative binding sites for transcription factors of the MYELOBLASTOMA (MYB) family, which suggests that a MYB transcription factor is the upstream regulator of PIN1 functional expression in leaf vein patterning. Below I present evidence consistent with this hypothesis.

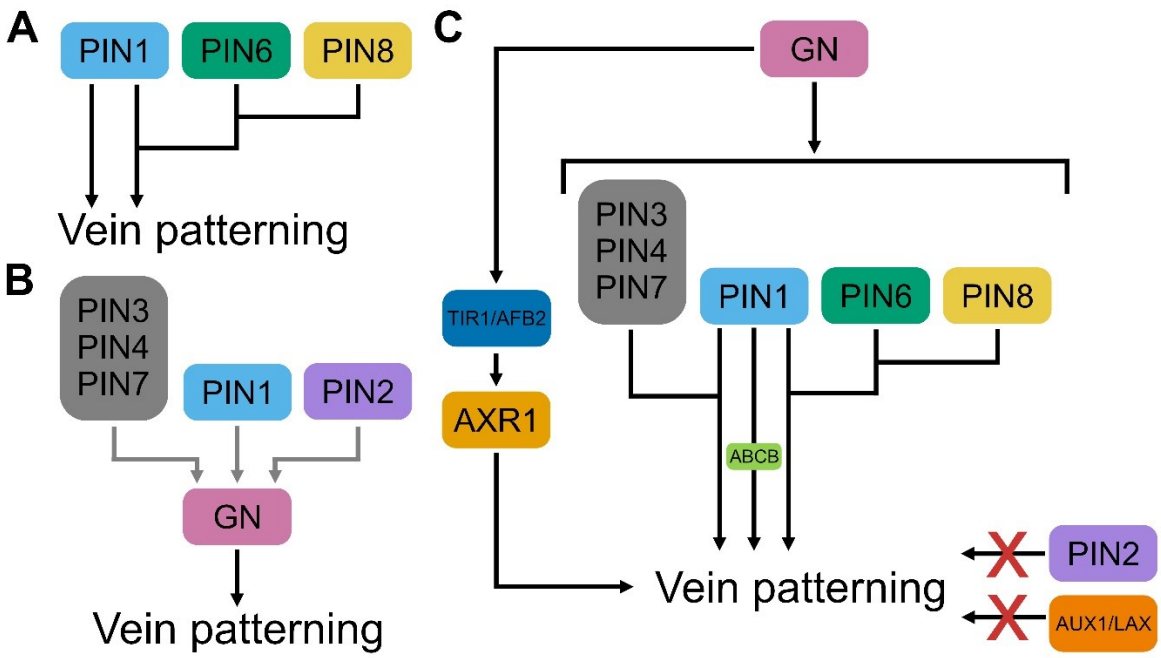

Figure 5.1. Contribution of thesis to knowledge of control of vein patterning by auxin. Summary of knowledge before and after thesis. Black arrows indicate gene functions and genetic interactions inferred from results of experimental tests; grey arrows indicate surmised functions and interactions. (A) Derived from results in Sawchuk et al. 2013. (B) Derived from results and hypotheses in Mayer et al. 1993 and Steinmann et al. 1999. (C) Derived from results in Chapter 4.

5.2.1 Evidence from expression analysis

The most parsimonious expectation is that a transcription factor and its target genes are expressed in overlapping domains. As *PIN1* (Scarpella et al. 2006; Wenzel et al. 2007), both the *ASYMMETRIC LEAVES1* (*AS1*) gene of Arabidopsis, which encodes a MYB transcription factor, and its homolog in maize *ROUGH SHEATH2* (*RS2*) are expressed in broad domains of leaf inner cells that over time become restricted to developing veins (Timmermans et al. 1999; Tsiantis et al. 1999b; Byrne et al. 2000; Iwakawa et al. 2007).

Though its expression in leaves is unknown, the *MYB77* gene of Arabidopsis is expressed in the root vascular cylinder (Shin et al. 2007), where *PIN1* is also expressed (Galweiler et al. 1998; Friml et al. 2002a).

5.2.2 Evidence from transcriptional activation studies

That the region of the *PIN1* promoter between -699 and -495 is *required* for PIN1 functional expression in leaf vein patterning (Chapter 3) suggest that that region is bound by a *positive* regulator of PIN1 functional expression in leaf vein patterning.

In barrelclover/Medicago, mutation of *MEDICAGO TRUNCULATA PHANTASTICA,* homologous to *AS1,* leads to lower expression of *MEDICAGO TRUNCULATA PIN-FORMED10* (Ge and Chen 2014).

In Arabidopsis, overexpression of *MYB77* leads to higher expression of *PIN1*, and mutation of *MYB77* leads to lower response of *PIN1* expression to auxin (Shin et al. 2007). Likewise, in *as1* mutants the expression of *LATERAL ORGAN BOUNDARIES*, *PHABULOSA*, *PHAVOLUTA* and *REVOLUTA* is reduced (Byrne et al. 2002; Fu et al. 2007).

Though indirect, these observations suggest that these *MYB* genes positively regulate the expression of their targets. However, direct evidence is available that at least some MYB transcription factors bind their targets and activate their expression. For example, AS1 forms a

complex with the zinc-finger CONSTANS that binds the promoter of *FLOWERING TIME* and activates its expression (Song et al. 2012), and the MYB transcription factor of Arabidopsis FOUR LIPS binds the promoters of *PIN3* and *PIN7* and activates their expression (Wang et al. 2015).

5.2.3 Evidence from genetic analysis

The most parsimonious expectation is that mutation of a transcription factor results in defects overlapping to those resulting from mutation in its targets.

As *pin1* (Okada et al. 1991), the *rs2* mutant of maize has defects in polar auxin transport (Tsiantis et al. 1999a). Furthermore, *rs2* leaves have multiple midveins, a defect that can be induced in WT by growth in the presence of auxin transport inhibitors (Tsiantis et al. 1999a), suggesting that those leaf vein pattern defects of *rs2* are the result of reduced auxin transport, as those of *pin1* are suggested to be (Mattsson et al. 1999).

As *pin1* leaves (Wenzel et al. 2007; Verna et al. 2015) (Chapter 2), the leaves of the *myb77* mutant of Arabidopsis have lower expression of DR5 (Shin et al. 2007), and in *as1* mutant leaves lateral veins fail to connect to the midvein, leading to "wide midveins" (Sun et al. 2002) like those induced by auxin transport inhibitors or by mutation in *PIN* genes (Mattsson et al. 1999; Sieburth 1999; Sawchuk et al. 2013) (Chapter 4).

One other expectation is that the defects resulting from double mutation of a transcription factor and its target would be no different from those resulting from mutation of the sole transcription factor. Because the defects of the *as1*;*pin1* double mutant are more severe than those of either *as1* or *pin1* (Hay et al. 2006), if *AS1* regulated PIN1 functional expression in leaf vein patterning it would have to do so redundantly with other transcription factors.

5.3 Hypothesis 2: a DNA-BINDING WITH ONE FINGER transcription factor is the upstream regulator of PIN1 functional expression in leaf vein patterning

The results in Chapter 3 suggest that the region of the *PIN1* promoter between -699 and -495 is required for *PIN1* function in leaf vein patterning. This promoter region contains three conserved, putative binding sites for transcription factors of the DNA-BINDING WITH ONE FINGER (DOF) family, which suggests that a DOF transcription factor is the upstream regulator of PIN1 functional expression in leaf vein patterning. Below I present evidence consistent with this hypothesis.

5.3.1 Evidence from expression analysis

As *PIN1* (Steinmann et al. 1999; Friml et al. 2003), the *DOF3.2*/*DOF6* gene of Arabidopsis is expressed in embryo vascular tissues (Rueda-Romero et al. 2012). As *PIN1* (Scarpella et al. 2006; Wenzel et al. 2007), *DOF1.1*/*OBP2*, *DOF2.1*, *DOF2.4*, *DOF4.6*, *DOF5.3* and *DOF5.8* are expressed in leaf veins (Skirycz et al. 2006; Konishi and Yanagisawa 2007; Gardiner et al. 2010). As *PIN1* (Galweiler et al. 1998; Friml et al. 2002a; Vieten et al. 2005), *DOF3.6*/*OBP3* is expressed in the vascular tissues of the cotyledons, hypocotyl and roots (Ward et al. 2005). Finally, as *PIN1* (Vieten et al. 2005; Scarpella et al. 2006; Wenzel et al. 2007), *AtDOF5.5*/*CYCLING DOF FACTOR1* (*CDF1*), *DOF5.2*/*CDF2*, *DOF3.3*/*CDF3* and *DOF2.3*/*CDF4* are expressed in veins of cotyledons and leaves (Imaizumi et al. 2005; Fornara et al. 2009).

5.3.2 Evidence from transcriptional activation studies

Mutation of the *DOF ACTING IN SEED EMBRYOGENESIS AND HORMONE ACCUMULATION* gene of Medicago/barrelclover leads to lower expression of the homolog of *PIN1* in Medicago/barrelclover (Noguero et al. 2015). Likewise, expression of many genes is lower in the *cdf1*;*2*;*3*;*5* quadruple mutant of Arabidopsis, suggesting that DOF transcription factors can activate expression of their targets (Fornara et al. 2015). More direct evidence of this ability is available, however.

The *PROLAMIN-BOX BINDING FACTOR* of barley binds the promoter and activates the expression of hordeins storage proteins (Mena et al. 1998). The *PROLAMIN-BOX BINDING FACTOR* of maize binds the promoter and activates the expression of zein storage proteins (Marzábal et al. 2008). The *ZmDof1* and *ZmDof2* of maize bind to promoters and activate expression of different genes in maize protoplasts (Yanagisawa and Sheen 1998; Yanagisawa 2000).

In Arabidopsis, DOF binding sites have been shown to be required for expression in leaf veins and guard cells (Gardner et al. 2009; Cominelli et al. 2011). Finally, DOF5.8 binds the promoter and activates the expression of *NAC DOMAIN CONTAINING PROTEING 69* (He et al. 2015).

5.3.3 Evidence from genetic analysis

Mutant phenotypes have revealed little about *DOF* function, possibly due to redundancy — Arabidopsis contains 37 putative *DOF* genes (Yanagisawa 2002). But overexpression of *DOF5.8*, as that of *PIN1* (Verna et al. 2015) (Chapter 2), represses the formation of minor veins (Konishi and Yanagisawa 2015).

5.4 Future approach

The evidence presented above is consistent with the possibility that MYB or DOF transcription factors regulate PIN1 functional expression in leaf vein patterning. Here I wish to suggest how this possibility could be tested experimentally and what the next steps could be should neither MYB nor DOF transcription factors be upstream regulators of PIN1 functional expression in leaf vein patterning.

1. To test whether the putative MYB or DOF binding-sites in the [-699,-14] promoter fragment are required for PIN1 functional expression in leaf vein patterning, I propose to mutate each of them separately in the [-699,-14] promoter fragment, use these mutant versions of the promoter fragment to drive *PIN1* expression in the *pin1* mutant background and test their ability to rescue the leaf vein pattern defects of *pin1*. Failure of either mutated version of the promoter fragment to rescue those defects would suggest requirement of the mutated binding site. Alternatively, the ability of both mutated versions of the promoter fragment to rescue the leaf vein pattern defects of *pin1* would suggest that neither binding site is required for PIN1 functional expression in leaf vein patterning.

2. Either way, to identify all the transcription factors that bind to the [-699,-14] promoter fragment I propose to use this sequence as bait in a yeast one-hybrid screen.

3. I propose to generate translational fusions to, for example, YFP of the transcription factors identified in the yeast one-hybrid screen (see point 2) to test whether their expression in leaves overlaps with the activity of the [-699,-14] promoter fragment.

4. I propose to test whether the transcription factors whose expression overlaps with the activity of the [-699,-14] promoter fragment (see point 3) bind that promoter region in vivo by chromatin immunopreciptation using translational fusions of those transcription factors to, for example YFP and anti-YFP antibodies.

5. I propose to identify mutants of the transcription factors whose expression overlaps with the activity of the [-699,-14] promoter fragment (see point 3) . The most parsimonious expectation is that those mutants have leaf vein pattern defects similar to those of *pin1*; however,

because of redundancy, they may not, in which case I would propose to overcome such redundancy by turning those activating transcription factors into repressors by fusion to portable repressor domains [e.g., ETHYLENE-RESPONSIVE ELEMENT-BINDING FACTOR—EAR; (Hiratsu et al. 2003)].

Further, I propose to analyze the activity of the [-699,-14] promoter fragment into those transcription factor mutants or transgenics; I expect the activity of the [-699,-14] promoter fragment to resemble that of the [-480,-14] promoter fragment, which lacks the region required for PIN1 functional expression in leaf vein patterning.

I also propose to analyze the genetic interaction between those transcription factor mutants or transgenics and *pin1*; I expect the double mutant between those mutants or transgenics and *pin1* to have leaf vein pattern defects similar to those of the transcription factor mutants or transgenics if no transcription factor other than that mutated regulated PIN1 functional expression in leaf vein patterning; otherwise, I expect those mutants or transgenics to enhance the leaf vein pattern defects of *pin1*.

Finally, I propose to overexpress *PIN1*by the *MP* or *RPS5A* promoter (Verna et al. 2015) (Chapter 2), for example in the transcription factor mutants or transgenics; I expect the leaf vein pattern defects of those mutants or transgenics to be, at least in part, rescued.

WORKS CITED

Abley K, Sauret-Güeto S, Marée AFM, Coen E (2016) Formation of polarity convergences underlying shoot outgrowths. eLife 5:e18165. doi:10.7554/eLife.18165

Aguilera A, Klein H (1989) Genetic and molecular analysis of recombination events in Saccharomyces cerevisiae occurring in the presence of the hyper-recombination mutation hpr1. Genetics 122 (3):503–517

Alim K, Frey E (2010) Quantitative predictions on auxin-induced polar distribution of PIN proteins during vein formation in leaves. The European Physical Journal E 33 (2):165–173. doi:10.1140/epje/i2010-10604-5

Aloni R (2010) The induction of vascular tissues by auxin. In: PJ D (ed) Plant hormones: biosynthesis, signal transduction, action. Kluwer Academic Publishers, Dordrecht, pp 485–506

Aloni R, Schwalm K, Langhans M, Ullrich CI (2003) Gradual shifts in sites of free-auxin production during leaf-primordium development and their role in vascular differentiation and leaf morphogenesis in Arabidopsis. Planta 216 (5):841–853

Alonso-Peral MM, Candela H, del Pozo JC, Martinez-Laborda A, Ponce MR, Micol JL (2006) The HVE/CAND1 gene is required for the early patterning of leaf venation in Arabidopsis. Development 133 (19):3755–3766

Alonso JM, Stepanova AN, Leisse TJ, Kim CJ, Chen H, Shinn P, Stevenson DK, Zimmerman J, Barajas P, Cheuk R, Gadrinab C, Heller C, Jeske A, Koesema E, Meyers CC, Parker H, Prednis L, Ansari Y, Choy N, Deen H, Geralt M, Hazari N, Hom E, Karnes M, Mulholland C, Ndubaku R, Schmidt I, Guzman P, Aguilar-Henonin L, Schmid M, Weigel D, Carter DE, Marchand T, Risseeuw E, Brogden D, Zeko A, Crosby WL, Berry CC, Ecker JR (2003) Genome-wide insertional mutagenesis of Arabidopsis thaliana. Science 301 (5633):653–657

Alvarez JP, Furumizu C, Efroni I, Eshed Y, Bowman JL (2016) Active suppression of a leaf meristem orchestrates determinate leaf growth. Elife 5:e15023

Ash A, Ellis B, Hickey L, Johnson K, Wilf P, Wing S (1999) Manual of leaf architecture. Smithsonian Institution: Washington

Avery GS, Jr. (1935) Differential Distribution of a Phytohormone in the Developing Leaf of Nicotiana, and Its Relation to Polarized Growth. Bulletin of the Torrey Botanical Club 62 (6):313–330

Bailly A, Sovero V, Vincenzetti V, Santelia D, Bartnik D, Koenig BW, Mancuso S, Martinoia E, Geisler M (2008) Modulation of P-glycoproteins by auxin transport inhibitors is mediated by interaction with immunophilins. J Biol Chem 283 (31):21817–21826

Baima S, Forte V, Possenti M, Penalosa A, Leoni G, Salvi S, Felici B, Ruberti I, Morelli G (2014) Negative feedback regulation of auxin signaling by ATHB8/ACL5-BUD2 transcription module. Mol Plant 7 (6):1006–1025

Bainbridge K, Guyomarc'h S, Bayer E, Swarup R, Bennett M, Mandel T, Kuhlemeier C (2008) Auxin influx carriers stabilize phyllotactic patterning. Genes Dev 22 (6):810–823

Balcells L, Modolell J, Ruiz-Gómez M (1988) A unitary basis for different Hairy-wing mutations of Drosophila melanogaster. The EMBO journal 7 (12):3899–3906

Band LR, Wells DM, Fozard JA, Ghetiu T, French AP, Pound MP, Wilson MH, Yu L, Li W, Hijazi HI, Oh J, Pearce SP, Perez-Amador MA, Yun J, Kramer E, Alonso JM, Godin C,

Vernoux T, Hodgman TC, Pridmore TP, Swarup R, King JR, Bennett MJ (2014) Systems analysis of auxin transport in the Arabidopsis root apex. Plant Cell 26 (3):862–875
Barbez E, Kubes M, Rolcik J, Beziat C, Pencik A, Wang B, Rosquete MR, Zhu J, Dobrev PI, Lee Y, Zazimalova E, Petrasek J, Geisler M, Friml J, Kleine-Vehn J (2012) A novel putative auxin carrier family regulates intracellular auxin homeostasis in plants. Nature 485 (7396):119–122
Bayer EM, Smith RS, Mandel T, Nakayama N, Sauer M, Prusinkiewicz P, Kuhlemeier C (2009) Integration of transport-based models for phyllotaxis and midvein formation. Genes Dev 23 (3):373–384
Beerling DJ, Fleming AJ (2007) Zimmermann's telome theory of megaphyll leaf evolution: a molecular and cellular critique. Current Opinion in Plant Biology 10 (1):4–12
Bender RL, Fekete ML, Klinkenberg PM, Hampton M, Bauer B, Malecha M, Lindgren K, J AM, Perera MA, Nikolau BJ, Carter CJ (2013) PIN6 is required for nectary auxin response and short stamen development. Plant J 74 (6):893-904
Benkova E, Michniewicz M, Sauer M, Teichmann T, Seifertova D, Jurgens G, Friml J (2003) Local, efflux-dependent auxin gradients as a common module for plant organ formation. Cell 115 (5):591–602
Bennett SRM, Alvarez J, Bossinger G, Smyth DR (1995) Morphogenesis in pinoid mutants of Arabidopsis thaliana. The Plant Journal 8 (4):505-520
Bennett T, Hines G, van Rongen M, Waldie T, Sawchuk MG, Scarpella E, Ljung K, Leyser O (2016) Connective Auxin Transport in the Shoot Facilitates Communication between Shoot Apices. PLoS Biol 14 (4):e1002446. doi:10.1371/journal.pbio.1002446
Berleth T, Mattsson J (2000) Vascular development: tracing signals along veins. Current Opinion in Plant Biology 3 (5):406–411
Berleth T, Mattsson J, Hardtke CS (2000) Vascular continuity and auxin signals. Trends Plant Sci 5 (9):387–393
Bier E (2000) Drawing lines in the Drosophila wing: initiation of wing vein development. Curr Opin Genet Dev 10 (4):393–398
Bilsborough GD, Runions A, Barkoulas M, Jenkins HW, Hasson A, Galinha C, Laufs P, Hay A, Prusinkiewicz P, Tsiantis M (2011) Model for the regulation of Arabidopsis thaliana leaf margin development. Proc Natl Acad Sci U S A 108 (8):3424–3429
Blakeslee JJ, Bandyopadhyay A, Lee OR, Mravec J, Titapiwatanakun B, Sauer M, Makam SN, Cheng Y, Bouchard R, Adamec J, Geisler M, Nagashima A, Sakai T, Martinoia E, Friml J, Peer WA, Murphy AS (2007) Interactions among PIN-FORMED and P-glycoprotein auxin transporters in Arabidopsis. Plant Cell 19 (1):131–147
Blilou I, Xu J, Wildwater M, Willemsen V, Paponov I, Friml J, Heidstra R, Aida M, Palme K, Scheres B (2005) The PIN auxin efflux facilitator network controls growth and patterning in Arabidopsis roots. Nature 433 (7021):39–44
Bosco CD, Dovzhenko A, Liu X, Woerner N, Rensch T, Eismann M, Eimer S, Hegermann J, Paponov IA, Ruperti B, Heberle-Bors E, Touraev A, Cohen JD, Palme K (2012) The endoplasmic reticulum localized PIN8 is a pollen specific auxin carrier involved in intracellular auxin homeostasis. Plant J
Bouchard R, Bailly A, Blakeslee JJ, Oehring SC, Vincenzetti V, Lee OR, Paponov I, Palme K, Mancuso S, Murphy AS, Schulz B, Geisler M (2006) Immunophilin-like TWISTED DWARF1 modulates auxin efflux activities of Arabidopsis P-glycoproteins. J Biol Chem 281 (41):30603–30612

Boutte Y, Ikeda Y, Grebe M (2007) Mechanisms of auxin-dependent cell and tissue polarity. Curr Opin Plant Biol 10 (6):616–623
Briscoe J, Pierani A, Jessell TM, Ericson J (2000) A homeodomain protein code specifies progenitor cell identity and neuronal fate in the ventral neural tube. Cell 101 (4):435–445
Brunoud G, Wells DM, Oliva M, Larrieu A, Mirabet V, Burrow AH, Beeckman T, Kepinski S, Traas J, Bennett MJ, Vernoux T (2012) A novel sensor to map auxin response and distribution at high spatio-temporal resolution. Nature 482 (7383):103–106
Bryant PJ (1970) Cell lineage relationships in the imaginal wing disc of Drosophila melanogaster. Developmental biology 22 (3):389–411
Busch M, Mayer U, Jurgens G (1996) Molecular analysis of the Arabidopsis pattern formation of gene GNOM: gene structure and intragenic complementation. Mol Gen Genet 250 (6):681–691
Byrne ME, Barley R, Curtis M, Arroyo JM, Dunham M, Hudson A, Martienssen RA (2000) Asymmetric leaves1 mediates leaf patterning and stem cell function in Arabidopsis. Nature 408 (6815):967
Byrne ME, Simorowski J, Martienssen RA (2002) ASYMMETRIC LEAVES1 reveals knox gene redundancy in Arabidopsis. Development 129 (8):1957–1965
Calderon-Villalobos LI, Tan X, Zheng N, Estelle M (2010) Auxin perception—structural insights. Cold Spring Harbor perspectives in biology:a005546
Candela H, Alonso-Peral MM, Ponce MR, Micol JL (2007) Role of HEMIVENATA and the Ubiquitin Pathway in Venation Pattern Formation. Plant Signal Behav 2 (4):258–259
Candela H, Martinez-Laborda A, Micol JL (1999) Venation pattern formation in Arabidopsis thaliana vegetative leaves. Dev Biol 205 (1):205–216
Carland F, Nelson T (2009) CVP2- and CVL1-mediated phosphoinositide signaling as a regulator of the ARF GAP SFC/VAN3 in establishment of foliar vein patterns. Plant J
Carland FM, Berg BL, FitzGerald JN, Jinamornphongs S, Nelson T, Keith B (1999) Genetic regulation of vascular tissue patterning in Arabidopsis. Plant Cell 11 (11):2123–2137
Carland FM, Nelson T (2004) Cotyledon vascular pattern2-mediated inositol (1,4,5) triphosphate signal transduction is essential for closed venation patterns of Arabidopsis foliar organs. Plant Cell 16 (5):1263–1275
Carraro N, Forestan C, Canova S, Traas J, Varotto S (2006) *ZmPIN1a* and *ZmPIN1b* Encode Two Novel Putative Candidates for Polar Auxin Transport and Plant Architecture Determination of Maize. Plant Physiology 142 (1):254
Carroll JS, Liu XS, Brodsky AS, Li W, Meyer CA, Szary AJ, Eeckhoute J, Shao W, Hestermann EV, Geistlinger TR (2005) Chromosome-wide mapping of estrogen receptor binding reveals long-range regulation requiring the forkhead protein FoxA1. Cell 122 (1):33–43
Casson SA, Chilley PM, Topping JF, Evans IM, Souter MA, Lindsey K (2002) The POLARIS gene of Arabidopsis encodes a predicted peptide required for correct root growth and leaf vascular patterning. The Plant Cell 14 (8):1705–1721
Cazzonelli CI, Vanstraelen M, Simon S, Yin K, Carron-Arthur A, Nisar N, Tarle G, Cuttriss AJ, Searle IR, Benkova E, Mathesius U, Masle J, Friml J, Pogson BJ (2013) Role of the Arabidopsis PIN6 auxin transporter in auxin homeostasis and auxin-mediated development. PLoS One 8 (7):e70069
Chen R, Hilson P, Sedbrook J, Rosen E, Caspar T, Masson PH (1998) The arabidopsis thaliana AGRAVITROPIC 1 gene encodes a component of the polar-auxin-transport efflux carrier. Proc Natl Acad Sci U S A 95 (25):15112–15117

Cheng Y, Dai X, Zhao Y (2006) Auxin biosynthesis by the YUCCA flavin monooxygenases controls the formation of floral organs and vascular tissues in Arabidopsis. Genes Dev 20 (13):1790–1799
Cieslak M, Runions A, Prusinkiewicz P (2015) Auxin-driven patterning with unidirectional fluxes. Journal of Experimental Botany 66 (16):5083–5102. doi:10.1093/jxb/erv262
Clay NK, Nelson T (2005) Arabidopsis thickvein mutation affects vein thickness and organ vascularization, and resides in a provascular cell-specific spermine synthase involved in vein definition and in polar auxin transport. Plant Physiol 138 (2):767–777
Cominelli E, Galbiati M, Albertini A, Fornara F, Conti L, Coupland G, Tonelli C (2011) DOF-binding sites additively contribute to guard cell-specificity of AtMYB60 promoter. BMC Plant Biology 11 (1):162
Dalessandro G, Roberts LW (1971) Induction of Xylogenesis in Pith Parenchyma Explants of Lactuca. American Journal of Botany 58 (5):378–385
De Celis JF (2003) Pattern formation in the Drosophila wing: The development of the veins. Bioessays 25 (5):443–451
Dengler N, Kang J (2001) Vascular patterning and leaf shape. Curr Opin Plant Biol 4 (1):50–56
Dengler NG (2006) The shoot apical meristem and development of vascular architecture. Canadian Journal of Botany 84 (11):1660–1671
Deyholos MK, Cordner G, Beebe D, Sieburth LE (2000) The SCARFACE gene is required for cotyledon and leaf vein patterning. Development 127 (15):3205–3213
Dharmasiri N, Dharmasiri S, Weijers D, Lechner E, Yamada M, Hobbie L, Ehrismann JS, Jurgens G, Estelle M (2005) Plant Development Is Regulated by a Family of Auxin Receptor F Box Proteins. Developmental Cell 9 (1):109–119
Dhondt S, Van Haerenborgh D, Van Cauwenbergh C, Merks RM, Philips W, Beemster GT, Inze D (2012) Quantitative analysis of venation patterns of Arabidopsis leaves by supervised image analysis. Plant J 69 (3):553–563
Dhonukshe P, Grigoriev I, Fischer R, Tominaga M, Robinson DG, Hasek J, Paciorek T, Petrasek J, Seifertova D, Tejos R, Meisel LA, Zazimalova E, Gadella TW, Jr., Stierhof YD, Ueda T, Oiwa K, Akhmanova A, Brock R, Spang A, Friml J (2008) Auxin transport inhibitors impair vesicle motility and actin cytoskeleton dynamics in diverse eukaryotes. Proc Natl Acad Sci U S A 105 (11):4489–4494
Dimitrov P, Zucker SW (2006) A constant production hypothesis guides leaf venation patterning. Proceedings of the National Academy of Sciences of the United States of America 103 (24):9363–9368
Ding Z, Wang B, Moreno I, Duplakova N, Simon S, Carraro N, Reemmer J, Pencik A, Chen X, Tejos R, Skupa P, Pollmann S, Mravec J, Petrasek J, Zazimalova E, Honys D, Rolcik J, Murphy A, Orellana A, Geisler M, Friml J (2012) ER-localized auxin transporter PIN8 regulates auxin homeostasis and male gametophyte development in Arabidopsis. Nat Commun 3:941
Ditengou FA, Gomes D, Nziengui H, Kochersperger P, Lasok H, Medeiros V, Paponov IA, Nagy SK, Nádai TV, Mészáros T (2018) Characterization of auxin transporter PIN6 plasma membrane targeting reveals a function for PIN6 in plant bolting. New Phytologist 217 (4):1610–1624
Donner TJ, Sherr I, Scarpella E (2009) Regulation of preprocambial cell state acquisition by auxin signaling in Arabidopsis leaves. Development 136 (19):3235–3246

Dowell RD (2010) Transcription factor binding variation in the evolution of gene regulation. Trends in genetics 26 (11):468–475
Esau K (1942) Vascular Differentiation in the Vegetative Shoot of Linum. I. The Procambium. American Journal of Botany 29 (9):738–747
Etchells JP, Turner SR (2010) The PXY-CLE41 receptor ligand pair defines a multifunctional pathway that controls the rate and orientation of vascular cell division. Development 137 (5):767–774
Ettinghausen Cv (1861) Die Blatt-Skelette der Dikotyledonen Kais. Kön. Hof- und Staatsdr., Vienna
Fabregas N, Formosa-Jordan P, Confraria A, Siligato R, Alonso JM, Swarup R, Bennett MJ, Mahonen AP, Cano-Delgado AI, Ibanes M (2015) Auxin influx carriers control vascular patterning and xylem differentiation in Arabidopsis thaliana. PLoS Genet 11 (4):e1005183. doi:10.1371/journal.pgen.1005183
Fan H-y, Klein HL (1994) Characterization of mutations that suppress the temperature-sensitive growth of the hpr1 delta mutant of Saccharomyces cerevisiae. Genetics 137 (4):945–956
Feugier FG, Iwasa Y (2006) How canalization can make loops: a new model of reticulated leaf vascular pattern formation. J Theor Biol 243 (2):235–244
Feugier FG, Mochizuki A, Iwasa Y (2005) Self-organization of the vascular system in plant leaves: Inter-dependent dynamics of auxin flux and carrier proteins. Journal of Theoretical Biology 236 (4):366–375
Fischer U, Ikeda Y, Ljung K, Serralbo O, Singh M, Heidstra R, Palme K, Scheres B, Grebe M (2006) Vectorial information for Arabidopsis planar polarity is mediated by combined AUX1, EIN2, and GNOM activity. Curr Biol 16 (21):2143–2149
Fornara F, De Montaigu A, Sánchez-Villarreal A, Takahashi Y, Ver Loren van Themaat E, Huettel B, Davis SJ, Coupland G (2015) The GI-CDF module of Arabidopsis affects freezing tolerance and growth as well as flowering. The Plant Journal 81 (5):695–706
Fornara F, Panigrahi KC, Gissot L, Sauerbrunn N, Ruhl M, Jarillo JA, Coupland G (2009) Arabidopsis DOF transcription factors act redundantly to reduce CONSTANS expression and are essential for a photoperiodic flowering response. Dev Cell 17 (1):75–86
Franzke A, Lysak MA, Al-Shehbaz IA, Koch MA, Mummenhoff K (2011) Cabbage family affairs: the evolutionary history of Brassicaceae. Trends in plant science 16 (2):108-116
Friml J, Benkova E, Blilou I, Wisniewska J, Hamann T, Ljung K, Woody S, Sandberg G, Scheres B, Jurgens G, Palme K (2002a) AtPIN4 mediates sink-driven auxin gradients and root patterning in Arabidopsis. Cell 108 (5):661–673
Friml J, Vieten A, Sauer M, Weijers D, Schwarz H, Hamann T, Offringa R, Jurgens G (2003) Efflux-dependent auxin gradients establish the apical-basal axis of Arabidopsis. Nature 426 (6963):147–153
Friml J, Wisniewska J, Benkova E, Mendgen K, Palme K (2002b) Lateral relocation of auxin efflux regulator PIN3 mediates tropism in Arabidopsis. Nature 415 (6873):806–809
Fu Y, Xu L, Xu B, Yang L, Ling Q, Wang H, Huang H (2007) Genetic interactions between leaf polarity-controlling genes and ASYMMETRIC LEAVES1 and 2 in Arabidopsis leaf patterning. Plant and cell physiology 48 (5):724–735
Fujita H, Mochizuki A (2006a) The origin of the diversity of leaf venation pattern. Developmental Dynamics 235 (10):2710–2721
Fujita H, Mochizuki A (2006b) Pattern formation of leaf veins by the positive feedback regulation between auxin flow and auxin efflux carrier. J Theor Biol 241 (3):541–551

Galweiler L, Guan C, Muller A, Wisman E, Mendgen K, Yephremov A, Palme K (1998) Regulation of polar auxin transport by AtPIN1 in Arabidopsis vascular tissue. Science 282 (5397):2226–2230

Ganguly A, Park M, Kesawat MS, Cho H-T (2014) Functional analysis of the hydrophilic loop in intracellular trafficking of Arabidopsis PIN-FORMED proteins. The Plant Cell:tpc. 113.118422

García-Bellido A, Merriam JR (1971) Parameters of the wing imaginal disc development ofDrosophila melanogaster. Developmental biology 24 (1):61–87

Gardiner J, Sherr I, Scarpella E (2010) Expression of DOF genes identifies early stages of vascular development in Arabidopsis leaves. Int J Dev Biol 54:1389–1396

Gardner MJ, Baker AJ, Assie JM, Poethig RS, Haseloff JP, Webb AA (2009) GAL4 GFP enhancer trap lines for analysis of stomatal guard cell development and gene expression. J Exp Bot 60 (1):213–226

Garrett JJ, Meents MJ, Blackshaw MT, Blackshaw LC, Hou H, Styranko DM, Kohalmi SE, Schultz EA (2012) A novel, semi-dominant allele of MONOPTEROS provides insight into leaf initiation and vein pattern formation. Planta 236 (1):297–312

Ge L, Chen R (2014) PHANTASTICA regulates leaf polarity and petiole identity in Medicago truncatula. Plant signaling & behavior 9 (3):e28121

Geisler M, Blakeslee JJ, Bouchard R, Lee OR, Vincenzetti V, Bandyopadhyay A, Titapiwatanakun B, Peer WA, Bailly A, Richards EL, Ejendal KF, Smith AP, Baroux C, Grossniklaus U, Muller A, Hrycyna CA, Dudler R, Murphy AS, Martinoia E (2005) Cellular efflux of auxin catalyzed by the Arabidopsis MDR/PGP transporter AtPGP1. Plant J 44 (2):179–194

Geisler M, Kolukisaoglu HU, Bouchard R, Billion K, Berger J, Saal B, Frangne N, Koncz-Kalman Z, Koncz C, Dudler R, Blakeslee JJ, Murphy AS, Martinoia E, Schulz B (2003) TWISTED DWARF1, a unique plasma membrane-anchored immunophilin-like protein, interacts with Arabidopsis multidrug resistance-like transporters AtPGP1 and AtPGP19. Mol Biol Cell 14 (10):4238–4249

Geisler M, Murphy AS (2006) The ABC of auxin transport: the role of p-glycoproteins in plant development. FEBS Lett 580 (4):1094–1102

Geldner N, Anders N, Wolters H, Keicher J, Kornberger W, Muller P, Delbarre A, Ueda T, Nakano A, Jürgens G (2003) The Arabidopsis GNOM ARF-GEF Mediates Endosomal Recycling, Auxin Transport, and Auxin-Dependent Plant Growth. Cell 112 (2):219–230

Geldner N, Richter S, Vieten A, Marquardt S, Torres-Ruiz RA, Mayer U, Jurgens G (2004) Partial loss-of-function alleles reveal a role for GNOM in auxin transport-related, post-embryonic development of Arabidopsis. Development 131 (2):389–400

Gerhardt H, Golding M, Fruttiger M, Ruhrberg C, Lundkvist A, Abramsson A, Jeltsch M, Mitchell C, Alitalo K, Shima D, Betsholtz C (2003) VEGF guides angiogenic sprouting utilizing endothelial tip cell filopodia. The Journal of Cell Biology 161 (6):1163

Gersani M (1987) The Induction of Differentiation of Organized Vessels in a Storage Organ. Annals of Botany 59 (1):31–34

Gifford EM, Foster AS (1988) Morphology and evolution of vascular plants W.H. Freeman and Co.,

Goodrich LV, Strutt D (2011) Principles of planar polarity in animal development. Development 138 (10):1877-1892

Goodstein DM, Shu S, Howson R, Neupane R, Hayes RD, Fazo J, Mitros T, Dirks W, Hellsten U, Putnam N, Rokhsar DS (2012) Phytozome: a comparative platform for green plant genomics. Nucleic Acids Res 40 (Database issue):D1178–1186

Gordon SP, Heisler MG, Reddy GV, Ohno C, Das P, Meyerowitz EM (2007) Pattern formation during de novo assembly of the Arabidopsis shoot meristem. Development 134 (19):3539–3548

Goto N, Starke M, Kranz AR (1987) Effect of gibberellins on flower development of the pin-formed mutant of Arabidopsis thaliana. Arabidopsis Information Service 23:66–71

Graumann K, Evans DE (2011) Nuclear envelope dynamics during plant cell division suggest common mechanisms between kingdoms. Biochem J 435 (3):661–667

Griffith ME, Mayer U, Capron A, Ngo QA, Surendrarao A, McClinton R, Jurgens G, Sundaresan V (2007) The TORMOZ gene encodes a nucleolar protein required for regulated division planes and embryo development in Arabidopsis. Plant Cell 19 (7):2246–2263. doi:10.1105/tpc.106.042697

Guenot B, Bayer E, Kierzkowski D, Smith RS, Mandel T, Zadnikova P, Benkova E, Kuhlemeier C (2012) PIN1-Independent Leaf Initiation in Arabidopsis. Plant Physiol 159 (4):1501–1510

Hadwiger JA, Wittenberg C, Richardson HE, de Barros Lopes M, Reed SI (1989) A family of cyclin homologs that control the G1 phase in yeast. Proceedings of the National Academy of Sciences 86 (16):6255–6259

Han M, Aroian RV, Sternberg PW (1990) The let-60 locus controls the switch between vulval and nonvulval cell fates in Caenorhabditis elegans. Genetics 126 (4):899–913

Han X, Hyun TK, Zhang M, Kumar R, Koh EJ, Kang BH, Lucas WJ, Kim JY (2014) Auxin-callose-mediated plasmodesmal gating is essential for tropic auxin gradient formation and signaling. Dev Cell 28 (2):132–146

Hardtke CS, Berleth T (1998) The Arabidopsis gene MONOPTEROS encodes a transcription factor mediating embryo axis formation and vascular development. Embo J 17 (5):1405–1411

Hardtke CS, Ckurshumova W, Vidaurre DP, Singh SA, Stamatiou G, Tiwari SB, Hagen G, Guilfoyle TJ, Berleth T (2004) Overlapping and non-redundant functions of the Arabidopsis auxin response factors MONOPTEROS and NONPHOTOTROPIC HYPOCOTYL 4. Development 131 (5):1089–1100

Hay A, Barkoulas M, Tsiantis M (2006) ASYMMETRIC LEAVES1 and auxin activities converge to repress BREVIPEDICELLUS expression and promote leaf development in Arabidopsis. Development 133 (20):3955–3961

He L, Su C, Wang Y, Wei Z (2015) ATDOF5. 8 protein is the upstream regulator of ANAC069 and is responsive to abiotic stress. Biochimie 110:17–24

Heisler MG, Hamant O, Krupinski P, Uyttewaal M, Ohno C, Jonsson H, Traas J, Meyerowitz EM (2010) Alignment between PIN1 polarity and microtubule orientation in the shoot apical meristem reveals a tight coupling between morphogenesis and auxin transport. PLoS Biol 8 (10):e1000516

Heisler MG, Ohno C, Das P, Sieber P, Reddy GV, Long JA, Meyerowitz EM (2005) Patterns of Auxin Transport and Gene Expression during Primordium Development Revealed by Live Imaging of the Arabidopsis Inflorescence Meristem. Curr Biol 15 (21):1899–1911

Higo K, Ugawa Y, Iwamoto M, Korenaga T (1999) Plant cis-acting regulatory DNA elements (PLACE) database: 1999. Nucleic acids research 27 (1):297–300

Hirakawa Y, Shinohara H, Kondo Y, Inoue A, Nakanomyo I, Ogawa M, Sawa S, Ohashi-Ito K, Matsubayashi Y, Fukuda H (2008) Non-cell-autonomous control of vascular stem cell fate by a CLE peptide/receptor system. Proceedings of the National Academy of Sciences 105 (39):15208–15213
Hiratsu K, Matsui K, Koyama T, Ohme-Takagi M (2003) Dominant repression of target genes by chimeric repressors that include the EAR motif, a repression domain, in Arabidopsis. Plant J 34 (5):733–739
Hodgkin J (1986) Sex determination in the nematode C. elegans: analysis of tra-3 suppressors and characterization of fem genes. Genetics 114 (1):15–52
Hou H, Erickson J, Meservy J, Schultz EA (2010) FORKED1 encodes a PH domain protein that is required for PIN1 localization in developing leaf veins. Plant J
Hsu Y-C, Fuchs E (2012) A family business: stem cell progeny join the niche to regulate homeostasis. Nature reviews Molecular cell biology 13 (2):103
Hsu Y-C, Li L, Fuchs E (2014) Emerging interactions between skin stem cells and their niches. Nature medicine 20 (8):847
Hudson J, Feilotter H, Young P (1990) stf1: non-wee mutations epistatic to cdc25 in the fission yeast Schizosaccharomyces pombe. Genetics 126 (2):309–315
Imaizumi T, Schultz TF, Harmon FG, Ho LA, Kay SA (2005) FKF1 F-box protein mediates cyclic degradation of a repressor of CONSTANS in Arabidopsis. Science 309 (5732):293–297
Iwakawa H, Iwasaki M, Kojima S, Ueno Y, Soma T, Tanaka H, Semiarti E, Machida Y, Machida C (2007) Expression of the ASYMMETRIC LEAVES2 gene in the adaxial domain of Arabidopsis leaves represses cell proliferation in this domain and is critical for the development of properly expanded leaves. The Plant Journal 51 (2):173–184
Jacobs WP (1952) The role of auxin in differentiation of xylem around a wound American Journal of Botany 39:301–309
Jin Z, Homola EM, Tiong S, Campbell SD (2008) Drosophila myt1 is the major cdk1 inhibitory kinase for wing imaginal disc development. Genetics
Johnston R, Leiboff S, Scanlon MJ (2015) Ontogeny of the sheathing leaf base in maize (Zea mays). New Phytologist 205 (1):306–315. doi:doi:10.1111/nph.13010
Jönsson H, Krupinski P (2010) Modeling plant growth and pattern formation. Current opinion in plant biology 13 (1):5–11
Kamphausen T, Fanghanel J, Neumann D, Schulz B, Rahfeld JU (2002) Characterization of Arabidopsis thaliana AtFKBP42 that is membrane-bound and interacts with Hsp90. Plant J 32 (3):263–276
Kang J, Dengler N (2004) Vein pattern development in adult leaves of Arabidopsis thaliana. International Journal of Plant Sciences 165 (2):231–242
Katekar GF, Geissler AE (1980) Auxin Transport Inhibitors: IV. EVIDENCE OF A COMMON MODE OF ACTION FOR A PROPOSED CLASS OF AUXIN TRANSPORT INHIBITORS: THE PHYTOTROPINS. Plant Physiol 66 (6):1190–1195
Keller CP, Stahlberg R, Barkawi LS, Cohen JD (2004) Long-term inhibition by auxin of leaf blade expansion in bean and Arabidopsis. Plant Physiol 134 (3):1217–1226
Kierzkowski D, Lenhard M, Smith R, Kuhlemeier C (2013) Interaction between meristem tissue layers controls phyllotaxis. Dev Cell 26 (6):616–628

Kim I, Cho E, Crawford K, Hempel FD, Zambryski PC (2005) Cell-to-cell movement of GFP during embryogenesis and early seedling development in Arabidopsis. Proc Natl Acad Sci U S A 102 (6):2227–2231
Kinsman EA, Pyke KA (1998) Bundle sheath cells and cell-specific plastid development in Arabidopsis leaves. Development 125 (10):1815–1822
Kleinboelting N, Huep G, Kloetgen A, Viehoever P, Weisshaar B (2012) GABI-Kat SimpleSearch: new features of the Arabidopsis thaliana T-DNA mutant database. Nucleic Acids Res 40 (Database issue):D1211–1215. doi:10.1093/nar/gkr1047
Kleine-Vehn J, Dhonukshe P, Sauer M, Brewer PB, Wi, Paciorek T, Benková E, Friml J (2008) ARF GEF-Dependent Transcytosis and Polar Delivery of PIN Auxin Carriers in Arabidopsis. Current biology 18 (7):526–531
Klucking EP (1995) Leaf Venation Patterns. J. Cramer, Berlin
Koizumi K, Naramoto S, Sawa S, Yahara N, Ueda T, Nakano A, Sugiyama M, Fukuda H (2005) VAN3 ARF-GAP-mediated vesicle transport is involved in leaf vascular network formation. Development 132 (7):1699–1711
Koizumi K, Sugiyama M, Fukuda H (2000) A series of novel mutants of Arabidopsis thaliana that are defective in the formation of continuous vascular network: calling the auxin signal flow canalization hypothesis into question. Development 127 (15):3197–3204
Konishi M, Yanagisawa S (2007) Sequential activation of two Dof transcription factor gene promoters during vascular development in Arabidopsis thaliana. Plant Physiol Biochem 45 (8):623–629
Konishi M, Yanagisawa S (2015) Transcriptional repression caused by Dof5. 8 is involved in proper vein network formation in Arabidopsis thaliana leaves. Journal of plant research 128 (4):643–652
Kouranti I, McLean JR, Feoktistova A, Liang P, Johnson AE, Roberts-Galbraith RH, Gould KL (2010) A Global Census of Fission Yeast Deubiquitinating Enzyme Localization and Interaction Networks Reveals Distinct Compartmentalization Profiles and Overlapping Functions in Endocytosis and Polarity. PLOS Biology 8 (9):e1000471. doi:10.1371/journal.pbio.1000471
Kramer EM (2004) PIN and AUX/LAX proteins: their role in auxin accumulation. Trends Plant Sci 9 (12):578–582
Kraus EJ, Brown NA, Hamner KC (1936) Histological Reactions of Bean Plants to Indoleacetic Acid. Botanical Gazette 98 (2):370–420
Krecek P, Skupa P, Libus J, Naramoto S, Tejos R, Friml J, Zazimalova E (2009) The PIN-FORMED (PIN) protein family of auxin transporters. Genome Biol 10 (12):249
Krogan NT, Ckurshumova W, Marcos D, Caragea AE, Berleth T (2012) Deletion of MP/ARF5 domains III and IV reveals a requirement for Aux/IAA regulation in Arabidopsis leaf vascular patterning. New Phytol
Kuchen EE, Fox S, De Reuille PB, Kennaway R, Bensmihen S, Avondo J, Calder GM, Southam P, Robinson S, Bangham A (2012) Generation of leaf shape through early patterns of growth and tissue polarity. Science 335 (6072):1092–1096
Lee MH, Kim B, Song SK, Heo JO, Yu NI, Lee SA, Kim M, Kim DG, Sohn SO, Lim CE, Chang KS, Lee MM, Lim J (2008) Large-scale analysis of the GRAS gene family in Arabidopsis thaliana. Plant Mol Biol 67 (6):659–670

Lee S-W, Feugier FG, Morishita Y (2014) Canalization-based vein formation in a growing leaf. Journal of Theoretical Biology 353:104–120. doi:https://doi.org/10.1016/j.jtbi.2014.03.005
Lescot M, Déhais P, Thijs G, Marchal K, Moreau Y, Van de Peer Y, Rouzé P, Rombauts S (2002) PlantCARE, a database of plant cis-acting regulatory elements and a portal to tools for in silico analysis of promoter sequences. Nucleic acids research 30 (1):325–327
Lin RC, Wang HY (2005) Two homologous ATP-binding cassette transporter proteins, AtMDR1 and AtPGP1, regulate Arabidopsis photomorphogenesis and root development by mediating polar auxin transport. Plant Physiology 138 (2):949–964. doi:10.1104/pp105.061572
Lincoln C, Britton JH, Estelle M (1990) Growth and development of the axr1 mutants of Arabidopsis. The Plant Cell Online 2 (11):1071–1080
Ljung K, Bhalerao RP, Sandberg G (2001) Sites and homeostatic control of auxin biosynthesis in Arabidopsis during vegetative growth. Plant J 28 (4):465–474
Loots GG, Ovcharenko I (2004) rVISTA 2.0: evolutionary analysis of transcription factor binding sites. Nucleic Acids Res 32 (Web Server issue):W217–221
Lowe DG (2004) Distinctive image features from scale-invariant keypoints. International journal of computer vision 60 (2):91–110
Lu P, Werb Z (2008) Patterning mechanisms of branched organs. Science 322 (5907):1506–1509
Ludwig-Muller J (2012) Auxin conjugates: their role for plant development and in the evolution of land plants. J Exp Bot 62 (6):1757–1773
Luschnig C, Gaxiola RA, Grisafi P, Fink GR (1998) EIR1, a root-specific protein involved in auxin transport, is required for gravitropism in Arabidopsis thaliana. Genes Dev 12 (14):2175–2187
Marcos D, Berleth T (2014) Dynamic auxin transport patterns preceding vein formation revealed by live-imaging of Arabidopsis leaf primordia. Frontiers in Plant Science 5
Maruyama IN, Miller DM, Brenner S (1989) Myosin heavy chain gene amplification as a suppressor mutation in Caenorhabditis elegans. Molecular and General Genetics MGG 219 (1–2):113–118
Marzábal P, Gas E, Fontanet P, Vicente-Carbajosa J, Torrent M, Ludevid MD (2008) The maize Dof protein PBF activates transcription of γ-zein during maize seed development. Plant molecular biology 67 (5):441–454
Masucci JD, Schiefelbein JW (1994) The rhd6 Mutation of Arabidopsis thaliana Alters Root-Hair Initiation through an Auxin- and Ethylene-Associated Process. Plant Physiol 106 (4):1335–1346
Mattsson J, Ckurshumova W, Berleth T (2003) Auxin signaling in Arabidopsis leaf vascular development. Plant Physiol 131 (3):1327–1339
Mattsson J, Sung ZR, Berleth T (1999) Responses of plant vascular systems to auxin transport inhibition. Development 126 (13):2979–2991
Mayer U, Buttner G, Jurgens G (1993) Apical-basal pattern formation in the Arabidopsis embryo: studies on the role of the gnom gene. Development 117 (1):149–162
Mena M, Vicente-Carbajosa J, Schmidt RJ, Carbonero P (1998) An endosperm-specific DOF protein from barley, highly conserved in wheat, binds to and activates transcription from the prolamin-box of a native B-hordein promoter in barley endosperm. The Plant Journal 16 (1):53–62

Mitchison G (1980a) A model for vein formation in higher plants. Proc R Soc Lond B 207 (1166):79–109
Mitchison GJ (1980b) The Dynamics of Auxin Transport. Proceedings of the Royal Society of London Series B, Biological Sciences 209 (1177):489–511
Mitchison GJ (1981) The Polar Transport of Auxin and Vein Patterns in Plants. Philosophical Transactions of the Royal Society of London Series B-Biological Sciences 295 (1078):461–471
Moriwaki T, Miyazawa Y, Fujii N, Takahashi H (2013) GNOM regulates root hydrotropism and phototropism independently of PIN-mediated auxin transport. Plant Sci 215–216:141–149
Moyroud E, Minguet EG, Ott F, Yant L, Posé D, Monniaux M, Blanchet S, Bastien O, Thévenon E, Weigel D (2011) Prediction of regulatory interactions from genome sequences using a biophysical model for the Arabidopsis LEAFY transcription factor. The Plant Cell:tpc. 111.083329
Mravec J, Kubes M, Bielach A, Gaykova V, Petrasek J, Skupa P, Chand S, Benkova E, Zazimalova E, Friml J (2008) Interaction of PIN and PGP transport mechanisms in auxin distribution-dependent development. Development 135 (20):3345–3354
Mravec J, Skupa P, Bailly A, Hoyerova K, Krecek P, Bielach A, Petrasek J, Zhang J, Gaykova V, Stierhof YD, Dobrev PI, Schwarzerova K, Rolcik J, Seifertova D, Luschnig C, Benkova E, Zazimalova E, Geisler M, Friml J (2009) Subcellular homeostasis of phytohormone auxin is mediated by the ER-localized PIN5 transporter. Nature 459 (7250):1136–1140
Muller A, Guan C, Galweiler L, Tanzler P, Huijser P, Marchant A, Parry G, Bennett M, Wisman E, Palme K (1998) AtPIN2 defines a locus of Arabidopsis for root gravitropism control. Embo J 17 (23):6903–6911
Nakamura M, Kiefer CS, Grebe M (2012) Planar polarity, tissue polarity and planar morphogenesis in plants. Curr Opin Plant Biol 15 (6):593–600
Naramoto S, Kleine-Vehn J, Robert S, Fujimoto M, Dainobu T, Paciorek T, Ueda T, Nakano A, Van Montagu MCE, Fukuda H, Friml J (2010) ADP-ribosylation factor machinery mediates endocytosis in plant cells. Proceedings of the National Academy of Sciences of the United States of America 107 (50):21890–21895
Naramoto S, Sawa S, Koizumi K, Uemura T, Ueda T, Friml J, Nakano A, Fukuda H (2009) Phosphoinositide-dependent regulation of VAN3 ARF-GAP localization and activity essential for vascular tissue continuity in plants. Development 136 (9):1529–1538
Nelson T, Dengler N (1997) Leaf Vascular Pattern Formation. Plant Cell 9 (7):1121–1135
Noguero M, Le Signor C, Vernoud V, Bandyopadhyay K, Sanchez M, Fu C, Torres-Jerez I, Wen J, Mysore KS, Gallardo K (2015) DASH transcription factor impacts Medicago truncatula seed size by its action on embryo morphogenesis and auxin homeostasis. The Plant Journal 81 (3):453–466
O'Connor DL, Runions A, Sluis A, Bragg J, Vogel JP, Prusinkiewicz P, Hake S (2014) A Division in PIN-Mediated Auxin Patterning during Organ Initiation in Grasses. PLOS Computational Biology 10 (1):e1003447. doi:10.1371/journal.pcbi.1003447
Oda Y, Fukuda H (2011) Dynamics of Arabidopsis SUN proteins during mitosis and their involvement in nuclear shaping. Plant J 66 (4):629–641
Odat O, Gardiner J, Sawchuk MG, Verna C, Donner TJ, Scarpella E (2014) Characterization of an allelic series in the MONOPTEROS gene of arabidopsis. Genesis

Okada K, Ueda J, Komaki MK, Bell CJ, Shimura Y (1991) Requirement of the Auxin Polar Transport System in Early Stages of Arabidopsis Floral Bud Formation. Plant Cell 3 (7):677–684

Okumura K, Goh T, Toyokura K, Kasahara H, Takebayashi Y, Mimura T, Kamiya Y, Fukaki H (2013) GNOM/FEWER ROOTS is required for the establishment of an auxin response maximum for arabidopsis lateral root initiation. Plant Cell Physiol 54 (3):406–417

Paponov IA, Teale WD, Trebar M, Blilou I, Palme K (2005) The PIN auxin efflux facilitators: evolutionary and functional perspectives. Trends Plant Sci 10 (4):170–177

Parkhurst SM, Bopp D, Ish-Horowicz D (1990) X: A ratio, the primary sex-determining signal in Drosophila, is transduced by helix-loop-helix proteins. Cell 63 (6):1179–1191

Parry G, Marchant A, May S, Swarup R, Swarup K, James N, Graham N, Allen T, Martucci T, Yemm A, Napier R, Manning K, King G, Bennett M (2001) Quick on the uptake: Characterization of a family of plant auxin influx carriers. Journal of Plant Growth Regulation 20 (3):217–225

Peret B, Swarup K, Ferguson A, Seth M, Yang YD, Dhondt S, James N, Casimiro I, Perry P, Syed A, Yang HB, Reemmer J, Venison E, Howells C, Perez-Amador MA, Yun JG, Alonso J, Beemster GTS, Laplaze L, Murphy A, Bennett MJ, Nielsen E, Swarup R (2012) AUX/LAX Genes Encode a Family of Auxin Influx Transporters That Perform Distinct Functions during Arabidopsis Development. Plant Cell 24 (7):2874–2885

Pérez-Pérez JM, Candela H, Robles P, López-Torrejón G, Del Pozo JC, Micol JL (2010) A role for AUXIN RESISTANT3 in the coordination of leaf growth. Plant and cell physiology 51 (10):1661–1673

Perez-Perez JM, Ponce MR, Micol JL (2004) The ULTRACURVATA2 gene of Arabidopsis encodes an FK506-binding protein involved in auxin and brassinosteroid signaling. Plant Physiol 134 (1):101–117

Petrasek J, Cerna A, Schwarzerova K, Elckner M, Morris DA, Zazimalova E (2003) Do phytotropins inhibit auxin efflux by impairing vesicle traffic? Plant Physiol 131 (1):254–263

Petrasek J, Mravec J, Bouchard R, Blakeslee JJ, Abas M, Seifertova D, Wisniewska J, Tadele Z, Kubes M, Covanova M, Dhonukshe P, Skupa P, Benkova E, Perry L, Krecek P, Lee OR, Fink GR, Geisler M, Murphy AS, Luschnig C, Zazimalova E, Friml J (2006) PIN proteins perform a rate-limiting function in cellular auxin efflux. Science 312 (5775):914–918

Petricka JJ, Clay NK, Nelson TM (2008) Vein patterning screens and the defectively organized tributaries mutants in Arabidopsis thaliana. The Plant Journal 56 (2):251–263

Prabhakaran Mariyamma N, Hou H, Carland FM, Nelson T, Schultz EA (2017) Localization of Arabidopsis FORKED1 to a RABA-positive compartment suggests a role in secretion. Journal of Experimental Botany 68 (13):3375–3390. doi:10.1093/jxb/erx180

Price CA, Symonova O, Mileyko Y, Hilley T, Weitz JS (2011) Leaf extraction and analysis framework graphical user interface: segmenting and analyzing the structure of leaf veins and areoles. Plant Physiol 155 (1):236–245

Prouse MB, Campbell MM (2012) The interaction between MYB proteins and their target DNA binding sites. Biochim Biophys Acta 1819 (1):67–77

Prusinkiewicz P, Runions A (2012) Computational models of plant development and form. New Phytol 193 (3):549–569

Przemeck GK, Mattsson J, Hardtke CS, Sung ZR, Berleth T (1996) Studies on the role of the Arabidopsis gene MONOPTEROS in vascular development and plant cell axialization. Planta 200 (2):229–237
Raven JA (1975) Transport of indole acetic acid in plant cells in relation to pH and electrical potential gradients, and its significance for polar IAA transport. New Phytologist 74:163–172
Reddy GV, Heisler MG, Ehrhardt DW, Meyerowitz EM (2004) Real-time lineage analysis reveals oriented cell divisions associated with morphogenesis at the shoot apex of Arabidopsis thaliana. Development 131 (17):4225–4237
Reinhardt D, Mandel T, Kuhlemeier C (2000) Auxin regulates the initiation and radial position of plant lateral organs. Plant Cell 12 (4):507–518
Reinhardt D, Pesce ER, Stieger P, Mandel T, Baltensperger K, Bennett M, Traas J, Friml J, Kuhlemeier C (2003) Regulation of phyllotaxis by polar auxin transport. Nature 426 (6964):255–260
Richter S, Geldner N, Schrader J, Wolters H, Stierhof YD, Rios G, Koncz C, Robinson DG, Jurgens G (2007) Functional diversification of closely related ARF-GEFs in protein secretion and recycling. Nature 448 (7152):488–492
Rolland-Lagan AG, Amin M, Pakulska M (2009) Quantifying leaf venation patterns: two-dimensional maps. Plant J 57 (1):195–205
Rolland-Lagan AG, Prusinkiewicz P (2005) Reviewing models of auxin canalization in the context of leaf vein pattern formation in Arabidopsis. Plant J 44 (5):854–865
Roman G, Lubarsky B, Kieber JJ, Rothenberg M, Ecker JR (1995) Genetic analysis of ethylene signal transduction in Arabidopsis thaliana: five novel mutant loci integrated into a stress response pathway. Genetics 139 (3):1393–1409
Roth-Nebelsick A, Uhl D, Mosbrugger V, Kerp H (2001) Evolution and Function of Leaf Venation Architecture: A Review. Annals of Botany 87 (5):553–566. doi:10.1006/anbo.2001.1391
Rubery PH (1990) Phytotropins: receptors and endogenous ligands. Symp Soc Exp Biol 44:119–146
Rubery PH, Sheldrake AR (1974) Carrier-Mediated Auxin Transport. Planta 118 (2):101–121
Rueden CT, Schindelin J, Hiner MC, DeZonia BE, Walter AE, Arena ET, Eliceiri KW (2017) ImageJ2: ImageJ for the next generation of scientific image data. BMC bioinformatics 18 (1):529
Runions A, Fuhrer M, Lane B, Federl P, Rolland-Lagan A-G, Prusinkiewicz P (2005) Modeling and visualization of leaf venation patterns. ACM Transactions on Graphics 24:702–711
Runions A, Smith RS, Prusinkiewicz P (2014) Computational Models of Auxin-Driven Development. In: Zažímalová E, Petrášek J, Benková E (eds) Auxin and Its Role in Plant Development. Springer Vienna, Vienna, pp 315–357. doi:10.1007/978-3-7091-1526-8_15
Sachs T (1968) On determination of pattern of vascular tissues in peas. Annals of Botany 32 (128):781–790
Sachs T (1975) Control of Differentiation of Vascular Networks. Annals of Botany 39 (160):197–204
Sachs T (1981) The control of the patterned differentiation of vascular tissues. Advances in Botanical Research 9:151–262

Sachs T (1989) The development of vascular networks during leaf development. Current Topics in Plant Biochemistry and Physiology 8:168–183
Sachs T (1991a) Cell Polarity and Tissue Patterning in Plants. Development Suppl 1:83–93
Sachs T (1991b) Pattern Formation in Plant Tissues. Development and cell biology series. Cambridge University Press, Cambridge
Sachs T (2000) Integrating Cellular and Organismic Aspects of Vascular Differentiation. Plant and Cell Physiology 41 (6):649–656. doi:10.1093/pcp/41.6.649
Sachs T (2003) Collective specification of cellular development. BioEssays 25 (9):897–903
Sack L, Scoffoni C (2013) Leaf venation: structure, function, development, evolution, ecology and applications in the past, present and future. New Phytol
Samakovlis C, Hacohen N, Manning G, Sutherland DC, Guillemin K, Krasnow MA (1996) Development of the Drosophila tracheal system occurs by a series of morphologically distinct but genetically coupled branching events. Development 122 (5):1395–1407
Sauer M, Balla J, Luschnig C, Wisniewska J, Reinohl V, Friml J, Benkova E (2006) Canalization of auxin flow by Aux/IAA-ARF-dependent feedback regulation of PIN polarity. Genes Dev 20 (20):2902–2911
Savaldi-Goldstein S, Baiga TJ, Pojer F, Dabi T, Butterfield C, Parry G, Santner A, Dharmasiri N, Tao Y, Estelle M, Noel JP, Chory J (2008) New auxin analogs with growth-promoting effects in intact plants reveal a chemical strategy to improve hormone delivery. Proc Natl Acad Sci U S A 105 (39):15190–15195. doi:10.1073/pnas.0806324105
Sawchuk MG, Donner TJ, Head P, Scarpella E (2008) Unique and overlapping expression patterns among members of photosynthesis-associated nuclear gene families in Arabidopsis. Plant Physiol 148 (4):1908–1924
Sawchuk MG, Edgar A, Scarpella E (2013) Patterning of Leaf Vein Networks by Convergent Auxin Transport Pathways. PLoS Genet 9 (2):e1003294
Sawchuk MG, Head P, Donner TJ, Scarpella E (2007) Time-lapse imaging of Arabidopsis leaf development shows dynamic patterns of procambium formation. New Phytol 176 (3):560–571
Sawchuk MG, Scarpella E (2013) Polarity, continuity, and alignment in plant vascular strands. J Integr Plant Biol 55 (9):824–834
Scarpella E, Francis P, Berleth T (2004) Stage-specific markers define early steps of procambium development in Arabidopsis leaves and correlate termination of vein formation with mesophyll differentiation. Development 131 (14):3445–3455
Scarpella E, Helariutta Y (2010) Vascular pattern formation in plants. Curr Top Dev Biol 91:221–265
Scarpella E, Marcos D, Friml J, Berleth T (2006) Control of leaf vascular patterning by polar auxin transport. Genes Dev 20 (8):1015–1027
Scarpella E, Rueb S, Meijer AH (2003) The RADICLELESS1 gene is required for vascular pattern formation in rice. Development 130 (4):645–658
Schindelin J, Arganda-Carreras I, Frise E, Kaynig V, Longair M, Pietzsch T, Preibisch S, Rueden C, Saalfeld S, Schmid B (2012) Fiji: an open-source platform for biological-image analysis. Nature methods 9 (7):676
Schindelin J, Rueden CT, Hiner MC, Eliceiri KW (2015) The ImageJ ecosystem: an open platform for biomedical image analysis. Molecular reproduction and development 82 (7-8):518–529

Schneider CA, Rasband WS, Eliceiri KW (2012) NIH Image to ImageJ: 25 years of image analysis. Nature methods 9 (7):671
Sessions A, Weigel D, Yanofsky MF (1999) The Arabidopsis thaliana MERISTEM LAYER 1 promoter specifies epidermal expression in meristems and young primordia. The Plant Journal 20 (2):259–263
She W, Lin W, Zhu Y, Chen Y, Jin W, Yang Y, Han N, Bian H, Zhu M, Wang J (2010) The gypsy insulator of Drosophila melanogaster, together with its binding protein suppressor of Hairy-wing, facilitate high and precise expression of transgenes in Arabidopsis thaliana. Genetics 185 (4):1141–1150
Shevell DE, Kunkel T, Chua NH (2000) Cell wall alterations in the arabidopsis emb30 mutant. Plant Cell 12 (11):2047–2060
Shevell DE, Leu WM, Gillmor CS, Xia G, Feldmann KA, Chua NH (1994) EMB30 is essential for normal cell division, cell expansion, and cell adhesion in Arabidopsis and encodes a protein that has similarity to Sec7. Cell 77 (7):1051–1062
Shin R, Burch AY, Huppert KA, Tiwari SB, Murphy AS, Guilfoyle TJ, Schachtman DP (2007) The Arabidopsis transcription factor MYB77 modulates auxin signal transduction. The Plant Cell 19 (8):2440–2453
Sieburth LE (1999) Auxin is required for leaf vein pattern in Arabidopsis. Plant Physiol 121 (4):1179–1190
Sieburth LE, Muday GK, King EJ, Benton G, Kim S, Metcalf KE, Meyers L, Seamen E, Van Norman JM (2006) SCARFACE encodes an ARF-GAP that is required for normal auxin efflux and vein patterning in Arabidopsis. Plant Cell 18 (6):1396–1411
Simon S, Skůpa P, Viaene T, Zwiewka M, Tejos R, Klíma P, Čarná M, Rolčík J, De Rycke R, Moreno I (2016) PIN6 auxin transporter at endoplasmic reticulum and plasma membrane mediates auxin homeostasis and organogenesis in Arabidopsis. New Phytologist 211 (1):65–74
Sims D, Duchek P, Baum B (2009) PDGF/VEGF signaling controls cell size in Drosophila. Genome biology 10 (2):R20
Skirycz A, Reichelt M, Burow M, Birkemeyer C, Rolcik J, Kopka J, Zanor MI, Gershenzon J, Strnad M, Szopa J, Mueller-Roeber B, Witt I (2006) DOF transcription factor AtDof1.1 (OBP2) is part of a regulatory network controlling glucosinolate biosynthesis in Arabidopsis. Plant J 47 (1):10–24
Smith RS, Bayer EM (2009) Auxin transport-feedback models of patterning in plants. Plant Cell Environ 32 (9):1258–1271
Song YH, Lee I, Lee SY, Imaizumi T, Hong JC (2012) CONSTANS and ASYMMETRIC LEAVES 1 complex is involved in the induction of FLOWERING LOCUS T in photoperiodic flowering in Arabidopsis. The Plant Journal 69 (2):332–342
Steffens NO, Galuschka C, Schindler M, BuÈlow L, Hehl R (2004) AthaMap: an online resource for in silico transcription factor binding sites in the Arabidopsis thaliana genome. Nucleic acids research 32 (suppl_1):D368–D372
Stein KK, Nesmith JE, Ross BD, Golden A (2010) Functional Redundancy of Paralogs of an Anaphase Promoting Complex/Cyclosome Subunit in Caenorhabditis elegans Meiosis. Genetics 186 (4):1285
Steinmann T, Geldner N, Grebe M, Mangold S, Jackson CL, Paris S, Galweiler L, Palme K, Jurgens G (1999) Coordinated polar localization of auxin efflux carrier PIN1 by GNOM ARF GEF. Science 286 (5438):316–318

Steynen QJ, Schultz EA (2003) The FORKED genes are essential for distal vein meeting in Arabidopsis. Development 130 (19):4695–4708
Stoma S, Lucas M, Chopard J, Schaedel M, Traas J, Godin C (2008) Flux-Based Transport Enhancement as a Plausible Unifying Mechanism for Auxin Transport in Meristem Development. PLOS Computational Biology 4 (10):e1000207. doi:10.1371/journal.pcbi.1000207
Sun Y, Zhou QW, Zhang W, Fu YL, Huang H (2002) ASYMMETRIC LEAVES1, an Arabidopsis gene that is involved in the control of cell differentiation in leaves. Planta 214 (5):694–702
Sussman MR, Goldsmith MH (1981) Auxin uptake and action of N-1-naphthylphthalamic acid in corn coleoptiles. Planta 151 (1):15–25
Swarup K, Benkova E, Swarup R, Casimiro I, Peret B, Yang Y, Parry G, Nielsen E, De Smet I, Vanneste S, Levesque MP, Carrier D, James N, Calvo V, Ljung K, Kramer E, Roberts R, Graham N, Marillonnet S, Patel K, Jones JDG, Taylor CG, Schachtman DP, May S, Sandberg G, Benfey P, Friml J, Kerr I, Beeckman T, Laplaze L, Bennett MJ (2008) The auxin influx carrier LAX3 promotes lateral root emergence. Nature Cell Biology 10 (8):946–954
Telfer A, Poethig RS (1994) Leaf development in Arabidopsis. In: Meyerowitz EM, Somerville CR (eds) Arabidopsis. Cold Spring Harbor Press, New York, pp 379–401
Thimann KV, Skoog F (1934) On the Inhibition of Bud Development and other Functions of Growth Substance in Vicia Faba. Proceedings of the Royal Society of London Series B, Containing Papers of a Biological Character 114 (789):317–339. doi:10.1098/rspb.1934.0010
Thompson PM, Ge T, Glahn DC, Jahanshad N, Nichols TE (2013) Genetics of the connectome. Neuroimage 80:475–488
Timmermans MCP, Hudson A, Becraft PW, Nelson T (1999) ROUGH SHEATH2: A Myb Protein That Represses knox Homeobox Genes in Maize Lateral Organ Primordia. Science 284 (5411):151
Troll W (1939) Vergleichende Morphologie der höhren Pflanzen. Gebrüder Borntraeger, Berlin
Tsiantis M, Brown MI, Skibinski G, Langdale JA (1999a) Disruption of auxin transport is associated with aberrant leaf development in maize. Plant Physiol 121 (4):1163–1168
Tsiantis M, Schneeberger R, Golz JF, Freeling M, Langdale JA (1999b) The maize rough sheath2 gene and leaf development programs in monocot and dicot plants. Science 284 (5411):154–156
Verna C, Sawchuk MG, Linh NM, Scarpella E (2015) Control of vein network topology by auxin transport. BMC Biol 13:94
Viaene T, Delwiche CF, Rensing SA, Friml J (2012) Origin and evolution of PIN auxin transporters in the green lineage. Trends Plant Sci
Vieten A, Vanneste S, Wisniewska J, Benkova E, Benjamins R, Beeckman T, Luschnig C, Friml J (2005) Functional redundancy of PIN proteins is accompanied by auxin-dependent cross-regulation of PIN expression. Development 132 (20):4521–4531
Wabnik K, Kleine-Vehn J, Balla J, Sauer M, Naramoto S, Reinohl V, Merks RM, Govaerts W, Friml J (2010) Emergence of tissue polarization from synergy of intracellular and extracellular auxin signaling. Mol Syst Biol 6:447

Walker ML, Farcot E, Traas J, Godin C (2013) The Flux-Based PIN Allocation Mechanism Can Generate Either Canalyzed or Diffuse Distribution Patterns Depending on Geometry and Boundary Conditions. PLOS ONE 8 (1):e54802. doi:10.1371/journal.pone.0054802
Wang B, Bailly A, Zwiewka M, Henrichs S, Azzarello E, Mancuso S, Maeshima M, Friml J, Schulz A, Geisler M (2013) Arabidopsis TWISTED DWARF1 functionally interacts with auxin exporter ABCB1 on the root plasma membrane. Plant Cell 25 (1):202–214
Wang H-Z, Yang K-Z, Zou J-J, Zhu L-L, Xie ZD, Morita MT, Tasaka M, Friml J, Grotewold E, Beeckman T (2015) Transcriptional regulation of PIN genes by FOUR LIPS and MYB88 during Arabidopsis root gravitropism. Nature communications 6:8822
Wangermann E (1974) The pathway of transport of applied indolyl-acetic acid through internode segments. New Phytologist 73 (4):623–636
Ward JM, Cufr CA, Denzel MA, Neff MM (2005) The Dof transcription factor OBP3 modulates phytochrome and cryptochrome signaling in Arabidopsis. Plant Cell 17 (2):475–485
Weijers D, Franke-van Dijk M, Vencken RJ, Quint A, Hooykaas P, Offringa R (2001) An Arabidopsis Minute-like phenotype caused by a semi-dominant mutation in a RIBOSOMAL PROTEIN S5 gene. Development 128 (21):4289–4299
Weijers D, Schlereth A, Ehrismann JS, Schwank G, Kientz M, Jurgens G (2006) Auxin triggers transient local signaling for cell specification in Arabidopsis embryogenesis. Developmental Cell 10 (2):265–270
Went FW (1928) Wuchsstoff und Wachstum. Recueil des travaux botaniques néerlandais 25:IV–116
Wenzel CL, Schuetz M, Yu Q, Mattsson J (2007) Dynamics of MONOPTEROS and PIN-FORMED1 expression during leaf vein pattern formation in Arabidopsis thaliana. Plant J 49 (3):387–398
Wilson MD, Odom DT (2009) Evolution of transcriptional control in mammals. Current opinion in genetics & development 19 (6):579–585
Wisniewska J, Xu J, Seifertova D, Brewer PB, Ruzicka K, Blilou I, Rouquie D, Benkova E, Scheres B, Friml J (2006) Polar PIN localization directs auxin flow in plants. Science 312 (5775):883
Wolpert L, Tickle C, Arias AM (2015) Principles of development. Oxford University Press, USA,
Wray GA (2007) The evolutionary significance of cis-regulatory mutations. Nature Reviews Genetics 8 (3):206
Wu G, Lewis DR, Spalding EP (2007) Mutations in Arabidopsis multidrug resistance-like ABC transporters separate the roles of acropetal and basipetal auxin transport in lateral root development. Plant Cell 19 (6):1826–1837
Wu G, Otegui MS, Spalding EP (2010) The ER-localized TWD1 immunophilin is necessary for localization of multidrug resistance-like proteins required for polar auxin transport in Arabidopsis roots. Plant Cell 22 (10):3295–3304
Xu J, Hofhuis H, Heidstra R, Sauer M, Friml J, Scheres B (2006) A molecular framework for plant regeneration. Science 311 (5759):385–388
Xu J, Scheres B (2005) Dissection of Arabidopsis ADP-RIBOSYLATION FACTOR 1 function in epidermal cell polarity. Plant Cell 17 (2):525–536
Yanagisawa S (2000) Dof1 and Dof2 transcription factors are associated with expression of multiple genes involved in carbon metabolism in maize. The Plant Journal 21 (3):281–288

Yanagisawa S (2002) The Dof family of plant transcription factors. Trends Plant Sci 7 (12):555–560
Yanagisawa S, Sheen J (1998) Involvement of maize Dof zinc finger proteins in tissue-specific and light-regulated gene expression. The Plant Cell 10 (1):75–89
Yang Y, Hammes UZ, Taylor CG, Schachtman DP, Nielsen E (2006) High-affinity auxin transport by the AUX1 influx carrier protein. Curr Biol 16 (11):1123–1127
Zadnikova P, Petrasek J, Marhavy P, Raz V, Vandenbussche F, Ding Z, Schwarzerova K, Morita MT, Tasaka M, Hejatko J, Van Der Straeten D, Friml J, Benkova E (2010) Role of PIN-mediated auxin efflux in apical hook development of Arabidopsis thaliana. Development 137 (4):607–617
Zhang C, Gong FC, Lambert GM, Galbraith DW (2005) Cell type-specific characterization of nuclear DNA contents within complex tissues and organs. Plant Methods 1 (1):7